LASER PYROLYSIS OF SELECTED HALOGENATED COMPOUNDS WITH $W(CO)_6$

Grant Richard Allen

A thesis submitted in fulfilment of the requirements for the degree of Doctor of Philosophy in Chemistry

The University of Auckland

2000

Abstract

The pyrolysis of selected halogenated compounds in the absence and presence of $W(CO)_6$ has been investigated using infrared laser powered homogeneous pyrolysis (IR LPHP). The chemistry of these compounds in the absence of $W(CO)_6$ is dominated by the themes of dehydrohalogenation (where available) and C–X bond homolysis (where X = halogen).

The pyrolysis of $W(CO)_6$ in the gas phase at moderate temperatures leads to unsaturated $W(CO)_x$ species; these prove to be very effective and selective abstractors of Cl and Br atoms from the selected halogenated compounds. The subsequent chemistry is dominated by the resulting organic radical moiety; observed end products are ascribed to disproportionation, combination, addition, rearrangement, abstraction and fragmentation of this species.

The results pertaining to the pyrolysis of several of the oxygen-containing halogenated compounds in the presence of $W(CO)_6$ suggest that unsaturated $W(CO)_x$ species are also effective abstractors of atomic oxygen. A number of the products observed can be attributed to intramolecular insertion of the resulting divalent carbon.

Acknowledgements

I would like to express my gratitude to those people, without whose help, this thesis would not have been possible. In particular, Professor Douglas Russell, for his untiring assistance and enthusiasm, and to Dr Rebecca Berrigan for her constructive insight. Many thanks are also extended to my fellow researchers, in particular, Anna Yee and Dr Nathan Hore, and to our brilliant technician Dr Noel Renner. I would also like to thank my family and friends for their support and encouragement. Lastly, I would like to thank the University of Auckland for my doctoral scholarship, for which I am extremely grateful.

Table of Contents

List of Tables

List of Figures

List of Abbreviations

AIBN	azobisisobutyronitrile
CIDNP	chemically induced dynamic nuclear polarisation
CW	continuous wave
EPA	ether, isopentane and ethanol (alcohol)
ESR	electron spin resonance
FT-IR	Fourier transform infrared spectroscopy
GC-MS	gas chromatography mass spectroscopy
HOMO	highest occupied molecular orbital
IR LPHP	infrared laser powered homogeneous pyrolysis
LIA	lock in amplifier
LUMO	lowest unoccupied molecular orbital
MSD	mass selective detector
NLUMO	next lowest unoccupied molecular orbital
NMR	nuclear magnetic resonance
PTFE	polytetrafluoroethene
TDLS	tuneable diode laser spectroscopy
TIC	total ion chromatogram
XPS	X-ray photoelectron spectroscopy

Chapter One

INTRODUCTION

1.1 Review of Organic Radical Chemistry

The importance of free radical species in a number of organic reactions has long been recognised. The discovery of triphenylmethyl in 1900, following the reaction of triphenylmethyl chloride and silver in benzene, heralded the beginning of contemporary organic radical chemistry [1]. It was, however, not until 1937, when Hey and Waters rationalised the products and kinetics of a wide range of organic reactions in terms of free radical chemistry, that synthetic radical mechanisms were accepted [2]. The subject of organic radical chemistry has advanced considerably over the interim, particularly with regard to the generation and detection of an organic radical species.

1.1.1 Generation of an Organic Radical Species

The generation of an organic radical species may involve direct homolysis of a covalent bond; alternatively, homolysis may be induced by another reactive species. The one-electron oxidation or reduction of an organic compound will also effect the formation of an organic radical species. The direct homolysis of a covalent bond is initiated in three ways:

1. *Thermolysis.* An increase in reaction temperature raises the vibrational energy of a molecule. The internal energy is lost by collision and dispersion in the medium, or by homolytic cleavage of one or more covalent bonds. At elevated temperature (approximately 1100 K) all bonds may be broken. The thermolysis of certain azoalkanes, peroxides and organometallic compounds (which have relatively weak

bonds) can occur in solution at temperatures below 423 K, providing a convenient method for producing radicals [3].

2. *Radiolysis.* An organic molecule that is exposed to high-energy radiation in the form of X-rays or γ-radiation will expel an electron. The homolytic fragmentation of the resultant radical cation will result in the formation of a radical and cation species. The irradiation of water is used as a source of hydroxyl radicals [4]. These are in turn employed in the production of other radical species. The radiation absorbed by the organic molecule is highly energetic; consequently, the bond breaking process is rather unselective.

3. *Photolysis.* The ultraviolet radiation absorbed by a molecule that contains a suitable chromophore will effect the excitation of n or π electrons to a singlet π^* state in which the electron spins are paired. The excited state may return to the ground state through a number of radiative or non-radiative decay processes. The energy of an electronically excited state may also be lost through chemical reaction; homolytic dissociation of a covalent bond can be induced by the absorption of ultraviolet radiation. A number of photochemical processes are illustrated in Figure 1.1. The energy absorbed by an organic molecule is of a distinct value; consequently, photolysis is a more selective method of effecting the homolytic fragmentation of a covalent bond than radiolysis or thermolysis [5].

The homolysis of a covalent bond is limited to molecules that possess a relatively weak bond; homolytic fragmentation of a molecule that does not have a weak bond may be

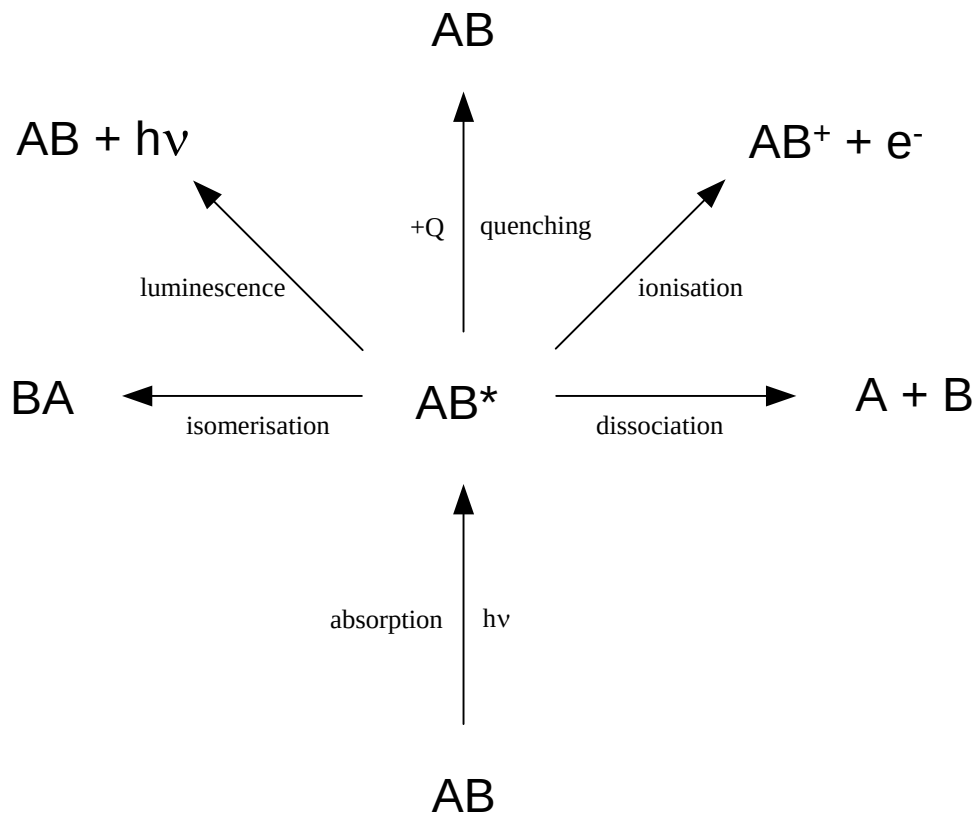

Figure 1.1 A schematic illustrating the various photochemical processes of a species, AB

induced by another species. A radical, molecule or photochemical sensitiser species can effect the induced homolysis of a covalent bond:

1. *Radical-induced decomposition.* The photolysis or thermolysis of an organic species with a relatively weak bond may effect the formation of a radical moiety; these species are referred to as initiators, and by energetically favourable processes initiate abstraction or addition reactions. The oxyl radicals derived from the photolysis or thermolysis of a peroxide compound (through homolysis of the O–O bond) can abstract atomic hydrogen from a wide range of organic substrates to yield an organic radical species [6]. The decomposition of certain azoalkanes will generate molecular nitrogen through concurrent homolysis of the weak C–N bonds (approximately 200 kJ mol^{-1}) to yield two alkyl radicals [7]; these can abstract atomic hydrogen from a range of organic substrates to generate another organic radical species. The tri-*n*-butyltin radical is obtained by the reaction of azobisisobutyronitrile (AIBN), an azoalkane, with the corresponding organometallic hydride, $Bu_3Sn–H$ [8]; similarly, the reaction of AIBN with $(Me_3Si)_3Si–H$ will afford the tris(trimethylsilyl)silyl radical. The tri-*n*-butyltin [8] and tris(trimethylsilyl)silyl [9] radicals are themselves effective abstractors of atomic halogen from a wide range of organohalide species. The organometallic radicals derived from the photolysis of a metal carbonyl dimer in solution (through homolysis of the metal-metal bond) have also been shown to abstract halogen from a range of organohalide substrates to yield an organic radical [10-13].

2. *Molecule-induced homolysis.* A radical may be generated through the interaction of two or more molecules; for example, the reaction of styrene with *tert*-butyl hypochlorite will yield the radical addition product in the dark at 273 K [14]. The

mechanism of reaction between two or more molecules that effects formation of a radical species is not yet understood.

3. *Photochemical sensitiser-induced homolysis.* The infrared or ultraviolet energy absorbed by a photosensitiser can be quenched by a reaction that yields a radical moiety; irradiation of benzophenone at 320 nm yields a triplet that can abstract atomic hydrogen from a range of organic species [15]. Alternatively, energy absorbed by a photosensitiser can be transferred to a radical precursor; the energy transferred to 2-ethylhexanal from the excited triplet of benzophenone will effect homolytic cleavage of the resulting excited species, yielding the formyl and 1-ethyl-1-pentyl radicals [16].

The oxidation or reduction of an organic compound may be chemical or electrochemical in nature and will effect the formation of an organic radical species through the loss or acquisition of a single electron. The electrochemical oxidation of a carboxylate will yield an acyloxyl radical that will expel molecular CO_2; combination of the resultant alkyl radical will generate an alkane (Kolbe alkane synthesis). The Fenton reaction between iron(II) salts and hydrogen peroxide is an extremely rapid process; iron(II) is oxidised to iron(III), while the peroxide is reduced, dissociating into hydroxide and a hydroxyl radical.

1.1.2 Detection of an Organic Radical Species

The presence of an organic radical species can be inferred from the nature of the reactants and products, and from the chemical behaviour of the system under investigation; products of a radical reaction may include combination addends that enable the reactive species to

be characterised. There are also a number of physical methods that may be employed in order to detect an organic radical species:

1. *Magnetic susceptibility.* An organic radical species has an unpaired electron that confers a permanent magnetic moment on the molecule. A substance that possesses a permanent magnetic moment is paramagnetic. The paramagnetic properties of a stable organic radical species in high concentration may be detected by way of a magnetic susceptibility measurement. A measure of the paramagnetic properties of an organic radical species that is present in low concentration is not possible; consequently, a more sensitive procedure, such as chemically induced dynamic nuclear polarisation (CIDNP) spectroscopy or electron spin resonance (ESR), is used.

2. *Chemically induced dynamic nuclear polarisation (CIDNP).* A nuclear magnetic resonance (NMR) spectrum recorded during the progress of an organic radical reaction may exhibit anomalous behaviour: certain signals may be much more intense than would be possible for a 100 % product yield, while others may be in emission. The presence of a radical species in an organic reaction may be diagnosed from the enhanced absorption and or emission lines observed in the NMR spectrum. It is evident from the observed phenomena (referred to as chemically induced dynamic nuclear polarisation) that the normal population of nuclear spins in the product molecules is disturbed during the course of a reaction. Only at the completion of reaction do the spin populations relax to their normal Boltzmann values, as determined by the strength of the magnetic field; the spectra then exhibit normal intensities that reflect the varying concentrations of each of the different products [17]. A qualitative explanation for the

deviation in the nuclear spin state populations (of the products) from the thermal equilibrium value has been given by Fischer and Bargon [18].

3. *Electron spin resonance (ESR).* An unpaired electron can exist in two spin states of equal energy. In the presence of an applied magnetic field, H, the orientation of the electron is quantised in two states (parallel or antiparallel to the magnetic field) which differ in energy. The frequency associated with the change from one energy level to the other is given by the equation:

$$\nu = \frac{g\beta H}{h}$$

where g = gyromagnetic or g-value and β = the Bohr magneton. The absorption or emission of a quantum, $h\nu$, induces a transition between energy states that is diagnostic of an unpaired electron. An excess population of approximately 10^{-3} in the lower level (which is maintained by relaxation phenomena) results in a net absorption of resonance radiation that is typically observed in a magnetic field of 0.3 T and a frequency of 9 GHz (3 cm). ESR is a very sensitive technique that is capable of detecting organic radicals at concentrations of the order of 10^{-8} M [3]; a very short-lived radical, however, can not be detected if the concentration does not reach this level. The creation or trapping of a radical in a solid matrix at low temperature increases the lifetime, and therefore concentration, of the transient species by effectively preventing dimerisation of the radical. A reactive radical may be generated in the presence of a nitroso derivative or nitrone; addition of the radical species to the nitroso derivative or nitrone (spin-trapping) will effect formation of a stable ESR-observable nitroxide radical.

1.1.3 Characteristic Reactions of an Organic Radical Species

An organic radical is a highly reactive species because it contains an atom with an odd number of electrons (usually seven) in the outer shell; the driving force for radical reaction is formation of a stable octet. There are seven classes of radical reaction that can be divided into four categories:

1. *Radical-radical reaction.* An organic radical species can collide and interact with another to form one or more stable products. The *combination* of two identical radicals will effect formation of the corresponding dimer; in a system containing two unlike radicals, cross-combination is also possible. The *disproportionation* of organic radical species is restricted to those that possess a β-hydrogen and involves the transfer of atomic hydrogen from one radical to another; disproportionation effects the formation of an unsaturated and saturated product. The pairing of electrons, which occurs when two radicals interact, is a highly exothermic process; consequently, such reactions are without an activation barrier and occur so rapidly that the rate is determined by diffusive encounter. An important factor in determining the competition between combination and disproportionation is rotational diffusion at the point of encounter. The dimerisation of a primary alkyl radical will usually predominate; conversely, a tertiary alkyl radical will disproportionate in preference to combination [17].

2. *Radical-molecule reaction.* An organic radical will undergo *addition* reactions with many unsaturated species, including olefins, aromatic compounds, azo compounds and carbonyl compounds [3]. The addition of an organic radical to the double bond of an olefin is regiospecific and is predicted to occur at the least substituted position to form the more stable radical intermediate. A reactive organic radical species may acquire

stability through the *abstraction* of an atom. The most prevalent radical abstraction reaction is that of hydrogen transfer; the abstraction of halogen (excluding fluorine) is also possible. The feasibility of abstraction can be estimated from the difference in the bond dissociation energies involved. The relative rate of hydrogen abstraction will decrease with increasing C–H bond strength: tertiary > secondary > primary hydrogen. In a similar manner, the rate of abstraction of halogen decreases with increasing C–X bond strength (where X = halogen): –I > –Br > –Cl [5].

3. *Unimolecular reaction.* The *homolytic fragmentation* of an organic radical species (through cleavage of a radical fragment β to the radical centre) is essentially the reverse of radical addition to a double bond; decarboxylation of an acyloxyl radical is an example of β-cleavage. The decomposition of a tertiary alkoxy radical will effect the formation of an alkyl radical and ketone through homolytic fragmentation of a C_α–C_β bond. The predominant decomposition pathway is determined by the stability of the resulting alkyl radical; a secondary radical is ejected in preference to a primary radical and a primary radical is ejected in preference to a methyl radical [19]. The *rearrangement* of an organic radical may involve migration of a monovalent atom or group. The *migration* of a monovalent atom may be referred to as intramolecular abstraction; intramolecular hydrogen abstraction via a five or six-membered cyclic transition state is frequently observed. 1,2-migrations are relatively rare [17]. The *cyclisation* of 5-hexenyl to the thermodynamically less stable cyclopentylmethyl radical is a radical rearrangement; it may, however, equally be viewed as an intramolecular example of radical addition [20-22]. The unimolecular conversion of a cyclopropylmethyl radical to a 3-butenyl derivative through *ring opening* is an example of a fast radical rearrangement [23-28].

4. *Electron transfer reactions.* A radical may undergo one-electron oxidation or reduction that is electrochemical or chemical in nature to yield a cationic or anionic species. The chemical oxidation or reduction of a radical is proposed to involve either electron or ligand transfer [29]. The reaction of $CuCl_2$ with an organic radical species is an example of ligand transfer oxidation and will effect the formation of CuCl and an alkyl chloride.

1.2 A Mild Route into Gas Phase Organic Radical Chemistry

The technique of infrared laser powered homogeneous pyrolysis (IR LPHP) [30-32] has been successfully exploited for over 20 years in the investigation of the mechanisms of thermal decomposition of volatile organometallic [33-35] and organic compounds [36, 37]. The pyrolysis of many organochlorine compounds has been investigated using IR LPHP by Pola [38]; as in conventional pyrolysis, the chemistry of these compounds is dominated by the themes of dehydrochlorination (where available) and C–Cl bond homolysis.

The IR LPHP technique is described in detail in section 2.2 and therefore only a brief description will be given here. A gaseous mixture of the target species and an inert photosensitiser (SF_6) is exposed to the output of a CO_2 IR laser; SF_6 strongly absorbs the laser energy, which is rapidly converted to heat via efficient intra- and inter-molecular relaxation [30, 31]. The advantages of this technique are well documented; only a small quantity of the target species is required, initiation of reaction is unambiguously homogenous and short-lived intermediates are readily trapped (physically or chemically). The progress of reaction may be monitored by conventional analytical techniques; in the

present work, Fourier transform infrared (FT-IR) spectroscopy and gas chromatography mass spectroscopy (GC-MS) were employed.

The IR LPHP of $W(CO)_6$ in the gas phase at low laser power leads to copious amounts of CO and a grey deposit, shown elsewhere to be more or less pure tungsten [39]. It is assumed that these products result from the successive homolytic loss of carbonyl groups. In the presence of vapours of various chlorinated organic compounds, the deposits were found in previous work to also contain chlorine; X-ray photoelectron spectroscopy (XPS) and reflectance infrared spectroscopy suggested a composition approximating to $W(CO)_4Cl_2$ [40, 41]. It appears, therefore, that unsaturated $W(CO)_x$ ($x < 6$) species are highly efficient abstractors of atomic chlorine from such compounds, and consequently offer a clean and low-energy route into gas phase radical chemistry. This is in contrast to conventional generative methods that are often complex and unselective due to the high energies involved.

The principal aim of this study is to illustrate the various reaction mechanisms of organic radical species by investigating the pyrolysis of a number of appropriate organochlorine precursors in the presence of $W(CO)_6$. Chapter Three focuses on radical-radical and radical-molecule reactions. Chapter Six focuses on unimolecular reactions, including rearrangement and homolytic fragmentation. The mechanism of pyrolysis of the precursor in the absence of $W(CO)_6$ was also established so as to provide a means of reference; in several systems (where there had been no previous attempt to construct a comprehensive gas phase decomposition scheme) this provided an opportune avenue for study. The pyrolysis of a number of acyl and diacyl chlorides in the absence of $W(CO)_6$ (which is described in Chapters Four and Five, respectively) generated transient ketene species that

were particularly interesting from a spectroscopic point of view. The pyrolysis of the acyl chlorides in the presence of $W(CO)_6$ illustrated a combination of various radical reactions; in contrast, the selective abstraction of both chlorine atoms from a diacyl chloride was accompanied by successive loss of carbonyl groups, affording a stable non-radical species.

1.3 References

[1] M. Gomberg, *J. Am. Chem. Soc.*, 1900, **22**, 757.

[2] D. H. Hey and W. A. Waters, *Chem. Rev.*, 1937, **21**, 202.

[3] J. Fossey, D. Lefort and J. Sorba, *Free Radicals in Organic Chemistry,* John Wiley & Sons, Chichester, 1995.

[4] D. C. Nonhebel and J. C. Walton, *Free-radical Chemistry,* University Press, Cambridge, 1974.

[5] N. S. Isaacs, *Physical Organic Chemistry,* Longman Group Limited, Essex, 1995.

[6] Y. Ogata, K. Tomizawa and K. Furuta, In *The Chemistry of Peroxides,* S. Patai, Ed., John Wiley & Sons, Chichester, 1983; pp. 710-771.

[7] P. S. Engel, *Chem. Rev.*, 1980, **80**, 99.

[8] W. P. Neumann, *Synthesis*, 1987, 665.

[9] C. Chatgilialoglu, *Acc. Chem. Res.*, 1992, **25**, 188.

[10] M. S. Wrighton and D. D. Ginley, *J. Am. Chem. Soc.*, 1975, **97**, 2065.

[11] M. S. Wrighton and D. D. Ginley, *J. Am. Chem. Soc.*, 1975, **97**, 4246.

[12] J. L. Hughey, C. B. Bock and T. J. Meyer, *J. Chem. Soc.*, 1975, **97**, 4440.

[13] A. Freeman and R. Bersohn, *J. Am. Chem. Soc.*, 1978, **100**, 4116.

[14] C. Walling, L. Heaton and D. D. Tanner, *J. Am. Chem. Soc.*, 1965, **87**, 1715.

[15] C. Walling and M. J. Gibian, *J. Am. Chem. Soc.*, 1965, **87**, 3361.

[16] J. D. Berman, J. H. Stanley, W. V. Sherman and S. G. Cohen, *J. Am. Chem. Soc.*, 1963, **85**, 4010.

[17] M. J. Perkins, *Radical Chemistry,* Ellis Horwood Limited, Hertfordshire, 1994.

[18] H. Fischer and J. Bargon, *Acc. Chem. Res.*, 1969, **2**, 110.

[19] F. D. Green, M. L. Savitz and F. D. Osterhaltz, *J. Am. Chem. Soc.*, 1961, **83**, 2196.

[20] D. J. Carlson and K. U. Ingold, *J. Am. Chem. Soc.*, 1968, **90**, 7047.

[21] D. Lal, D. Griller, S. Husband and K. U. Ingold, *J. Am. Chem. Soc.*, 1974, **96**, 6355.

[22] P. Schmid, D. Griller and K. U. Ingold, *Int. J. Chem. Kinet.*, 1979, **11**, 333.

[23] M. Newcombe, *Tetrahedron*, 1993, **49**, 1151.

[24] V. W. Bowry, J. Lusztyk and K. U. Ingold, *J. Am. Chem. Soc.*, 1991, **113**, 5687.

[25] A. L. J. Beckwith and V. W. Bowry, *J. Am. Chem. Soc.*, 1994, **116**, 2710.

[26] P. S. Engel, S. L. He, J. T. Banks, K. U. Ingold and J. Lusztyk, *J. Org. Chem.*, 1997, **62**, 1210.

[27] A. Effio, D. Griller, K. U. Ingold, A. L. J. Beckwith and A. K. Serelis, *J. Am. Chem. Soc.*, 1980, **102**, 1734 and references therein.

[28] M. Newcombe and A. G. Glenn, *J. Am. Chem. Soc.*, 1989, **111**, 265.

[29] J. K. Kochi, *Science*, 1967, **155**, 415.

[30] D. K. Russell, *Chem. Vap. Deposition*, 1996, **2**, 223.

[31] D. K. Russell, *Chem. Soc. Rev.*, 1990, **19**, 407.

[32] W. M. Shaub and S. H. Bauer, *Int. J. Chem. Kinet.*, 1975, **7**, 509.

[33] D. K. Russell, I. M. T. Davidson, A. M. Ellis, G. P. Mills, M. Pennington, I. M. Povey, J. B. Raynor, S. Saydam and A. D. Workman, *Organometallics*, 1995, **14**, 3717.

[34] R. E. Linney and D. K. Russell, *J. Mater. Chem.*, 1993, **3**, 587.

[35] A. S. Grady, R. D. Markwell and D. K. Russell, *J. Chem. Soc., Chem. Commun.*, 1991, 929.

[36] N. R. Hore and D. K. Russell, *J. Chem. Soc., Perkin Trans. II*, 1998, 269.

[37] H. Hettema, N. R. Hore, N. D. Renner and D. K. Russell, *Aust. J. Chem.*, 1997, **50**, 363.

[38] J. Pola, *Spectrochim. Acta, Part A*, 1990, **46**, 607.

[39] K. E. Lewis, D. M. Golden and G. P. Smith, *J. Am. Chem. Soc.*, 1986, **106**, 3905.

[40] G. R. Allen, BSc. (Honours) Dissertation, University of Auckland, 1996.

[41] G. R. Allen, N. D. Renner and D. K. Russell, *J. Chem. Soc., Chem. Commun.*, 1998, 703.

Chapter Two

EXPERIMENTAL

2.1 Introduction

In this chapter, the equipment and experimental techniques used specific to this investigation will be described, with particular emphasis given to infrared laser powered homogeneous pyrolysis (IR LPHP), the method by which the compounds studied were decomposed. Methods of experimental analysis including Fourier transform infrared (FT-IR) spectroscopy, matrix isolation and infrared tuneable diode laser (TDL) spectroscopy will also be described. A brief description of the theoretical calculations performed during the course of this investigation will also be given.

2.2 Infrared Laser Powered Homogeneous Pyrolysis

The use of lasers in chemistry, particularly with regard to inducing chemical reactions, can be attributed to the considerable advantages laser light has over conventional light sources. Laser radiation is coherent, linear and highly monochromatic in nature. Early studies involving laser-induced chemistry were limited to those molecules that could absorb infrared radiation directly [1, 2]. It was found that this problem could be overcome by introducing a chemically inert, infrared absorber to the system [3]. Energy absorbed in a specific vibrational mode of the photosensitiser could be rapidly converted to translational energy through very efficient intra- and inter-molecular relaxation. By selecting a photosensitiser with a low thermal conductivity, that heat, while expeditiously transferred to the target species via intermolecular collisions, was confined to the centre of the reaction cell. Infrared laser powered homogeneous pyrolysis (IR LPHP), by which the technique is known, provides a number of distinct advantages over its conventional counterpart. Most significantly, the process is entirely homogeneous, in that energy is conveyed directly into

the gas phase at the centre of the pyrolysis cell. The resultant inhomogeneous temperature profile has a twofold advantage:

- surface initiated reactions are eliminated;

- the primary products of pyrolysis are initially ejected into the cooler regions of the cell; thereby inhibiting their further reaction.

In addition, IR LPHP requires only a small quantity of sample, and consequently it is possible to investigate the decomposition of compounds that are both expensive and rare. A disadvantage of IR LPHP is that it is difficult to discern the absolute temperature at which reaction occurs. The collection of kinetic data is consequently limited, as reaction rates are dependent on that unequivocal temperature. Moreover, the generation of reaction products can alter both the thermal conductivity and heat capacity of a system, thereby modifying the temperature distribution. It is possible to ascertain the spatially averaged temperature at which a reaction is occurring by comparing that system with another whose kinetic parameters are well known, *i.e.* by utilising a chemical thermometer, an example being ethyl ethanoate.

Notwithstanding these disadvantages, IR LPHP has provided a valuable tool for the investigation of gas phase reactions. Infrared laser powered homogeneous pyrolysis has been extensively reviewed in an article by Russell [4].

2.3 Equipment

2.3.1 Vacuum Line

The vacuum manifold, illustrated in Figure 2.1, was constructed from Pyrex glass of 15 mm in diameter and 2 mm in thickness, and used for the manipulation of the photosensitiser and selected sample gases. The line was fitted with J. Young 'O' ring vacuum taps and PTFE high vacuum screw cap joints to which reagent containing Pyrex sample tubes could be attached. Photosensitiser was stored within a U-tube on the vacuum line.

The vacuum obtained when both the rotary (Edwards E2M5 two stage) and oil diffusion (Edwards EO2) pumps were operating was of the order of 10^{-5} Torr (1 Torr = 133.332 Pa). A second vacuum line was used primarily for the matrix isolation of reactive intermediates for subsequent FT-IR analysis. This technique will be discussed in section 2.7.

2.3.2 Pyrolysis Cell

The static or standard pyrolysis cell consisted of a Pyrex cylinder of 100 mm in length and 38 mm in diameter. Sample and photosensitiser were admitted to the cell through a double 'O' ring Teflon screw cap. Protruding from the base and side of the cell were two small reservoirs (the latter of which could be sealed) that could be used to retain liquids or chemicals of low vapour pressure. To the cell wall was appended a Pyrex tube of length 25 mm and diameter 8 mm capped with a Shimadzu 2920 rubber injection plug, through which a gas tight lockable syringe could extract a sample for subsequent GC-MS analysis.

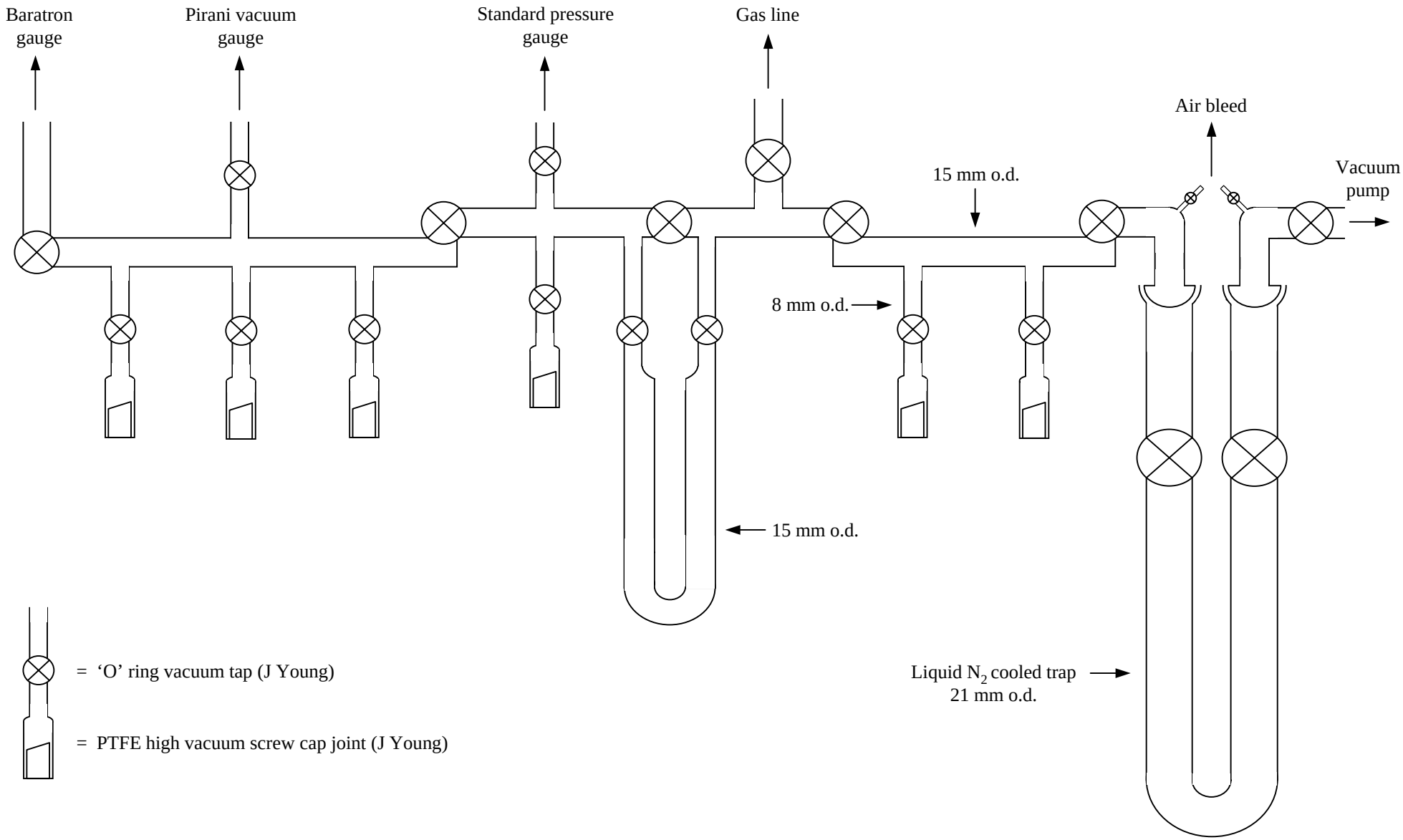

Figure 2.1 A schematic of the vacuum manifold

Zinc selenide (ZnSe) windows were fitted to each end of the reaction cell for axial irradiation, with quick setting epoxy resin. The standard pyrolysis cell without the side reservoir is illustrated in Figure 2.2.

The pyrolysis cell used during the matrix isolation of a transient species differed to the standard or static IR LPHP cell in that there were Pyrex ports appended such that a vacuum line could be attached. A zinc selenide window was attached to the end of the cell through which laser radiation entered and fitted to the opposite end was a reflective stainless steel disk. At the base of the pyrolysis cell a small reservoir protruded, similar to that located on the underside of the static IR LPHP cell.

2.3.3 Window Material

To each end of a standard pyrolysis cell was attached a zinc selenide window. An IR LPHP pyrolysis cell window must be:

- transparent to the CO_2 laser radiation;
- transparent to the infrared spectrometer radiation;
- thermally stable and strong;
- chemically inert;

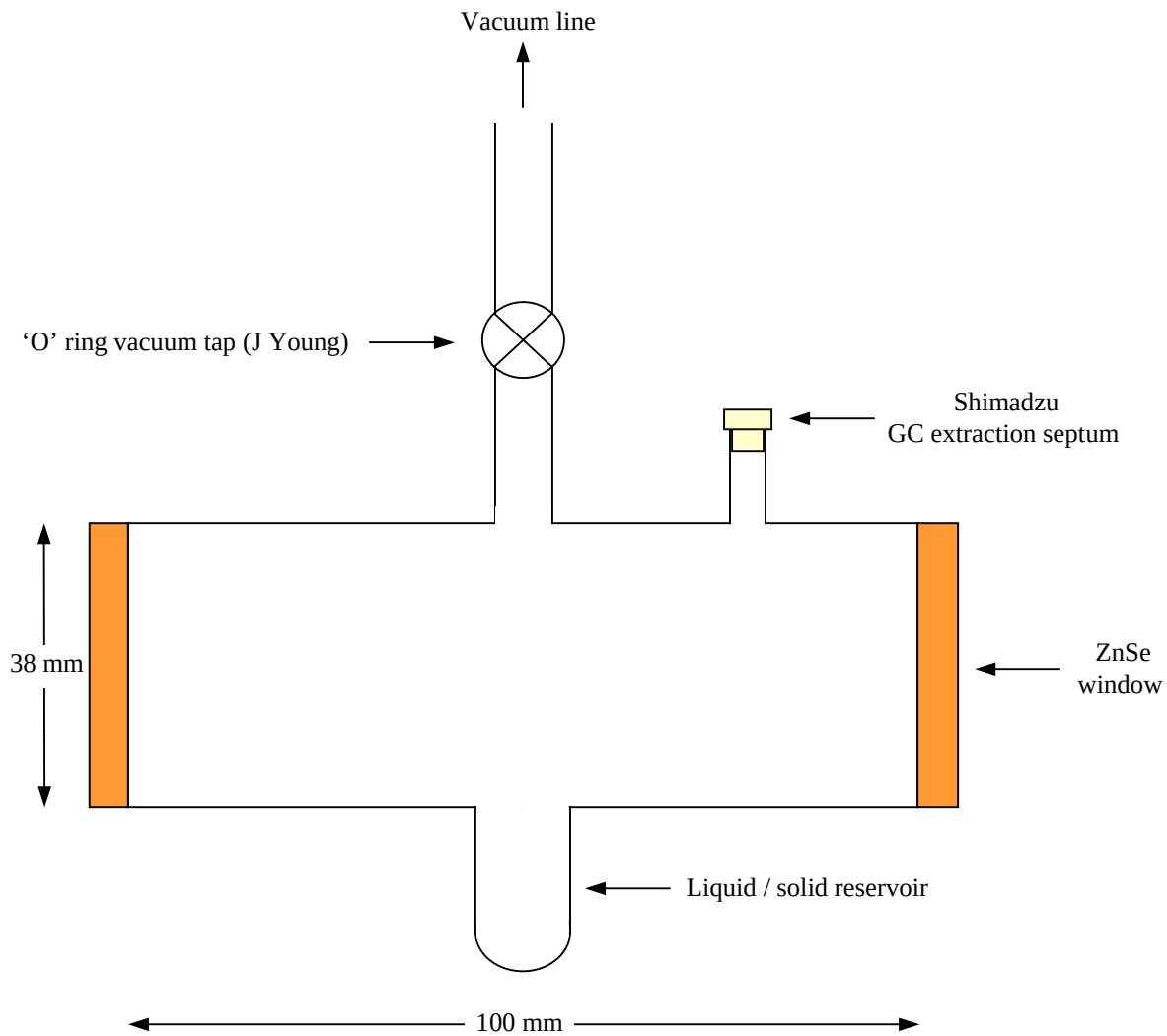

Figure 2.2 A schematic of the standard IR LPHP cell

- of low thermal expansion.

Zinc selenide satisfies all of the above requirements, and unlike its alkali halide counterparts, is non-hygroscopic. This enables the study of moisture sensitive organometallic compounds. One significant disadvantage of zinc selenide windows is their cost; intrinsically expensive, they also require an anti-reflective Al_2O_3 coating to counter the high refractive index of ZnSe. Additionally the IR cut-off is relatively high at 500 cm^{-1}, which while sometimes inconvenient, has not been a significant problem in this investigation.

2.3.4 Photosensitiser

The addition of a photosensitiser to the pyrolysis cell allows for the IR LPHP of compounds that will not directly absorb infrared radiation. The photosensitiser of choice, sulfur hexafluoride (SF_6) is ideal, as it possesses the following characteristics:

- strong absorption of radiation at 10.6 μm that corresponds to that generated by the CO_2 laser. Disregarding the effects of bleaching and temperature dependence, an absorption value of 0.995 over a path of 5 mm and a pressure of 10 Torr has been estimated [5];

- a very efficient inter- and intra-molecular relaxation process, thus enabling it to transfer translational energy to the reagent molecule. The vibrational relaxation time of SF_6 has been reported as 10 μs Torr [6];

- high thermal stability, reportedly up to 1500 K [7];

- chemically inert;

- low thermal conductivity [8]; thus the heat generated by laser irradiation is confined to the centre of the cell.

While the peaks attributable to SF_6 were present when characterising reactions with FT-IR spectroscopy, these rarely proved problematic when interpreting infrared spectra, product and reactant bands infrequently overlapped with those of SF_6 [9]. The FT-IR spectrum of SF_6, including the vibrational assignment of absorbance bands [10], is illustrated in Figure 2.3.

2.3.5 CO_2 Laser

The CO_2 laser is of immense importance in both industry and research. Its operation is based on transitions between the vibrational levels of the CO_2 molecule. Passing an electric discharge through the carbon dioxide laser gas mixture (0.8 He, 0.1 N_2 and 0.1 CO_2) effects the ionisation of helium. The ejected electrons collide with molecules of nitrogen which are in turn vibrationally excited to the $\nu = 1$ level. Energy is transferred from this vibrational level to the commensurate anti-symmetric stretching energy level (001) of CO_2 via intermolecular collisions. Subsequent relaxation of the resultant population inversion occurs as energy is transferred into the lower CO_2 symmetric stretching mode (100) and CO_2 bending mode (020) via intermolecular collisions with helium. Laser emission at 10.6 μm and 9.6 μm respectively, accompanies this process.

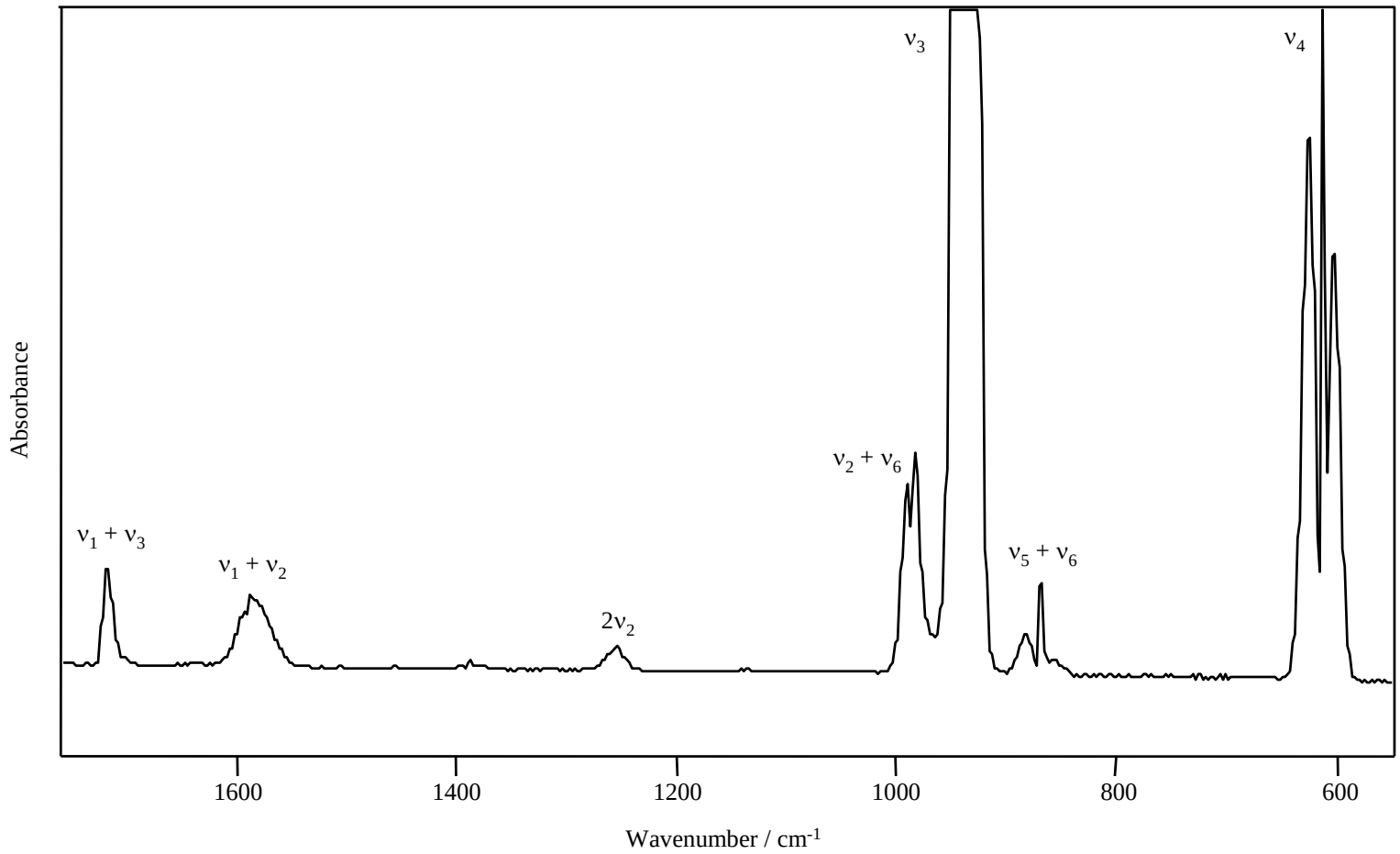

Figure 2.3 Assigned FT-IR spectrum of SF_6 [10]

The IR LPHP experiments discussed herein were performed using an Electrox Industrial 'M-80' free running carbon dioxide laser. This operated at a wavelength of 10.6 μm, with a total power output range of between 60 and 85 W. The beam size, and hence the power output, could be manipulated by adjusting the aperture at the beam exit. Aperture diameters are given in Table 2.1. To a first approximation, the power output was taken to be proportional to the square of the diameter of the exiting beam. Aperture 1 allowed the complete transmission of the exiting beam; thus the total power output was not reduced. Conversely, the utilisation of aperture 18, having a diameter approximately a tenth that of aperture 1 would reduce the total power output by a factor of a hundred.

Table 2.1 Aperture Diameters

Aperture	**1**	**2**	**3**	**4**	**5**	**6**	**7**	**8**	**9**
Diameter / mm	11.3	8.4	7.6	6.7	6.0	5.3	4.6	4.3	4.0

Aperture	**10**	**11**	**12**	**13**	**14**	**15**	**16**	**17**	**18**
Diameter / mm	3.7	3.4	3.1	2.8	2.5	2.2	1.9	1.6	1.3

2.4 Chemicals

With the exception of cyclobutylmethyl chloride, 4-(bromomethyl)-2-oxetanone and acryloyl chloride, the compounds used in this investigation were obtained commercially and of analytical grade. These and SF_6 were purified prior to use by repeated freeze-pump-thaw cycles, where the compound is cooled to liquid nitrogen temperature (77 K) and degassed, before being thawed to ambient temperature. Provided care was taken not to

displace the entire sample it was possible to outgas those compounds with a relatively low vapour pressure at room temperature.

In the course of this investigation it was necessary to synthesise 4-(bromomethyl)-2-oxetanone and cyclobutylmethyl chloride. The latter was prepared by treating cyclobutanemethanol with thionyl chloride according to the literature procedure [11]. The synthesis of 4-(bromomethyl)-2-oxetanone was effected by the bromolactonisation of vinylacetic acid in accord with Somerville [12]. In both cases product identification and purity was established using both GC-MS and NMR spectroscopy. Acryloyl chloride was kindly supplied by Dr S. Horner. Table 2.2 lists the common names and formulae of those compounds investigated and their source.

2.5 Experimental Procedure

2.5.1 Introduction

Experiments involving the IR LPHP of a compound or compounds in a static pyrolysis cell required prior sample manipulation using the vacuum manifold illustrated in Figure 2.1. Those experiments involving the matrix isolation of a reactive species were performed on the alternative vacuum line. Both vacuum lines were set up when required according to instructions detailed in the accompanying manual [13]. Once a pressure of 10^{-5} Torr was attained, preparation of the sample could proceed.

Table 2.2 Chemicals used and source

Common Name	Formula	Source
Acetaldehyde	C_2H_4O	Riedel-de Haën
Acetone	C_3H_6O	Bulk
Acetyl chloride	C_2H_3ClO	Prosynth
Acryloyl chloride	C_3H_3ClO	Aldrich
Benzyl chloride	C_7H_7Cl	May and Baker
4-(Bromomethyl)-2-oxetanone	$C_4H_5BrO_2$	Synthesised [12]
E-2-Butenoyl chloride	C_4H_5ClO	Aldrich
Chloroacetic acid	$C_2H_3ClO_2$	Aldrich
Chloroacetonitrile	C_2H_2ClN	Aldrich
Chloroacetyl chloride	$C_2H_2Cl_2O$	Aldrich
Cyclobutylmethyl chloride	C_5H_9Cl	Synthesised [11]
Cyclopropylmethyl chloride	C_4H_7Cl	Aldrich
2-Chloro-2-methylpropane	C_4H_9Cl	Merck
2-Chloropropane	C_3H_7Cl	BDH
3-Chloropropanoyl chloride	$C_3H_4Cl_2O$	Aldrich
Cyclopropanecarbonyl chloride	C_4H_5ClO	Aldrich
E-1,2-Dichloroethene	$C_2H_2Cl_2$	Riedel-de Haën
α,α′-Dichloro-*o*-xylene	$C_8H_4Cl_2$	Aldrich
Diglycoloyl chloride (2,2′-oxydiacetyl chloride)	$C_4H_4Cl_2O_3$	Aldrich
Epichlorohydrin	C_3H_5ClO	BDH
Fumaroyl chloride (2-Butenedioyl dichloride)	$C_4H_2Cl_2O_2$	Aldrich
Malonyl chloride (Propanedioyl dichloride)	$C_3H_2Cl_2O_2$	Aldrich
Methacryloyl chloride	C_4H_5ClO	Lancaster
Propanoyl chloride	C_3H_5ClO	Aldrich
Propargyl chloride	C_3H_3Cl	Aldrich

Table 2.2. *Continued*

Common Name	Formula	Source
Propylene oxide	C_3H_6O	BDH
Succinyl chloride (Butanedioyl dichloride)	$C_4H_4Cl_2O_2$	Aldrich
Sulfur hexafluoride	SF_6	BOC
Tungsten hexacarbonyl	$W(CO)_6$	Prosynth

2.5.2 Procedure for Sample Preparation

The static pyrolysis cell was fitted to the vacuum manifold and evacuated. Introduction into the cell of the selected compounds was achieved through one of two ways. Samples with sufficient vapour pressure were stored in Pyrex reagent tubes that could be fitted to the line through PTFE high vacuum screw cap joints. Once attached, the sample was subjected to repeated freeze-pump-thaw cycles to remove any unwanted gases, a process known as degassing. A quantity of vapour, of the order of 1 to 2 Torr, was then transferred to the cell. Samples of low vapour pressure, including $W(CO)_6$, were placed directly into the non-isolated cell reservoir, where they were then outgassed. In all static pyrolysis experiments, approximately 10 Torr of degassed SF_6 was introduced into the cell as the photosensitiser. After the required components had been added, the cell was removed from the line and, in order to provide a means of reference, analysed using FT-IR spectroscopy.

2.5.3 Pyrolysis Set-up

For successful IR LPHP the cell had to be positioned such that the ZnSe window was perpendicular to the beam. After selecting the power and aperture setting the cell was appropriately placed approximately 20 mm from the laser. Several procedures were implemented prior to an IR LPHP experiment in order to eliminate any associated hazards:

- a firebrick was placed behind the cell to absorb the emerging beam;
- protective eyewear, impermeable to infrared radiation, was worn while operating the CO_2 laser;

- an interlock system was fitted to all entrances of the laboratory in which the laser was housed. Laser operation was possible only if all entries were sealed.

The contents of the pyrolysis cell were exposed to the output of the CO_2 laser for a period of between one and two minutes, at a power level sufficiently high enough to induce pyrolysis. The progress of reaction, in particular the decrease in starting material, was monitored *ex situ* using FT-IR spectroscopy. When required, the vapour pressure of those solid or liquid samples contained within the cell reservoir, specifically $W(CO)_6$, could be increased by gently warming the exterior of the cell with a hairdryer.

2.6 Experimental Analysis

2.6.1 Introduction

Throughout this study a number of analytical techniques were employed in order to resolve the mechanism of substrate decomposition. In the first instance, the progress and products of reaction were monitored *ex situ* using Fourier transform infrared (FT-IR) spectroscopy (refer to section 2.6.2). Product identification was confirmed with gas chromatography mass spectroscopy (GC-MS) (refer to section 2.6.3). In several systems, the proposed pyrolysis scheme predicted one or more transient species. The technique of matrix isolation spectroscopy, which is described in section 2.7, was used to detect such species. It was possible to generate and observe transient species *in situ* using IR laser powered homogeneous pyrolysis – tuneable diode laser spectroscopy (IR LPHP–TDLS). This technique is outlined in section 2.8.

2.6.2 Fourier Transform Infrared Spectroscopy

Fourier transform infrared (FT-IR) spectroscopy provides a convenient, non-invasive method by which molecules (with a permanent electric dipole or a vibration that induces a change in the electric dipole moment) can be detected and characterised. The FT-IR spectrometer uses a Michelson interferometer to produce an interferogram representing the variation in intensity with path difference. The variation in intensity with wavelength, or the absorption spectrum, can be obtained by Fourier transformation of this interferogram. If a sample is placed in the path of an infrared source, it will absorb at a particular frequency, thereby reducing that component of the composite signal that passes through the Michelson interferometer. Subsequent Fourier transformation affords the absorption spectrum of the sample [14, 15].

Fourier transform infrared spectroscopy has a number of advantages over conventional infrared spectroscopy, all of which can be attributed to the Michelson interferometer:

- all frequencies emitted from the source fall on the detector all of the time. Known as the multiplex, or Fellgett advantage, this effects an increase in sensitivity [14];

- greater acquisition speed, which is particularly useful for recording spectra of short-lived species;

- spectra can be manipulated mathematically; it is possible to subtract certain components *e.g.* water, from the spectrum;

- high level of accuracy owing to the continuous calibration by the internal helium neon (HeNe) laser;

- the entrance aperture is circular and so allows the source radiation to pass more efficiently than in conventional spectrometers, where a slit is employed. This is known as the Jacquinot, or étendu, advantage.

All infrared spectra were recorded using a Digilab FTS 60 Fourier transform infrared spectrometer at a resolution of 1 cm^{-1}. In order to inhibit peaks attributed to atmospheric CO_2 or water, a dry nitrogen purge was attached to the sample entry chamber of the spectrometer.

2.6.3 Gas Chromatography Mass Spectroscopy

Gas chromatography is an analytical technique used to separate composite mixtures. The sample components are carried through the chromatographic column (stationary phase) by the carrier gas (mobile phase), each component partitioning between the stationary and mobile phase. The partitioning of a component between these phases is an equilibrium process that can be described by the distribution coefficient, K_D, of that component. If the separation of two components is to occur (*i.e*. if they are to have different retention times), the distribution coefficient of each must differ [16].

Temperature-programmed gas chromatography, where the temperature of the column is increased during the separation, allows one to separate those higher boiling components from the more volatile solutes without having to wait an immoderate length of time for the

former to elute. As the temperature of the column is increased those compounds that have condensed on the stationary phase are vaporised according to their respective boiling points and migrate down the column. Conversely, by lowering the temperature of the column it is possible to separate those components that possess overlapping retention times at higher temperature. Temperature-programmed gas chromatography was utilised in all GC-MS experiments performed during the course of this investigation.

GC-MS data was recorded using a Hewlett Packard 6890 gas chromatograph coupled with a Hewlett Packard 5973 mass selective detector (MSD). The gas chromatograph employed a cross-linked phenyl methyl siloxane gum capillary column with an internal diameter of 0.25 mm and length 29.2 m. The film thickness was 0.25 μm. A GS GasPro column of unidentified film thickness, with an internal diameter of 0.32 mm and length 30 m was used for those systems where the expected decomposition products were of low molecular weight. In all experiments the carrier gas was helium.

The mass selective detector recorded spectra at a rate of three scans per second over the mass range 15 to 400 AMU. To ensure that the normal operating conditions were not compromised, the split ratio (the ratio of sample injected to that passing the MSD) was maintained at 30:1 for all experiments. The sum of all ion abundances for each scan, known as the total ion chromatogram (TIC), was instrumental in detecting species that were in such low quantities to not be observed with FT-IR spectroscopy. Consequently, the elucidation of an accurate pyrolysis scheme was greatly aided through GC-MS.

GC-MS samples were extracted from the pyrolysis cell through a Shimadzu 2920 rubber injection plug with a gas tight lockable syringe. A volume of pyrolysis gas of the order of

2.5 mL was withdrawn prior to locking the syringe; the contents were then compressed to approximately 0.1 mL – equating to the gas volume at atmospheric pressure. The sample was then injected into the GC-MS inlet valve. This technique, although considerably more quantitative than other methods (*e.g.* dissolving the products in a suitable GC solvent), could only be used to evaluate relative product yields – by comparing peak heights. The absolute product yield could not be ascertained. The pyrolysis products were, in general, relatively simple compounds, and as such identified on the basis of mass spectroscopy using the Chemstation database. An acceptable product match was of the order of ≥ 90 %.

2.7 Matrix Isolation Spectroscopy

2.7.1 Introduction

Matrix isolation spectroscopy is a technique that permits the isolation and characterisation of a short-lived reactive species and has been utilised extensively in this investigation. The lifetime of a reactive moiety may be prolonged considerably by inhibiting further reaction with another species. This concept is the underlying principle behind the technique of matrix isolation. The reactive species, or guest molecule, is trapped in sites within a rigid host material, and as such is prevented from diffusing to, and consequently reacting with, another species. The host material comprises a crystalline solid or glass formed by freezing a liquid or solidifying a gas, typically the latter, at very low temperature [17, 18]. In addition, these low temperatures inhibit molecular decomposition of the reactive species.

The matrix materials of early investigations were solvent mixtures that froze to clear glasses at liquid nitrogen temperature (77 K) [19, 20]. It was found that a mixture of ether,

isopentane and ethanol (ratio of 5 : 5 : 2), known as EPA formed a glass at this temperature that was transparent throughout the UV-visible region. While EPA was (and still is) used extensively as a matrix material it has a significant disadvantage in that it is not always chemically inert to very reactive species. Moreover, low temperature solvent glasses are not particularly transparent to infrared radiation, thereby precluding the use of infrared spectroscopy, an analytical technique that yields significantly more structural data about a trapped species than UV-visible spectroscopy.

The use of solidified inert gases as trapping media was contrived in the 1950's by Whittle and co-workers [21], and had several advantages over low temperature solvent glasses; specifically, chemical inertness, transparency to a wide region of the electromagnetic region (including the infrared) and a tendency to form clear glasses. Moreover, perturbation of the reactive species was kept to a minimum, the ground state of most species perturbed less than 1 % from their gas phase levels [22].

To create a rigid matrix from an inert gas required a significantly lower temperature than had been used in the past. Whittle and co-workers were initially limited to xenon matrices, as the lowest temperature obtained in their laboratory was 66 K, too high to condense Kr, Ar or Ne. Subsequent developments in cryostat technology, utilising liquid H_2 or He coolants, realised temperatures of the order of 4 to 20 K, low enough to maintain a rigid matrix of any of the inert gases, and in fact, a number of other more reactive matrix materials, including CO, CH_4 and SF_6. The closed-cycle helium refrigerator, which is more convenient to use, has largely superseded the liquid refrigerant. It does not have any of the associated hazards: H_2 is highly flammable, while He, having a very low heat of vaporisation, requires only a small amount of heat to generate a large volume of gas.

The reactive species can be generated and trapped in the low temperature matrix in a number of ways:

- the reactive species is generated in the gas phase externally through irradiation of a suitable precursor, followed by deposition in a stream of the host gas, *e.g.* the formation of NX_3 in discharges through $Ar/N_2/X_2$ mixtures [23];

- the stable precursor is co-deposited with the matrix material and then irradiated with one of either UV light, an electron beam or X-rays, *e.g.* the formation of $Cr(CO)_5$ in matrices from the photolysis of $Cr(CO)_6$ [24];

- two streams of material, one of which incorporates the matrix material is condensed onto the cryogenically cooled window, whereupon reaction occurs yielding the short lived species;

- annealing the matrix (warming the matrix to a softening point) such that the guest species, which has been generated by one of those three methods listed above, diffuses to a location in the matrix where further reaction occurs, either with a reactive host or another guest species.

As a technique by which products of an intermediate nature can be both entrapped and characterised, matrix isolation spectroscopy is unsurpassed. Many of the difficulties that were encountered in early matrix isolation experiments have been resolved affording a robust method ideally suited to verifying a proposed decomposition or pyrolysis mechanism.

2.7.2 Procedure

The matrix isolation assembly, illustrated in Figures 2.4 and 2.5, was designed and built by Dr N. D. Renner. The assembly was constructed such that a reactive species, generated externally through the IR LPHP or conventional hot-walled pyrolysis of an appropriate precursor, would rapidly co-deposit with the matrix material on the cold sample holder. A two-stage closed cycle helium refrigerator, the second stage (heat station) of which was in direct contact with the sample holder (a copper block), maintained a temperature of between 15 and 20 K. All matrices were collected at this temperature.

The matrix cold cell (the cavity enclosing the cold stage and sample holder) was fitted with two valves, one of which connected to that part of the vacuum line where pyrolysis occurred (the spray-on line). The main vacuum line, to which the spray-on line linked, was connected to the second valve of the matrix cold cell. An inlet port on the spray-on line, fitted with a needle valve, permitted attachment of a gas bulb containing a mixture of matrix material and degassed precursor. The matrix and precursor gas mix was prepared on the standard vacuum line, at a ratio of between 100 : 1 and 2000 : 1 (dependent on the experiment) at a pressure of at least 200 Torr. The method by which decomposition was initiated determined the matrix gas used, IR LPHP experiments employed SF_6, while conventional hot-walled pyrolysis used Ar as the host gas. Prior to experiment the entire assembly (excluding the gas bulb) was evacuated using a rotary (Edwards E2M5 two stage) and oil diffusion (Edwards EO2) pump. Having attained a sufficient vacuum, the valve connecting the spray-on manifold to the main vacuum line (V1 in Figure 2.4) was closed and a pressure of source gas (of the order of 0.15 Torr) introduced through the needle valve.

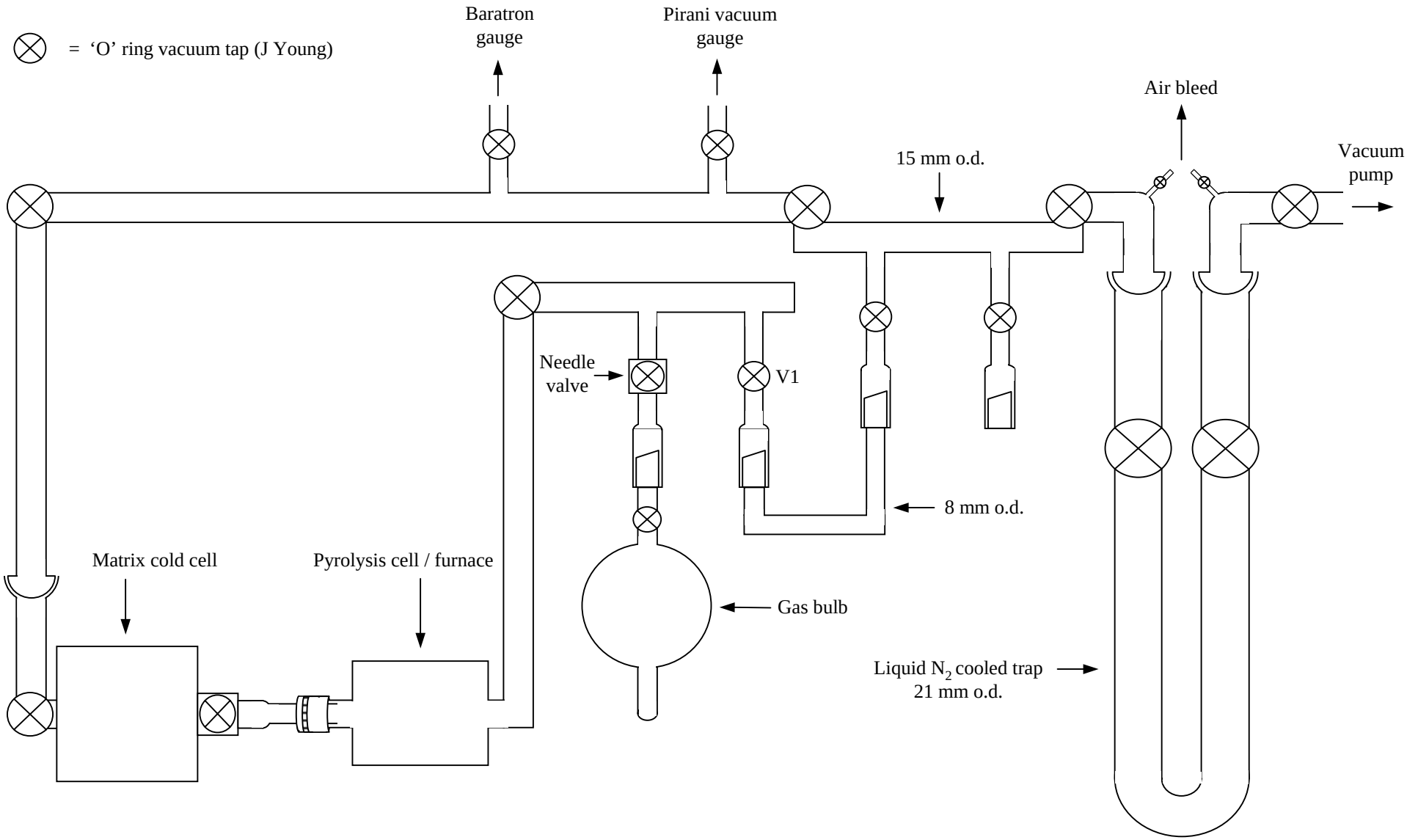

Figure 2.4 A schematic of the matrix isolation assembly

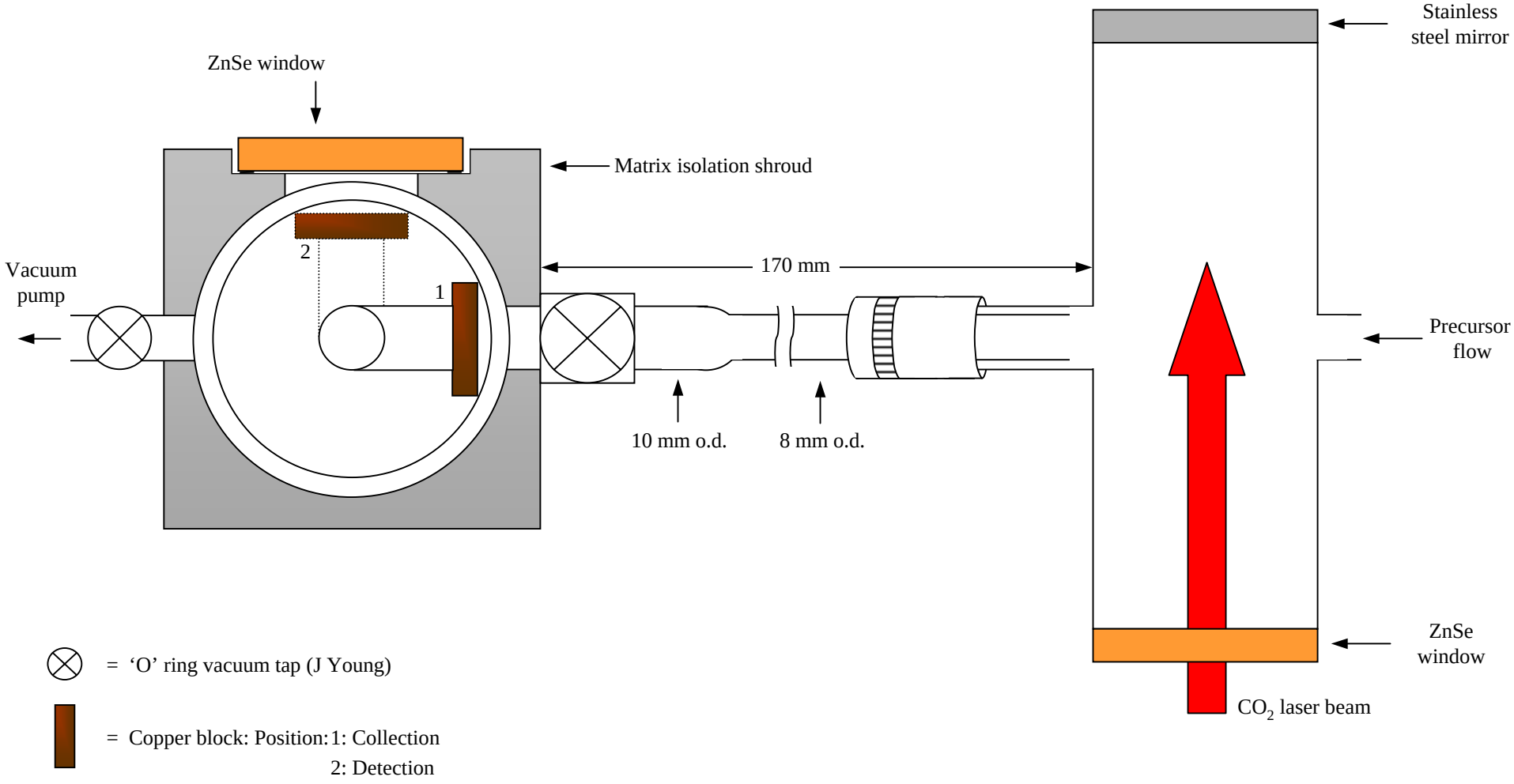

Figure 2.5 Top view of the IR LPHP matrix isolation assembly

With conventional hot-walled pyrolysis the precursor was decomposed in silica tube (8 mm i.d.) heated to between 673 and 1073 K (dependent on experiment) with a 300 mm long electric oven. In IR LPHP initiated decomposition laser radiation was directed at a ZnSe fronted reaction cell through which the mixture flowed. The reaction products were collected at the conductively cooled copper block within 170 mm of the pyrolysis tube or reaction cell at such a rate that an appreciable matrix was acquired. The duration over which the matrix was collected was of the order of 30 minutes when Ar matrices were collected and 0.5 minutes when SF_6 was employed, the difference in part, ascribed to their different formula weights. At the cessation of experiment the matrix cold cell was disengaged from the vacuum line and the cold stage, to which the sample holder was appended, rotated 90° to permit FT-IR analysis. The temperature of the cold sample holder was maintained at between 15 and 20 K during spectrum acquisition.

The IR LPHP matrix isolation experiment could be modified such that the path between the reaction cell and cold sample holder was restricted. By utilising a length of Pyrex with an aperture (0.5 mm) at that end adjacent to the reaction cell, an extremely short-lived species could be prevented from reaching the cold stage before reacting further. Consequently, it was possible to differentiate species based on transient lifetimes.

The utilisation of an aperture to restrict flow had the additional affect of increasing the pressure of source gas at the IR LPHP cell; an increase in the pressure of SF_6 effects an increase in the temperature that can be attained by laser irradiation. In an unmodified IR LPHP matrix isolation experiment it was found that the highest effective temperature reached when utilising aperture 1 (the highest power) was equivalent to that attained when executing a static IR LPHP experiment at aperture 12. Those compounds that required an

effective temperature greater than this were consequently not decomposed. The modification of the matrix isolation assembly, while inhibiting the collection of very short-lived species allowed the IR LPHP of those compounds that would otherwise not decompose. In experiments where the flow was restricted it was found that the total pressure at the reaction cell could be maintained at approximately 10 Torr (equivalent to the pressure in a static IR LPHP cell) by admitting 20 Torr of source gas to the spray-on line. This was effected by employing a gas bulb containing a mix of the matrix and precursor gas at a pressure of 20 Torr and introducing the entire contents to the isolated spray-on line.

2.8 IR LPHP Tuneable Diode Laser Spectroscopy

The combination of infrared laser powered homogeneous pyrolysis (IR LPHP) and tuneable diode laser spectroscopy (TDLS) provides an ideal and novel technique by which to generate and characterise the high-resolution spectra of a transient species *in situ*. In this investigation, the technique of IR LPHP–TDLS was utilised exclusively for the generation and detection of a transient moiety, specifically those substituted ketene species that ensue from the dehydrohalogenation of an appropriate acyl or diacyl chloride precursor.

The IRLP-TDLS assembly is illustrated in Figure 2.6. The transient species is generated in a specially adapted cell (the multipass cell) through IR LPHP of an appropriate precursor, and spectroscopically probed *in situ* with a diode laser source. There are numerous examples of infrared diode lasers, each capable of covering a region of the infrared spectrum of the order of 100 cm^{-1}. While most of the spectral range between 400 and 3500 cm^{-1} is covered, there are significant regions that are not; consequently, the

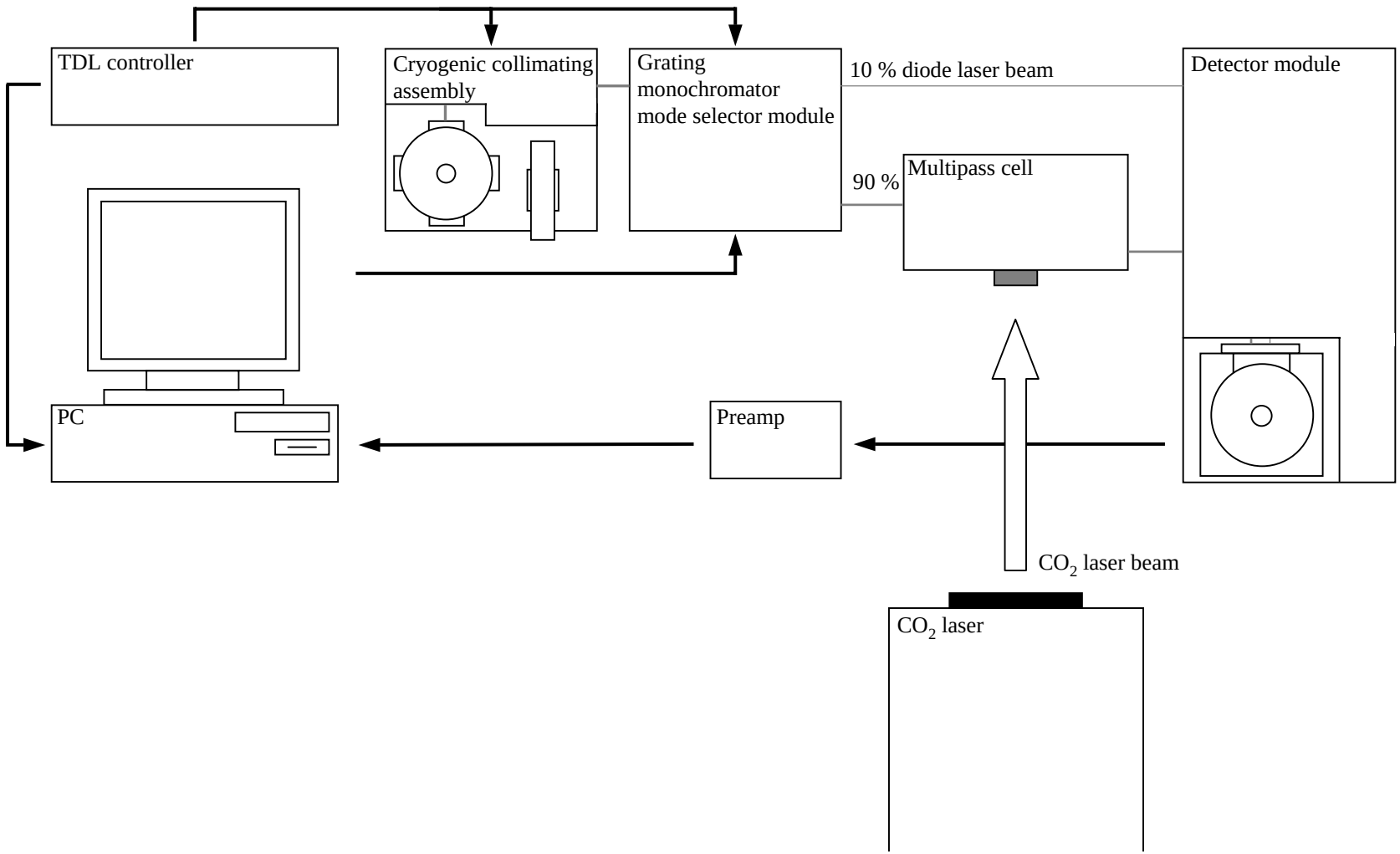

Figure 2.6 Schematic of the IR LPHP-TDLS assembly for absorption experiments

characterisation of species that absorb in that part of the spectrum affected is not possible. Diode laser emission results from the relaxation of electrons in the conduction band of a n-type semiconductor (a material comprising a dopant with excess electrons) to the holes in the valence band of a p-type semiconductor (a material comprising a dopant that can trap electrons). The frequency of the laser output mode is determined by the width of this band gap, and can be manipulated by varying the operating current or temperature of the semi-conductor material. Semiconductor materials used to emit infrared light include ternary compounds such as $Pb_{1-x}Sn_xTe$ and $Ga_{1-x}Al_xAs$; the latter is widely used in compact disc players. The promotion of electrons to the conduction band (a population inversion) can be created in a number of ways, however for the most part tuneable diode lasers employ electron injection at the p–n junction [15].

The semiconductor diode used in this investigation, was one of four available and emitted infrared light between 1950 and 2200 cm^{-1}, ideal for the detection of transient ketene type species. The frequency of the output laser mode was broadly determined by regulating the current and temperature settings with a Laser Photonics TDL controller. The maximum temperature and current allowed was of the order of 123 K and 1000 mA respectively [25]. The output laser beam was reflected off an Al collimating mirror and passed through a grating monochromator, which was used to select and isolate a discrete frequency. The beam was then split, with 90 % entering the multipass cell for signal detection and, for the purpose of referencing, the remaining 10 % relayed through a germanium etalon that could be used as an internal calibrant. The level of accuracy at which the position of absorption bands were measured in this investigation (the characterisation of high resolution spectra was not executed) was such that an internal calibrant was not required; the accuracy attained via the grating monochromator was sufficient.

The multipass cell, illustrated in Figure 2.7, was designed and built by Dr N. D. Renner. The cell was constructed such that the incoming diode beam was reflected between two adjacent gold plated mirrors, thereby increasing the effective path length to approximately 2 m. The CO_2 laser beam entered the cell perpendicular to the diode laser, through a ZnSe window located at the front of the multipass cell. IR LPHP of the cell contents (of the order of 1 Torr of precursor and 4 Torr of SF_6) was confined to the centre of the cell where the diode laser beam was focussed. This effected an increase in the probability of detecting the transient species. The output diode laser beam exited the multipass cell diagonally opposite to the point where it had entered, and passed into the detector module.

It was necessary to use a lock-in amplifier (LIA) to increase the signal to noise ratio in systems that had weak or short-lived bands. The mechanics of lock-in amplification is beyond the scope of this text; a thorough account is given in Ref [26, 27]. In contrast to standard operating conditions (where an absorption spectrum is observed), the operating principles of a LIA are such that the output signal is represented as the first derivative.

The acquisition, manipulation and analysis of spectral information was executed on an IBM compatible PC with a virtual oscilloscope that was designed and developed by Dr N. R. Hore using the LabVIEW program development application. The reader is referred to Ref. [27] for a comprehensive description of this software.

2.9 Theoretical Calculations

In the course of this investigation, it was necessary to execute a number of theoretical calculations in order to corroborate a proposed species, or pyrolysis scheme. The former

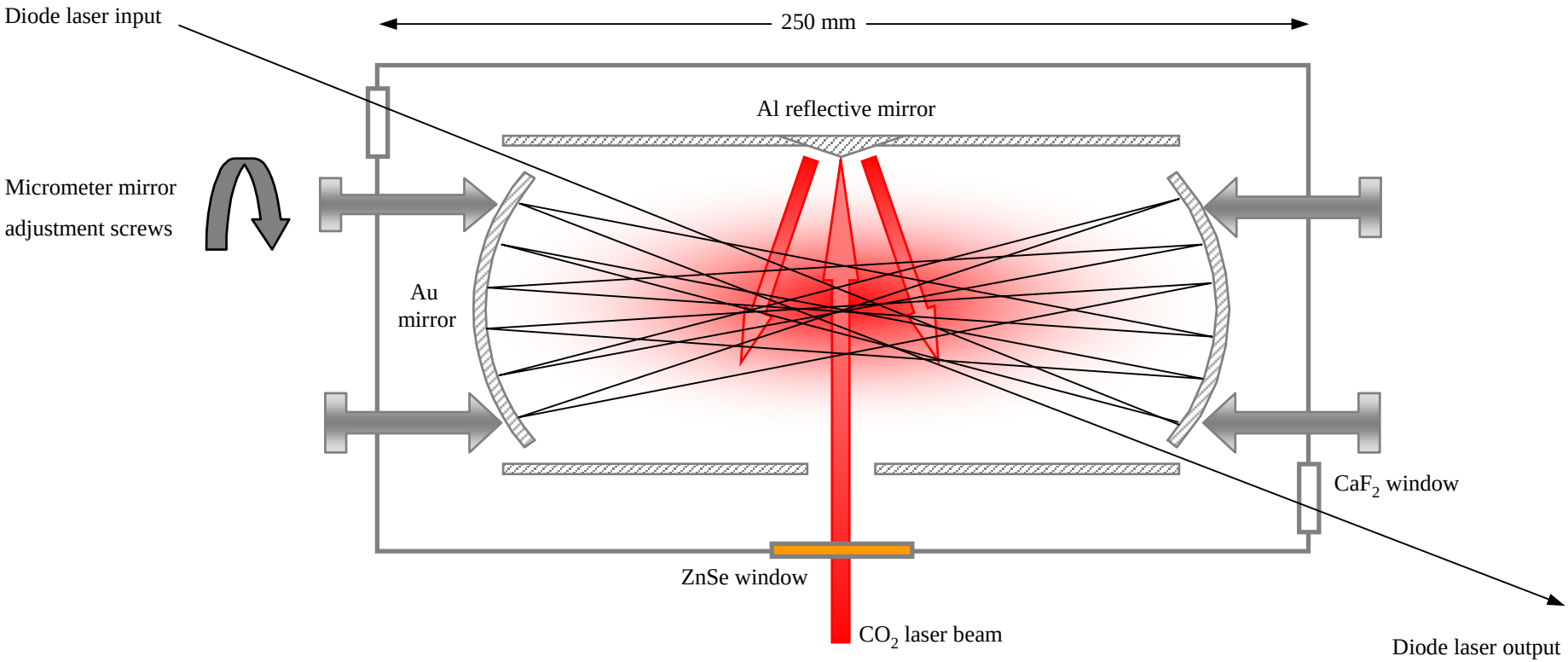

Figure 2.7 Top view of the TDL multipass cell

was realised by calculating the vibrational frequencies of the moiety in question and comparing that with the post-pyrolysis infrared spectrum. This was particularly useful for systems in which a substituted ketene intermediate was proffered. Such species possess a characteristic carbonyl stretching frequency between 2100 and 2200 cm^{-1}, the precise position of which is determined by the substituent present [28]. A proposed species was verified by comparing the observed value with that calculated. To account for anharmonicity, it was necessary to scale the calculated frequency by 0.9155 – this corresponded to the observed signal for ketene in the gas phase (2150.7 cm^{-1}) divided by the calculated value for the cumulenic stretch of ketene (2349.1 cm^{-1}).

The feasibility of a proposed pyrolysis scheme could be evaluated by determining the relative activation energies involved. For the most part, this involved calculating the activation barrier to dehydrohalogenation, the predominant decomposition route when $W(CO)_6$ was absent, and comparing this value with that of an alternate system, whose actual pyrolysis temperature (*i.e.* the laser power required to initiate decomposition) was known. It was found that theory agreed well with experiment; a system calculated to possess relatively higher activation energy required a higher decomposition temperature.

All theoretical calculations were executed on a conventional IBM compatible computer (Pentium II 200 MHz CPU) using the PC Spartan *Plus* molecular orbital program [29, 30]. While PC Spartan *Plus* provides a full range of molecular mechanics and quantum chemical methods, it was found that for the purpose of this study the PM3 semi-empirical molecular orbital method [31] would suffice. An absolute value of the activation energy of a particular reaction pathway was of little value in the present investigation; rather, the relative values of the various pathways available were of greater significance. Hettema and

co-workers have shown that among others, the PM3 semi-empirical method is not an immoderately inaccurate technique by which to calculate the relative activation energy of reaction [32]. For example, the activation energy for the decarboxylation of acetic acid was calculated using the PM3 Hamiltonian to be 368 kJ mol^{-1} – comparable to the experimentally determined values of between 271.5 – 304.2 kJ mol^{-1} [32].

PC Spartan *Plus* employs a builder function to construct reactant or product geometries that correspond to well minima on a multi-dimensional potential energy surface. All structures were located by minimising the norm of the gradient to less than 5×10^{-9} N. The geometry of a particular transition state (the lowest energy maximum) can be located by specifying critical bond lengths and angles in the starting molecular geometry in accord with the proposed mechanism. For example, the elimination of HCl across a single bond in a chlorinated organic compound involves an increase in the C–Cl and C–H bond lengths with a concomitant decrease in the distance between H and Cl. The transition state geometry is verified using frequency analysis calculations; transition states possess only one imaginary frequency that can be visually represented using PC Spartan *Plus*. The imaginary frequency corresponds to the intrinsic reaction coordinate. The intrinsic reaction coordinate is the lowest energy path between the reactant and products that passes through the desired transition state. The activation energy of reaction can be evaluated by determining the difference in energies between the reactant (or for the reverse reaction, the product) and the proposed transition state.

2.10 References

[1] C. Bordé, A. Henry and L. Henry, *Compt. Rend. Acad. Sci. Paris, Ser. B*, 1966, **262**, 1389.

[2] C. Bordé, C. Cohen and L. Henry, *Compt. Rend. Acad. Sci. Paris, Ser. B*, 1967, **265**, 267.

[3] J. Tardieu de Maliesse, *Compt. Rend. Acad. Sci. Paris, Ser. B*, 1972, **275**, 989.

[4] D. K. Russell, *Chem. Soc. Rev.*, 1990, **19**, 407.

[5] A. V. Nowak and J. L. Lyman, *J. Quant. Spectrosc. Radiat. Transfer*, 1975, **15**, 945.

[6] K. Sugawara, T. Nakanaga, H. Takeo and C. Matsumura, *Chem. Phys.*, 1989, **135**, 301.

[7] J. L. Lyman, *J. Chem. Phys.*, 1977, **67**, 1868.

[8] *Physical Properties of Inorganic Compounds,* A. L. Horvath, Ed., Arnold, London, 1975.

[9] E. A. Jones and R. T. Lagemann, *J. Chem. Phys.*, 1951, **19**, 534.

[10] G. Herzberg, *Infrared and Raman Spectra of Polyatomic Molecules,* Litton Educational, New York, 1945.

[11] S. P. Ermer, G. E. Struck, S. P. Bitler, R. Richards, R. Bau and T. C. Flood, *Organometallics*, 1993, **12**, 2634.

[12] R. F. Somerville, Ph.D. Thesis, The University of Auckland, 1987.

[13] R. Linney, *Laser Pyrolysis Techniques; Experimental Methods,* 1994.

[14] J. M. Hollas, *High Resolution Spectroscopy,* 2nd Ed, John Wiley and Sons Ltd, West Sussex, 1998.

[15] P. W. Atkins, *Physical Chemistry,* 4th Ed, Oxford University Press, Oxford, 1990.

[16] L. G. Hargis, *Analytical Chemistry Principles and Techniques,* Prentice Hall, New Jersey, 1988.

[17] *Chemistry and Physics of Matrix-Isolated Species,* L. Andrews and M. Moskovits, Eds., Elsevier Science, Amsterdam, 1989.

[18] I. R. Dunkin, *Matrix-Isolation Techniques,* Oxford University Press, Oxford, 1998.

[19] G. N. Lewis, D. Lipkin and T. T. Magel, *J. Am. Chem. Soc.*, 1944, **66**, 1579.

[20] G. N. Lewis and D. Lipkin, *J. Am. Chem. Soc.*, 1942, **64**, 2801.

[21] E. Whittle, D. A. Dows and G. C. Pimentel, *J. Chem. Phys.*, 1954, **22**, 1943.

[22] M. E. Jacox, *J. Mol. Spec.*, 1985, **113**, 286.

[23] C. K. Kohlmiller and L. Andrews, *Inorg. Chem.*, 1982, **21**, 1519.

[24] R. N. Perutz and J. J. Turner, *J. Am. Chem. Soc.*, 1975, **97**, 4791.

[25] Laser Photonics Inc., Tuneable Diode Laser Test Report, 1996.

[26] Stanford Research Systems, *SR810 DSP Lock-in Amplifier Operating Manual and Programming Reference,* Sunnyvale, CA, 1993.

[27] N. R. Hore, Ph.D. Thesis, The University of Auckland, 1999.

[28] M. A. McAllister and T. T. Tidwell, *Can. J. Chem.*, 1994, **72**, 882.

[29] Wavefunction Inc., *PC Spartan Plus Tutorial and User's Guide,* Irvine, CA, 1997.

[30] Wavefunction Inc., PC Spartan *Plus*, Irvine, CA, 1997.

[31] J. J. P. Stewart, *J. Computer Aided Molecular Design*, 1990, **4**, 1.

[32] H. Hettema, N. R. Hore, N. D. Renner and D. K. Russell, *Aust. J. Chem.*, 1997, **50**, 363.

Chapter Three

SELECTED CHLORINATED COMPOUNDS

3.1 Introduction

The IR LPHP of $W(CO)_6$ in the gas phase leads to unsaturated $W(CO)_x$ species; these have been shown to be very effective and selective abstractors of chlorine atoms from a wide range of organic substrates, and offer a clean and low energy route into gas phase organic radical chemistry [1]. The principal aim of this study is to illustrate the various reactions of a particular organic radical by investigating the pyrolysis of selected organochlorine precursors in the presence of $W(CO)_6$. The chemistry of these organic radical species is dominated by radical-radical and radical-molecule reactions; namely, combination, disproportionation, addition and abstraction.

A comprehensive investigation demands that the mechanism pertaining to pyrolysis of the organochlorine precursor in the absence of $W(CO)_6$ be understood. The decomposition of an organochlorine compound is initiated by dehydrochlorination or C–Cl fission, the latter effecting formation of an organic radical. The molecular β-elimination of HCl from an organochlorine species will afford the corresponding olefin through formation of an additional carbon-carbon bond; conversely, in organochlorine compounds that do not possess a β-hydrogen, decomposition proceeds through α-elimination of HCl yielding a carbene moiety [2, 3].

A number of techniques, including photolysis and conventional pyrolysis, have been used to initiate decomposition of an organochlorine species; all have associated drawbacks. Photolysis is limited to compounds that absorb radiation directly, while conventional pyrolysis, unlike IR LPHP, is not homogeneous; consequently, reaction is complicated by heterogeneous contributions. In this investigation, the gas phase decomposition of

2-chloropropane, 2-chloro-2-methylpropane, *E*-1,2-dichloroethene, propargyl chloride (3-chloro-1-propyne), chloroacetonitrile, benzyl chloride ((chloromethyl)benzene), α,α'-dichloro-*o*-xylene (1,2-bis(chloromethyl)benzene) and chloroacetic acid, in the presence and absence of $W(CO)_6$, was initiated by IR LPHP and the products characterised using a combination of FT-IR, GC-MS and matrix isolation spectroscopy.

3.2 2-Chloropropane

The IR LPHP of 2-chloropropane has been investigated by Kubat and Pola [4], with the conclusion that reaction proceeds through the molecular elimination of HCl yielding propene. In the present work, a sample of 2-chloropropane and $W(CO)_6$ was exposed to low laser power (*i.e.* temperature); the most significant products were propene, propane, and 2,3-dimethylbutane. These results are consistent with the selective abstraction of Cl to yield the isopropyl radical, which either combines to 2,3-dimethylbutane or undergoes disproportionation to propane and propene.

The disproportionation to combination ratio of isopropyl, which is reported to be in the range of 0.54 to 0.69 [5-8], predicts formation of propane and propene in preference to 2,3-dimethylbutane. In this study, propane was detected at a level slightly greater than that of the combination product, while the level of propene exceeded that of propane. It is evident from these results that an alternative pathway to propene exists, most probably involving molecular dehydrochlorination of starting material; certainly, the decomposition of 2-chloropropane alone commenced at a temperature comparable to that of the alkyl chloride in the presence of $W(CO)_6$.

3.3 2-Chloro-2-Methylpropane

The thermolysis of 2-chloro-2-methylpropane in incident and reflected shock waves has been investigated by Lifshitz [9], with the conclusion that reaction proceeds through molecular elimination of HCl to form 2-methyl-1-propene. In the present study, a sample of 2-chloro-2-methylpropane alone was exposed to the output of a continuous wave (CW) CO_2 laser at low laser power with comparable results.

On co-pyrolysis with $W(CO)_6$ at a similar temperature, the major products were 2-methyl-1-propene, 2,4,4-trimethyl-1-pentene, 2,4,4-trimethyl-2-pentene, 2,2,4,6,6-pentamethyl-3-heptene and 3-methylene-2,2,6,6-tetramethylheptane; isobutane was detected in trace amount. These results are consistent with the selective abstraction of Cl to yield the tertiary butyl radical; this can undergo addition reactions (with an olefin) or disproportionation to 2-methyl-1-propene and isobutane. The absence of 2,2,3,3-tetramethylbutane precludes combination, which given the low yield of isobutane, is consistent with the reported disproportionation to combination ratio of 2.32 of the tertiary butyl radical [5].

2-methyl-1-propene was detected at a level significantly greater than that of isobutane, suggesting an alternative formation mechanism, probably involving dehydrochlorination of starting material. Certainly, the decomposition of 2-chloro-2-methylpropane alone, like 2-chloropropane, commenced at a temperature comparable to that of the alkyl chloride in the presence of $W(CO)_6$.

Addition of the tertiary butyl radical to the least substituted sp^2 carbon atom of 2-methyl-1-propene (followed by homolytic fragmentation of a single C_β–H bond in the resulting

addend radical) will afford 2,4,4-trimethyl-1-pentene or 2,4,4-trimethyl-2-pentene. There are a total of eight C_β–H bonds in the addend radical; homolytic cleavage of any one of six (which are equivalent) will yield 2,4,4-trimethyl-1-pentene, while homolysis of any one of the remaining two (which are also equivalent) will afford 2,4,4-trimethyl-2-pentene. Consequently, the former is expected at a greater yield than that of the latter; in this study, 2,4,4-trimethyl-2-pentene was detected at a level considerably less than that of 2,4,4-trimethyl-1-pentene.

In a manner analogous to the formation of 2,4,4-trimethyl-1-pentene and 2,4,4-trimethyl-2-pentene, addition of the tertiary butyl radical to the least substituted sp^2 carbon of the former (followed by homolytic cleavage of a C_β–H bond in the resulting addend radical) will afford 2,2,4,6,6-pentamethyl-3-heptene or 3-methylene-2,2,6,6-tetramethylheptane. In contrast to the addend radical effected from addition of the tertiary butyl radical to 2-methyl-1-propene, this addend radical has a total of seven C_β–H bonds of which homolytic cleavage of any one of four (which are equivalent) will generate 2,2,4,6,6-pentamethyl-3-heptene; scission of any one of the remaining three (which are also equivalent) will afford 3-methylene-2,2,6,6-tetramethyl-heptane. As a result, the yield of each is expected to be similar; in this investigation, 2,2,4,6,6-pentamethyl-3-heptene was detected at a level comparable to that of the latter.

There was no evidence to indicate addition of the tertiary butyl radical to 2,4,4-trimethyl-2-pentene. This is consistent with the relative population of each of the primary addition products; the yield of 2,4,4-trimethyl-2-pentene was less than that of 2,4,4-trimethyl-1-pentene. A proposed pyrolysis scheme for 2-chloro-2-methylpropane with $W(CO)_6$ is illustrated in Figure 3.1.

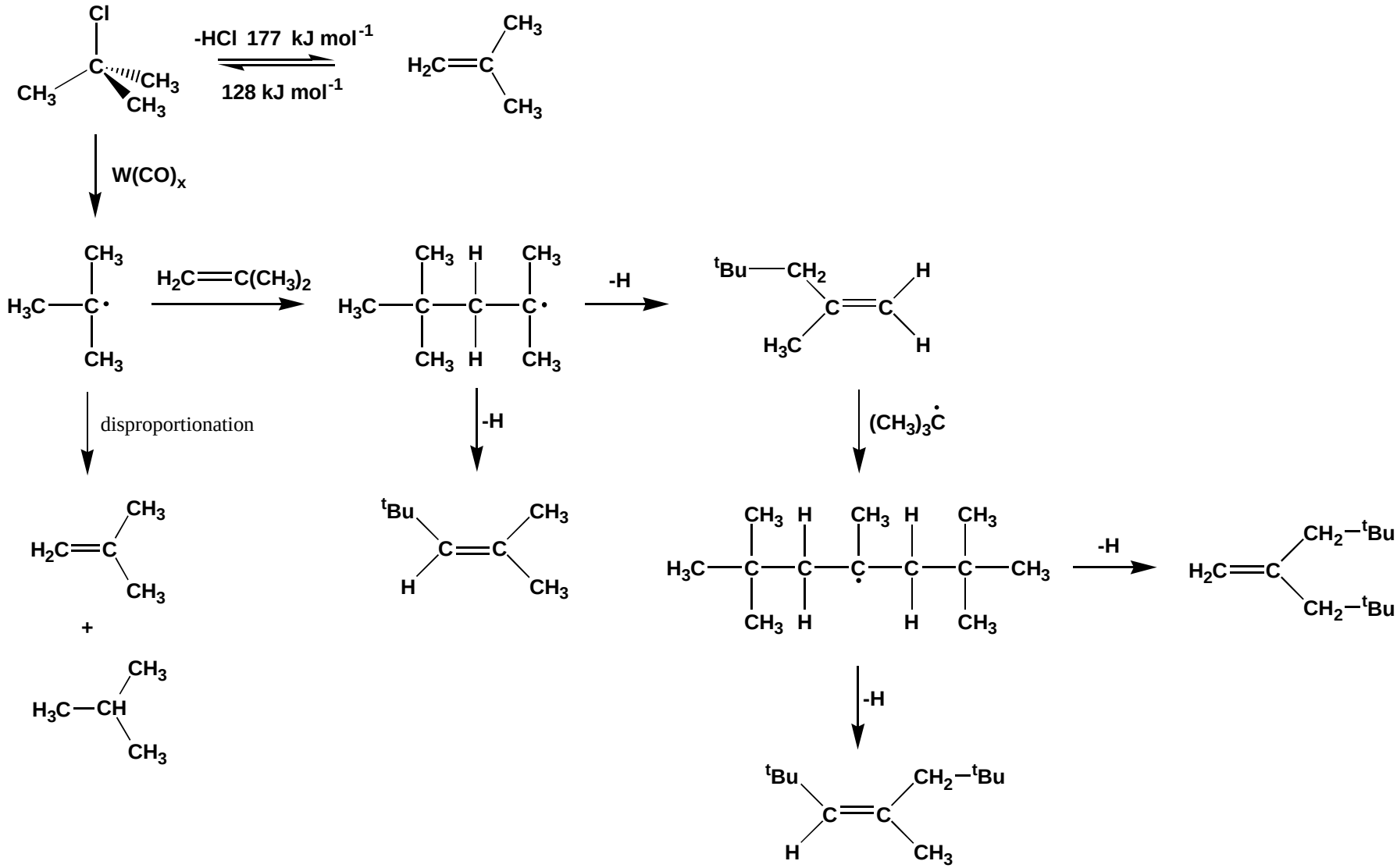

Figure 3.1 A proposed scheme for 2-chloro-2-methylpropane and $W(CO)_6$ IR LPHP

3.4 E-1,2-Dichloroethene

The IR LPHP of *E*-1,2-dichloroethene has been investigated by Kubat and Pola [4]; pyrolysis at low temperature leads to *E*-*Z* isomerisation, which is succeeded at higher laser power (*i.e.* temperature) by dehydrochlorination to form chloroacetylene. A moderate amount of acetylene was observed and ascribed to the elimination of molecular chlorine. The isomerisation of *E*- and *Z*-1,2-dichloroethene has been extensively studied by several other workers [10-12].

In the present investigation, a mixture of SF_6 and *E*-1,2-dichloroethene was exposed to the output of a CW CO_2 laser at a power level so as to promote only isomerisation, producing an approximately equimolar mixture of the *E* and *Z* isomers. A small quantity of outgassed $W(CO)_6$ was then admitted to the reaction cell, and continued irradiation of the gaseous contents at a level insufficient for isomerisation led to decay of IR features of the two isomers at different rates. The first-order kinetic plots, which are illustrated in Figure 3.2, are consistent with reactions whose activation energies differ by the known zero point energy difference of 1840 ± 380 J mol^{-1} [10], and an effective temperature of 650 ± 150 K. This 'kinetic isomer effect' suggests that loss reactions of the two isomers involve Cl abstraction pathways whose transition states differ little in energy.

The stable products derived from the pyrolysis of *E*-and *Z*-1,2-dichloroethene and $W(CO)_6$ were identified using FT-IR and GC-MS spectroscopy as chloroethene, ethylene, benzene and acetylene, the latter observed in only trace amount. There were no peaks in the post-pyrolysis infrared spectrum that could be attributed to chloroacetylene or HCl. These

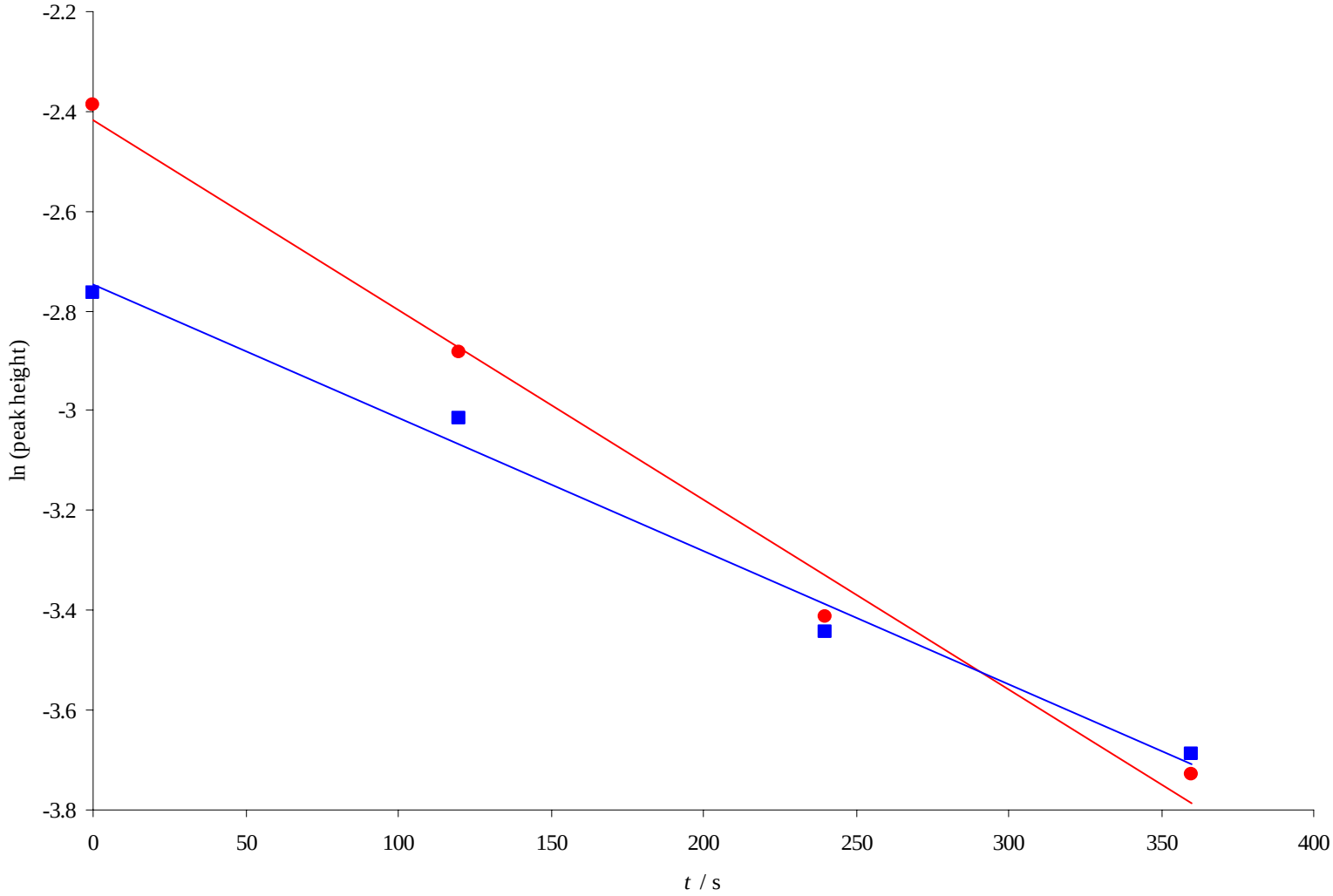

Figure 3.2 First-order kinetic plots for the decay of *E*-1,2-$C_2H_2Cl_2$ (—) and *Z*-1,2-$C_2H_2Cl_2$ (—) on laser pyrolysis in the presence of $W(CO)_6$

results are consistent with a mechanism involving the 2-chloroethenyl radical, the species effected through the abstraction of atomic chlorine from starting material.

The transfer of atomic hydrogen to an alkyl or alkenyl radical (of which 2-chloroethenyl is an example) is the most common abstraction reaction [13], and will account for the production of chloroethene. While the elimination of molecular chlorine from starting material will account for the formation of acetylene at a higher temperature in the absence of $W(CO)_6$, it can be discounted in the present investigation as pyrolysis was initiated at a significantly lower temperature. Presumably, the production of acetylene is, in part, attributable to homolytic fragmentation of the 2-chloroethenyl radical through cleavage of the C–Cl bond.

The intensity of absorbance bands ascribed to ethylene and benzene was found to increase at the expense of those assigned to chloroethene as the duration of pyrolysis was extended; this is consistent with a mechanism involving the selective abstraction of atomic chlorine from chloroethene to yield the vinyl radical. The disproportionation of vinyl radical, while accounting for the production of ethylene (and acetylene), can be discounted; the absence of 1,3-butadiene (the combination product) is not consistent with the reported disproportionation to combination ratio of the vinyl radical, namely 0.22 [14]. It is possible to rationalise this result in terms of the radical concentration. The population of vinyl radicals as a proportion of the total population is expected to be relatively low (vinyl radicals are effected through secondary reaction); consequently, the probability of collision and, by corollary reaction, is lowered. An alternative mechanism, in which the vinyl radical abstracts atomic hydrogen, may account for the formation of ethylene. Homolytic

fragmentation of the vinyl radical through cleavage of the C–H bond will effect the production of acetylene.

The level of acetylene and benzene effected from the pyrolysis of *E*-1,2-dichloroethene in the presence of $W(CO)_6$ is ostensibly inconsistent with that expected; this can be rationalised on the basis of a mechanism involving the trimerisation of acetylene to benzene, a process well known to be catalysed by transition metals [15-20]. The intensity of absorbance bands ascribed to acetylene was not observed to vary significantly with the duration of pyrolysis, suggesting that the mechanism responsible for production, specifically homolysis of 2-chloroethenyl (C–Cl bond scission) or vinyl (C–H bond scission), was approximately equivalent to that associated with depletion. A proposed scheme for *E*-1,2-dichloroethene IR LPHP in the presence of $W(CO)_6$ is illustrated in Figure 3.3.

3.5 Propargyl Chloride

The thermal isomerisation and decomposition of propargyl chloride (3-chloro-1-propyne) has been extensively studied using shock tube techniques [21-24] in the light of its role in the formation of the propargyl radical (an intermediate recognised in the production of benzene in fuel-rich systems) through homolysis of the C–Cl bond. In all cases, scission of the C–Cl bond competes with molecular elimination of HCl with a branching ratio that is dependent on the temperature [21-24]. Kumaran and co-workers have reported that the elimination of HCl from propargyl chloride dominates at $T < 1455$ K [24], while Kern and co-workers have derived a branching ratio (HCl elimination to C–Cl fission) of 0.86 : 0.14

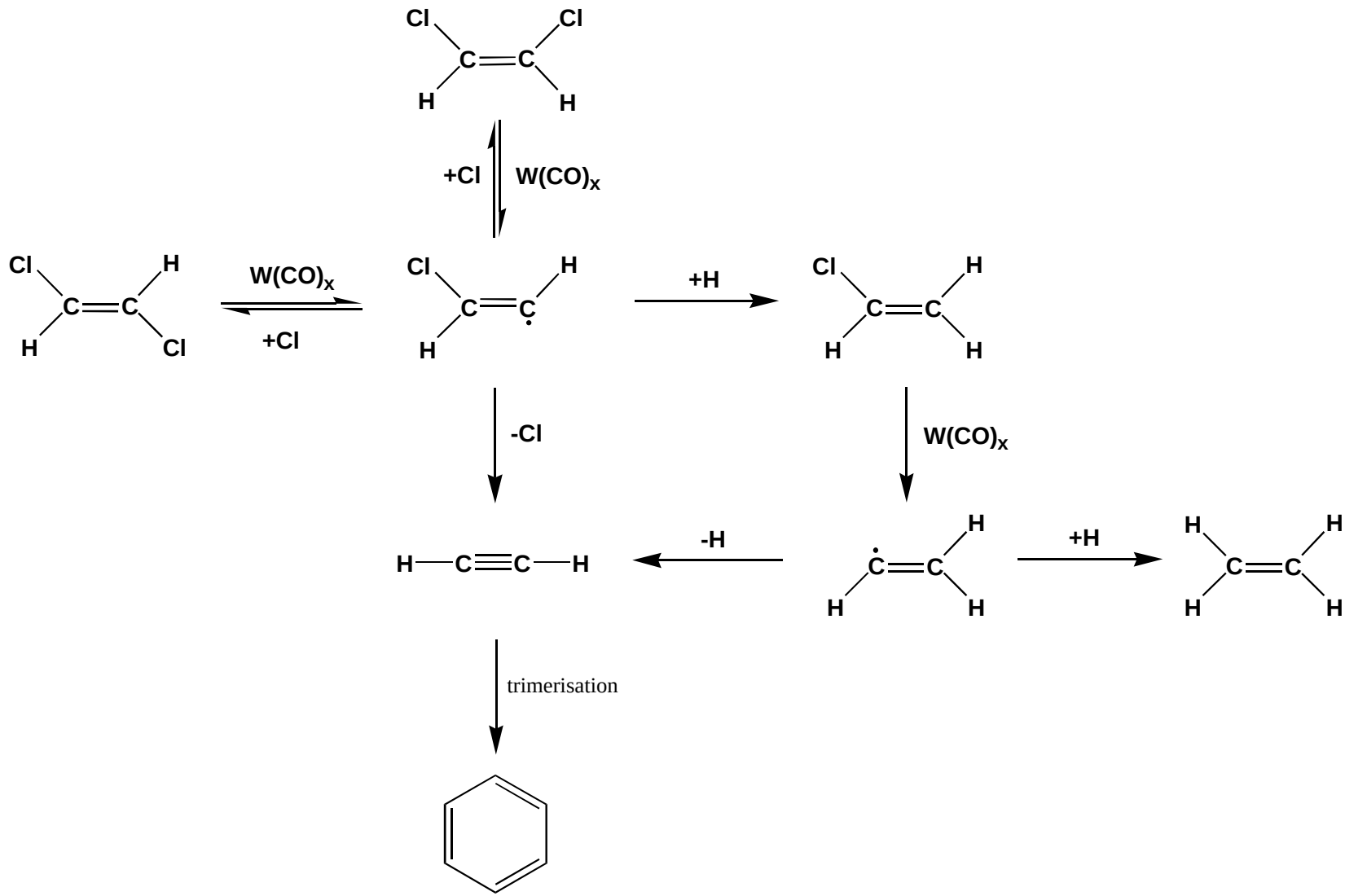

Figure 3.3 A proposed scheme for *E*-1,2-dichloroethene and $W(CO)_6$ IR LPHP

at 1350 K ≤ T ≤ 1700 K [21]. It is proposed that molecular dehydrochlorination will effect the formation of singlet cyclopropenylidene [21, 22], the predicted global minimum on the C_3H_2 potential energy hypersurface [25]. The subsequent insertion of singlet cyclopropenylidene into C–H bonds and addition to multiple bonds is postulated to account for the formation of C_2H_2, C_4H_2 and C_6H_2, the predominant products observed following thermolysis of propargyl chloride [21, 22].

In contrast, the thermolysis of propargyl chloride in the presence of sodium vapour at 623 K ≤ T ≤ 673 K is reported to effect formation of C_3H_3 exclusively, through selective abstraction of atomic chlorine [26]. While combination of C_3H_3, of which H–C≡C–CH_2· (2-propynyl) is the preferred constitutional isomer [27, 28], was expected to yield 1,5-hexadiyne, and to a lesser extent 1,2,4,5-hexatetraene and 1,2-hexadien-5-yne, the major products were in fact benzene and 1,3-hexadien-5-yne. In fact, the yield of 1,5-hexadiyne was significantly lower than all other C_6H_6 isomers; this suggested that chemically activated 1,5-hexadiyne expeditiously rearranged to 1,3-hexadien-5-yne or benzene. Alternatively, rearrangement of 2-propynyl prior to combination would account for the low yield of 1,5-hexadiyne [26].

The photolysis of propargyl chloride has been studied by a number of workers [29-36], with an express focus on the initial decomposition step, specifically the elimination of HCl or C–Cl bond fission. In all cases, it was concluded that the predominant dissociation channel, in contrast to that pertaining to thermolysis, is C–Cl bond fission with a minor channel generating HCl and C_3H_2 fragments. Lee and Lin [36] have reported a branching ratio (H–Cl elimination to C–Cl fission) of 0.16 : 0.84, which is in marked contrast to that derived by Kern and co-workers from the thermolysis of propargyl chloride [21].

In the present investigation, a sample of propargyl chloride was exposed to the output of a CW CO_2 laser in the absence and presence of $W(CO)_6$. The most significant product observed following the pyrolysis of propargyl chloride in the absence of $W(CO)_6$ and at lower powers (*i.e.* temperature) was 1-chloro-1-propyne, which is consistent with isomerisation of the starting material. In contrast to earlier shock tube studies [21-24], there was no evidence to indicate formation of 1-chloro-1,2-propadiene (chloroallene); 3-chlorocyclopropene, another C_3H_3Cl isomer, was not detected in this investigation. At a slightly elevated temperature, the isomerisation of propargyl chloride was followed by the molecular elimination of HCl to yield C_3H_2; homolytic fragmentation of the C–Cl bond, which effected the formation of C_3H_3, occurred to a lesser extent.

The most significant pyrolysis product at a higher temperature in the absence of $W(CO)_6$ was chlorobenzene, and is ascribed to intermolecular insertion of the divalent carbon of C_3H_2 (specifically, singlet cyclopropenylidene) into the acetylenic or saturated C–H bonds of propargyl chloride, with rearrangement of the resultant addend. Intermolecular insertion of singlet cyclopropenylidene into the saturated C–H bonds of 1-chloro-1-propyne will also yield chlorobenzene, following rearrangement of the vibrationally excited intermediate.

Intramolecular reaction of cyclopropenylidene can be discounted; insertion of the divalent carbon into the C_γ–H bond is not possible, while the instability of the olefinic species derived from insertion at the C_β–H bond will ostensibly prohibit its formation. At very high temperatures, the absorbance band ascribed to benzene intensified at the expense of those assigned to chlorobenzene; this is consistent with homolysis of the C–Cl bond in the latter to yield the phenyl radical, which will abstract atomic hydrogen to form benzene.

The formation of propyne, 1,5-hexadiyne, 1,2-hexadien-5-yne, 1,2,4,5-hexatetraene and benzene, which were detected at a modest level following the pyrolysis of propargyl chloride in the absence of $W(CO)_6$, is consistent with C–Cl fission to yield C_3H_3. The propargyl radical will yield propyne through the abstraction of atomic hydrogen, while C_3H_3 combination will lead to the three activated isomers of C_6H_6: 1,5-hexadiyne, 1,2-hexadien-5-yne and 1,2,4,5-hexatetraene. These products are consistent respectively, with head-to-head, head-to-tail and tail-to-tail collision between two propargyl radicals, followed by deactivation of the resulting addend. Presumably, rearrangement of each of the vibrationally excited C_6H_6 isomers will afford benzene exclusively; there was no evidence to indicate formation of 1,3-hexadien-5-yne, which was observed and ascribed by Alkemade and Homann, to rearrangement of the C_6H_6 isomers [26]. At a higher power, the peak assigned to benzene intensified at the expense of those ascribed to each of the three C_6H_6 isomers, suggesting that rearrangement will predominate at elevated temperature. On co-pyrolysis with $W(CO)_6$ at a much lower temperature, propyne, 1,5-hexadiyne, 1,2-hexadien-5-yne, 1,2,4,5-hexatetraene and benzene were the only observed products; this indicates exclusive formation of C_3H_3 through the selective abstraction of atomic chlorine from starting material.

The formation of acetylene and 1-buten-3-yne, which were observed at a modest level in this investigation, has been ascribed by Kern and co-workers (who also reported these products) to intermolecular insertion of cyclopropenylidene at the acetylenic C–H bond of propyne with further rearrangement and fragmentation of the resultant addend [22]. The insertion of cyclopropenylidene into the saturated C–H bonds of propyne with subsequent fragmentation of the resulting intermediate will effect the formation of three acetylene molecules. A proposed scheme for propargyl chloride IR LPHP is given in Figure 3.4.

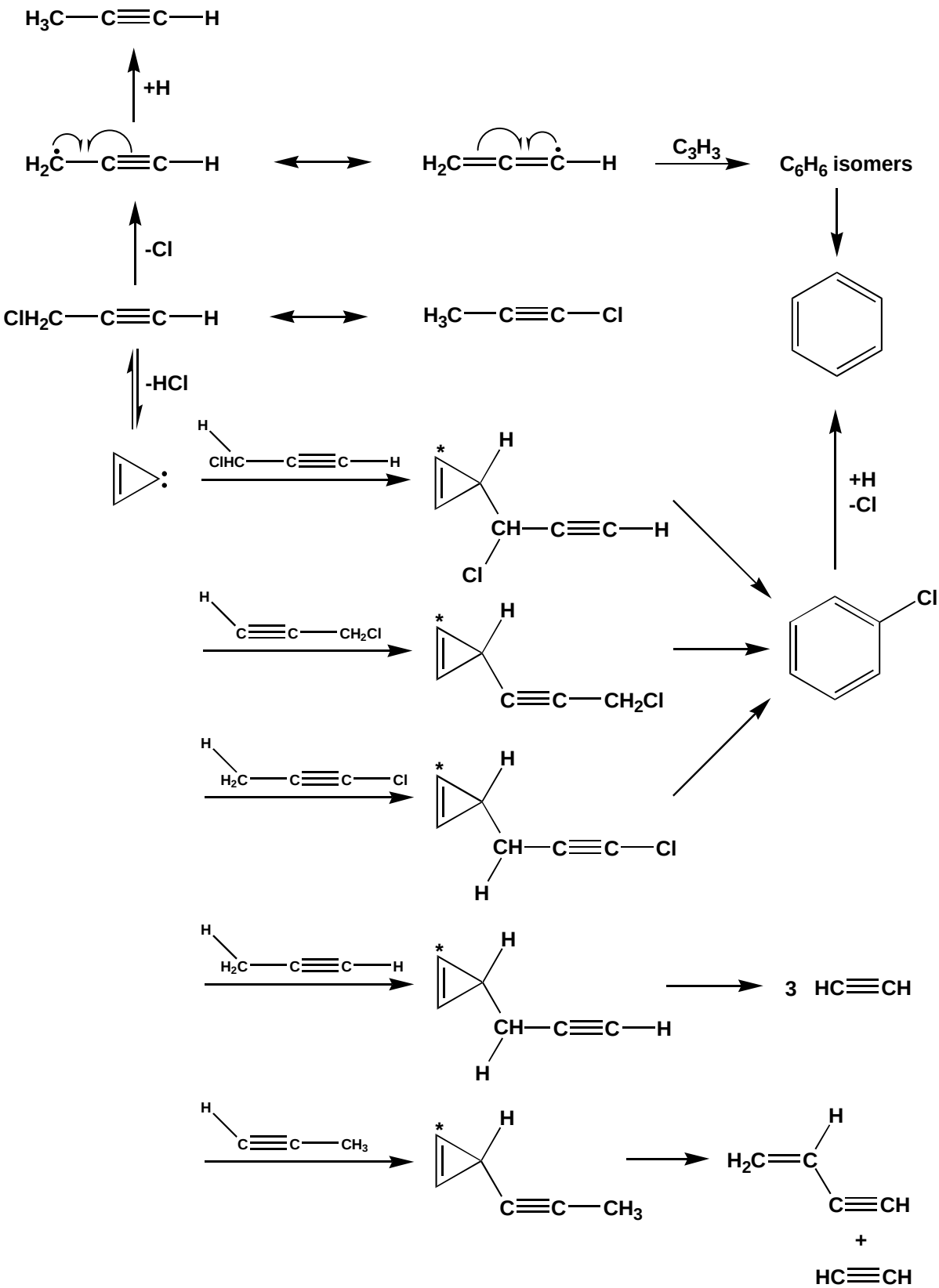

Figure 3.4 A proposed scheme for propargyl chloride IR LPHP; activated species are labelled *****

3.6 Chloroacetonitrile

The pyrolysis of monohalogenoacetonitriles at 1073-1273 K under reduced pressure has been investigated by Hashimoto and co-workers [37], and is reported to effect the production of *E*- and *Z*-2-butenedinitrile (fumaronitrile and maleonitrile, respectively) in 50-60 % yield. This was ascribed to unimolecular elimination of the hydrogen halide followed by combination of the resultant cyanocarbene. An alternative mechanism, involving cross-combination of $\cdot CH_2CN$ and $\cdot CHXCN$ (where X = halogen), followed by dehydrohalogenation of the resultant species, has been promulgated by Brown [2]. The formation of $\cdot CH_2CN$ and $\cdot CHXCN$ was attributed to the elimination of atomic chlorine and hydrogen, respectively, from the halogenated acetonitrile.

The abstraction of atomic chlorine from chloroacetonitrile by the tri-*n*-butyltin [38] and cyclohexyl radicals [39] has been studied in the liquid phase, with an express focus on the stability of the resultant cyanomethyl radical. It was found that the electron withdrawing cyano group effected delocalisation of the unpaired electron, resulting in a decrease in the spin density at the radical centre; this has the effect of diminishing the tendency of the radical to undergo reaction. The IR spectrum of cyanomethyl radical, which was generated by the excimer laser photolysis of chloroacetonitrile at 193 nm, was observed using time resolved diode laser spectroscopy by Sumiyoshi and co-workers [40].

3.6.1 Co-pyrolysis with $W(CO)_6$

In the present work, a sample of chloroacetonitrile was exposed to the output of a CW CO_2 laser in the absence and presence of $W(CO)_6$. On co-pyrolysis with $W(CO)_6$ at a low power

(*i.e.* temperature), the most significant products were acetonitrile and succinonitrile; 2-propenenitrile (acrylonitrile) and HCN were detected in trace amount. These results are consistent with the selective abstraction of Cl to yield the $\cdot CH_2CN$ radical; this either combines or abstracts atomic hydrogen to effect formation of acetonitrile. Presumably, the formation of acrylonitrile is ascribed to unimolecular elimination of HCN from succinonitrile.

3.6.2 Pyrolysis

The products derived from the pyrolysis of chloroacetonitrile in the absence of $W(CO)_6$ include HCN, acetonitrile, succinonitrile, acrylonitrile, 2-propynenitrile (propiolonitrile), cyanogen chloride (chlorine cyanide), HCl and acetylene, and are consistent with molecular elimination of HCl or homolytic fragmentation of the C–Cl bond. The formation of acetonitrile and succinonitrile is consistent with the latter (see above), while production of propiolonitrile and cyanogen chloride is initiated via elimination of molecular HCl. The distribution of products, specifically the presence of acetonitrile and succinonitrile at a level in excess of that of propiolonitrile, suggests that the predominant decomposition channel is C–Cl fission. The production of acetylene, which was observed at a modest level, is ascribed to elimination of molecular HCN from acrylonitrile (effected by the elimination of HCN from succinonitrile); the yield of acetylene increased substantially, at the expense of acrylonitrile, at elevated temperature.

In a manner analogous to that of propargyl chloride, it is proposed that the carbene resulting from dehydrochlorination of chloroacetonitrile will insert into a saturated C–H bond of a second molecule of starting material (the predominant species present) yielding

1-chloro-1,2-dicyanoethane. The fact that 1-chloro-1,2-dicyanoethane was not detected in this study suggests that at such a temperature it may expeditiously decompose; certainly, the formation of propiolonitrile and cyanogen chloride can be accounted for through the decomposition of 1-chloro-1,2-dicyanoethane.

It is postulated that the formation of propiolonitrile involves dehydrochlorination of 1-chloro-1,2-dicyanoethane, followed by molecular elimination of HCN from the resultant species, specifically *E*- or *Z*-2-butenedinitrile (fumaronitrile or maleonitrile). While neither was detected in this study, one can not preclude such a mechanism; in a manner analogous to that of 1-chloro-1,2-dicyanoethane, the pyrolysis temperature is probably sufficient to initiate decomposition of both species. The formation of cyanogen chloride is consistent with homolytic fragmentation of the C(1)–C(2) single bond of 1-chloro-1,2-dicyanoethane. Presumably, this is accompanied by a hydrogen and chlorine shift (from C(3) to C(2) and C(2) to C(1), respectively), which effects the formation of cyanogen chloride and acrylonitrile. A proposed scheme for chloroacetonitrile IR LPHP is depicted in Figure 3.5.

3.7 Benzyl Chloride

The flash vacuum pyrolysis (FVP) of the benzyl halides has been investigated in the gas phase by Schissel and co-workers [41], with the conclusion that reaction proceeds by homolysis of the C–X bond (where X = halogen) to yield the benzyl radical and molecular (α-elimination) or stepwise elimination of the hydrogen halide. The phenylcarbene afforded from dehydrochlorination of the benzyl halide undergoes ring expansion at $T \leq 873$ K to cycloheptatrienylidene that combines to yield heptafulvalene, and ring

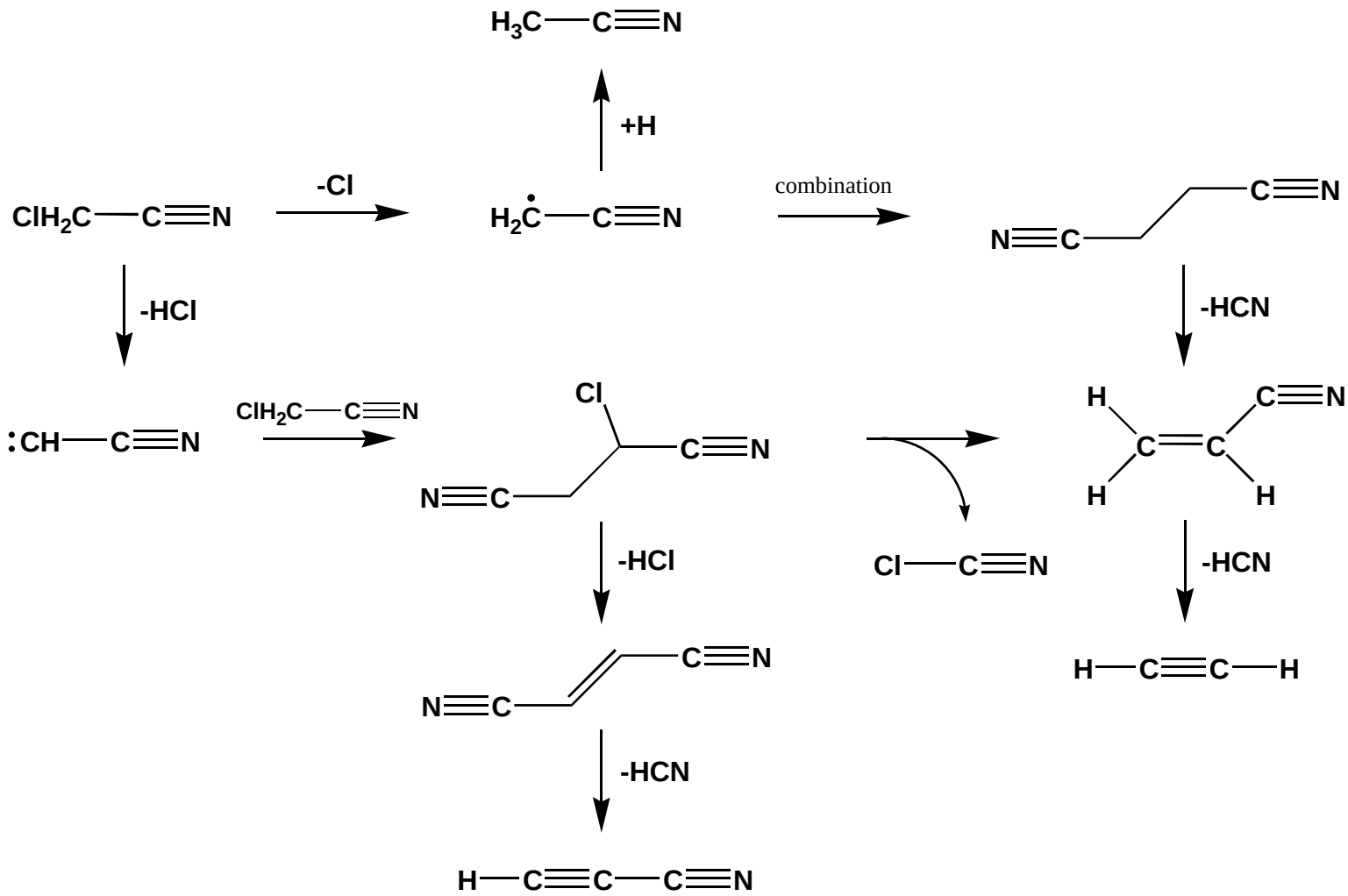

Figure 3.5 A proposed scheme for chloroacetonitrile IR LPHP

contraction at T > 873 K to form metastable 5-vinylidenecyclopentadiene (fulvenallene). The formation of stilbene and anthracene in low yield at T > 873 K was ascribed to the decomposition of heptafulvalene, FVP of a pure sample affording the same products [41]. Voronkov and co-workers [42] studied the decomposition of benzyl chloride ((chloromethyl)benzene) at 923 K and concluded that reaction proceeds through Cl fission and α-elimination of molecular HCl. In contrast to the work of Schissel and co-workers, these workers were unable to confirm the presence of heptafulvalene and fulvenallene, ostensibly precluding rearrangement of the arylcarbene formed through molecular dehydrochlorination of starting material.

Müller-Markgraf and Troe have investigated the thermal decomposition of the benzyl halides in incident and reflected shock waves [43], with the conclusion that reaction proceeds by C–Cl fission exclusively, to form the benzyl radical. The ascendant reaction of benzyl at low temperature is reversible combination to bibenzyl; at elevated temperature equilibrium favours the dissociation of bibenzyl, and fragmentation of the benzyl radical predominates. While the fragmentation of benzyl was not characterised by these workers, a preliminary investigation into the decomposition of the benzyl radical was reported by Smith [44, 45]; two channels, leading to $C_3H_3 + C_4H_4$ or $C_2H_2 + C_5H_5$ were tentatively identified using Knudsen mass spectroscopy.

3.7.1 Co-pyrolysis with $W(CO)_6$

In the present investigation, a sample of benzyl chloride was exposed to low laser power in the presence of $W(CO)_6$, the most significant products were toluene and bibenzyl (1,1'-(1,2-ethanediyl)bisbenzene). These results are analogous to those of Müller-Markgraf

and Troe, and are consistent with selective abstraction of atomic chlorine to yield the benzyl radical, this either combines, or abstracts atomic hydrogen to effect formation of toluene; there was no evidence to indicate decomposition of toluene or bibenzyl.

3.7.2 Pyrolysis

The products detected following pyrolysis of benzyl chloride without $W(CO)_6$, while comprising those consistent with homolytic fragmentation of the C–Cl bond, also included 1-chloro-1,2-diphenylethane (1,1'-(1-chloro-1,2-ethanediyl)bisbenzene), *E*-stilbene (*E*-1,1'-(1,2-ethenediyl)bisbenzene), phenylacetylene (ethynylbenzene), styrene (ethenylbenzene), and benzene, all of which may be accounted for through molecular elimination of HCl from starting material. The formation of heptafulvalene and metastable fulvenallene, the products ascribed to rearrangement of the arylcarbene, could not be confirmed. It is possible, however, that neither survive under these conditions. The dehydrochlorination of benzyl chloride, like propargyl chloride and chloroacetonitrile, affords the benzylidene carbene through α-elimination; β-elimination of HCl can be precluded, as there is no β-hydrogen atom. The intermolecular insertion of the divalent carbon of benzylidene into the benzylic C–H bonds of benzyl chloride (the predominant species present) will account for the formation of 1-chloro-1,2-diphenylethane.

The production of *E*-stilbene is consistent with the molecular elimination of HCl from 1-chloro-1,2-diphenylethane; presumably, dehydrochlorination is favoured by a periplanar geometry in which the appropriate hydrogen and chlorine atoms are adjacent. This is in contrast to E2 reactions (which take place when an alkyl halide is treated with a strong base), where elimination occurs from a periplanar geometry in which the hydrogen and

chorine atoms are on opposite sides of the molecule [3]. Although combination of benzylidene will yield *E*-stilbene, and to a lesser extent (on account of steric repulsion) the *Z* isomer, it can be discounted in the present study as there was no evidence to indicate formation of the latter. The production of phenylacetylene may involve β-elimination of benzene from *E*-stilbene; certainly, phenylacetylene became more prevalent at a higher temperature. An alternative pathway to phenylacetylene involving loss of atomic hydrogen from *E*-stilbene, followed by the elimination of phenyl radical from the resulting species can not be discounted.

The intensity of the peak (in the gas chromatogram) assigned to styrene intensified at elevated temperatures, at the expense of those ascribed to 1-chloro-1,2-diphenylethane. These results are consistent with the elimination of atomic chlorine from 1-chloro-1,2-diphenylethane to yield the 1,2-diphenylethyl radical; homolytic fragmentation (cleavage of a C–Ph bond) will effect the formation of styrene and the phenyl radical. The phenyl radical may abstract atomic hydrogen, accounting for the observed benzene.

An alternative mechanism that may account for the formation of 1,2-diphenylethyl involves the loss of atomic hydrogen from bibenzyl; certainly, the intensity of the peak ascribed to bibenzyl decreased, albeit marginally, at elevated temperatures. C–Cl fission, however, represents a more likely decomposition pathway, given that the C–Cl bond enthalpy is significantly lower than that of the C–H bond [46]. It is conceivable that the production of styrene proceeds through a molecular elimination route in a manner analogous to that of phenylacetylene through β-elimination of benzene from bibenzyl. A proposed pyrolysis scheme for benzyl chloride is illustrated in Figure 3.6.

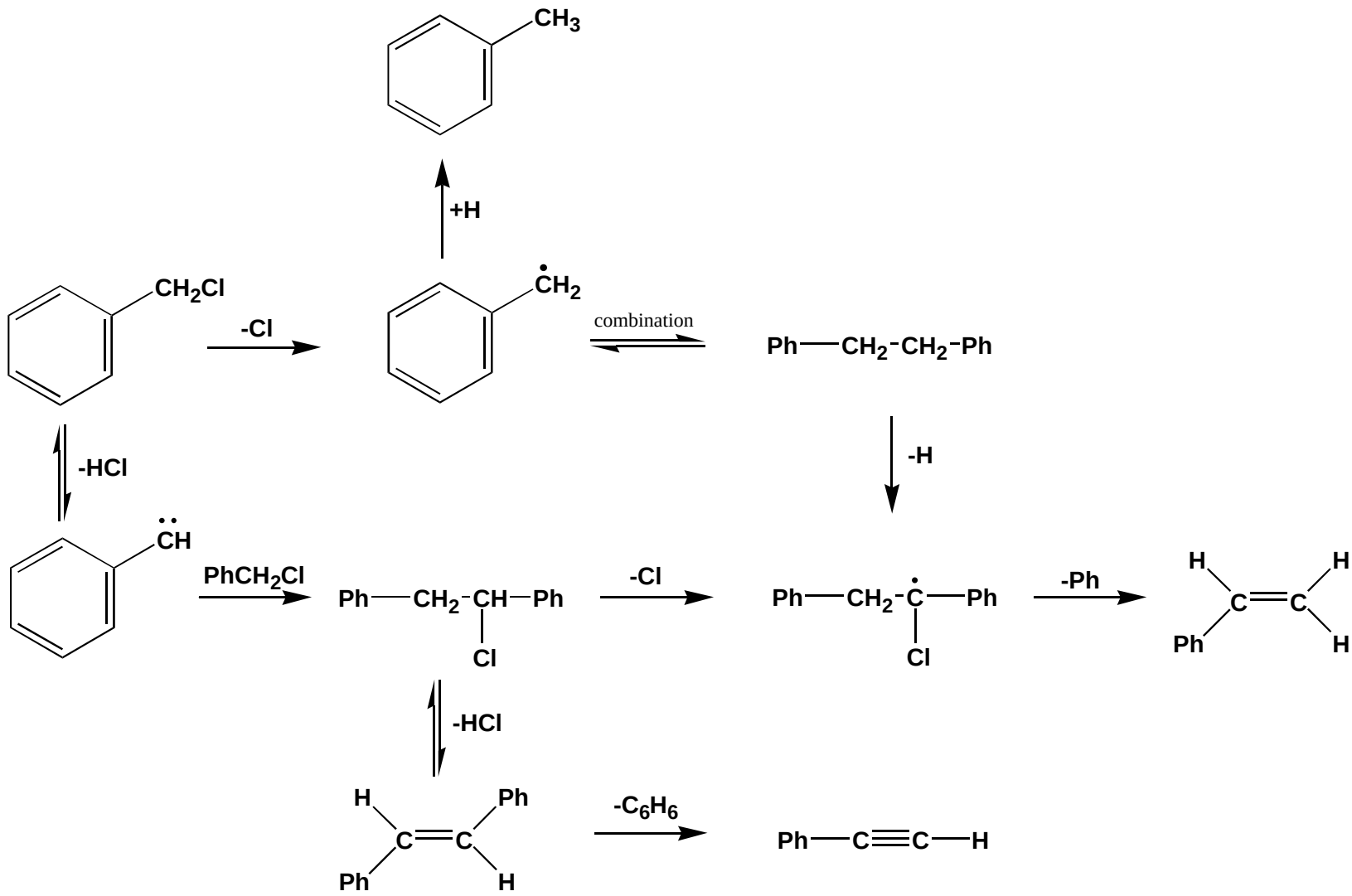

Figure 3.6 A proposed scheme for benzyl chloride IR LPHP

3.8 α,α'-Dichloro-o-xylene

The flash vacuum pyrolysis of α,α'-dichloro-*o*-xylene (1,2-bis(chloromethyl)benzene) has been investigated by Schiess and co-workers [47, 48], with the conclusion that reaction proceeds through dehydrochlorination yielding the α-monosubstituted benzocyclobutene, 7-chlorobicyclo[4.2.0]octa-1,3,5-triene. 2-chlorostyrene and phenylacetylene, which were detected at a modest level, are ascribed to ring cleavage, preceded (or succeeded) in the latter case by molecular elimination of HCl. The formation of 2-chlorostyrene indicates an accompanying chlorine shift.

In contrast, the flash vacuum pyrolysis of a variety of organic halides over magnesium at 873 K is reported to effect efficient dehalogenation; reaction of 1,2-bis(chloromethyl) benzene derivatives leads to the benzocyclobutene [49], through cyclisation of the less stable *o*-xylylene [50]. The UV photolysis of α,α'-dichloro-*o*-xylene has been investigated by a number of workers [51, 52]; in all cases, the observed products were *o*-xylylene and HCl. It is reported that the photolysis of α,α'-dichloro-*o*-xylene leads to double homolytic bond cleavage to produce *o*-xylylene and two chlorine atoms, the latter expected to rapidly abstract atomic hydrogen effecting the formation of HCl.

3.8.1 Pyrolysis

In the present work, a sample of α,α'-dichloro-*o*-xylene was exposed to the output of a CW CO_2 laser in the absence and presence of $W(CO)_6$. The most significant products observed following pyrolysis of α,α'-dichloro-*o*-xylene in the absence of $W(CO)_6$ are consistent

with a mechanism that proceeds through the molecular elimination of HCl, and include phenylacetylene, chlorobenzene, (2-chloroethenyl)benzene, acetylene, benzene and 1,3-butadiene, the latter observed in trace amount. In contrast to the findings of earlier workers, the species derived from the dehydrochlorination of starting material, namely 7-chlorobicyclo[4.2.0]octa-1,3,5-triene, was not detected in this investigation. Presumably, the decomposition of 7-chlorobicyclo[4.2.0]octa-1,3,5-triene succeeds α,α'-dichloro-*o*-xylene dehydrochlorination, yielding benzocyclobutadiene via the molecular elimination of HCl, and (2-chloroethenyl)benzene through homolysis of the four-membered ring (with an accompanying hydrogen shift). The absence of 2-chlorostyrene ostensibly precludes concomitant migration of chlorine. The post-pyrolysis gas chromatogram of α,α'-dichloro-*o*-xylene is illustrated in Figure 3.7.

The production of phenylacetylene is consistent with the molecular elimination of HCl from (2-chloroethenyl)benzene; an alternative mechanism, involving the decomposition of benzocyclobutadiene (through rupture of the four-membered ring, with accompanying hydrogen shift) can not, however, be discounted. It is presumed that the latter occurs expeditiously; benzocyclobutadiene, which is identified by an intense absorbance band at 737 cm^{-1} [53], was not detected directly by infrared spectroscopy in the gas phase or in a SF_6 matrix (dilution 100 : 1).

The intensity of the band ascribed to benzene increased at the expense of phenylacetylene as the temperature of pyrolysis was raised. These results are consistent with homolytic fragmentation of the latter to yield the phenyl and ethynyl radical; the former will abstract atomic chlorine or hydrogen, resulting in the observed chlorobenzene and benzene. The absence of bibenzyl precludes combination of the phenyl radical. In contrast, ethynyl

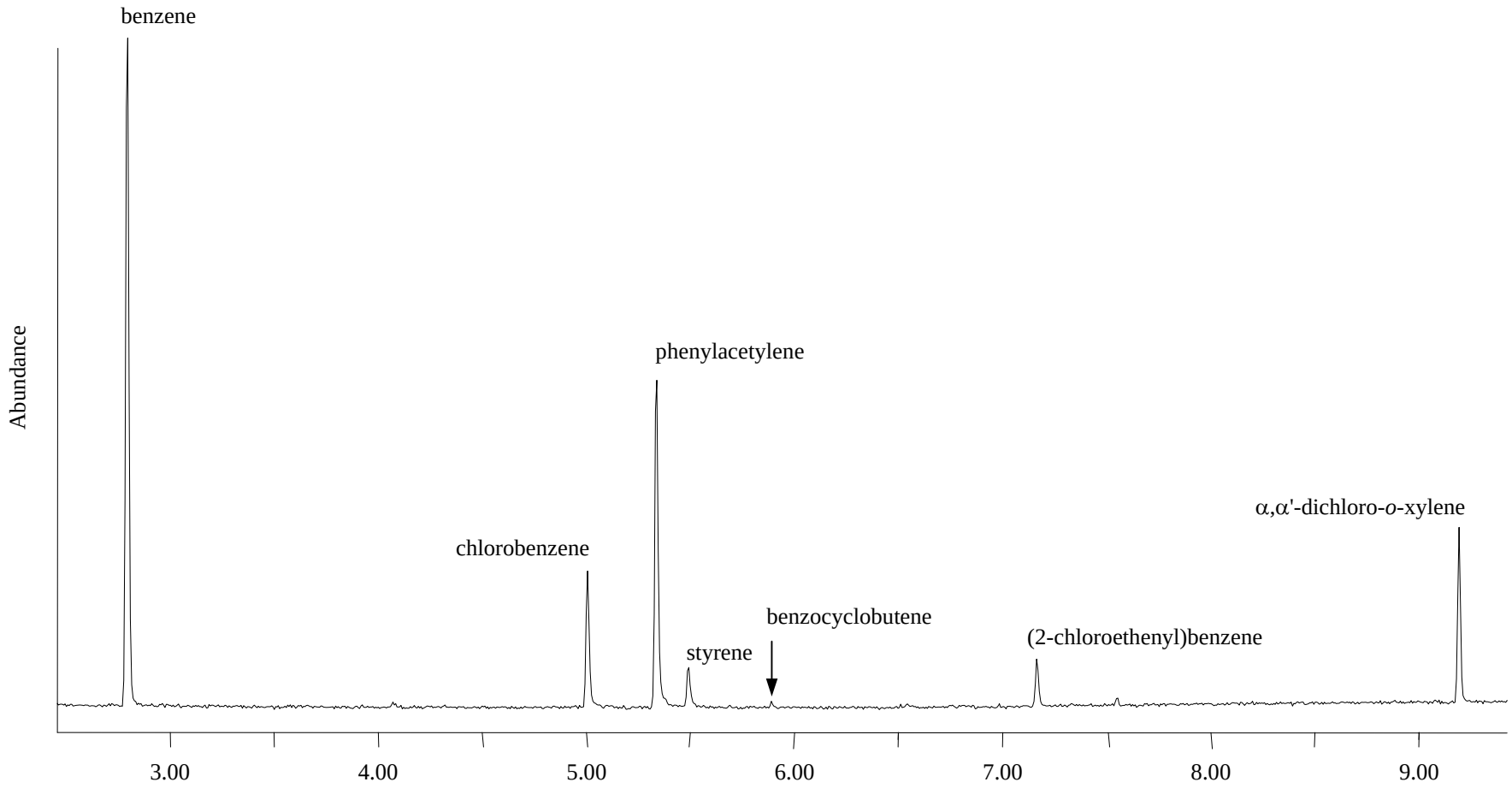

Figure 3.7 Gas chromatogram of α,α'-dichloro-*o*-xylene after IR LPHP

combination, while not predominant, is indicated by the formation of 1,3-butadiene. Presumably, loss of atomic hydrogen from ethynyl accounts for formation of acetylene.

There were a number of weaker signals in the post pyrolysis spectrum and gas chromatogram of α,α'-dichloro-*o*-xylene that are ascribed to benzocyclobutene and styrene, the former detected in only trace amount. The production of benzocyclobutene is consistent with homolytic cleavage of each of the C–Cl bonds; presumably, intramolecular combination (cyclisation) of the resultant diradical is favoured over *o*-xylylene formation, which was not detected in this study. Homolytic fragmentation of benzocyclobutene (via cleavage of the four-membered ring), with an accompanying hydrogen shift will account for the formation of styrene; that styrene was observed at a greater level than benzocyclobutene suggests that such a process occurs rapidly at these temperatures.

In a manner analogous to that of phenylacetylene decomposition, scission of the exocyclic carbon-carbon single bond in styrene, will effect production of the phenyl and vinyl radical. The absence of those products ascribed to combination or disproportionation of the vinyl radical suggests that the decomposition of styrene is a minor pathway under these conditions. A proposed scheme for the pyrolysis of α,α'-dichloro-*o*-xylene is illustrated in Figure 3.8.

3.8.2 Co-pyrolysis with $W(CO)_6$

The most significant products observed following pyrolysis of α,α'-dichloro-*o*-xylene in the presence of $W(CO)_6$, are consistent with a mechanism that proceeds through the selective abstraction of atomic chlorine, and include benzocyclobutene, 2-methylbenzyl

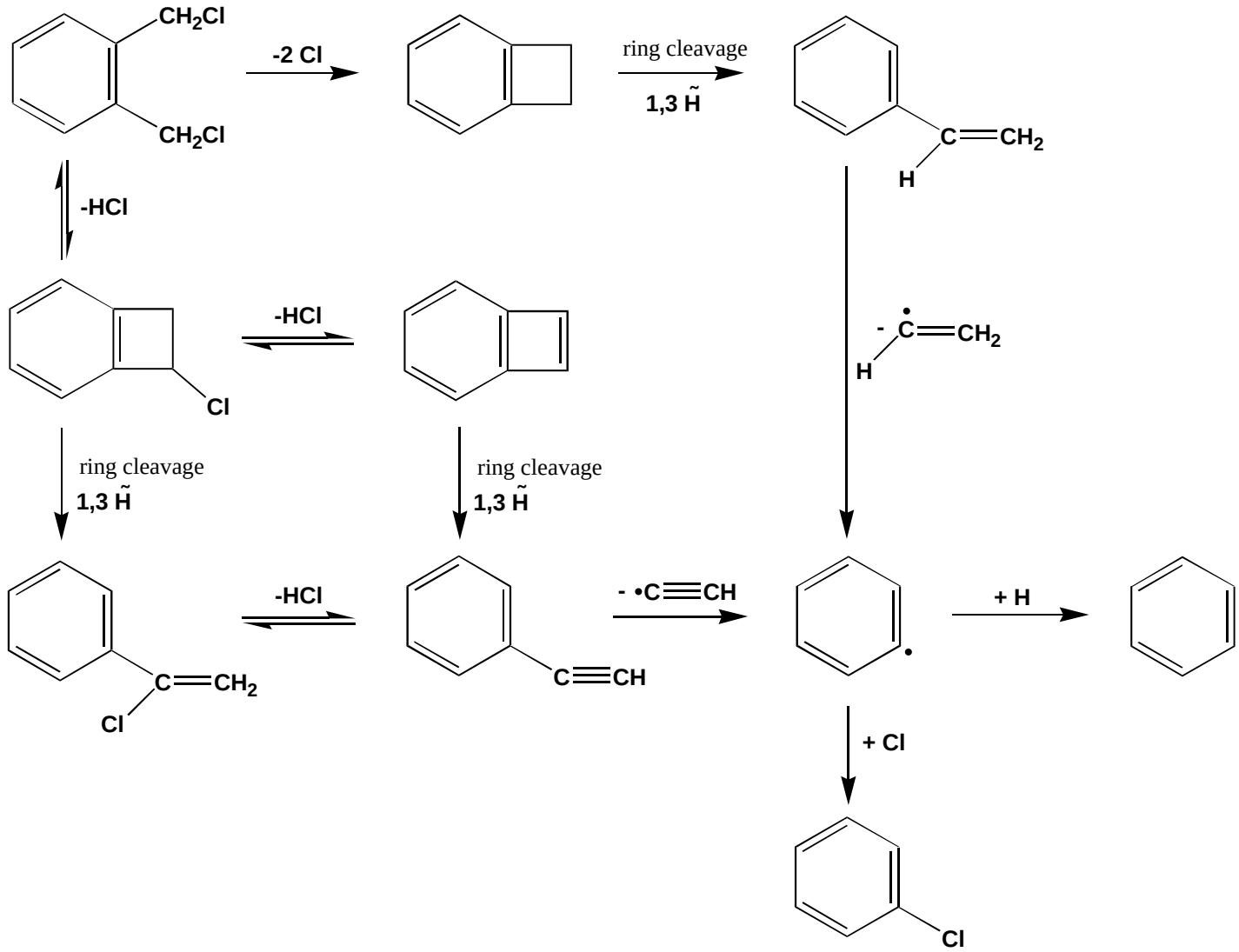

Figure 3.8 A proposed scheme for α,α'-dichloro-*o*-xylene IR LPHP

chloride (1-(chloromethyl)-2-methylbenzene) and *o*-xylene (1,2-dimethylbenzene). The post-pyrolysis spectrum and gas chromatogram of α,α'-dichloro-*o*-xylene and $W(CO)_6$ was devoid of peaks ascribed to phenylacetylene, (2-chloroethenyl)benzene and chlorobenzene, suggesting that the dehydrochlorination of starting material is inhibited in the presence of $W(CO)_6$.

It is apparent that the radical effected through the abstraction of a single chlorine atom is able to abstract hydrogen atoms prior to the elimination of a second chlorine atom to yield 2-methylbenzyl chloride. The diradical effected through abstraction of both chlorine atoms will afford benzocyclobutene through intramolecular combination; in contrast to the photolysis of α,α'-dichloro-*o*-xylene, the rearrangement product, specifically *o*-xylylene, was not detected under these conditions. The absence of styrene precludes homolytic cleavage of the four-membered ring in benzocyclobutene, and can be rationalised in terms of reaction temperature; presumably, benzocyclobutene is stable at the temperatures required to initiate the IR LPHP of α,α'-dichloro-*o*-xylene in the presence of $W(CO)_6$.

The abstraction of atomic chlorine from starting material is not unique; peaks in the post-pyrolysis infrared spectrum that were attributed to 2-methylbenzyl chloride were found to decrease, albeit marginally, as the duration of pyrolysis was increased. A corresponding increase in those bands ascribed to *o*-xylene was observed over the same period. The radical generated through the abstraction of Cl from 2-methylbenzyl chloride is also formed by the diradical intermediate abstracting a single hydrogen atom; presumably, intramolecular combination does not immediately follow the abstraction of a second Cl from starting material. A proposed pyrolysis scheme for α,α'-dichloro-*o*-xylene in the presence of $W(CO)_6$ is illustrated in Figure 3.9.

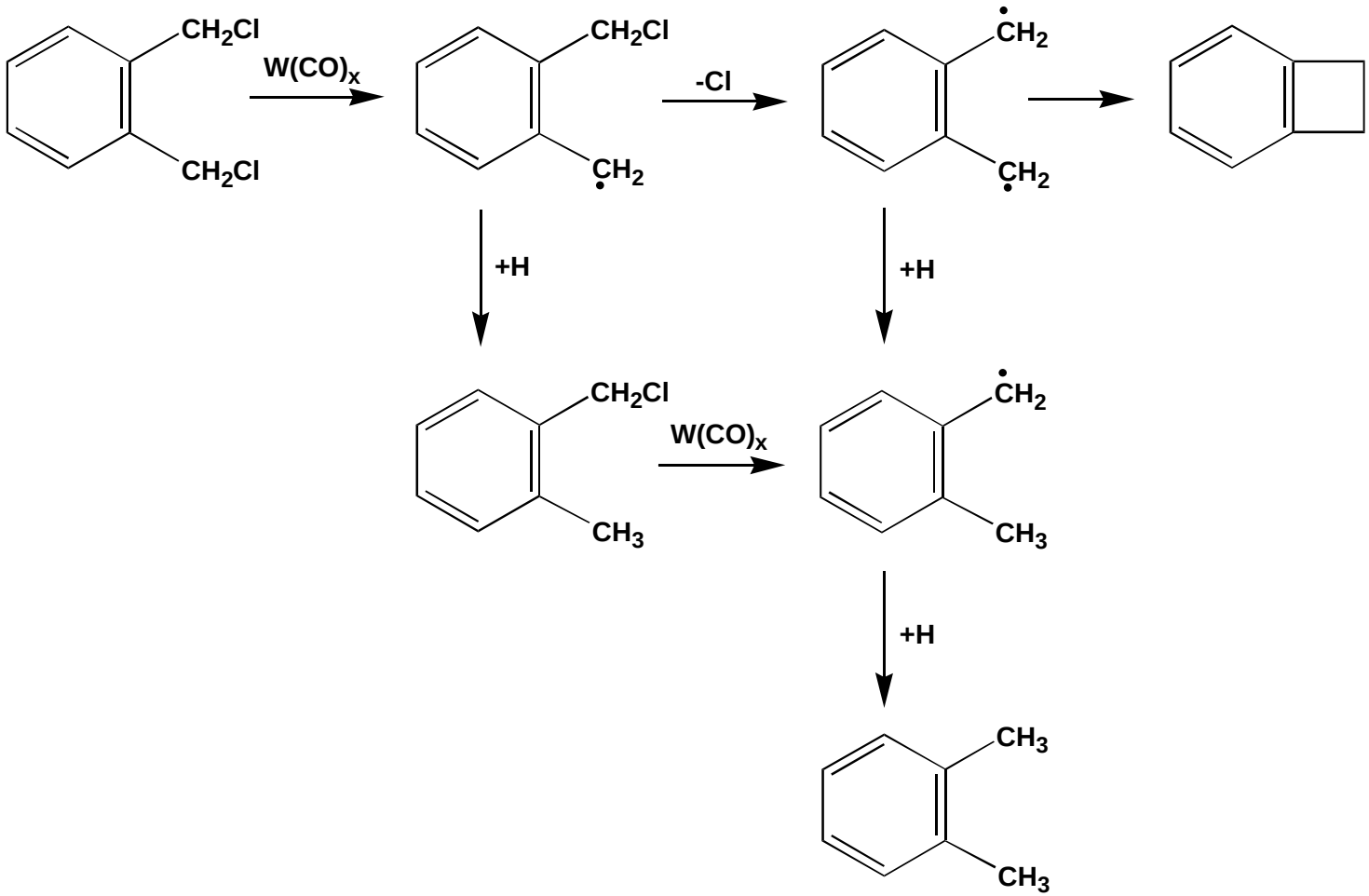

Figure 3.9 A proposed scheme for α,α'-dichloro-*o*-xylene and $W(CO)_6$ IR LPHP

3.9 Chloroacetic Acid

The series of halogenated acetic acids provides an interesting example of a change in pyrolysis mechanism down a series [54]. The decarbonylation of the oxiranone intermediate formed by elimination of HCl from chloroacetic acid yields formaldehyde, CO and HCl as the observed pyrolysis products. On the other hand, homolysis of the C–I bond in iodoacetic acid, followed by a hydrogen shift and decarboxylation, effects formation of the methyl radical and CO_2, the former affording methane through the abstraction of atomic hydrogen; bromoacetic acid follows both routes concurrently.

The pyrolysis of chloroacetic acid with $W(CO)_6$ at very low temperatures was found to yield the radical abstraction end products methane and CO_2. In addition, a number of other products (specifically ethylene, propene, methyl ethanoate and acetaldehyde, the latter observed in trace amount) were detected. This is consistent with a mechanism that proceeds through the selective abstraction of atomic chlorine from starting material. There was no evidence to indicate formation of formaldehyde. The FT-IR spectra of the products of laser pyrolysis of chloroacetic acid in the absence and presence of $W(CO)_6$ is illustrated in Fig. 3.10.

The abstraction of atomic chlorine from chloroacetic acid yields 2-hydroxy-2-oxoethyl, the homolytic fragmentation of which will effect the production of methylene through cleavage of the carbon-carbon single bond. The combination of methylene effects the formation of ethylene, while the addition of methylene to the double bond of ethylene will afford propene, through rearrangement of the vibrationally excited cyclopropane intermediate. The exothermicity of methylene addition is predicted to exceed the activation energy of isomerisation and consequently the transformation of the initial product by

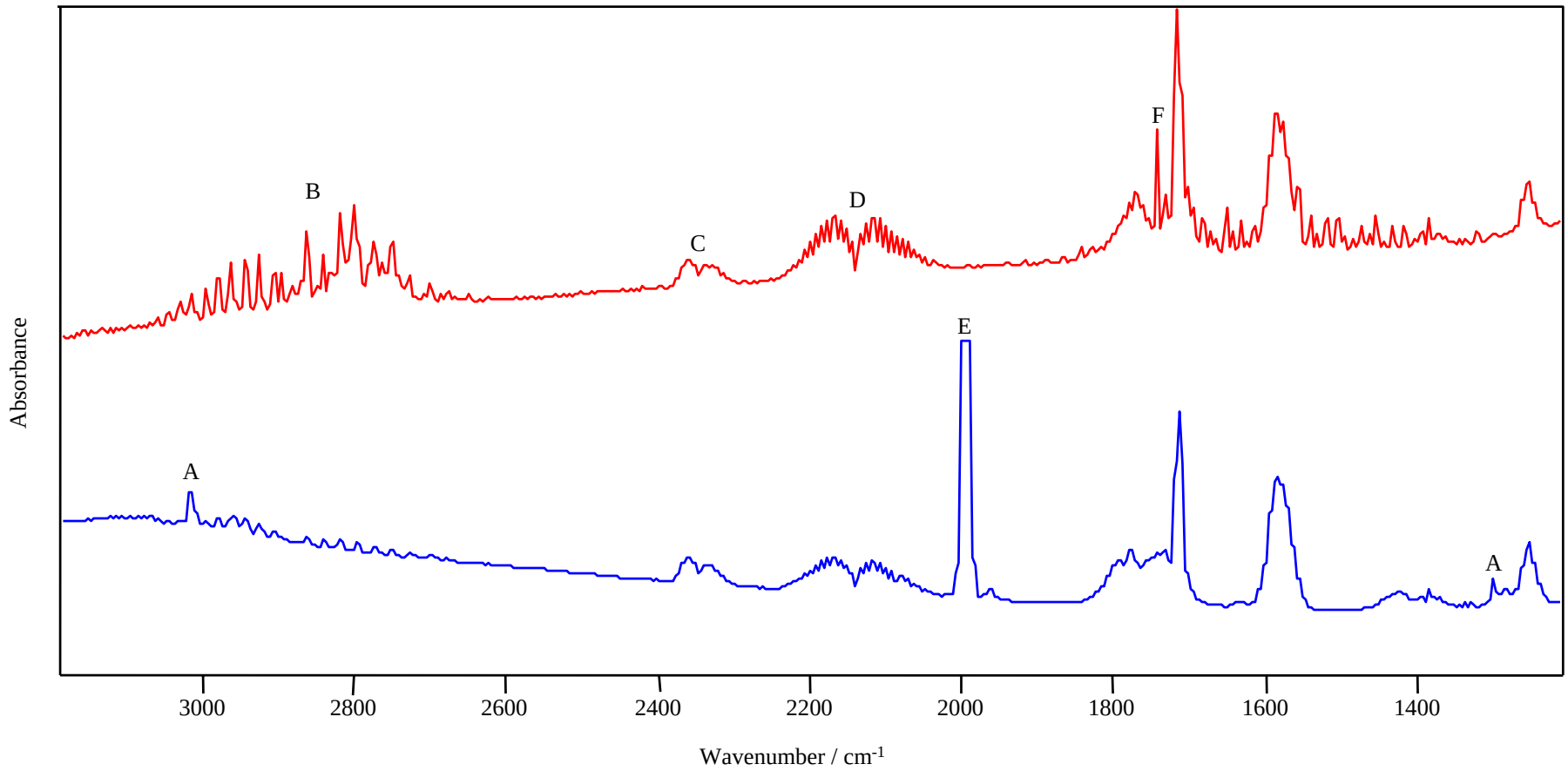

Figure 3.10 FT-IR spectra of the products of laser pyrolysis of $ClCH_2CO_2H$ in the absence (—) and presence (—) of $W(CO)_6$; A = CH_4; B = HCl; C = CO_2; D = CO; E = $W(CO)_6$; F = CH_2O; unassigned peaks are attributable to SF_6; the small amount of HCl evident in the lower trace was present in the original sample; the small amount of CO_2 present in the upper trace is atmospheric CO_2

structural or geometrical isomerisation is practicable [55]. In his systematic studies of the stereochemistry of the addition of methylene to the double bond of a selection of olefins, Frey reported that the yield of the cyclopropane increased with rising pressure and was more stereospecific at higher pressures [56, 57]. It was proposed that deactivating collisions of the vibrationally excited cyclopropane would inhibit rearrangement to the isomeric cyclopropane and to the thermodynamically more stable alkene. Consequently, the yield of the initial deactivated adduct will be greater at higher pressure, where the likelihood of a collision is increased. The fact that cyclopropane was not observed in this investigation reflects the low pressure employed when executing IR LPHP.

Combination of the methyl radical formed by the successive rearrangement (hydrogen shift) and fragmentation (decarboxylation) of 2-hydroxy-2-oxoethyl will afford ethane. The addition of methyl to ethylene, followed by the loss of H may offer an alternative pathway to propene. The presence of methyl ethanoate, albeit in trace amount, is consistent with cross-combination of the methyl and CH_3CO_2 radical. This suggests that decarboxylation of 2-hydroxy-2-oxoethyl does not immediately follow hydrogen migration.

The formation of acetaldehyde is consistent with homolytic fragmentation of the CH_3CO_2 radical; abstraction of atomic hydrogen by the organic radical species effected through scission of the carbon-oxygen single bond will effect production of the aldehyde. The unimolecular rate expressions for the decomposition of several larger radicals are known to have activation energies of the order of 120 to 160 kJ mol^{-1} and normal pre-exponential factors; consequently, such species are less stable than the analogous alkanes and alkenes [58]. A proposed scheme for chloroacetic acid and $W(CO)_6$ IR LPHP is illustrated in Figure 3.11.

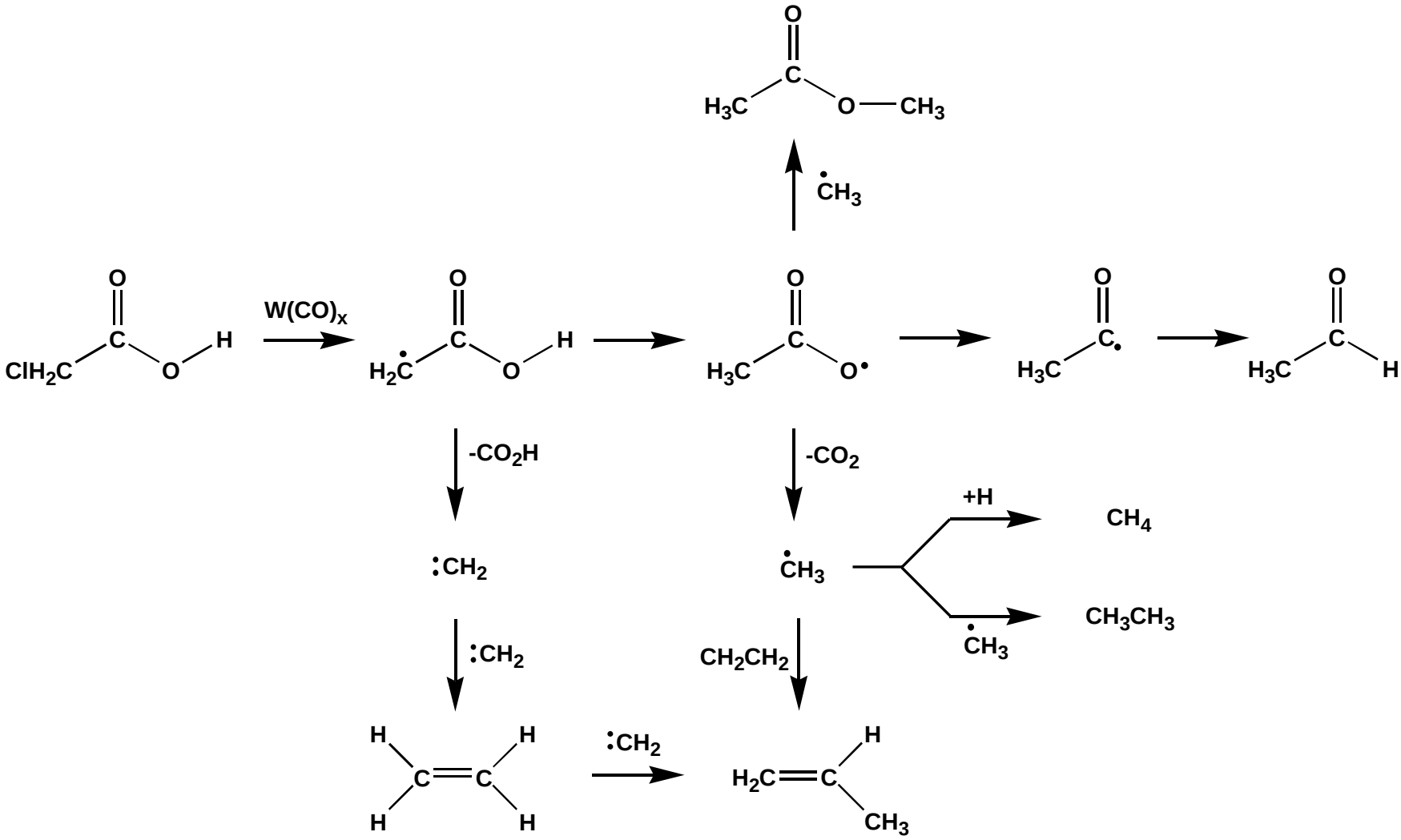

Figure 3.11 A proposed scheme for chloroacetic acid and $W(CO)_6$ IR LPHP

3.10 Conclusion

The results presented in this chapter confirm that $W(CO)_x$ species are effective and selective abstractors of atomic chlorine from a range of organochlorine compounds under comparatively mild conditions. The subsequent chemistry is dominated by the resulting organic radical moiety; observed end products can be ascribed to combination and disproportionation (the two types of radical-radical reactions), addition, abstraction and, to a lesser extent, fragmentation of the resultant radical species.

The combination or disproportionation of the resultant radical was for the most part, a dominant reaction pathway; only in systems where the radical concentration was relatively low were radical-radical reactions not significant. In general, the known disproportionation to combination ratio was reflected in experimental observation; in cases where the observed distribution of self-reaction products differed from that expected, an additional mechanism was proposed to account for the apparent deviation. β-elimination of HCl from starting material, the predominant pyrolysis pathway of an organochlorine compound without $W(CO)_6$, may account for such a discrepancy; the olefin formed is identical to the unsaturated species derived from disproportionation of the organic radical. This was especially evident in systems that decomposed in the absence of $W(CO)_6$ at a temperature comparable to that in the presence of $W(CO)_6$. The decomposition of organochlorine compounds that did not possess a β-hydrogen, in the absence of $W(CO)_6$, involved α-elimination of HCl; the subsequent chemistry was dominated by the resulting carbene.

Addition reactions of the resultant organic radical were predominant in systems where pyrolysis, in the absence of $W(CO)_6$, was found to initiate molecular dehydrochlorination

at a relatively low temperature. In such cases, there was competition between the selective abstraction of atomic chlorine and HCl elimination, the latter effecting the formation of an olefinic species. The addition of an organic radical species to the double bond of an olefin occurred primarily at the least substituted carbon; homolytic fragmentation of the resulting radical addend involved, for the most part, cleavage of the C_{β}–H bond.

The pyrolysis of a number of organochlorine compounds in the presence of $W(CO)_6$, resulted in the abstraction of atomic hydrogen by the inaugural organic radical species; in several cases this was the dominant pyrolysis mechanism. The compound afforded is identical to the saturated product derived from disproportionation of the organic radical. Consequently, it is possible to rationalise a deviation in the expected distribution of disproportionation products in terms of the abstraction of atomic hydrogen. The capacity of an organic radical to abstract Cl in preference to H is significantly less than that expected, given that the enthalpy of the C–Cl bond is lower than that of the C–H bond [46]. This suggests that $W(CO)_x$ species are considerably more efficient at abstracting atomic chlorine than organic radical species, which is in accord with the relative strengths of the W–Cl and C–Cl bonds [59].

The fragmentation of the resultant organic radical was rarely a predominant pyrolysis mechanism; in contrast, homolytic fragmentation of a radical formed by secondary reaction was frequently observed. It is possible to rationalise this difference in terms of radical concentration; the concentration of a radical formed through primary reaction should be higher than that effected through secondary reaction. Consequently, the probability of a collision, and as such reaction, between radicals formed from secondary reaction is considerably less than that afforded from primary reaction.

3.11 References

[1] G. R. Allen, N. D. Renner and D. K. Russell, *J. Chem. Soc., Chem. Commun.*, 1998, 703.

[2] R. F. C. Brown, *Pyrolytic Methods in Organic Chemistry,* Academic Press, New York, 1980.

[3] J. McMurray, *Organic Chemistry,* 3rd Ed, Brookes/Cole Publishing Company, Pacific Grove, CA, 1992.

[4] P. Kubat and J. Pola, *Z. Phys. Chemie*, 1987, **268**, 849.

[5] J. O. Terry and J. H. Futrell, *Can. J. Chem.*, 1967, **45**, 2327.

[6] J. Thynne, *J. Chem. Soc., Faraday Trans.*, 1961, **57**, 676.

[7] C. Heller and A. Gordon, *J. Phys. Chem.*, 1958, **62**, 709.

[8] R. Riem and K. Kutschke, *Can. J. Chem.*, 1960, **38**, 2332.

[9] A. Lifshitz, A. Bar-Nun, A. Burcat, A. Ofir and R. D. Levine, *J. Phys. Chem.*, 1982, **86**, 791.

[10] N. C. Craig, L. G. Piper and V. L. Wheeler, *J. Phys. Chem.*, 1971, **75**, 1453.

[11] R. V. Ambartzumian, N. V. Chekalin, V. S. Doljikov, V. S. Letokhov and V. N. Lokhman, *Opt. Commun.*, 1976, **18**, 400.

[12] J. L. Jones and R. L. Taylor, *J. Am. Chem. Soc.*, 1940, **62**, 3480.

[13] J. Fossey, D. Lefort and J. Sorba, *Free Radicals in Organic Chemistry,* John Wiley & Sons, Chichester, 1995.

[14] A. Fahr and A. H. Laufer, *J. Phys. Chem.*, 1990, **94**, 726.

[15] J. C. Bertolini, J. Massardiner and G. Dalmai-Imerdik, *J. Chem. Soc., Farad. Trans. I*, 1978, **74**, 1720.

[16] S. Lie, L. Wang, M. Xie, X. Guo and Y. Wu, *Catal. Lett.*, 1995, **30**, 135.

[17] P. M. Maitlis, *Pure Appl. Chem.*, 1973, **33**, 489.

[18] G. N. Schauzer and S. Eichlwer, *Chem. Ber.*, 1962, **95**, 550.

[19] F. Solymosi, A. Erdohelyi and A. Szoke, *Catal. Lett.*, 1995, **32**, 43.

[20] J. E. Germaine, *Catalytic Conversion of Hydrocarbons,* Academic Press, London, 1969.

[21] R. D. Kern, H. Chen, Z. Qin and K. Xie, In *Shock Waves at Marseille, Vol. II, Proc. 19th Symp. (Int.) on Shock Waves*. 1993. Marseille, R. Brun and L. Dumitrescu, Eds., Springer, Berlin, 1995; pp. 113-118.

[22] R. D. Kern, H. Chen, J. H. Kiefer and P. S. Mudipalli, *Combust. Flame*, 1995, **100**, 177.

[23] R. W. Gallant, *US Patent,* US 3,364,271; *Chem. Abstr.* 1968, **68**, 104549f.

[24] S. S. Kumaran, K. P. Lim, J. V. Michael, J. L. Tilson, A. Suslensky and A. Lifshitz, *Israel J. Chem.*, 1996, **36**, 223.

[25] V. Jonas, M. Bohme and G. Frenking, *J. Phys. Chem.*, 1993, **96**, 1640.

[26] U. Alkemade and K. H. Homann, *Z. Phys. Chem. N. F.*, 1989, **161**, 19.

[27] I. Haller and R. Srinivasan, *J. Am. Chem. Soc.*, 1966, **88**, 3694.

[28] J. Collin and F. P. Lossing, *Can. J. Chem.*, 1957, **35**, 778.

[29] D. B. Atkinson and J. W. Hudgens, *J. Phys. Chem. A*, 1999, **103**, 4242.

[30] A. Fahr, P. Hassanzadeh, B. Laszlo and R. E. Huie, *Chem. Phys.*, 1997, **215**, 59.

[31] P. W. Browning, D. C. Kitchen, M. F. Arendt and L. J. Butler, *J. Phys. Chem.*, 1996, **100**, 7765.

[32] C. L. Morter, S. K. Farhat, J. D. Adamson, G. P. Glass and R. F. Curl, *J. Phys. Chem.*, 1994, **98**, 7029.

[33] Y. Sumiyoshi, T. Imajo, K. Tanaka and T. Tanaka, *Chem. Phys. Lett.*, 1994, **231**, 569.

[34] M. Kawasaki, K. Kasatani, H. Sato, H. Shinohara and N. Nishi, *Chem. Phys.*, 1984, **88**, 135.

[35] D. A. Ramsay and P. Thistlethwaite, *Can. J. Chem.*, 1966, **44**, 1381.

[36] Y. Lee and S. Lin, *J. Chem. Phys.*, 1998, **108**, 134.

[37] N. Hashimoto, K. Matsumura and K. Morita, *J. Org. Chem.*, 1969, **34**, 3410.

[38] J. Cooper, A. Hudson and R. Jackson, *J. Chem. Soc., Perkin Trans. II*, 1975, 1056.

[39] Y. Gonen, A. Horowitz and L. Rajbenbach, *J. Chem. Soc., Faraday Trans. I*, 1977, **73**, 866.

[40] Y. Sumiyoshi, K. Tanaka and T. Tanaka, *J. Chem. Phys.*, 1996, **104**, 1839.

[41] P. Schissel, M. E. Kent, D. J. McAdoo and E. Hedaya, *J. Am. Chem. Soc.*, 1970, **92**, 2147.

[42] M. G. Voronkov, E. N. Deryagina and L. G. Shagun, *Zh. Org. Khim.*, 1982, **18**, 902.

[43] W. Müller-Markgraf and J. Troe, *J. Phys. Chem*, 1988, **92**, 4899.

[44] R. D. Smith, *J. Phys. Chem.*, 1979, **83**, 1553.

[45] R. D. Smith, *Combust. Flame*, 1979, **35**, 179.

[46] P. W. Atkins, *Physical Chemistry*, 4th Ed, Oxford University Press, Oxford, 1990.

[47] P. Schiess, S. Rutschmann and V. V. Toan, *Tet. Lett.*, 1982, **23**, 3669.

[48] P. Schiess, M. Heitzmann and S. Rutschmann, *Tet. Lett.*, 1978, 4569.

[49] R. A. Aitken, P. K. G. Hodgson, A. O. Oyewale and J. J. Morrison, *J. Chem. Soc., Chem. Commun.*, 1997, 1163.

[50] W. R. Roth, M. Biermann, H. Dekker, R. Jochems, C. Mosselman and H. Hermann, *Chem. Ber.*, 1978, **111**, 3892.

[51] M. Fujiwara, K. Mishima, K. Tamai, Y. Tanimoto, K. Mizuno and Y. Ishii, *J. Phys. Chem. A*, 1997, **101**, 4912.

[52] K. Haider and M. S. Platz, *J. Am. Chem. Soc.*, 1988, **110**, 2318.

[53] O. L. Chapman, C. C. Chang and N. R. Rosenquist, *J. Am. Chem. Soc.*, 1976, **98**, 261.

[54] H. Hettema, N. R. Hore, N. D. Renner and D. K. Russell, *Aust. J. Chem.*, 1997, **50**, 363.

[55] W. Kirmse, *Carbene Chemistry,* Academic Press, New York, 1971.

[56] H. M. Frey, *Proc. Roy. Soc., Ser. A*, 1959, **250**, 409.

[57] H. M. Frey, *Proc. Roy. Soc., Ser. A*, 1959, **251**, 575.

[58] W. Tsang and J. H. Kiefer, In *The Chemical Dynamics and Kinetics of Small Radicals,* K. Liu and A. Wagner, Eds., World Scientific, Singapore, 1995; pp. 58-119.

[59] *CRC Handbook of Chemistry and Physics,* 60th Ed, R. C. Weast, Ed., CRC Press, Boca Raton, Fl., 1979.

Chapter Four

ACYL CHLORIDES

4.1 Introduction

The principal intention of this study was to elucidate the reaction mechanisms of organic radical species resulting from the selective abstraction of atomic chlorine from selected acyl chlorides. It has been shown that IR LPHP of $W(CO)_6$ in the gas phase leads to unsaturated $W(CO)_x$ species that are very effective and selective abstractors of chlorine atoms from a wide range of organic substrates [1]. The chemistry of the resultant organic radical species is dominated by the themes of combination, disproportionation, addition, abstraction, fragmentation and rearrangement; these have been described in section 1.1.3.

A comprehensive investigation of the decomposition of an acyl chloride in the presence of $W(CO)_6$ required that the pyrolysis mechanism of the precursor in the absence of $W(CO)_6$ be understood. While the decomposition of several acyl chlorides has been the subject of some work, there has been no previous attempt to construct a comprehensive gas phase decomposition scheme of any of the selected acyl chlorides. In general, the decomposition of an acyl chloride is initiated through molecular elimination of HCl, effecting formation of the analogous ketene [2-4]. Ketenes are often transient species, whose chemical utility, particularly in organic synthesis, has long been recognised [2, 5-8]; for example, hydration of ketene was, for many years, a major industrial process for the preparation of acetic acid.

In this investigation, the gas phase decomposition of chloroacetyl chloride, propanoyl chloride, 3-chloropropanoyl chloride, acryloyl chloride (2-propenoyl chloride), *E*-2-butenoyl chloride, methacryloyl chloride (2-methyl-2-propenoyl chloride) and cyclopropanecarbonyl chloride was initiated in the absence and presence of $W(CO)_6$ using IR LPHP, and characterised using a combination of FT-IR, GC-MS, TDL and matrix isolation spectroscopy.

4.2 Chloroacetyl Chloride

The thermolysis [9-13] and photolysis [14] of chloroacetyl chloride has been studied by a number of workers with an express focus on the initial decomposition step, specifically, molecular elimination of HCl. The dehydrochlorination of chloroacetyl chloride yields the unstable ketene derivative, chloroketene. Microwave [10] and photoelectron [11, 13] spectra have been obtained for chloroketene. Xu and co-workers have used laser-induced fluorescence excitation spectroscopy to identify and characterise the product of chloroketene decarbonylation, namely chloromethylene [9].

Masters and co-workers have executed a theoretical investigation of ketene forming reactions that involve halogen abstraction of an alkyl or acyl halide [15]. The reaction of an anionic metal carbonyl ($Mn(CO)_5^-$) with bromoacetyl chloride afforded $Mn(CO)_5Br$ and ketene (ethenone), not the acyl complex expected from nucleophilic displacement of the halide by the metal centre via a S_N2 mechanism [16, 17]. The reaction of $Mn(CO)_5^-$ with chloroacetyl chloride is less facile, generating the acetyl complex. These workers attribute this difference to the contrasting energies and composition of the LUMO and NLUMO (next lowest unoccupied molecular orbital) of each system. The driving force of reaction is a donor-acceptor interaction between the HOMO (highest occupied molecular orbital) of $Mn(CO)_5^-$ and, respectively, the LUMO and NLUMO of the 2-haloacetyl chloride.

4.2.1 Pyrolysis

In the present work, the stable products of chloroacetyl chloride IR LPHP were identified as *E* and *Z*-1,2-dichloroethene, chloromethane, 1,1,2,2-tetrachloroethane, chloroform and

trichloroethene, the latter becoming a significant product at higher laser power (*i.e.* temperature). The decarbonylation product, namely dichloromethane, was also detected. The post-pyrolysis gas chromatogram of chloroacetyl chloride in the absence and presence of $W(CO)_6$ is illustrated in Figure 4.1. An ephemeral absorbance band was observed in the post-pyrolysis infrared spectrum at 2154 cm^{-1} and ascribed to chloroketene.

The intermediate ketene was also detected directly by IR spectroscopy in both an Ar and SF_6 matrix (dilution 2000 : 1). At 16 K, an intense band at 2147 cm^{-1} (2149 cm^{-1} in a SF_6 matrix), attributable to the cumulenic stretch, ν_2, of chloroketene, was observed. Davidovics and co-workers observed chloroketene, following photolysis of chloroacetyl chloride in a Xe matrix at 2141 cm^{-1} [14]. In the present study, chloroketene was also detected directly in the gas phase by TDL spectroscopy. At 2145, 2158 and 2195 cm^{-1}, a series of absorption bands developed while the contents of the cell were exposed to the output of a CW CO_2 laser. The spectrum returned to its original state within five minutes of the cessation of irradiation.

The formation of chloroketene is consistent with the molecular dehydrochlorination of chloroacetyl chloride. This is in accord with earlier investigations that have concentrated on the initial decomposition step [9-14]. The increase in the intensity of absorbance bands ascribed to starting material (during the acquisition of a spectrum) at the expense of the band ascribed to chloroketene suggests that molecular dehydrochlorination is reversible. The absence of dichloroacetaldehyde, the product effected from *anti*-Markovnikov addition of HCl to chloroketene, suggests that the reversible nature of dehydrochlorination (at least during the time when the cell contents were not exposed to laser irradiation) is unilateral. Theoretical investigations support this proposition; the production of

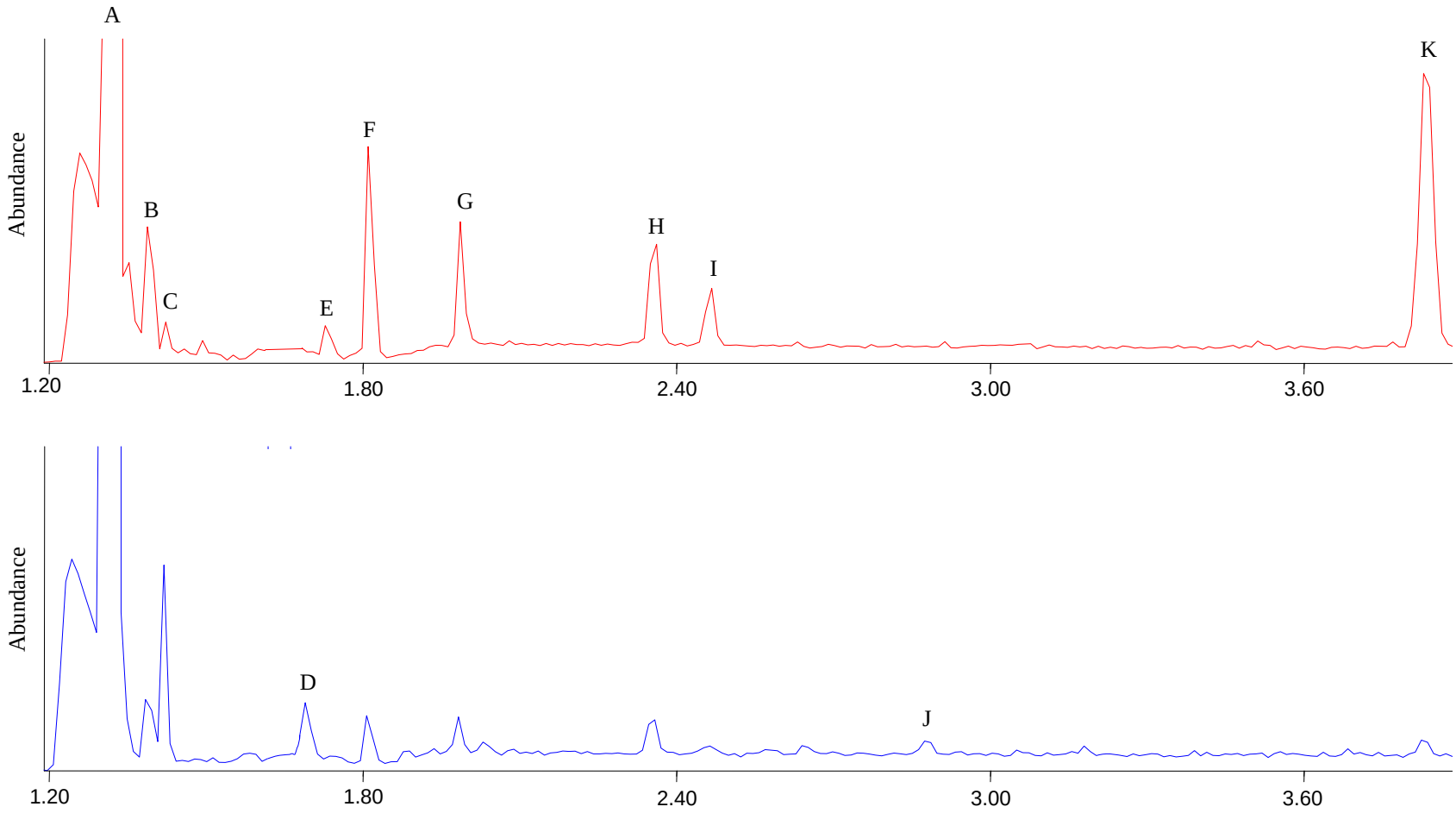

Figure 4.1 Partial gas chromatogram of the products of laser pyrolysis of chloroacetyl chloride in the absence (—) and presence (—) of $W(CO)_6$; A = SF_6; B = chloromethane; C = chloroethene; D = acetyl chloride; E = 1,2-dichloroethyne; F = dichloromethane; G = *E*-1,2-dichloroethene; H = *Z*-1,2-dichloroethene; I = chloroform; J = 1,2-dichloroethane; K = trichloroethylene; 1,1,2,2-tetrachloroethane was observed in the upper trace at 9.6 min

chloroacetyl chloride from Markovnikov addition of HCl to chloroketene is significantly lower in activation energy than that associated with the formation of dichloroacetaldehyde.

It is possible that the barrier to dichloroacetaldehyde formation is overcome at elevated temperature (*i.e.* when the cell is irradiated); the fact that it is not detected in the gas phase suggests that it expeditiously decompose under these conditions. Certainly, formation of trichloroethene and 1,1,2,2-tetrachloroethane may be explained through decomposition of dichloroacetaldehyde. The homolytic fragmentation of the C(1)–C(2) bond (numbered from the oxygen-bearing carbon) will yield the formyl and dichloromethyl radicals, respectively; combination of the latter will effect formation of 1,1,2,2-tetrachloroethane, from which the molecular elimination of HCl will afford trichloroethene.

The utilisation of ketenes as precursors of carbenes is well known; decarbonylation of a ketene, of which chloroketene is an example, will afford the analogous carbene [18]. The decarbonylation of chloroketene will yield chloromethylene [9]. The production of *E* and *Z*-1,2-dichloroethylene may be accounted for through combination of chloromethylene. Statistically, one would expect the yield of each to be approximately equivalent which, as illustrated by the comparable intensities of their respective peaks in the gas chromatogram (Figure 4.1), is indeed the case.

It is well known that carbenes can abstract atomic hydrogen [18]; the successive abstraction of hydrogen atoms by chloromethylene may account for the formation of chloromethane. It is conceivable that carbenes abstract atomic chlorine given that the enthalpy of the C–Cl bond is considerably lower than that of the C–H bond [19]. The abstraction of atomic chlorine by chloromethylene will afford the dichloromethyl radical,

an intermediate proposed in the decomposition of dichloroacetaldehyde. In addition to combination, the dichloromethyl radical may abstract H or Cl to generate dichloromethane or chloroform, respectively. It is difficult to define the precise mechanism of pyrolysis for chloroacetyl chloride given that each of the proposed pathways is practicable. Consequently, a pyrolysis scheme is proposed that incorporates all possible mechanisms, and is illustrated in Figure 4.2.

4.2.2 Co-pyrolysis with $W(CO)_6$

In the present work, the stable products of chloroacetyl chloride IR LPHP in the presence of $W(CO)_6$ were identified as acetyl chloride, chloroacetaldehyde, dichloromethane, chloromethane, 1,2-dichloroethane, chloroethene, ethylene, propene, ethane, methane and CO. There were no peaks in the post-pyrolysis infrared spectrum or gas chromatogram that were attributable to chloroketene and HCl; trichloroethene, *E* and *Z*-1,2-dichloroethene, 1,2-tetrachloroethane and chloroform were observed in only trace amount. The absence of the HCl suggests that molecular dehydrochlorination is inhibited when $W(CO)_6$ is present.

These results are consistent with the selective abstraction of atomic chlorine at C(1) or C(2) to form the 2-chloro-1-oxoethyl or 2-chloro-2-oxoethyl radicals, respectively. It is evident from experimental observation that the elimination of a second chlorine atom does not immediately follow the elimination of the first. The molecular elimination of CO from either 2-chloro-1-oxoethyl or 2-chloro-2-oxoethyl will yield the chloromethyl radical; this either combines to yield 1,2-dichloroethane, or abstracts H or Cl to form chloromethane or dichloromethane, respectively. The formation of dichloromethane is also consistent with the decarbonylation of chloroacetyl chloride. The generation of chloroacetaldehyde and

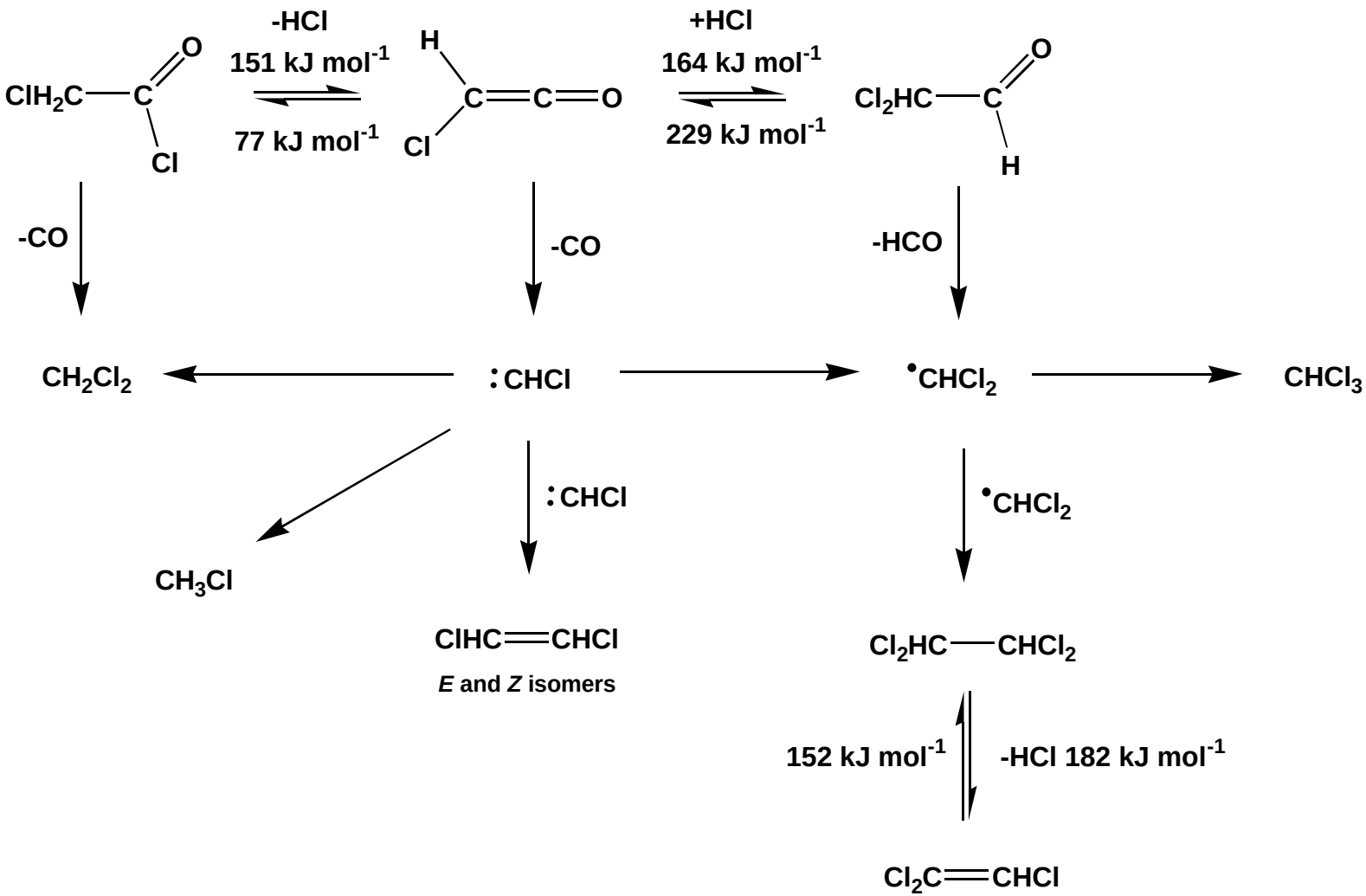

Figure 4.2 A proposed scheme for chloroacetyl chloride IR LPHP with calculated activation energies for reversible dehydrochlorination

acetyl chloride, albeit in trace amount, suggests that the elimination of molecular CO from 2-chloro-1-oxoethyl and 2-chloro-2-oxoethyl may be preceded by the abstraction of atomic hydrogen.

It is apparent from experimental observation that the abstraction of atomic chlorine from starting material is not unique; peaks in the post-pyrolysis gas chromatogram ascribed to 1,2-dichloroethane, dichloromethane, chloromethane and chloroethene decreased as the duration of pyrolysis was extended. A concomitant increase in bands attributable to the non-chlorinated alkanes and alkenes was also observed. The selective abstraction of atomic chlorine from chloroethene will afford the vinyl radical. The rates of formation of the combination and disproportionation products are proportional to the radical concentration [20]; consequently, the absence of 1,3-butadiene and acetylene (ascribed to combination and disproportionation of vinyl radicals) suggest that the mechanism responsible for the formation of vinyl radicals is a minor pathway. It is possible that vinyl radicals in low concentration abstract atomic hydrogen to yield the observed ethylene.

The abstraction of atomic chlorine from chloromethane and 1,2-dichloroethane will afford the methyl and 2-chloroethyl radicals, respectively. The methyl radical either combines, or abstracts atomic hydrogen to generate the observed methane. The homolytic fragmentation of 2-chloroethyl through cleavage of the C–Cl or C–H bond will afford ethylene or chloroethene, respectively. Theoretical calculations by Seetula [21] have shown that the predominant decomposition route for a β-chlorinated ethyl radical is through scission of the weakest bond, specifically C_β–Cl; however, an alternative route through C_β–H dissociation is also practicable, given the relatively low enthalpy of that bond [19]. The absence of chloroethane and 1,4-dichlorobutane preclude the disproportionation and

combination of 2-chloroethyl, and suggest that the mechanism responsible for its production (specifically, the selective abstraction of Cl from 1,2-dichloroethane) is a minor pathway.

It is apparent from the low level of propene observed in the post-pyrolysis spectrum and gas chromatogram of chloroacetyl chloride and $W(CO)_6$ that the mechanism involved is minor. The addition of methyl to ethylene with homolytic cleavage of the C_β–H bond in the resultant addend may account for the observed propene. The rate constant associated with each process can be calculated using the Arrhenius equation:

$$k = \mathrm{A}\exp(-\mathrm{E}/\mathrm{RT})$$

The pre-exponential factors (A) and activation energies (E) of methyl addition and C_β–H scission have been determined by Westly and co-workers [22] and Warnatz [23], respectively. In the present study, the reaction temperature was estimated to be approximately 550 K; an investigation into the pyrolysis of *E*-1,2-dichloroethene and $W(CO)_6$ (refer to section 3.4) concluded that the effective temperature of reaction at a slightly higher laser power was of the order of 650 ± 150 K. The resultant rate constant for methyl addition is $2.5 \cdot 10^8$ cm^3 $molecule^{-1}$ s^{-1}, while that associated with fragmentation of the C_β–H bond is 0.15 s^{-1}. The magnitude of the rate-limiting step, specifically the elimination of atomic hydrogen, is such that the mechanism responsible for the production of propene is practicable; the trace quantity observed reflects the low level of ethylene present. A proposed scheme for chloroacetyl chloride and $W(CO)_6$ IR LPHP is given in Figure 4.3.

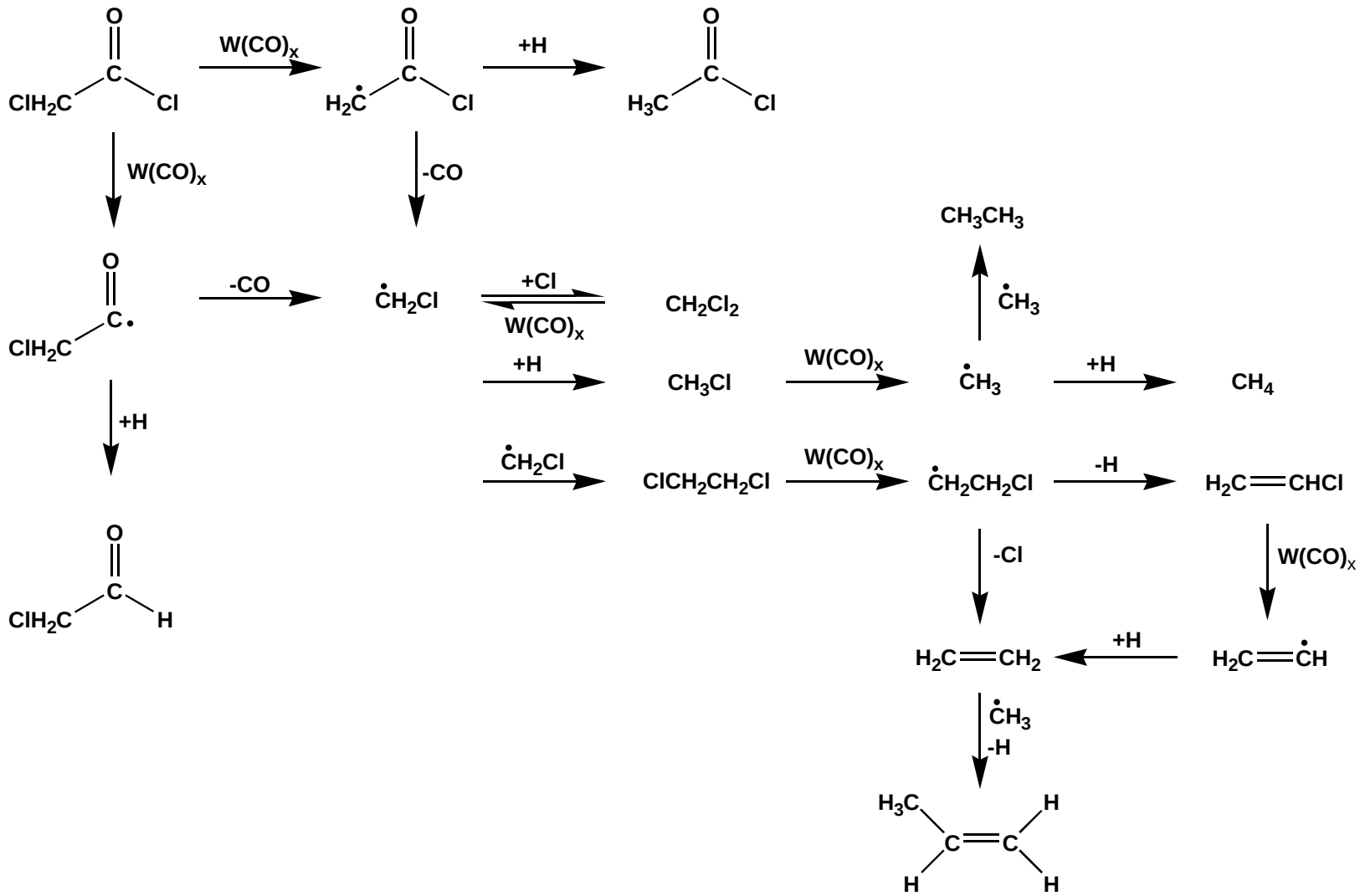

Figure 4.3 A proposed scheme for chloroacetyl chloride and $W(CO)_6$ IR LPHP

4.3 Propanoyl Chloride

Propanoyl chloride has been identified and utilised as a precursor to methyl ketene. Bock and co-workers observed that the thermal elimination of HCl from a number of acyl chlorides, including propanoyl chloride, generated the analogous ketene [24]. A radical mechanism was postulated to describe the dehydrohalogenation of the parent compound.

4.3.1 Pyrolysis

In the present study, the stable products of propanoyl chloride pyrolysis were identified as chloroethene, 1,3-butadiene, ethylene, acetylene and acrolein (2-propenal); the latter was less significant at higher temperature. The decarbonylation product, chloroethane, was detected in trace amount. A section of the post-pyrolysis FT-IR spectrum of propanoyl chloride in the absence and presence of $W(CO)_6$ is given in Figure 4.4. A transient band at 2133 cm^{-1} was ascribed to methylketene, and appeared to have a shorter lifetime than chloroketene.

Methylketene was also detected directly by IR spectroscopy in an Ar matrix (dilution 2000 : 1). At 16 K, an absorbance band at 2124 cm^{-1} with a shoulder at 2129 cm^{-1}, attributable to the cumulenic stretch, ν_2, of methylketene, was observed. Two weaker peaks were observed at 2137 and 2144 cm^{-1}, the former ascribed to CO. Johnstone and Sodeau detected absorbance bands in the post-photolysis spectrum of acrolein, at 2126 and 2129 cm^{-1} that they ascribed to methylketene [25]. The appearance of two additional signals at 2138 and 2146 cm^{-1}, the former ascribed to CO, and the latter a complexed

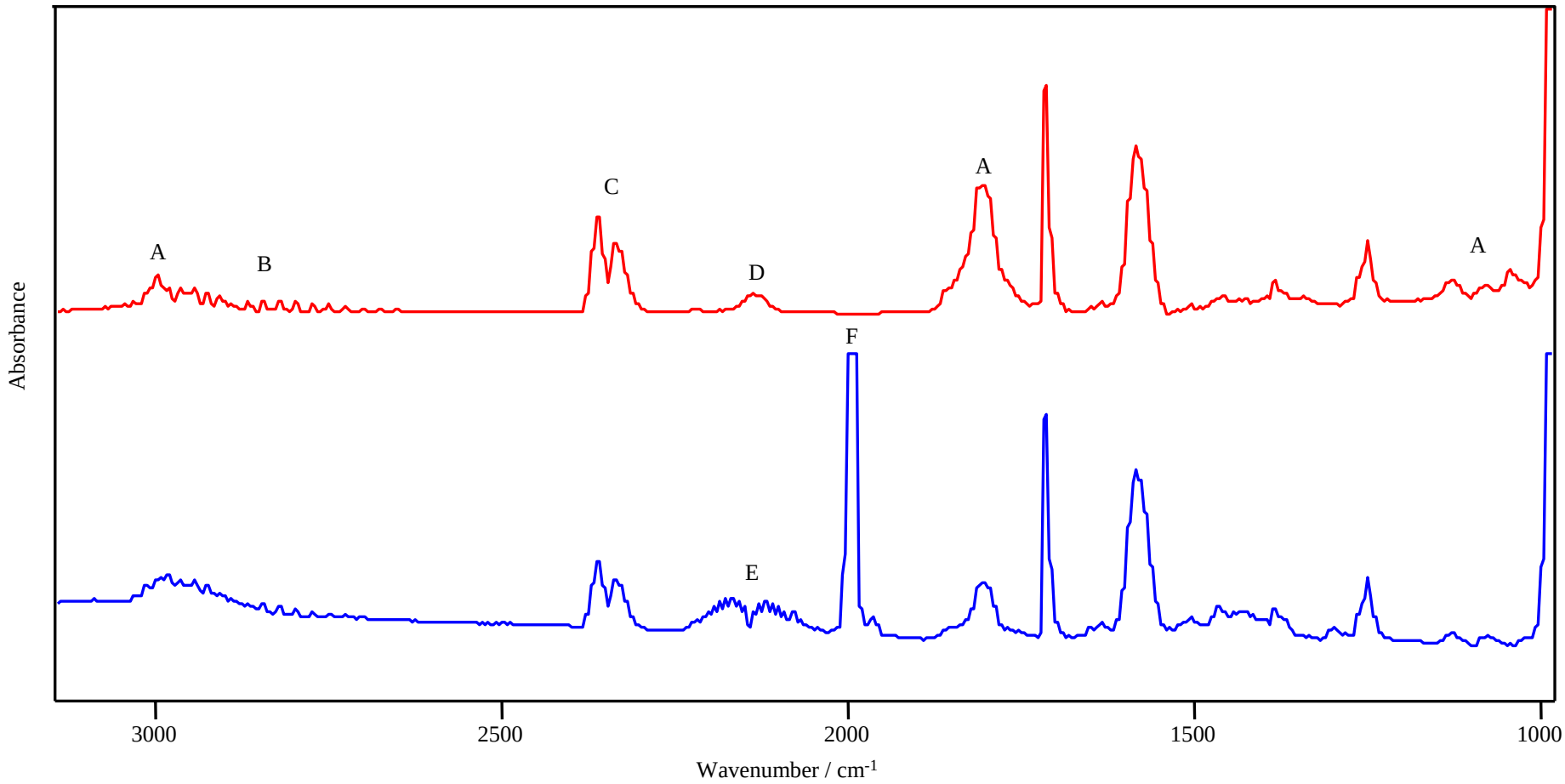

Figure 4.4 FT-IR spectra of the products of laser pyrolysis of propanoyl chloride in the absence (—) and presence (—) of $W(CO)_6$; A = propanoyl chloride; B = HCl; C = CO_2; D = methyl ketene; E = CO; F = $W(CO)_6$; unassigned peaks are attributable to SF_6; the small amount of HCl evident in the lower trace was present in the original sample; the CO_2 present is atmospheric in nature

CO-ethylidene pair, was also reported. The absorbance band at 2144 cm^{-1} observed in the present work coincides approximately with that observed by Johnstone and Sodeau.

In the present work, the IR LPHP of propanoyl chloride was monitored *in situ* by TDL spectroscopy. At 2122 and 2145 cm^{-1}, a blanket absorption was observed when the contents of the cell were exposed to the output of a CW CO_2 laser; this is ascribed to methylketene. Individual peaks were resolved using a lock in amplifier. The high resolution spectrum of methyl ketene is shown in Figure 4.5. Subsequent to irradiation the spectrum returned to its original state within several minutes.

The formation of methylketene is consistent with the molecular elimination of HCl from propanoyl chloride. The increase in propanoyl chloride at the expense of methylketene and HCl as the spectrum was acquired, indicates the reversibility of dehydrochlorination. Theoretical investigations predict that the predominant reaction of methylketene and HCl will yield propanoyl chloride as opposed to 2-chloropropanal, the latter consistent with *anti*-Markovnikov addition. It is possible that the activation barrier to formation of 2-chloropropanal is overcome at elevated temperature; the fact that this compound was not detected suggests that it will decompose under these conditions. The molecular elimination of HCl from 2-chloropropanal will yield methylketene or acrolein (2-propanal), the latter consistent with dehydrochlorination across the C(2)–C(3) bond. An alternative formation mechanism for acrolein involves a 1,3-H shift in propanoyl chloride.

The homolytic cleavage of the C(1)–C(2) bond in acrolein will yield the formyl and vinyl radicals [26]; similarly, homolytic fragmentation of 2-chloropropanal will yield the formyl and α-chlorinated ethyl radicals. Seetula [21] has shown that the predominant

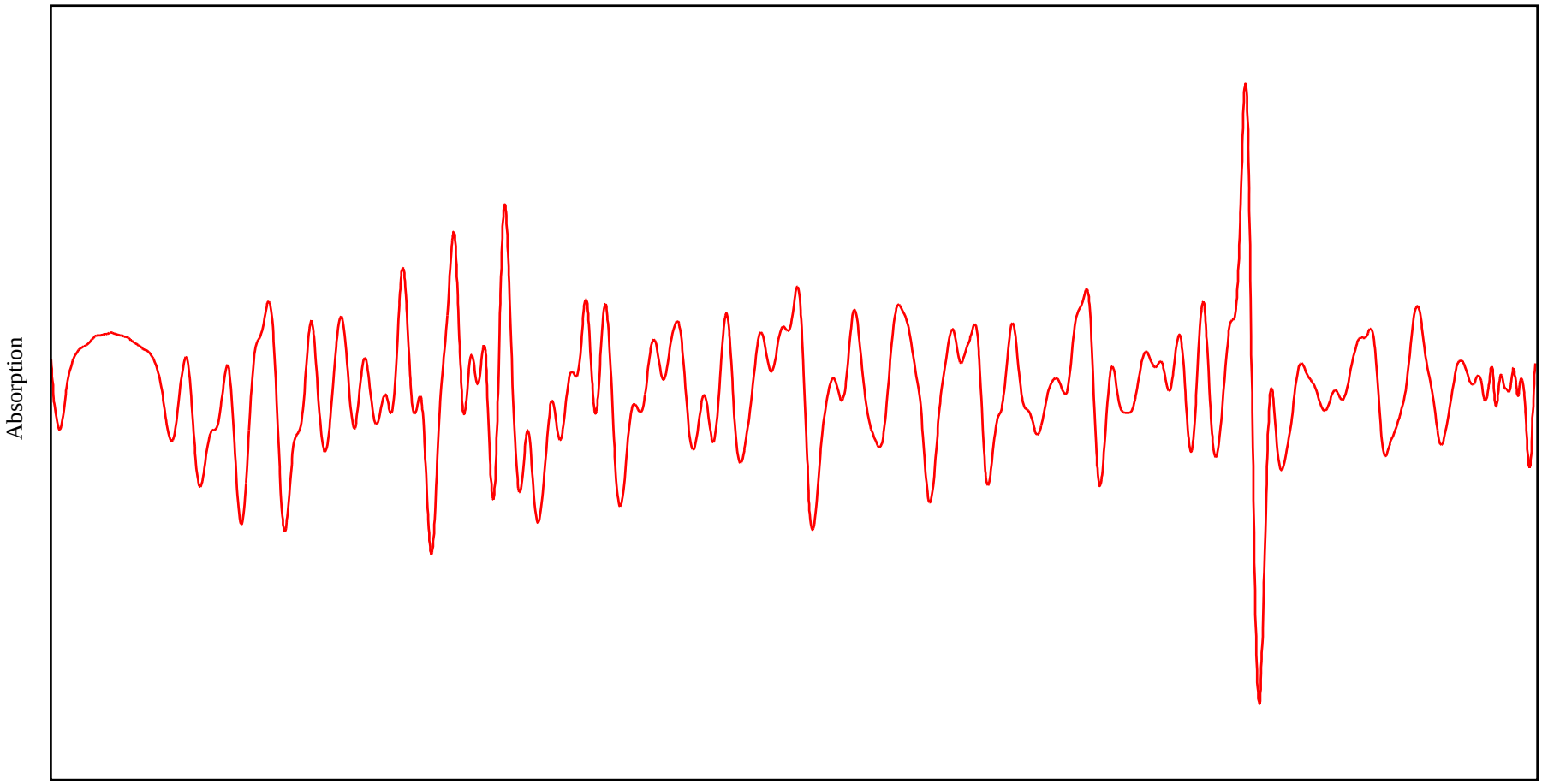

Figure 4.5 High resolution spectrum (centred at 2124 cm^{-1}) of methyl ketene

decomposition route for a α-chlorinated ethyl radical is through scission of the C_β–H bond (the weakest bond) to yield chloroethene, a significant product in this investigation. The formation of acetylene and ethylene, and 1,3-butadiene is consistent, respectively, with the disproportionation and combination of vinyl radicals. It is likely, therefore, that the formation mechanism (specifically, elimination of HCO from acrolein) is significant, resulting in a high concentration of vinyl radicals. The formation of ethylene is also consistent with the decarbonylation of methylketene, followed by rearrangement of the resultant ethylidene species. A proposed scheme for IR LPHP of propanoyl chloride is given in Figure 4.6.

4.3.2 Co-pyrolysis with $W(CO)_6$

In the present investigation, the stable products of propanoyl chloride and $W(CO)_6$ IR LPHP were identified using FT-IR and GC-MS spectroscopy as CO, ethylene, ethane, *n*-butane, propene and C_4H_8 isomers, namely 2-methyl-1-propene, 1- and 2-butene. The decarbonylation product, chloroethane was characterised by a weak signal in the gas chromatogram. The post-pyrolysis spectrum of propanoyl chloride and $W(CO)_6$ was devoid of peaks ascribed to methyl ketene or HCl, the products expected from molecular dehydrochlorination of starting material.

The pyrolysis of propanoyl chloride and $W(CO)_6$ is initiated through the selective abstraction of atomic chlorine effecting formation of the propanoyl radical. The subsequent decarbonylation of propanoyl generates ethyl, which can undergo disproportionation, combination or decomposition. The latter is known to proceed, primarily, through the elimination of atomic hydrogen to yield ethylene [27-33]. Feng and co-workers [33] have

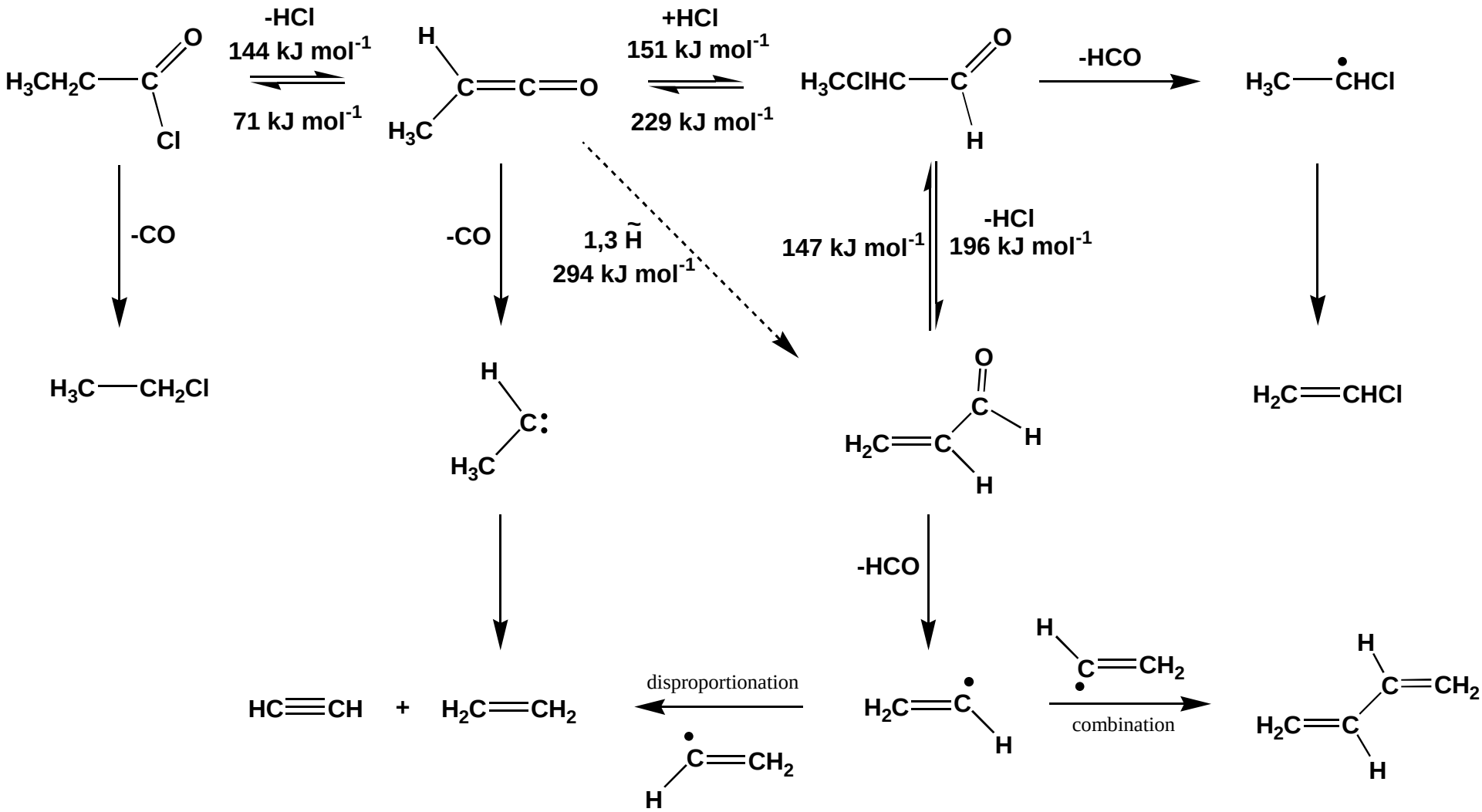

Figure 4.6 A proposed scheme for propanoyl chloride IR LPHP with calculated activation energies for reversible dehydrochlorination and 1,3-hydrogen migration

derived expressions for the low and high pressure limit rate constants of unimolecular decomposition of the ethyl radical between 198 and 1100 K:

$$k^0 = 6.63 \cdot 10^9 \, \mathrm{T}^{-4.99} \exp(-20130/\mathrm{T}) \, \mathrm{cm}^3 \text{ molecule} \, \mathrm{s}^{-1}$$

$$k^\infty = 1.11 \cdot 10^{10} \, \mathrm{T}^{1.037} \exp(-18504/\mathrm{T}) \, \mathrm{s}^{-1}$$

A plot of the reported values of *k* against the pressure of ethane (a precursor to ethyl) was reported; for a total pressure exceeding 1 Torr the rate constant was calculated at the high-pressure limit. In the present study, the rate constant of ethyl decomposition was determined using the expression at the high-pressure limit as the total pressure invariably exceeded 10 Torr. The pyrolysis of propanoyl chloride in the presence of $W(CO)_6$ was initiated at a similar laser power, and therefore temperature, to that required to initiate pyrolysis of chloroacetyl chloride in the presence of $W(CO)_6$. The temperature in the latter case was estimated to be of the order of 550 K (refer to section 4.2.2); consequently, the limiting high-pressure rate constant for IR LPHP initiated ethyl decomposition was calculated at 0.0189 s^{-1}.

Tsang and Hampson [34] have determined the rate constants for ethyl combination and disproportionation at $300 < T < 1000$ K as respectively, $1.8 \cdot 10^{-11}$ cm^3 $molecule^{-1}$ s^{-1} and $0.23 \cdot 10^{-11}$ cm^3 $molecule^{-1}$ s^{-1}. These values are significantly lower than that associated with ethyl decomposition. This is reflected in the distribution of products; the generation of ethylene far surpassed *n*-butane and ethane. The disproportionation of ethyl will afford ethylene in addition to ethane; consequently, it is difficult to compare the ratio of ethylene to ethane and *n*-butane (by relating their respective peak areas in the post-pyrolysis gas chromatogram) with the expected distribution of products based on the ratio of rate

constants. The disproportionation to combination ratio of ethyl, which is reported to be in the range of 0.13 to 0.14 [34-36], predicts preferential formation of *n*-butane. The fact that ethane was detected at a greater level than *n*-butane suggests an additional pathway to ethane, most probably, involving abstraction of atomic hydrogen by the ethyl radical.

The formation of propene can be rationalised in terms of radical addition; the addition of methyl to ethylene will yield propene, following homolytic cleavage of a C_β–H bond in the resultant addend. The rate-limiting step is scission of the C–H bond, and was calculated in section 4.2.2 as 0.15 s^{-1} at 550 K. This is significantly higher than the rate constants associated with ethyl disproportionation, combination or decomposition. Consequently, it is expected that the mechanism responsible for the production of propene is significant. The magnitude of the bands ascribed to propene observed in the post pyrolysis spectrum and gas chromatogram of propanoyl chloride in the presence of $W(CO)_6$ suggest that this is indeed the case.

It is necessary to account for the formation of the methyl radical, if the mechanism proposed for the production of propene is accepted. Tsang and Kiefer [37] have investigated the unimolecular reactions of large polyatomic molecules, including those of the ethyl radical. The unimolecular rate expressions for the decomposition of larger radicals were found to have activation energies of the order of 120-160 kJ mol^{-1} and normal pre-exponential factors. It was proposed that such moieties were significantly less stable than the comparable alkanes and alkenes, and would rapidly generate highly reactive species such as methyl or atomic hydrogen. Consequently, decomposition of the ethyl radical may yield methyl and methylene through homolytic cleavage of the carbon-carbon bond; dimerisation of the latter will afford ethylene.

The production of the C_4H_8 isomers may be accounted for through the addition of methyl to propene with loss of atomic hydrogen from the resultant addend. The isomeric distribution is dependent on which carbon the methyl radical appends to, and on which hydrogen atom is successively eliminated. According to the Hammond postulate, the structure of a transition state will resemble the structure of the nearest stable species; an endothermic process will have a transition state that resembles products, in contrast to the transition state of an exothermic step that will resemble starting materials [19]. While addition of the methyl radical to propene is slightly exothermic, there is a certain amount of developing radical character in the transition state and, consequently, the transition state for methyl addition will structurally resemble the radical product. The factors that increase the stability of the radical intermediate will also stabilise the nearby transition state and thereby promote reaction. Increasing alkyl substitution is known to stabilise an alkyl radical [19]; consequently, the addition of methyl to propene will occur predominantly at the least substituted carbon effecting formation of the more stable 1-methylpropyl radical. An additional bond can form with concomitant loss of atomic hydrogen, between C(2) and C(1) or C(3) of 1-methylpropyl affording 1- and 2-butene, respectively.

The addition of methyl to propene at the more highly substituted carbon will effect formation of the less stable radical, 2-methylpropyl. The elimination of atomic hydrogen from the resultant addend will afford 2-methyl-1-propene, exclusively. The ratio of the rates of attack at each end of the olefin is known to be dependent on the temperature [20]; as the temperature is raised, the ratio will approach 1 : 1. It is evident from experimental observation, specifically the fact that the ratio of 1- and 2-butene to 2-methyl-1-propene was approximately equivalent, that addition of the methyl radical to propene does not

occur at one end of the olefin in preference to the other. A proposed scheme for propanoyl chloride pyrolysis in the presence of $W(CO)_6$, is given in Figure 4.7.

4.4 3-Chloropropanoyl Chloride

Piétri and co-workers have recently investigated the photolysis of matrix isolated 3-chloropropanoyl chloride [38]. At $\lambda > 230$ nm, the primary products were reported as acryloyl chloride and 3-chloro-1-propen-1-one [39], attributable respectively to elimination of HCl across the C(2)–C(3) and C(1)–C(2) bond (numbered from the oxygen-bearing carbon). Subsequent decarbonylation of the latter yields 2-chloroethylidene that can rearrange to the observed chloroethene. Piétri and co-workers also observed methylene ketene (1,2-propadien-1-one) and contended that the formation of such was attributed to the dehydrochlorination of acryloyl chloride. A thorough search of the literature has failed to find any other reference to the decomposition of 3-chloropropanoyl chloride, with the exception of a patent detailing the preparation of acryloyl chloride from gas phase dehydrochlorination of 3-chloropropanoyl chloride [40].

4.4.1 Pyrolysis

In the present work, the most significant products detected following the pyrolysis of 3-chloropropanoyl chloride at low temperature was acryloyl chloride; chloroethene was the major product at higher laser power. The formation of the latter is consistent with the decarbonylation of acryloyl chloride; molecular elimination of HCl across the C(2)–C(3) bond of 3-chloropropanyol chloride will effect the formation of acryloyl chloride. In

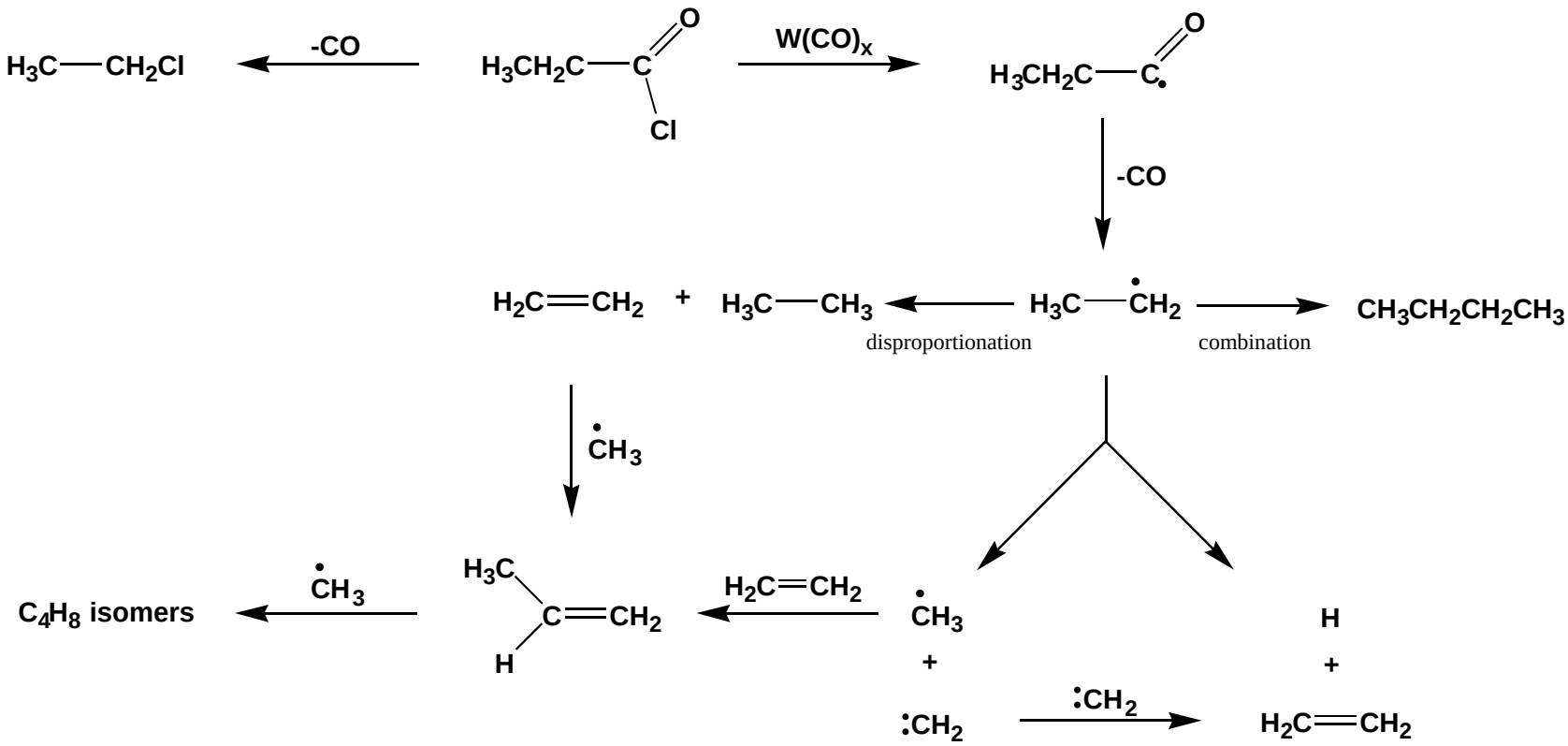

Figure 4.7 A proposed scheme for propanoyl chloride and $W(CO)_6$ IR LPHP

contrast to the post-pyrolysis spectra of chloroacetyl and propanoyl chloride, there were no absorbance bands attributable to a short-lived ketene species in the infrared spectrum at ambient temperature.

The low temperature post-pyrolysis FT-IR spectrum of 3-chloropropanoyl chloride, which is shown in Figure 4.8, revealed a series of absorbance bands between 2200 and 2100 cm^{-1}. Reaction was initiated at 748 K and the pyrolysate co-deposited with Ar (dilution 2000 : 1) at 16 K. The most intense band at 2122 cm^{-1} was attributable to the cumulenic stretch, ν_2, of methylene ketene, and is in agreement with the value (ascribed to the uncomplexed product) reported by Chapman and co-workers [41]. The formation of methylene ketene is consistent with the dehydrochlorination of acryloyl chloride. Subsequent decarbonylation of methylene ketene will yield ethenylidene that rearranges to the observed acetylene.

A number of weaker absorbance signals were also present at 2099, 2137, 2141 (shoulder) and 2169 cm^{-1}. In experiments initiated at a higher temperature, a weak band at 2147 cm^{-1} was observed that has yet to be identified. The peaks at 2137 and 2141 cm^{-1} are ascribed to uncomplexed CO and ketene respectively; the spectrum of an authentic sample of each, isolated in an Ar matrix, is spectroscopically identical with those peaks observed in the post-pyrolysis spectrum. The trace peak at 2099 cm^{-1} may be ascribed to complexed methylene ketene; Piétri and co-workers [42] proposed a propadienone-HCl complex to account for the signal observed at 2102 cm^{-1}.

The band at 2169 cm^{-1} is ascribed to 3-chloro-1-propen-1-one; this is consistent with the molecular dehydrochlorination of 3-chloropropanoyl chloride across the C(1)–C(2) bond, or a 1,3-chlorine shift in acryloyl chloride. In the present work, the cumulenic stretch of

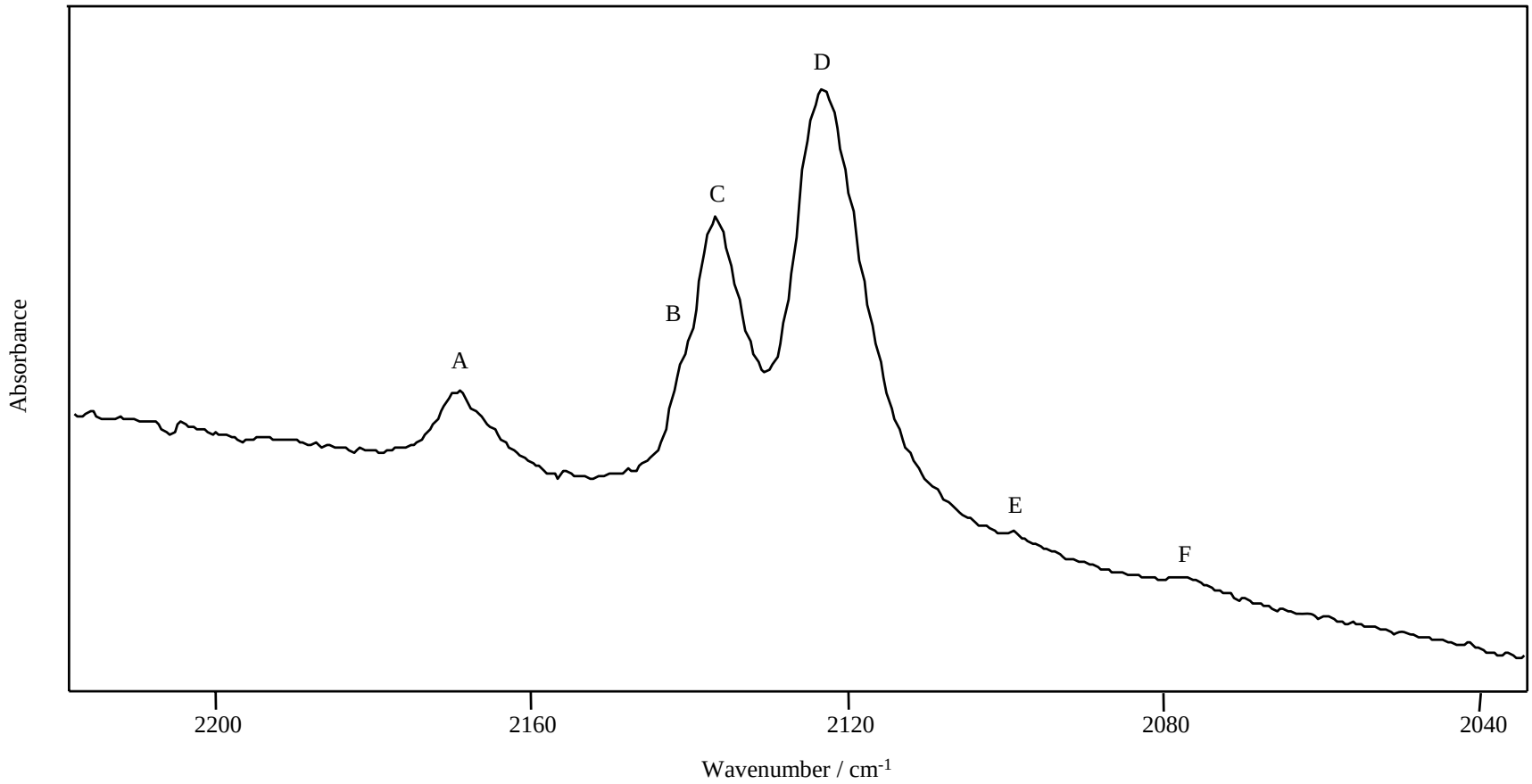

Figure 4.8 FT-IR spectrum of Ar matrix trapped (16 K) 3-chloropropanoyl chloride after pyrolysis at 748 K;
A = 3-chloro-1-propen-1-one; B = ketene; C = CO; D = methylene ketene; E = methylene ketene-HCl complex; F = acryloyl chloride

3-chloro-1-propen-1-one with scaling [43] was calculated at 2148 cm^{-1} and is in reasonable agreement with that observed. The Cartesian coordinates for 3-chloro-1-propen-1-one are given in Table 4.1. The activation barrier value of the proposed 1,3-chlorine shift must be considered; semi-empirical calculations predict that such a mechanism has a comparable activation energy to that associated with the molecular dehydrochlorination of 3-chloropropanoyl chloride and, consequently, represents a practicable pathway. It is conceivable that the formation of 3-chloro-1-propen-1-one also involve *anti*-Markovnikov addition of HCl to the C(2)–C(3) of methylene ketene, the most significant product of a transient nature observed in the post-pyrolysis spectrum. The molecular elimination of HCl from 3-chloro-1-propen-1-one will yield methylene ketene, while decarbonylation will effect the formation of 2-chloroethylidene that rapidly rearranges to chloroethene.

Table 4.1 Cartesian coordinates (Angstroms) for 3-chloro-1-propen-1-one

Atom	X	Y	Z
H 1	0.8238401	0.0767211	-1.7994989
C 2	0.5107775	-0.2331663	-0.7878554
H 3	0.4687527	-1.3354491	-0.7678406
C 4	-0.7571144	0.4057401	-0.4092048
Cl 5	1.7900413	0.2886131	0.3629904
C 6	-1.6920255	-0.2172845	0.2843537
H 7	-0.9176671	1.4547907	-0.6788867
O 8	-2.5394028	-0.7672393	0.8752395

In the present work, IR LPHP of 3-chloropropanoyl chloride was monitored *in situ* by TDL spectroscopy. At 2145 cm^{-1}, a series of minor absorption bands, attributable to ketene

(ethenone), developed while the contents of the cell were exposed to the output of a CW CO_2 laser. The spectrum obtained was spectroscopically identical to that observed for a pure sample of ketene, procured through the pyrolysis of acetyl chloride. Within ten minutes of the cessation of irradiation, the absorption bands attributable to ketene had disappeared. A proposed scheme for the pyrolysis of 3-chloropropanoyl chloride, excluding the mechanism responsible for ketene formation, is given in Figure 4.9.

4.4.2 Co-pyrolysis with $W(CO)_6$

The stable products derived from the pyrolysis of 3-chloropropanoyl chloride in the presence of $W(CO)_6$ were identified as CO, propanoyl chloride, chloroethene and ethylene. The level of chloroethene present was significantly greater than in the post-pyrolysis spectrum of 3-chloropropanoyl chloride in the absence of $W(CO)_6$. The gas chromatogram revealed a number of diminutive peaks that are ascribed to the pyrolysis products of propanoyl chloride and $W(CO)_6$, intensifying as the duration of pyrolysis was prolonged. The formation of HCl in only trace amount ostensibly precludes molecular dehydrochlorination of acryloyl chloride.

The pyrolysis of 3-chloropropanoyl chloride in the presence of $W(CO)_6$ is initiated through the selective abstraction of Cl from C(1) or C(3) to afford the 3-chloro-1-oxopropyl or 3-chloro-3-oxopropyl radicals, respectively. In an manner analogous to the pyrolysis of chloroacetyl chloride and $W(CO)_6$, it is evident that the elimination of a second chlorine atom is preceded by the decarbonylation of the intermediary radical, in each case affording the 2-chloroethyl radical. The presence of propanoyl chloride, albeit in trace amount, suggests that 3-chloro-3-oxopropyl is able to abstract atomic hydrogen prior to

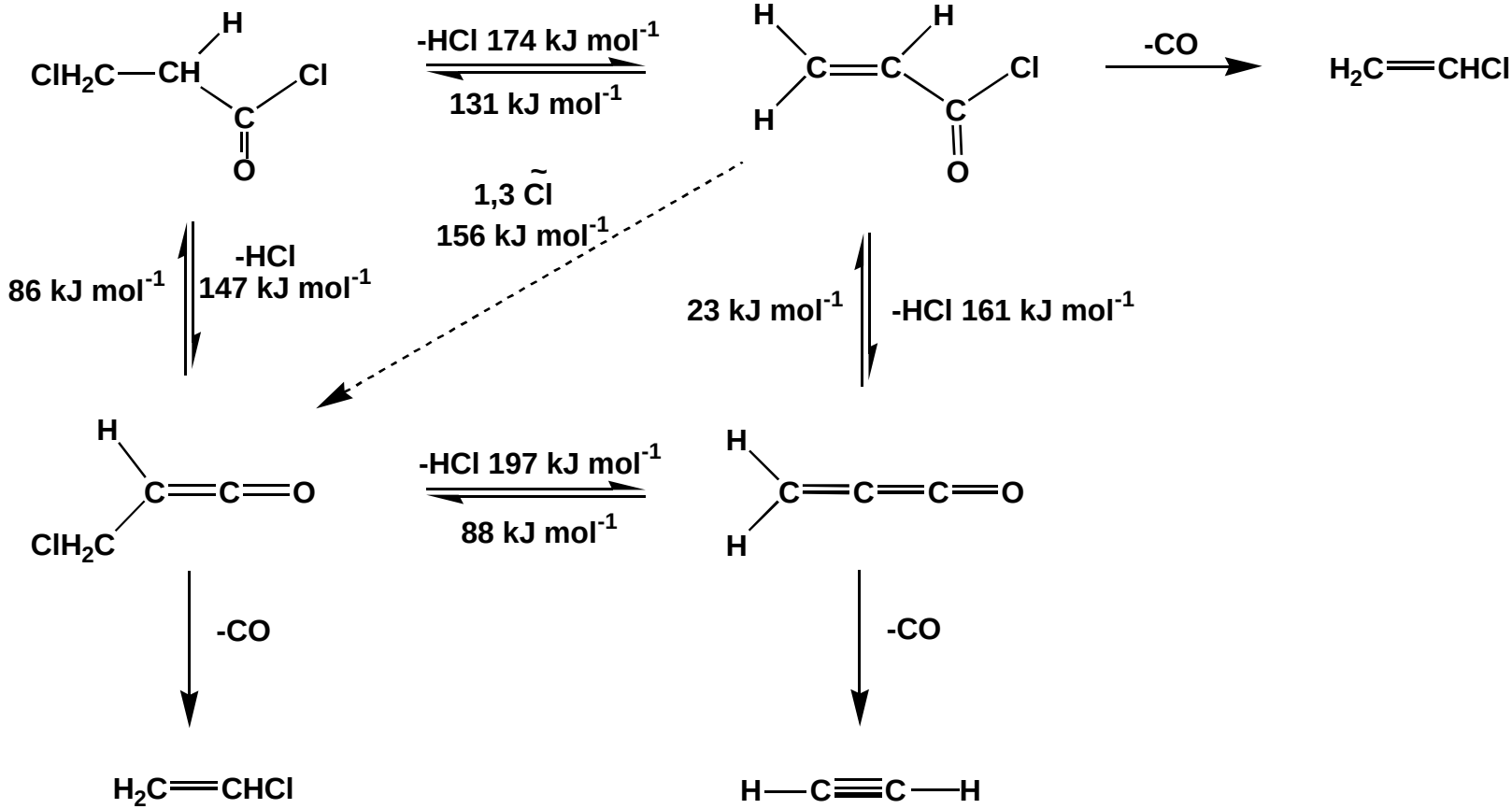

Figure 4.9 A proposed scheme for 3-chloropropanoyl IR LPHP with calculated activation energies for dehydrochlorination and 1,3-chlorine migration

decarbonylation. Conversely, the absence of 3-chloropropanal, the product generated from the abstraction of atomic hydrogen by the 3-chloro-1-oxopropyl radical, suggests that the latter is less stable than 3-chloro-3-oxopropyl.

The subsequent decomposition of 2-chloroethyl, an intermediate also postulated in the pyrolysis of chloroacetyl chloride and $W(CO)_6$, involves the elimination of atomic hydrogen or chlorine to afford chloroethene or ethylene, respectively. The predominant decomposition mechanism of a β-chlorinated ethyl radical is through scission of the C_β–Cl bond, which will afford ethylene [21]. The dissociation of C_β–H is a practicable route, given the relatively low bond enthalpy [19], and will yield chloroethene. The absence of chloroethane and 1,4-dichlorobutane, further reinforce the conclusion drawn from the pyrolysis of chloroacetyl chloride and $W(CO)_6$ (refer to section 4.2.2); namely, that the disproportionation and combination of 2-chloroethyl is not a practicable pathway.

It is evident from experimental observation that the selective abstraction of atomic chlorine from starting material is not unique; peaks in the post-pyrolysis infrared spectrum that were attributed to chloroethene were found to decrease, albeit marginally, as the duration of pyrolysis was increased. A corresponding increase in those bands ascribed to ethylene was observed over the same period. The vinyl radical generated from the abstraction of atomic chlorine from chloroethene can theoretically undergo disproportionation or combination effecting the formation of acetylene and ethylene, and 1,3-butadiene, respectively. In a manner analogous to the pyrolysis of chloroacetyl chloride and $W(CO)_6$, the exclusive generation of ethylene suggests that neither mechanism operates under these conditions. An alternative mechanism, in which the vinyl radical abstracts atomic hydrogen, may account for the formation of ethylene. The absence of acetylene suggests

that the elimination of atomic hydrogen from the vinyl radical is not a predominant mechanism under these conditions. A proposed pyrolysis scheme for 3-chloropropanoyl chloride in the presence of $W(CO)_6$ is illustrated in Figure 4.10.

4.5 Acryloyl Chloride

The thermolysis of acryloyl chloride has been studied by Bock and co-workers [24]; the results of photoelectron spectroscopy suggest that the initial decomposition step, specifically the elimination of HCl, is simultaneously accompanied by the loss of CO. Ostensibly, the expected product of molecular dehydrochlorination, methylene ketene, was not detected.

In an investigation by Piétri and co-workers, it was shown that at $\lambda > 230$ nm acryloyl chloride was photolytically decomposed to 1,2-propadien-1-one via 1,2-HCl elimination and 3-chloro-1-propen-1-one [39] via 1,3-chlorine migration [42]. The latter was expeditiously decomposed to 2-chloroethylidene and CO at such wavelengths; rearrangement of the former afforded the observed chloroethene. The subsequent decarbonylation of methylene ketene yielded acetylene. The non-concerted mechanism inferred is inconsistent with that proposed by Bock and co-workers.

Piétri and co-workers were able to corroborate the presence of 3-chloro-1-propen-1-one by comparing the value calculated for the cumulenic stretch, specifically 2146 cm^{-1} (after scaling), with the absorbance bands observed in the infrared spectrum between 2139 and 2145 cm^{-1}. Moreover, 3-chloro-1-propen-1-one derived from the photolysis of

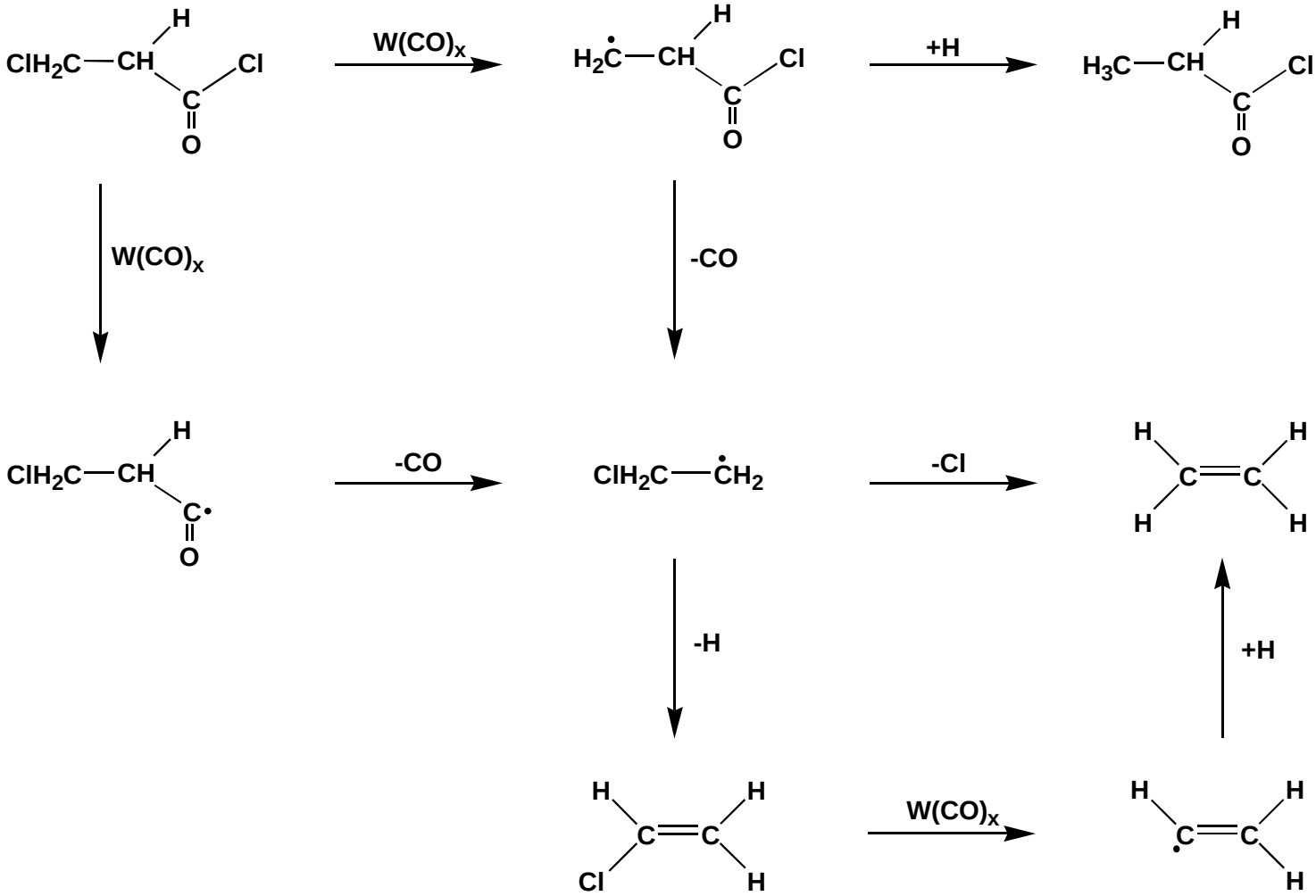

Figure 4.10 A proposed scheme for 3-chloropropanoyl chloride and $W(CO)_6$ IR LPHP

3-chloropropanoyl chloride at $\lambda > 230$ nm was reported to be spectroscopically similar to that observed from the photolytically induced 1,3-chlorine shift of acryloyl chloride. It is important to note, however, that the production of 3-chloro-1-propen-1-one from the photolysis of 3-chloropropanoyl chloride is accompanied by the formation of acryloyl chloride [38]. The decomposition of acryloyl chloride at $\lambda > 230$ nm effects the formation of methylene ketene and 3-chloro-1-propen-1-one [42]; consequently, it would appear that the execution of such an experiment so as to corroborate the existence of the latter is redundant.

4.5.1 Pyrolysis

In the present work, a sample of acryloyl chloride was exposed to the output of a CW CO_2 laser in the absence and presence of $W(CO)_6$. The products observed following the pyrolysis of acryloyl chloride in the absence of $W(CO)_6$ were entirely consistent with the chemistry associated with the decomposition of 3-chloropropanoyl chloride; the molecular dehydrochlorination of 3-chloropropanoyl chloride across the C(2)–C(3) bond was shown in section 4.4.1 to yield acryloyl chloride.

4.5.2 Co-pyrolysis with $W(CO)_6$

On co-pyrolysis with $W(CO)_6$ at much lower temperature, the most significant products were CO, 1,3-butadiene, ethylene and benzene; acetylene was detected in trace amount. Chloroethene, the decarbonylation product, was also observed. The absence of HCl precludes the molecular dehydrochlorination of acryloyl chloride in the presence of

$W(CO)_6$. The selective abstraction of atomic chlorine, followed by decarbonylation of the resultant species will afford the vinyl radical; this either undergoes combination or disproportionation, effecting the generation of 1,3-butadiene, or ethylene and acetylene, respectively. Several measurements of the rate constant of vinyl decay [44-48] and of the gas phase ratio of disproportionation to combination [46, 49-54] have been reported. The absolute rate constants of vinyl disproportionation and combination (as opposed to the rate constant of vinyl decay, where no distinction is made) are $1.8 \cdot 10^{-11}$ cm^3 $molecule^{-1}$ s^{-1} and $8.2 \cdot 10^{-11}$ cm^3 $molecule^{-1}$ s^{-1} at 298 K, respectively [46]; the resultant disproportionation to combination ratio is 0.22.

It is evident from experimental observation, that an additional mechanism is responsible for the formation of ethylene; the level of 1,3-butadiene (the combination product) was unexpectedly comparable to that of ethylene (a disproportionation product). The elevated temperature of reaction will affect the value of the rate constants, and may account for the difference; alternatively, an additional mechanism for ethylene production may be considered. The formation of ethylene is consistent with abstraction of atomic hydrogen by vinyl radicals.

The low level of acetylene observed is also consistent with a mechanism involving the trimerisation of acetylene to the observed benzene, a process well known to be catalysed by transition metals [55-60]. A proposed pyrolysis scheme for acryloyl chloride in the presence of $W(CO)_6$ is illustrated in Figure 4.11.

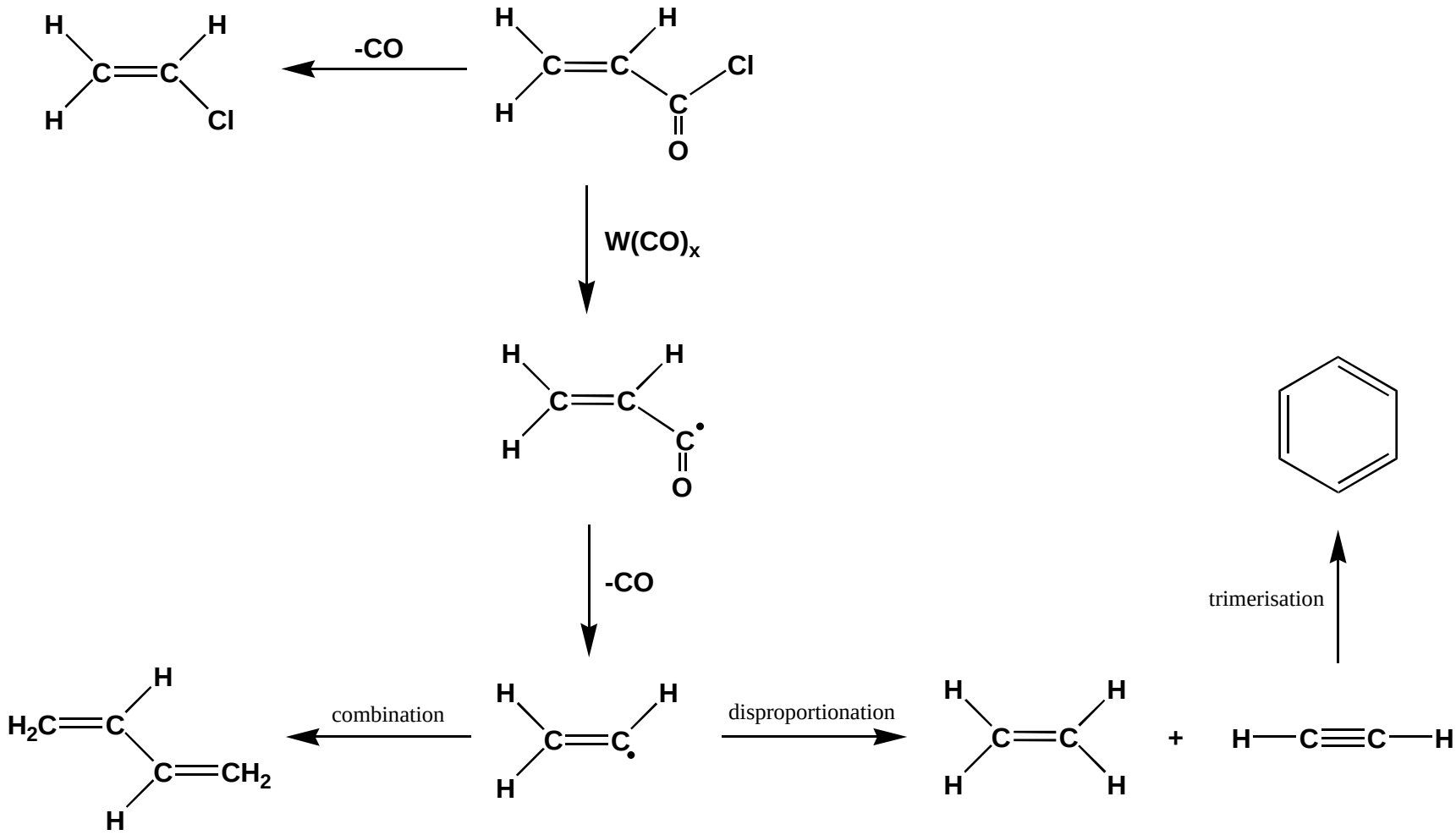

Figure 4.11 A proposed scheme for acryloyl chloride and $W(CO)_6$ IR LPHP

4.6 E-2-Butenoyl Chloride

The thermal or flash vacuum pyrolysis of *E*-2-butenoyl chloride has been investigated by a number of workers [61-63]. A combination of tandem mass spectrometry and low temperature (77 K) infrared spectroscopy was utilised by Maquestiau and co-workers to detect vinyl ketene and ethylidene ketene following flash vacuum pyrolysis [61, 62]. Ethylidene ketene, while observed by tandem mass spectroscopy, was not detected in the low temperature infrared spectrum; it was reasoned that the high efficiency of fragmentation of the ethylidene ketene ions would allow detection even if the concentration of such ions were extremely low. In the low temperature post-pyrolysis spectrum of *E*-2-butenoyl chloride, vinyl ketene was observed at 2118 cm^{-1}.

Mohmand and co-workers [63] used photoelectron spectroscopy to investigate the thermal decomposition of *E*-2-butenoyl chloride; the formation of ethylidene ketene was ascribed to 1,2-HCl elimination. Conversely, vinyl ketene, which was also observed, was consistent with 1,4-HCl elimination. Additionally, it was proposed that at higher temperature, ethylidene ketene rearrange to the thermodynamically more stable vinyl ketene.

4.6.1 Pyrolysis

In the present investigation, the stable products of *E*-2-butenoyl chloride pyrolysis were identified as HCl, CO, propyne and 3-butenoyl chloride; the trace amount of *Z*-2-butenoyl chloride observed is consistent with isomerisation of the starting material. The formation of allene at higher temperature is ascribed to the rearrangement of propyne; thermal interconversion of propyne and allene at high temperature is a well known process [64]. A

transient band at 2134 cm^{-1} is ascribed to vinyl ketene and appeared to have a much longer lifetime than either chloroketene or methylketene. In fact, when sufficient quantities were generated by extensive pyrolysis of the starting material, it was possible to detect vinyl ketene using GC-MS.

The formation of vinyl ketene is consistent with the molecular 1,4-elimination of HCl from *Z*-2-butenoyl chloride; the conformation of *E*-2-butenoyl chloride ostensibly precludes such a process. It is evident that the dehydrochlorination of *Z*-2-butenoyl chloride is rapid, as it was detected in only trace amount. The decarbonylation of vinyl ketene coupled with a hydrogen shift will afford propyne, a significant product in this investigation.

The low temperature post-pyrolysis FT-IR spectrum of *E*-2-butenoyl chloride revealed a number of bands between 2200 and 2100 cm^{-1}. The pyrolysate was co-deposited with Ar (dilution 2000 : 1) at 16 K. The most intense absorbance band at 2127 cm^{-1} is ascribed to uncomplexed vinyl ketene, and is in accord with the value reported by Maquestiau and co-workers [61, 62]. Brown and co-workers [65], and Bjarnov [66] have reported the infrared and microwave spectra of vinyl ketene generated by pyrolysis of vinylacetic anhydride. The cumulenic stretch of vinyl ketene in the gas phase was observed at 2137 cm^{-1} [66]; Brown and co-workers observed matrix-isolated (77 K) vinyl ketene at 2130 cm^{-1}.

A weak band that was observed at 2109 cm^{-1} is ascribed to ethylidene ketene; on annealing to 20 K, this peak decayed, to be replaced by a broad absorbance band at 2094 cm^{-1}. Wentrup and Lorencak observed ethylidene ketene at a comparable frequency, following the pyrolysis of an alternative precursor [67]. The formation of ethylidene ketene is

consistent with the molecular dehydrochlorination of *E*-2-butenoyl chloride across the C(1)–C(2) bond. The decarbonylation of ethylidene ketene will afford propenylidene that rapidly rearranges to propyne.

Vinyl ketene and ethylidene ketene, were also detected in a SF_6 matrix (dilution 2000 : 1) where initiation of reaction is homogeneous. At 16 K, a weak absorbance band at 2125 cm^{-1} was observed and ascribed to uncomplexed vinyl ketene; an intense band at 2100 cm^{-1} was assigned to ethylidene ketene. The relative intensities of the bands ascribed to vinyl and ethylidene ketene reflect a preference for ethylidene ketene formation, in contrast to isolation using an Ar matrix. It is conceivable, therefore, that the mechanism responsible for the formation of vinyl ketene, specifically molecular 1,4-elimination of HCl from *Z*-2-butenoyl chloride, is heterogeneous in nature.

In both an Ar and SF_6 matrix, vinyl ketene increased at the expense of ethylidene ketene on annealing the matrix to 25 K. In matrix experiments that utilised a restriction in the gas flow between reaction (the pyrolysis cell or furnace) and collection (the cold stage), the intensity of the peak assigned to ethylidene ketene was reduced; conversely, the band ascribed to vinyl ketene intensified. These results are consistent with the conversion of ethylidene ketene to vinyl ketene through a 1,3-hydrogen shift, and suggest that the lifetime of ethylidene ketene is brief and significantly more transient than that of vinyl ketene.

In contrast to the pyrolysis of chloroacetyl and propanoyl chloride, the decrease in bands assigned to the ketene was not accompanied by an increase in the bands ascribed to *E*-2-butenoyl chloride. This result precludes the addition of HCl to ethylidene ketene

across the C(1)–C(2) bond. The formation of 3-butenoyl chloride is consistent with Markovnikov addition of HCl to the less transient vinyl ketene across the C(1)–C(2) bond. The addition of HCl to vinyl ketene across the C(3)–C(4) bond, while affording either 4-chloro-1-buten-1-one or 3-chloro-1-buten-1-one (the latter in accord with Markovnikov's rule) can be discounted; there were no absorbance bands attributable to these products in the low temperature post-pyrolysis spectrum of *E*-2-butenoyl chloride. Moreover, theoretical calculations predict formation of 3-butenoyl chloride from the addition of HCl to vinyl ketene. A proposed scheme for the IR LPHP of *E*-2-butenoyl chloride is illustrated in Figure 4.12.

4.6.2 Co-pyrolysis with $W(CO)_6$

The products of *E*-2-butenoyl chloride and $W(CO)_6$ IR LPHP were characterised as benzene, CO, propene, 2-methyl-1-propene and the three stereoisomers of 2,4-hexadiene, the latter detected in trace amount. An increase in benzene at the expense of each of the stereoisomers of 2,4-hexadiene as the duration of pyrolysis was extended, suggests that the mechanism responsible involve decomposition of the latter. Stoichiometrically, the double elimination of molecular hydrogen from 2,4-hexadiene, with concurrent ring closure might account for the formation of benzene. The experimental techniques specific to this investigation are not capable of detecting molecular hydrogen, and consequently a definitive mechanism can not be established.

The formation of 2,4-hexadiene (*E,E*, *E,Z* and *Z,Z*) and propene is consistent with the selective abstraction of atomic chlorine to yield the 1-oxo-2-butenyl radical. The subsequent decarbonylation of 1-oxo-2-butenyl will yield the 1-propenyl radical; this either

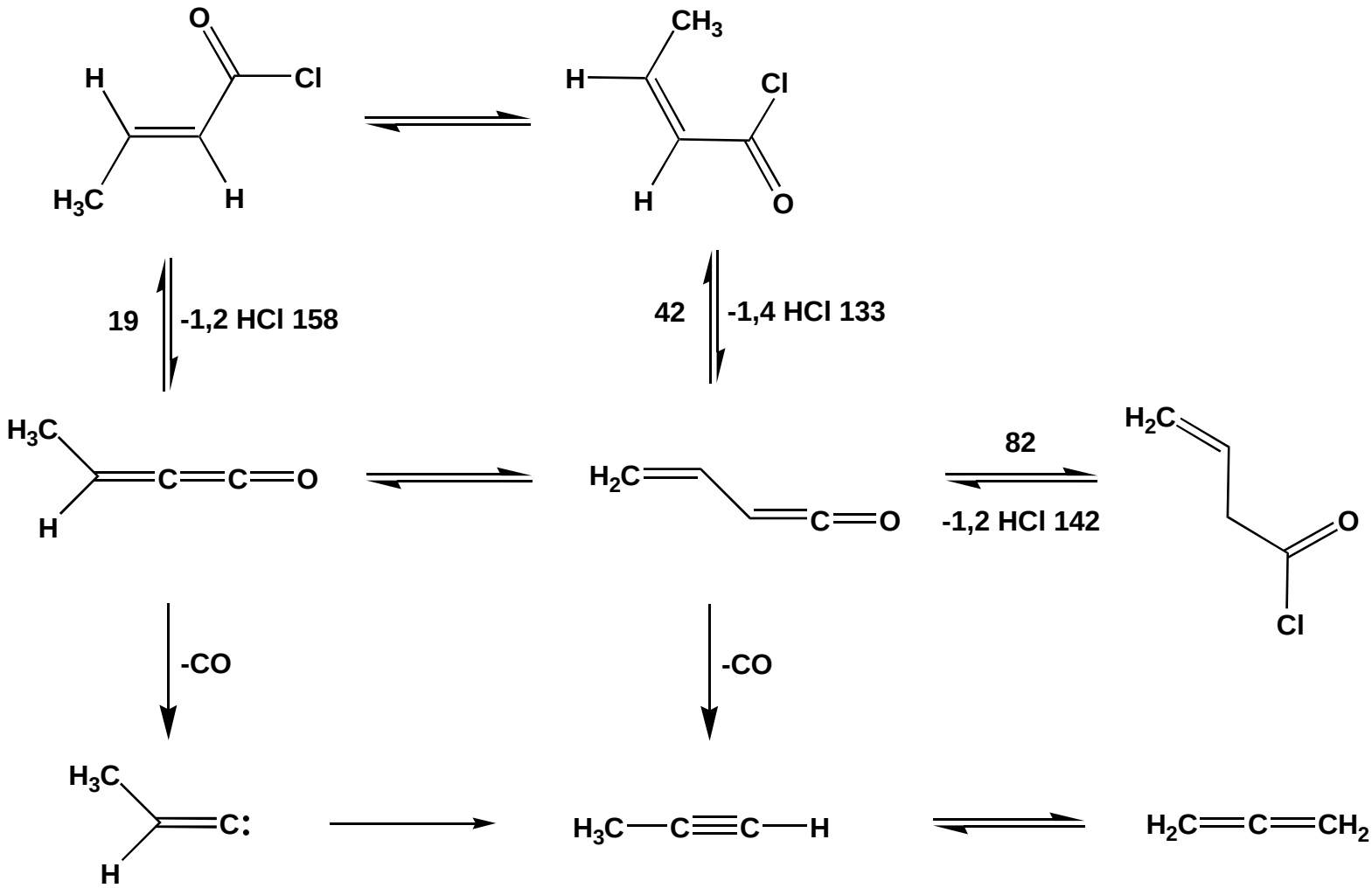

Figure 4.12 A proposed scheme for *E*-2-butenoyl chloride IR LPHP; calculated activation energies are in kJ mol^{-1}

combines to form 2,4-hexadiene (*E,E*, *E,Z* and *Z,Z*) or abstracts atomic hydrogen to form the observed propene, the most significant product (excluding CO) in this investigation. The absence of 2-butenal precludes the abstraction of atomic hydrogen by 1-oxo-2-butenyl, suggesting that decarbonylation is rapid. The intensities of the bands assigned to *E,E*, *E,Z* and *Z,Z*-2,4-hexadiene while diminutive, were comparable; statistically, the yield of each stereoisomer is expected to be approximately equivalent.

The disproportionation of 1-propenyl radicals will effect the generation of propene and propyne; that the latter is not observed in this work suggests that such a mechanism is not practicable under these conditions. It is evident from the zero or low yield of those products ascribed to the disproportionation and combination of 1-propenyl that the concentration remains low throughout reaction. The concentration of a radical reflects the stability of that species, a highly reactive radical will not be detected at a significant level; vinylic radicals, including 1-propenyl, are destabilised relative to methyl [68]. Consequently, the expected concentration of 1-propenyl radicals is low. The absence of 1,5-hexadiene and 2,3-dimethyl-1,3-butadiene, the products ascribed to combination of the 2-propenyl or 1-methylethenyl radicals, preclude isomerisation of the 1-propenyl radical.

The addition of methylene or methyl to propene, followed in the latter case by homolytic cleavage of the C_β–H bond in the resulting addend, may account for the formation of 2-methyl-1-propene. The addition of methyl to propene is predicted to occur predominantly at the least substituted carbon, yielding the more stable 1-methylpropyl radical. An additional bond can form, with concomitant loss of atomic hydrogen, between C(2) and C(1) or C(3) affording 1- and 2-butene, respectively. Although the ratio of the rates of attack at each end of the olefin will approach 1:1 as the temperature is raised [20],

the fact that 2-methyl-1-propene is produced exclusively suggests that the addition of methyl to propene is not a practicable mechanism.

The addition of methylene to the double bond of propene will afford methylcyclopropane, a product not observed in this investigation. The exothermicity of such a process is predicted to exceed the activation energy of isomerisation; consequently, the transformation of the initial product by structural or geometrical isomerisation is a practicable pathway [18]. It is conceivable that the subsequent rearrangement of activated methylcyclopropane leads exclusively to 2-methyl-1-propene, given that no other C_4H_8 isomers were detected.

It is necessary to account for the formation of methylene, if the mechanism proposed for the production of propene is accepted. It was shown in section 4.3.2 that the unimolecular rate expressions for the decomposition of larger radicals had activation energies of the order of 120-160 kJ mol^{-1} and normal pre-exponential factors [37]. As a result, such moieties are predicted to be significantly less stable than the comparable alkanes and alkenes, and will rapidly generate highly reactive species such as methyl or atomic hydrogen. While the decomposition of 1-propenyl will not directly form methylene, it is possible that the elimination of atomic hydrogen from methyl (afforded through homolytic cleavage of the C(2)–C(3) single bond in 1-propenyl) will afford the carbene. A proposed scheme for the pyrolysis of *E*-butenoyl chloride and $W(CO)_6$ is given in Figure 4.13.

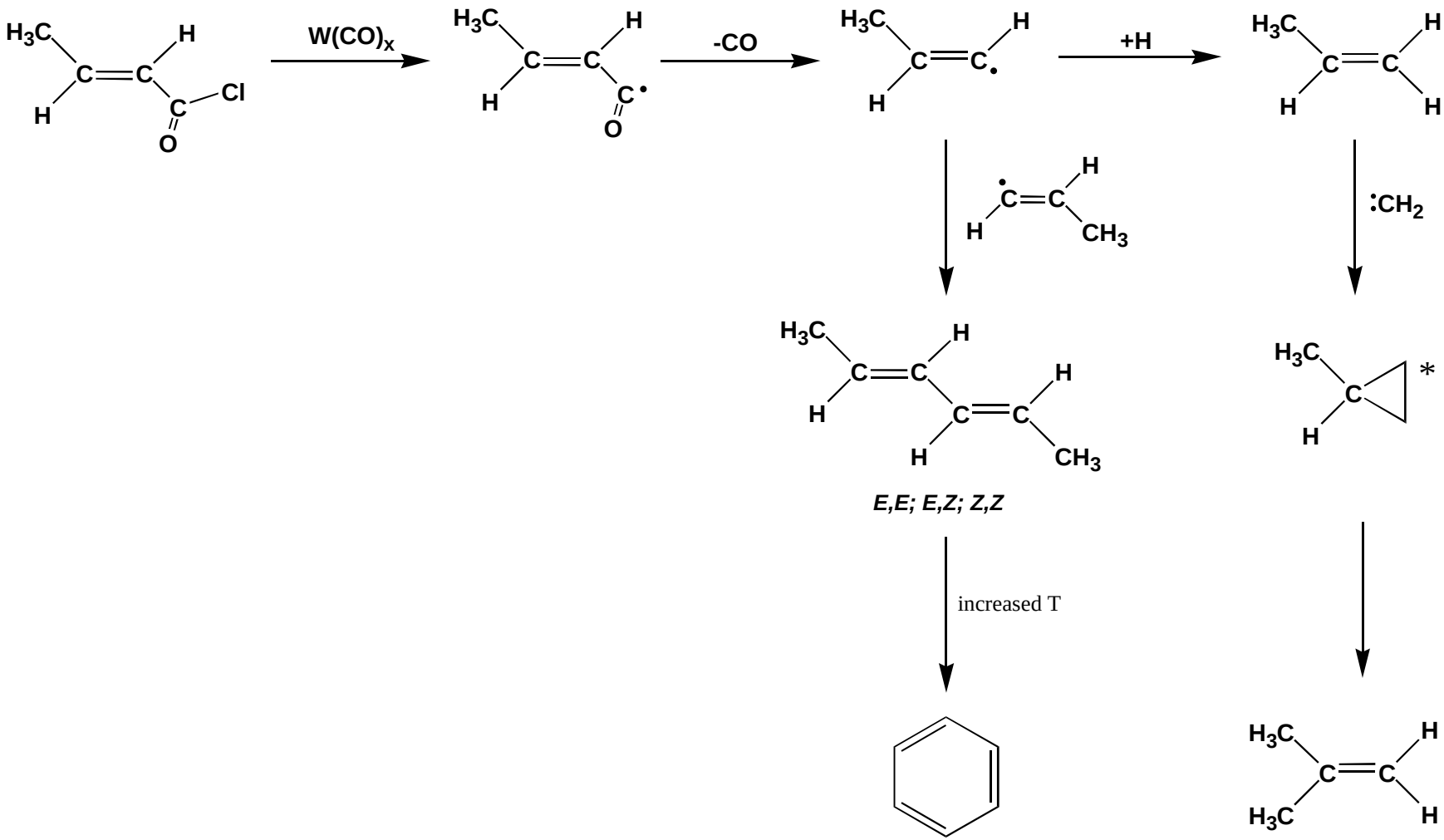

Figure 4.13 A proposed scheme for *E*-2-butenoyl chloride and $W(CO)_6$ IR LPHP; activated species are labelled *****

4.7 Methacryloyl Chloride

4.7.1 Pyrolysis

The decomposition of methacryloyl chloride (2-methyl-2-propenoyl chloride) has not been investigated previously. The products of methacryloyl chloride IR LPHP were identified using FT-IR and GC-MS spectroscopy at both ambient and low (16 K) temperature as CO, HCl, propyne and allene. The decarbonylation product, 2-chloro-propene was also detected in trace amount. There were no absorbance bands, attributable to a short-lived ketene species, in the post-pyrolysis infrared spectrum at ambient temperature.

The molecular dehydrochlorination of methacryloyl chloride is restricted to 1,3-HCl elimination, affording either propyne or (following rotation of the C(O)Cl group) allene; the absence of a β-hydrogen precludes 1,2-HCl elimination and, consequently, formation of the ketene. The experimental observations illustrate this point; the low temperature spectrum of the Ar matrix-isolated products of methacryloyl chloride thermolysis was devoid of bands ascribed to a short-lived ketene species. In the spectral region between 2200 and 2100 cm^{-1} there was only one peak observed at 2137 cm^{-1}, which was attributable to CO.

The elimination of HCl is accompanied by concurrent loss of CO. Semi-empirical calculations predict that the activation barrier value for formation of propyne is comparable to that of allene, and significantly higher than the acyl chlorides possessing a β-hydrogen. The conditions required for the successful decomposition of methacryloyl chloride reflect this result; IR LPHP of methacryloyl chloride employed a considerably higher temperature than for each of the other acyl chlorides investigated. It is likely that the conditions

pertaining to the pyrolysis of methacryloyl chloride are sufficient to initiate the thermal interconversion of propyne and allene, a well known process at high temperature [64]. Figure 4.14 illustrates the proposed pyrolysis scheme for methacryloyl chloride.

4.7.2 Co-pyrolysis with $W(CO)_6$

The products observed following pyrolysis of methacryloyl chloride in the presence of $W(CO)_6$ are consistent with the decomposition scheme derived for the pyrolysis of *E*-2-butenoyl chloride in the presence of $W(CO)_6$; this is described in section 4.6.2. In contrast, however, the selective abstraction of atomic chlorine from methacryloyl chloride will yield 2-methyl-1-oxo-2-propenyl radicals that undergo rapid decarbonylation to generate 1-methylethenyl radicals. A proposed scheme for the pyrolysis of methacryloyl chloride in the presence of $W(CO)_6$ is illustrated in Figure 4.15.

4.8 Cyclopropanecarbonyl Chloride

The pyrolysis [13, 24, 61, 62] and photolysis of matrix isolated [69] cyclopropanecarbonyl chloride has been investigated by several workers. It has been determined that decomposition commences through the elimination of HCl, affording cyclopropylidene ketene. Maquestiau and co-workers [61, 62] and Monnier and co-workers [69] observed this transient species directly using low temperature (77 and 15 K respectively) FT-IR spectroscopy. Bock and co-workers [13, 24] were unable to confirm the presence of cyclopropylidene ketene, and consequently proposed that dehydrochlorination was accompanied by concomitant loss of CO.

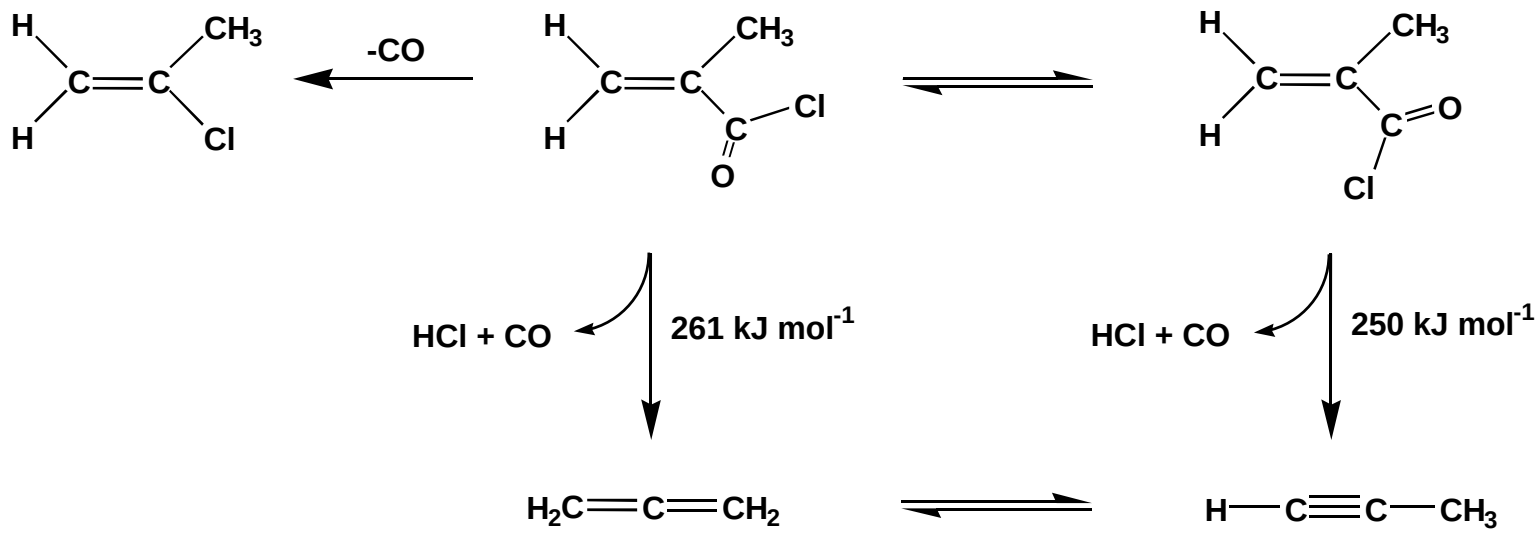

Figure 4.14 A proposed scheme for methacryloyl chloride IR LPHP with calculated activation energies

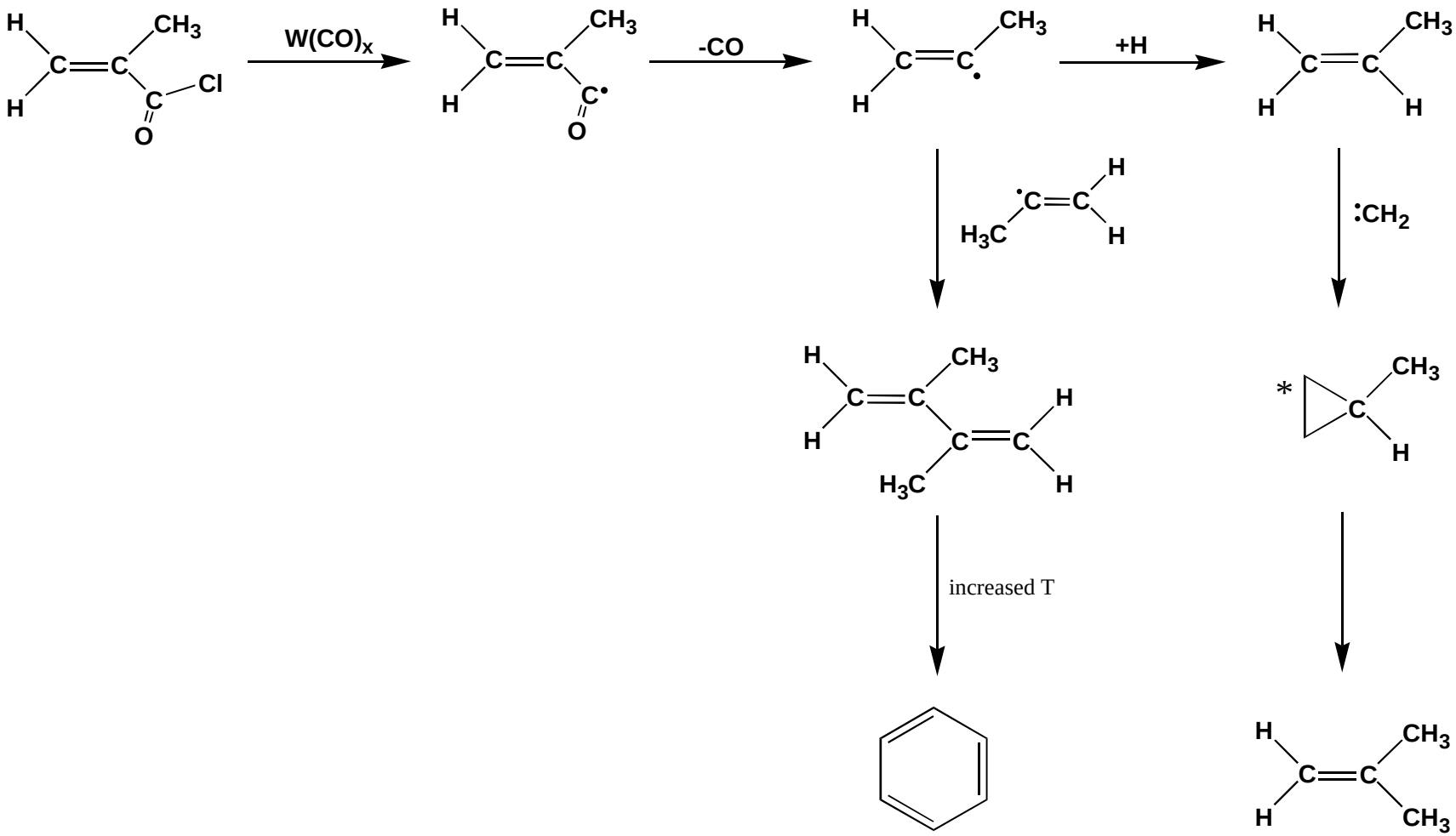

Figure 4.15 A proposed scheme for methacryloyl chloride and $W(CO)_6$ IR LPHP; activated species are labelled *****

There is some argument as to whether the subsequent decay of cyclopropylidene ketene occurs in a concerted or stepwise manner; decarbonylation may be simultaneously accompanied, or subsequently succeeded by ring opening. In any case, allene is the ultimate product. In a study of the photolysis of matrix isolated cyclopropanecarbonyl chloride, Monnier and co-workers [69] observed chlorocyclopropane; it was reasoned that this was the product of cyclopropylidene insertion into the single bond of HCl, and consequently corroborated a non-concerted mechanism. It is worth noting, however, that the decarbonylation of cyclopropanecarbonyl chloride will yield chlorocyclopropane directly.

4.8.1 Pyrolysis

The stable products of cyclopropanecarbonyl chloride pyrolysis were identified as HCl, CO and allene; the formation of chlorocyclopropane could not be confirmed. There was no evidence to indicate generation of the transient cyclopropylidene ketene at ambient temperature.

The low temperature post-pyrolysis spectrum of cyclopropanecarbonyl chloride in both an Ar and SF_6 matrix (dilution 2000 : 1) revealed a number of bands between 2200 and 2100 cm^{-1}. At 16 K, an intense band at 2175 cm^{-1} (2168 cm^{-1} in a SF_6 matrix) was observed, which was ascribed to the cumulenic stretch of uncomplexed cyclopropylidene ketene. A number of workers have isolated and spectroscopically investigated cyclopropylidene ketene at low temperature [62, 69-72]. The uncomplexed ketene, procured through thermolysis of the 1-pyrazoline-3,5-dione derivative, was observed by Maier and co-workers [70] at 2176 and 2154 cm^{-1}. Conversely, the absorbance band

pattern observed between 2145 and 2125 cm^{-1} by Monnier and co-workers [69] was ascribed to the complexed ketene. All other reports of cyclopropylidene ketene give the cumulenic stretch in this region and, consequently, indicate the complex.

The formation of cyclopropylidene ketene is consistent with the elimination of HCl from starting material. There was no evidence to suggest that this process is reversible; absorbance bands ascribed to starting material did not increase during the acquisition of a spectrum at the expense of HCl. The decarbonylation of cyclopropylidene ketene may be simultaneously accompanied, or subsequently succeeded by ring opening and will afford the observed allene. While the isolation and characterisation of cyclopropylidene has not eventuated in the course of this work, a stepwise mechanism can not be discounted.

There were several weaker bands at 2187, 2152 (2146 cm^{-1} in a SF_6 matrix) and 2128 cm^{-1}, the peaks at 2187 and 2128 cm^{-1} only evident in experiments that utilised an Ar matrix. On annealing an Ar matrix to 20 K, the absorbance band at 2128 cm^{-1} intensified at the expense of those at 2187 and 2175 cm^{-1}. The peak at 2152 cm^{-1} remained unchanged. The post-pyrolysis spectra of Ar matrix trapped cyclopropanecarbonyl chloride at 16 and 20 K is illustrated in Figure 4.16. The annealing pattern of the peaks observed, indicate three distinct products. The absorbance band at 2187 cm^{-1} is attributable to cyclopropylidene ketene, on account of its similar behaviour on annealing to the peak at 2175 cm^{-1}. The band at 2128 cm^{-1} is ascribed to vinyl ketene; the low temperature spectrum of an authentic sample (procured through the pyrolysis of *E*-2-butenoyl chloride) is spectroscopically identical with the band observed in this study.

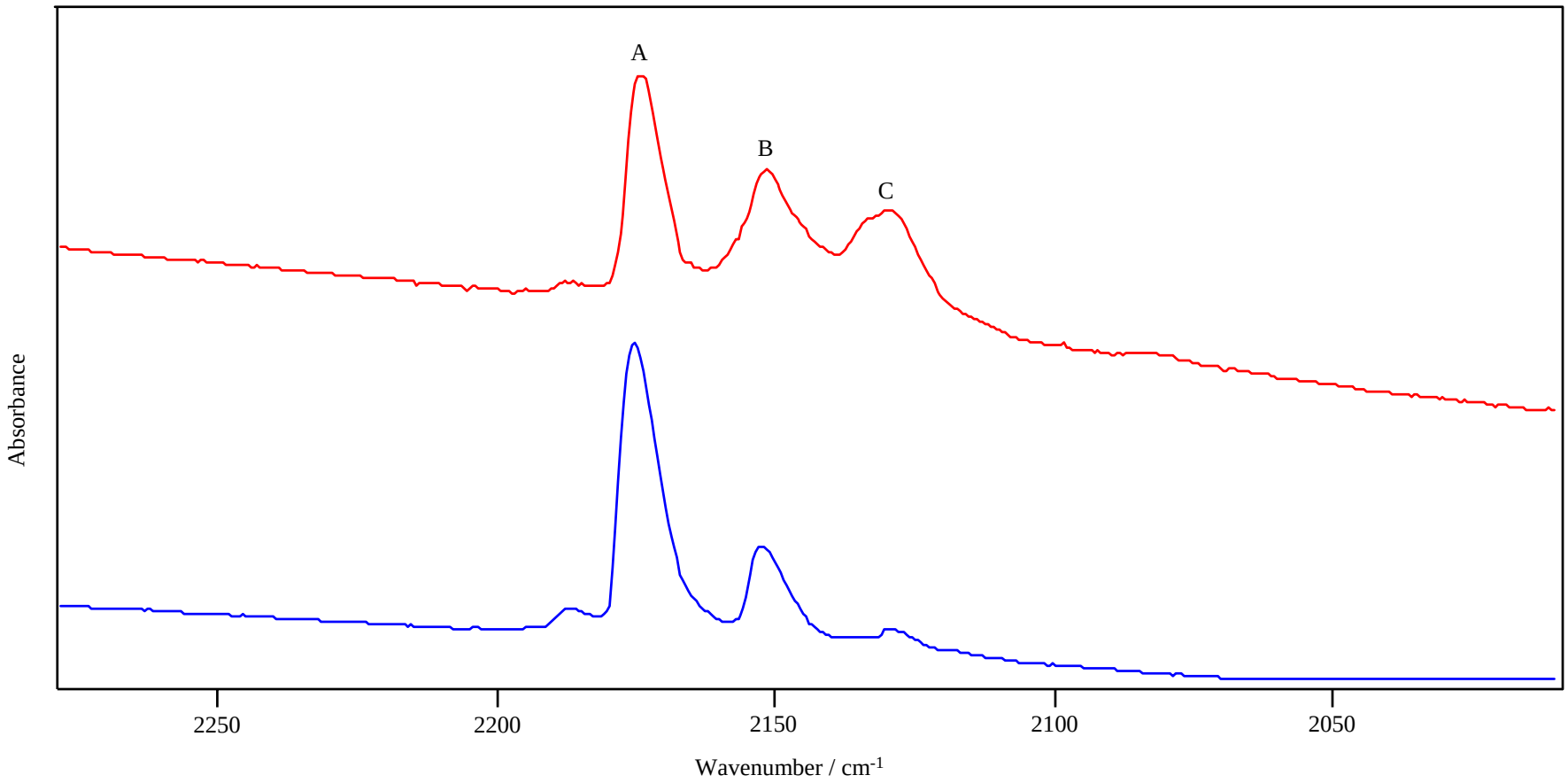

Figure 4.16 Post-pyrolysis FT-IR spectra of Ar matrix trapped cyclopropanecarbonyl chloride at 16 K (—) and 20 K (—); A = cyclopropylidene ketene; B = 4-chloro-1-buten-1-one; C = vinyl ketene

The increase in vinyl ketene at the expense of cyclopropylidene ketene is consistent with isomerisation of the latter through heterolytic cleavage of the three-membered ring with a 1,3-H shift. The fact that vinyl ketene was not observed in the gas phase, or at low temperature in a SF_6 matrix suggests that the mechanism responsible is heterogeneous in nature; in each case, decomposition is initiated by IR LPHP, thereby inhibiting reaction at the surface. Furthermore, the decomposition of vinyl ketene has been shown (in section 4.6.1) to yield propyne, which was not detected in this investigation. Maquestiau and co-workers could find no spectroscopic evidence for the isomerisation (ring opening) of cyclopropylidene ketene to vinyl ketene [62].

The band at 2152 cm^{-1} may be ascribed to 4-chloro-1-buten-1-one. The mechanism responsible for the formation of 4-chloro-1-buten-1-one involves heterolytic cleavage of the three-membered ring with a 1,3-chlorine shift. Semi-empirical calculations have shown that this mechanism represents a practicable decomposition route with activation energy of 248 kJ mol^{-1}. Moreover, the cumulenic stretch of the ketene is calculated at 2153 cm^{-1} with scaling [43], which is in excellent agreement with that observed. The decarbonylation or dehydrochlorination of 4-chloro-1-buten-1-one will afford 3-chloro-1-propene or vinyl ketene, respectively; that the former was not observed ostensibly indicates that this assignment is incorrect. It is possible, however, that 3-chloro-1-propene expeditiously decompose under these conditions; certainly, formation of allene (a significant product) is consistent with the molecular dehydrochlorination of 3-chloro-1-propene.

In the present study, IR LPHP of cyclopropanecarbonyl chloride was monitored *in situ* by TDL spectroscopy. In the region of the infrared spectrum centred at 2177 cm^{-1}, which is illustrated in Figure 4.17, a series of bands attributable to cyclopropylidene ketene was

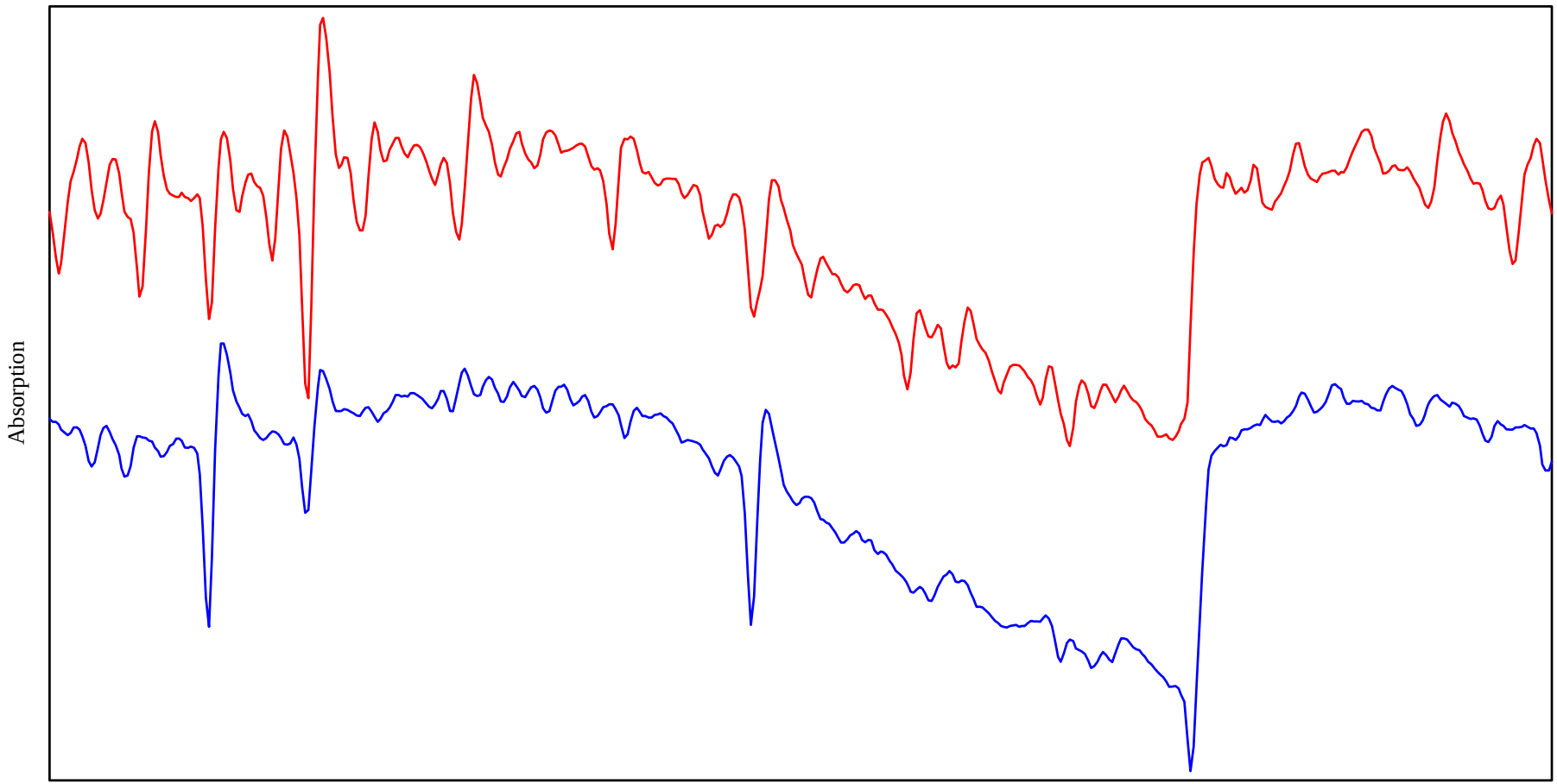

Figure 4.17 High resolution spectra (centred at 2177 cm^{-1}) of cyclopropanecarbonyl chloride before (—) and during (—) IR LPHP

observed when the contents of the cell were exposed to the output of a CW CO_2 laser. The spectrum returned to its original state immediately following cessation of irradiation. Additionally, a series of minor absorption bands appeared at 2164 cm^{-1}, that is ascribed to ketene; the spectrum obtained was spectroscopically identical to that observed for a pure sample of ketene, procured through the pyrolysis of acetyl chloride. Bands attributed to ketene were discernible for up to ten minutes following cessation of irradiation. A proposed pyrolysis scheme for cyclopropanecarbonyl chloride, without the mechanism responsible for the formation of 4-chloro-1-propen-1-one (which has not been definitively characterised) and ketene (which is formed in trace amount) is illustrated in Figure 4.18.

4.8.2 Co-pyrolysis with $W(CO)_6$

The products derived from the pyrolysis of cyclopropanecarbonyl chloride in the presence of $W(CO)_6$ at low temperature were CO, propene, 2-methyl-1-propene, 1,5-hexadiene and benzene; a trace amount of cyclopropane was also detected. An increase in benzene at the expense of 1,5-hexadiene as the duration of pyrolysis was extended, suggests that the mechanism responsible involve decomposition of the latter. The stoichiometric elimination of two hydrogen molecules from 1,5-hexadiene, with concomitant ring closure may account for the formation of benzene in a similar manner to that of 2,4-hexadiene, the combination product effected following pyrolysis of *E*-2-butenoyl chloride with $W(CO)_6$.

The formation 1,5-hexadiene and propene is consistent with the selective abstraction of Cl from cyclopropanecarbonyl chloride to yield cyclopropanecarbonyl radicals; these rapidly lose CO to generate cyclopropyl radicals that form 2-propenyl (allyl) radicals through

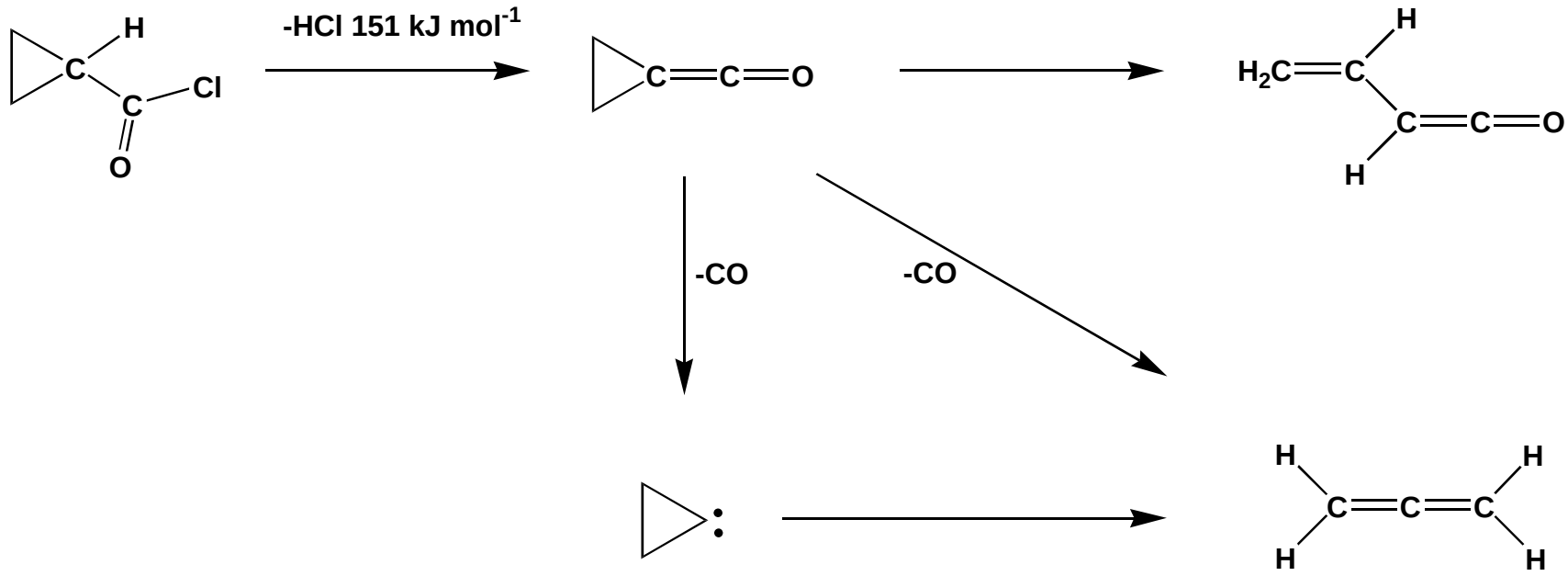

Figure 4.18 A proposed scheme for cyclopropanecarbonyl chloride IR LPHP with calculated activation energy for dehydrochlorination

homolytic cleavage of the three-membered ring. The allyl radicals combine or abstract atomic hydrogen to yield the observed propene.

A number of theoretical investigations into the thermal ring opening of cyclopropyl to allyl radical have been executed, with an express focus on the mode of reaction [73-82]. While there has been some disagreement as to whether reaction is conrotatory or disrotatory, a recent investigation has predicted that (in the absence of substituents in the methylene groups, which may lead to steric effects) there should be no preference between modes, as both possess a common transition state [73]. There has been no experimental evidence presented to support any of the theories proposed. Notwithstanding the mode of reaction, the thermal conversion of cyclopropyl to allyl is clearly a practicable mechanism. It is apparent, given the formation of cyclopropane, that cyclopropyl radicals may abstract atomic hydrogen prior to ring opening.

The allyl radical is predicted to be more stable, and by corollary, of greater concentration than either 1-propenyl or 1-methylethenyl, the radical intermediates effected, respectively, through pyrolysis of *E*-2-butenoyl or methacryloyl chloride in the presence of $W(CO)_6$. The stability of the allyl radical can be attributed to delocalisation of the unpaired electron across both ends of the π orbital system [83]. Consequently, the yield of 1,5-hexadiene is expected to be considerably higher than for either 2,4-hexadiene or 2,3-dimethyl-1,3-butadiene (combination products of 1-propenyl or 1-methylethenyl radicals, respectively), which is indeed the case. The disproportionation of allyl radicals will afford propene and allene; that the latter is not observed suggests that such a mechanism is not practicable; this is consistent with the reported disproportionation to combination ratio for the allyl radical of 0.008 [84].

In an analogous manner to *E*-2-butenoyl and methacryloyl chloride pyrolysis in the presence of $W(CO)_6$, the addition of methylene to propene with subsequent rearrangement of the resultant activated cycloalkane may account for the exclusive formation of 2-methyl-1-propene. The decomposition of allyl will yield methylene through homolytic cleavage of the carbon-carbon single bond. A proposed scheme for pyrolysis of cyclopropanecarbonyl chloride in the presence of $W(CO)_6$ is illustrated in Figure 4.19.

4.9 Conclusion

The results presented in this chapter confirm that $W(CO)_x$ species are effective and selective abstractors of Cl from selected acyl chlorides under comparatively mild conditions. The decarbonylation of the species afforded from the elimination of atomic chlorine resulted in an organic radical species that dominated the subsequent chemistry. The observed end products can be ascribed to combination, disproportionation, abstraction and fragmentation of the resultant radical species. In systems that possessed more than one chlorine atom it was found that the selective abstraction of atomic chlorine could occur at either site. Abstraction of the second chlorine atom was preceded by the molecular elimination of CO. The abstraction of atomic chlorine from starting material was not unique; in several cases a product could only be accounted for through a mechanism that involved Cl abstraction from a primary pyrolysis product.

The combination or disproportionation of the resultant radical was, for the most part, a dominant reaction pathway; only in systems where the radical concentration was relatively low were radical-radical reactions not significant. The distribution of products ascribed to either combination or disproportionation was generally in accord with the reported k_d / k_c

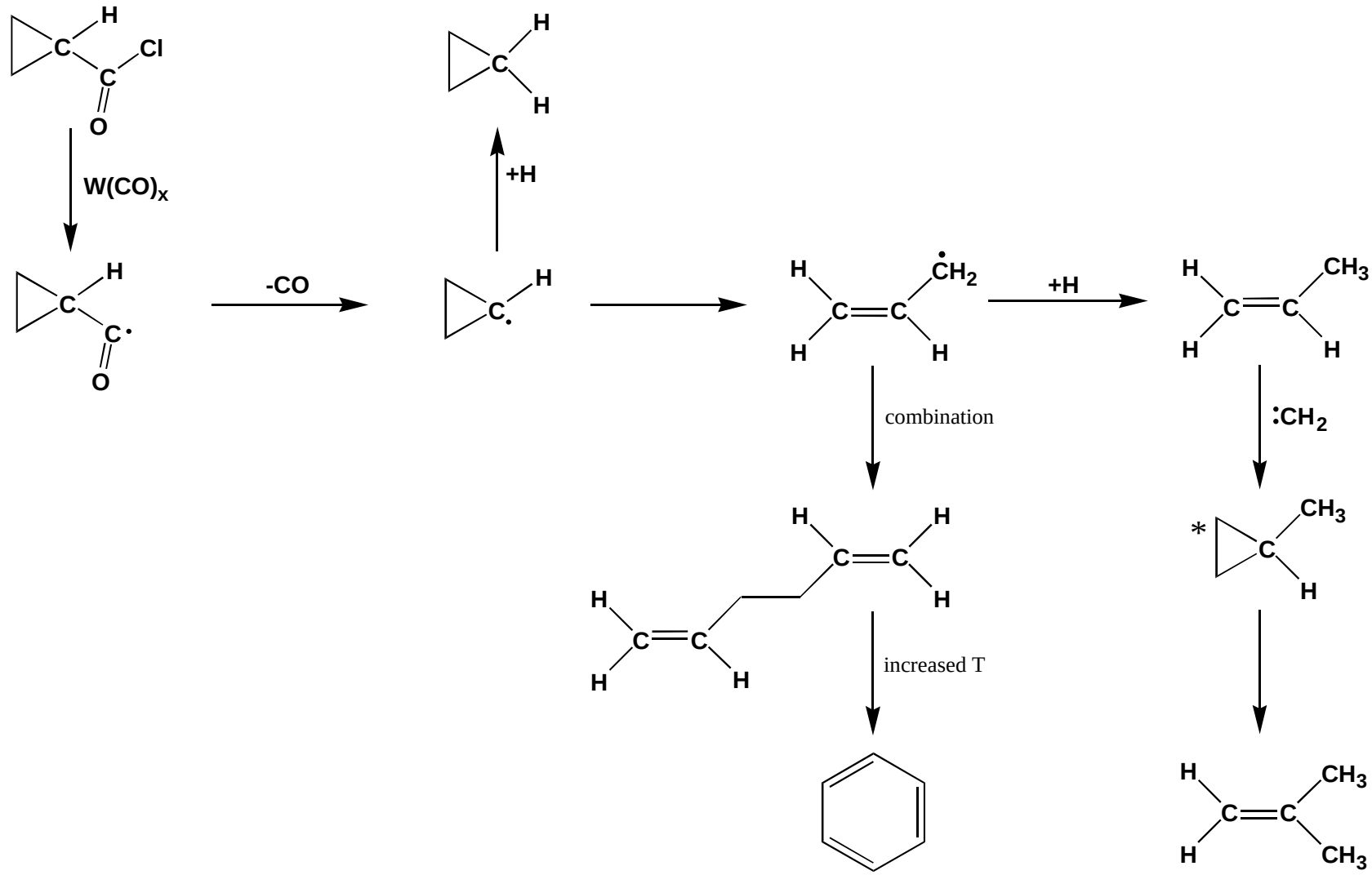

Figure 4.19 A proposed scheme for cyclopropanecarbonyl chloride and $W(CO)_6$ IR LPHP; activated species are labelled *****

value. In cases where the observed distribution of self-reaction products differed from that expected, an additional mechanism was proposed to account for the deviation; where the level of the saturated disproportionation product exceeded the combination product, abstraction of atomic hydrogen by the organic radical species was proposed.

The fragmentation of the resultant organic radical, with the exception of 2-chloroethyl (derived from the pyrolysis of 3-chloropropanoyl chloride and $W(CO)_6$) which involved homolytic cleavage of the C–H or C–Cl bond, was rarely a predominant pyrolysis mechanism. In contrast, homolytic fragmentation of a radical formed by secondary reaction was frequently observed. This difference can be rationalised in terms of radical concentration; the concentration of a radical formed through primary reaction is expected to be higher than that effected through secondary reaction. Consequently, the probability of collision, and as such reaction, between radicals formed from secondary reaction is considerably less than that afforded from primary reaction.

In the absence of $W(CO)_6$, the pyrolysis of the selected acyl chlorides was initiated through molecular 1,2-HCl elimination, affording (with the exception of methacryloyl chloride, which does not possess a β-hydrogen) the ketene. The molecular dehydrochlorination of *Z*-2-butenoyl chloride (effected through isomerisation of the *E* form) was restricted to 1,4-HCl elimination yielding vinyl ketene. The dehydrochlorination of a compound that possessed a second chlorine atom could occur in two ways; for example, the pyrolysis of 3-chloropropanoyl chloride effected formation of 3-chloro-1-propen-1-one and acryloyl chloride through HCl elimination across the C(1)–C(2) and C(2)–C(3) bonds, respectively.

The reversibility of dehydrochlorination was illustrated in systems where a relatively stable ketene was generated; during spectrum acquisition, bands ascribed to the precursor increased at the expense of those assigned to the ketene. The orientation of electrophilic addition was not restricted to that expected from Markovnikov's rule; presumably, the barrier to the *anti*-Markovnikov product was exceeded under IR LPHP conditions.

The decomposition of the ketene, primarily, involved homolytic loss of the carbonyl group yielding the analogous carbene. In several intermediate ketenes, a 1,3-hydrogen migration was also proposed to account for an observed end product; a hydrogen shift in cyclopropylidene ketene was accompanied by heterolytic cleavage of the three-membered ring, and resulted in the formation of vinyl ketene. The predominant reaction of a simple carbene (possessing a single carbon atom) involved combination or abstraction. In contrast, rearrangement of a more complex carbene (by insertion of the divalent carbon at the C_{β}–H bond) can account for the formation of several unsaturated products; for example, the formation of acetylene following the pyrolysis of acryloyl chloride is consistent with rearrangement of the intermediary carbene, ethenylidene.

4.10 References

[1] G. R. Allen, N. D. Renner and D. K. Russell, *J. Chem. Soc., Chem. Commun.*, 1998, 703.

[2] *The Chemistry of Ketenes, Allenes and Related Compounds,* S. Patai, Ed., John Wiley & Sons, New York, 1980.

[3] *The Chemistry of Acyl Chlorides,* S. Patai, Ed., John Wiley & Sons, London, 1972.

[4] T. T. Tidwell, *Ketenes,* John Wiley & Sons, New York, 1995.

[5] W. E. Hanford and J. C. Sauer, *Organic Reactions*, 1946, **3**, 108.

[6] R. N. Lacey, In *The Chemistry of the Alkenes,* S. Patai, Ed., Interscience, New York, 1964; pp. 1161-1227.

[7] D. Bormann, *Methoden der Organischen Chemie,* Theime Verlag, Stuttgart, 1968.

[8] E. Schaumann and S. Scheiblich, *Methoden der Organischen Chemie,* Theime Verlag, Stuttgart, 1993.

[9] S. Xu, K. A. Beran and M. D. Harmony, *J. Phys. Chem*, 1994, **98**, 2742.

[10] M. Gerry, W. Lewis-Bevan and N. P. C. Westwood, *J. Chem. Phys.*, 1983, **79**, 4655.

[11] D. Colbourne and N. P. C. Westwood, *J. Chem. Soc., Perkin Trans. II,* 1985, 2049.

[12] D. Colbourne, C. D. Frost, C. A. McDowell and N. P. C. Westwood, *J. Chem. Soc., Chem. Commun.*, 1980, 250.

[13] H. Bock, T. Hirabayashi and S. Mohmand, *Chem. Ber.*, 1981, **114**, 2595.

[14] G. Davidovics, M. Monnier and A. Allouche, *Chem. Phys.*, 1991, **150**, 395.

[15] A. P. Masters, T. S. Lorenson and T. Ziegler, *Organometallics*, 1989, **8**, 1088.

[16] A. Yamamoto, *Organotransition Metal Chemistry,* John Wiley & Sons, New York, 1986.

[17] J. P. Collman, L. S. Hegedus, J. R. Norton and R. G. Finke, *Principles and Applications of Organotransition Metal Chemistry,* University Science Books, Mill Valley, CA, 1987.

[18] W. Kirmse, *Carbene Chemistry,* 2nd Ed, Academic Press, New York, 1971.

[19] P. W. Atkins, *Physical Chemistry,* 4th Ed, Oxford University Press, Oxford, 1990.

[20] J. Fossey, D. Lefort and J. Sorba, *Free Radicals in Organic Chemistry,* John Wiley & Sons, Chichester, 1995.

[21] J. A. Seetula, *J. Chem. Soc., Faraday Trans.*, 1998, **94**, 1933.

[22] F. Westly, J. T. Herron, R. J. Cvetanovic, R. F. Hampson and W. G. Mallard, NIST-Chemical Kinetics Standard Reference Database Number 17, Version 5, National Institute of Standards and Technology, Gaithersburg MD.

[23] J. Warnatz, *Combustion Chemistry,* Springer, New York, 1984.

[24] H. Bock, T. Hirabayashi, S. Mohmand and B. Solouki, *Angew. Chem., Int. Ed. Engl.*, 1977, **16**, 105.

[25] D. Johnstone and J. Sodeau, *J. Chem. Soc., Faraday Trans.*, 1992, **88**, 409.

[26] E. W. R. Steacie, *Atomic and Free Radical Reactions,* Reinhold Publishing Corp., New York, 1954.

[27] W. L. Hase, H. B. Schlegel, V. Balbyshev and M. Page, *J. Phys. Chem.*, 1996, **97**, 5354.

[28] L. F. Loucks and K. J. Laidler, *Can. J. Chem*, 1967, **45**, 2795.

[29] M. C. Lin and M. H. Back, *Can. J. Chem.*, 1966, **44**, 2357.

[30] Y. Simon, J. F. Foucaut and G. Scacchi, *Can. J. Chem.*, 1988, **66**, 2142.

[31] A. B. Trenwith, *J. Chem. Soc., Faraday Trans. II*, 1986, **82**, 457.

[32] P. D. Pacey and J. H. Wimalasena, *J. Phys. Chem.*, 1984, **88**, 5657.

[33] Y. Feng, J. T. Niiranen, Á. Bencsura, V. D. Knyazev, D. Gutman and W. Tsang, *J. Phys. Chem.*, 1993, **97**, 871.

[34] W. Tsang and R. F. Hampson, *J. Phys. Chem., Ref. Data*, 1986, **15**, 1087.

[35] D. A. Parker and C. P. Quinn, *J. Chem. Soc., Faraday Trans. I*, 1976, **72**, 1952.

[36] J. O. Terry and J. H. Futrell, *Can. J. Chem.*, 1967, **45**, 2327.

[37] W. Tsang and J. H. Kiefer, In *The Chemical Dynamics and Kinetics of Small Radicals,* K. Liu and A. Wagner, Eds., World Scientific, Singapore, 1995; pp. 58-119.

[38] N. Piétri, J. Piot and J. Aycard, *J. Mol. Structure*, 1998, **443**, 163.

[39] This compound was labelled 3-chloro-1,2-propenone by Piétri and co-workers.

[40] N. Kraus, U. Mueller, B. Wohlfarth, M. Raetzsch, D. Plaschnick and (VEB Filmfabrik Wolften Fotochemisches Kombinat), *Ger. (East) Patent,* DD 248,581; *Chem. Abstr.* 1988, **109**, 54328a.

[41] O. Chapman, M. Miller and S. Pitzenberger, *J. Am. Chem. Soc.*, 1987, **109**, 6867.

[42] N. Piétri, M. Monnier and J. Aycard, *J. Org. Chem.*, 1998, **63**, 2462.

[43] Calculated values are scaled by 2150.7 / 2349.1 (*i.e.* the observed signal for ketene in the gas phase / the calculated value for the cumulenic stretch of ketene).

[44] C. Kubitza, Ph.D. Thesis, Technische Hochschule Darmstadt, 1995.

[45] A. Fahr, A. H. Laufer, R. Klien and W. Braun, *J. Phys. Chem.*, 1991, **95**, 3218.

[46] A. Fahr and A. H. Laufer, *J. Phys. Chem.*, 1990, **94**, 726.

[47] K. O. MacFadden and C. L. Currie, *J. Chem. Phys.*, 1973, **58**, 1213.

[48] R. P. Thorn, W. A. Payne, L. J. Stief and D. C. Tardy, *J. Phys. Chem.*, 1996, **100**, 13594.

[49] A. Fahr, W. Braun and A. H. Laufer, *J. Phys. Chem.*, 1993, **97**, 1502.

[50] A. W. Tickner and D. J. Le Roy, *J. Chem. Phys.*, 1951, **19**, 1247.

[51] A. G. Sherwood and H. E. Gunning, *J. Phys. Chem.*, 1965, **69**, 2323.

[52] N. A. Weir, *J. Chem. Soc.*, 1965, 6870.

[53] S. Takita, Y. Mori and I. Tanaka, *J. Phys. Chem.*, 1968, **72**, 4360.

[54] L. Szirovicza, *Int. J. Chem. Kinet.*, 1985, **17**, 117.

[55] J. C. Bertolini, J. Massardiner and G. Dalmai-Imerdik, *J. Chem. Soc., Farad. Trans. I*, 1978, **74**, 1720.

[56] S. Lie, L. Wang, M. Xie, X. Guo and Y. Wu, *Catal. Lett.*, 1995, **30**, 135.

[57] P. M. Maitlis, *Pure Appl. Chem.*, 1973, **33**, 489.

[58] G. N. Schauzer and S. Eichlwer, *Chem. Ber.*, 1962, **95**, 550.

[59] F. Solymosi, A. Erdohelyi and A. Szoke, *Catal. Lett.*, 1995, **32**, 43.

[60] J. E. Germaine, *Catalytic Conversion of Hydrocarbons,* Academic Press, London, 1969.

[61] A. Maquestiau, P. Pauwells, R. Flammang, P. Lorencak and C. Wentrup, *Spectrosc.: Int. J.*, 1984, **3**, 173.

[62] A. Maquestiau, P. Pauwels, R. Flammang, P. Lorencak and C. Wentrup, *Org. Mass Spec.*, 1986, **21**, 259.

[63] S. Mohmand, T. Hirabayashi and H. Bock, *Chem. Ber.*, 1981, **114**, 2609.

[64] A. Lifshitz, M. J. Frenklach and A. Burcat, *J. Phys. Chem.*, 1975, **79**, 1148.

[65] R. D. Brown, P. D. Godfrey and M. Woodruff, *Aust. J. Chem.*, 1979, **32**, 2103.

[66] E. Bjarnov, *Z. Naturforsch. A*, 1979, **34**, 1269.

[67] C. Wentrup and P. Lorencak, *J. Am. Chem. Soc.*, 1988, **110**, 1880.

[68] P. H. Scudder, *Electron Flow in Organic Chemistry,* John Wiley & Sons, New York, 1992.

[69] M. Monnier, A. Allouche, P. Verlaque and J. Aycard, *J. Phys. Chem*, 1995, **99**, 5977.

[70] G. Maier, M. Heider and C. Sierakowski, *Tetrahedron Lett.*, 1991, **32**, 1961.

[71] R. Leung-Toung and C. Wentrup, *J. Org. Chem.*, 1992, **57**, 4850.

[72] G. J. Baxter, R. F. C. Brown, F. W. Eastwood and K. J. Harrington, *Tetrahedron Lett.*, 1975, 4283.

[73] S. Olivella, A. Solé and J. M. Bofill, *J. Am. Chem. Soc.*, 1990, **112**, 2160.

[74] P. Merlet, S. D. Peyerimhoff, R. Buenker and S. Shih, *J. Am. Chem. Soc.*, 1974, **96**, 959.

[75] L. Farnell and W. G. Richards, *J. Chem. Soc., Chem. Commun.*, 1973, 334.

[76] J. R. Bews, C. Glidwell and J. C. Walton, *J. Chem. Soc., Perkin Trans. II*, 1982, 1447.

[77] S. Beran and R. Zahradnik, *Collect. Czech. Chem. Commun.*, 1976, **41**, 2303.

[78] M. J. S. Dewar, *Chem. Br.*, 1975, **11**, 97.

[79] M. J. S. Dewar and S. J. Kirschner, *J. Am. Chem. Soc.*, 1974, **96**, 5244.

[80] M. J. S. Dewar and S. J. Kirschner, *J. Am. Chem. Soc.*, 1971, **93**, 4290.

[81] G. Szeimies and G. Boche, *Angew. Chem., Int. Ed. Engl.*, 1971, **10**, 912.

[82] R. B. Woodward and R. Hoffmann, *J. Am. Chem. Soc.*, 1965, **87**, 395.

[83] J. McMurray, *Organic Chemistry,* 3rd Ed, Brookes/Cole Publishing Company, Pacific Grove, CA, 1992.

[84] D. G. L. James and S. M. Kambanis, *Trans. Faraday Soc.*, 1969, **65**, 1350.

Chapter Five

DIACYL CHLORIDES

5.1 Introduction

The intention of this investigation was to evaluate the mechanisms pertaining to the pyrolysis of selected diacyl chlorides in the presence of $W(CO)_6$. The pyrolysis of $W(CO)_6$ in the gas phase leads to unsaturated $W(CO)_x$ species, which have been shown to be very effective and selective abstractors of chlorine atoms from a wide range of organic substrates [1]. The chemistry of the resultant organic radicals is dominated by the themes of combination, disproportionation, fragmentation, rearrangement, abstraction and addition; these have been described in section 1.1.3.

An extensive investigation necessitates an understanding of the mechanism of pyrolysis of each of the selected diacyl chlorides without $W(CO)_6$. The decomposition of a diacyl halide is presumably analogous to that of an acyl chloride, initiated by molecular dehydrochlorination [2-4]. The resultant species, in contrast to the ketene derived from the decomposition of an acyl chloride (that possesses only a single chlorine atom) is capable of relinquishing a second molecule of HCl to effect the formation of a bisketene, a species having two ketene groups. The bisketenes, which have been reviewed by a number of workers [5-8], are often transient species that have long been proposed as intermediates in many important reactions [2].

In this study, the gas phase decomposition of several diacyl chlorides, including malonyl chloride (propanedioyl dichloride), fumaroyl dichloride (*E*-2-butenedioyl dichloride), succinyl chloride (butanedioyl dichloride) and diglycoloyl chloride (2,2'-oxybisacetyl chloride) was initiated in the presence and absence of $W(CO)_6$ using IR LPHP. A combination of FT-IR, GC-MS and matrix isolation spectroscopy was employed to characterise reaction.

5.2 Malonyl Chloride

Malonyl chloride (propanedioyl dichloride) has been identified and utilised as a precursor to chloroformyl ketene (3-oxo-2-propenoyl chloride) by Piétri and co-workers [9]; the *s-cis* and *s-trans* conformers were generated through thermal dehydrochlorination of malonyl dichloride at 323 K, and isolated in an Ar or Xe matrix. In contrast to the β-diketones and β-diesters, for which the enol form predominates, malonyl chloride presents only the diketo form, of which the structure of lowest energy belongs to the C_1 symmetry group with one C(O)Cl group rotated by ϕ_1 ($CCCO_1$) = 90° to the other C(O)Cl group [10]. It was proposed that a skewed conformation would assist the molecular dehydrochlorination of malonyl chloride, thus accounting for the low temperature of thermolysis. The subsequent photolysis of matrix-isolated chloroformyl ketene at $\lambda > 310$ nm, initiated interconversion of the conformers and dehydrochlorination of the *s-cis* form, effecting the formation of carbon suboxide (1,2-propadiene-1,3-dione).

5.2.1 Pyrolysis

In the present work, the most significant products observed following the pyrolysis of malonyl chloride at low laser power (*i.e.* temperature) were HCl, carbon suboxide and chloroformyl ketene, the latter also observed prior to IR LPHP. These results are consistent with the molecular dehydrochlorination of malonyl chloride to yield chloroformyl ketene; the subsequent elimination of HCl from this species will afford the observed carbon suboxide. The mild conditions employed reflect the low activation energy of malonyl chloride dehydrochlorination, which is calculated at 136 kJ mol^{-1} in the present study. Moreover, the presence of chloroformyl ketene in spectra prior to pyrolysis indicates that

this process can occur at ambient temperature. The decarbonylation of chloroformyl ketene does not appear to be a practicable decomposition pathway; the structure of the resultant carbene is such that rearrangement to a more stable species (through intramolecular insertion of the divalent carbon into a C_β–H bond) is not possible.

The intrinsic stability of carbon suboxide is reflected in experimental observation; the decarbonylation of carbon suboxide was initiated at a significantly higher temperature than that necessary to initiate the decay of chloroformyl ketene or malonyl chloride. The dioxides of carbon with an odd number of carbon atoms (of which carbon suboxide is an example) have long been known [11, 12], and are inherently more stable than those that possess an even number [2]. There have been numerous studies of carbon suboxide that have been periodically reviewed [13-20]. A number of investigations have focussed on the photolysis and thermolysis of carbon suboxide in the light of its role in the formation of interstellar species [21-24]. The presence of C_3O_2 in the coma and nucleus of comet Halley was reported by Huntress and co-workers [21]. At cometary temperatures C_3O_2 in the gas phase was found to dissociate at the C–CO bond upon absorption of UV light, producing CO and elemental carbon in a 2:1 ratio. The thermolysis of C_3O_2 behind shock waves has been investigated by Friedrichs and Wagner [22]; decarbonylation was initiated at temperatures between 1750 and 2300 K, illustrating the thermal stability of the bisketene.

5.2.2 Co-pyrolysis with $W(CO)_6$

The stable products derived from the pyrolysis of malonyl chloride and $W(CO)_6$ were identified as ethylene, propene and 2-methyl-1-propene. The formation of chloroformyl ketene, carbon suboxide and HCl in moderate amount indicates molecular

dehydrochlorination, a result not unexpected given that the temperature associated with the pyrolysis of malonyl chloride alone was comparable to that in the presence of $W(CO)_6$.

The generation of ethylene, propene and 2-methyl-1-propene is consistent with the selective abstraction of chlorine atoms from malonyl chloride; successive homolytic loss of carbonyl groups from the resultant diradical will yield methylene. Combination of methylene will effect the formation of ethylene, while the addition of methylene to the double bond of ethylene will afford propene, through rearrangement of the vibrationally excited cyclopropane intermediate. Similarly, the addition of methylene to the double bond of propene will generate vibrationally excited methylcyclopropane. The subsequent rearrangement of activated methylcyclopropane is likely to lead exclusively to 2-methyl-1-propene, given that no other C_4H_8 isomers were detected.

The exothermicity of methylene addition is predicted to exceed the activation energy of isomerisation; consequently, the transformation of the initial addend by structural or geometrical isomerisation is practicable [25]. In his systematic studies of the stereochemistry of the addition of methylene to the double bond of a selection of olefins, Frey reported that the yield of cyclopropane derivative increased with rising pressure [26, 27]. It was proposed that deactivating collisions of the vibrationally excited cyclopropane would inhibit rearrangement to the isomeric cyclopropane or the thermodynamically more stable alkene. Consequently, the yield of the initial deactivated adduct will be greater at higher pressure where the likelihood of a collision is increased. The fact that cyclopropane and methylcyclopropane were not observed in this investigation, reflects the low pressure employed when executing photosensitised IR laser pyrolysis. A proposed scheme for malonyl chloride and $W(CO)_6$ IR LPHP is given in Figure 5.1.

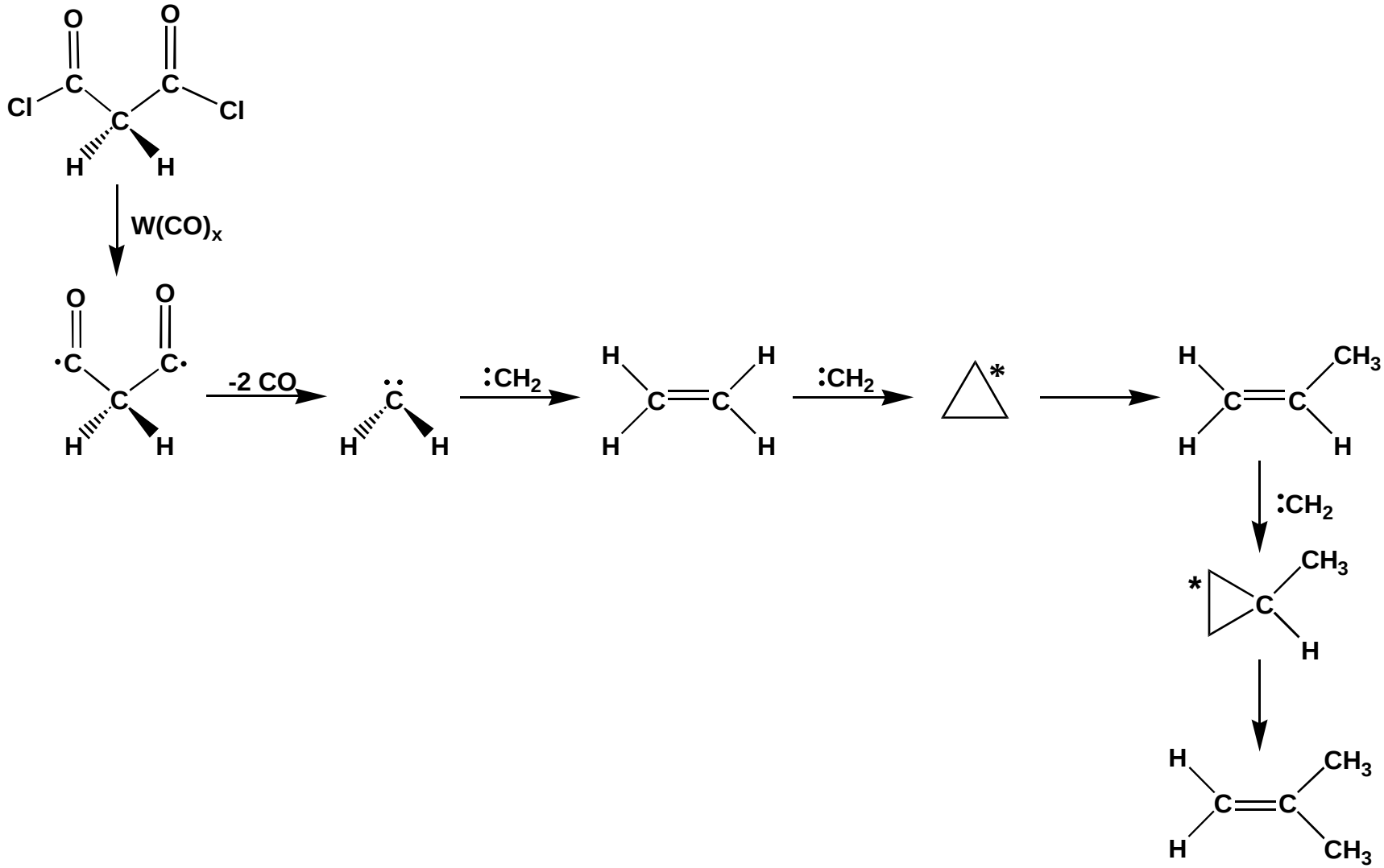

Figure 5.1 A proposed scheme for malonyl chloride and $W(CO)_6$ IR LPHP; activated species are labelled *****

5.3 Fumaroyl Chloride

The pyrolysis of fumaroyl chloride (*E*-2-butenedioyl dichloride) has been studied by several workers with a view to generating the transient species, tricarbon monoxide (3-oxo-1,2-propadienylidene) [28-30]. Brown and co-workers have proposed two possible reaction pathways, which are depicted in Figure 5.2, to account for the formation of this species [30]. In each case, reaction is initiated by the dehydrochlorination of starting material; subsequent decarbonylation of the resultant ketene (4-oxo-2,3-butadienoyl chloride) affords a carbene from which the loss of molecular HCl will afford tricarbon monoxide.

Although 1,2,3-butatriene-1,4-dione (the transient species derived from the molecular dehydrochlorination of 4-oxo-2,3-butadienoyl chloride) was not observed by Brown and co-workers, an alternative mechanism involving subsequent decarbonylation of 1,2,3-butatriene-1,4-dione was not discounted. It was proposed that a lack of sufficient amounts of highly enriched isotopes of the dichloride prevented the search for the cumulenone.

McNaughton and co-workers have used high and low resolution FT-IR spectroscopy to monitor the gaseous pyrolysis products of fumaroyl chloride [29]. At low temperature, the most significant product was 2-propynoyl chloride, which was ascribed to rearrangement of the carbene generated by successive dehydrochlorination and decarbonylation of starting material. The formation of tricarbon monoxide was ascribed to dehydrochlorination of the carbene intermediate. At higher temperature, the major product was chloroacetylene, which was ascribed to the decarbonylation of 2-propynoyl chloride.

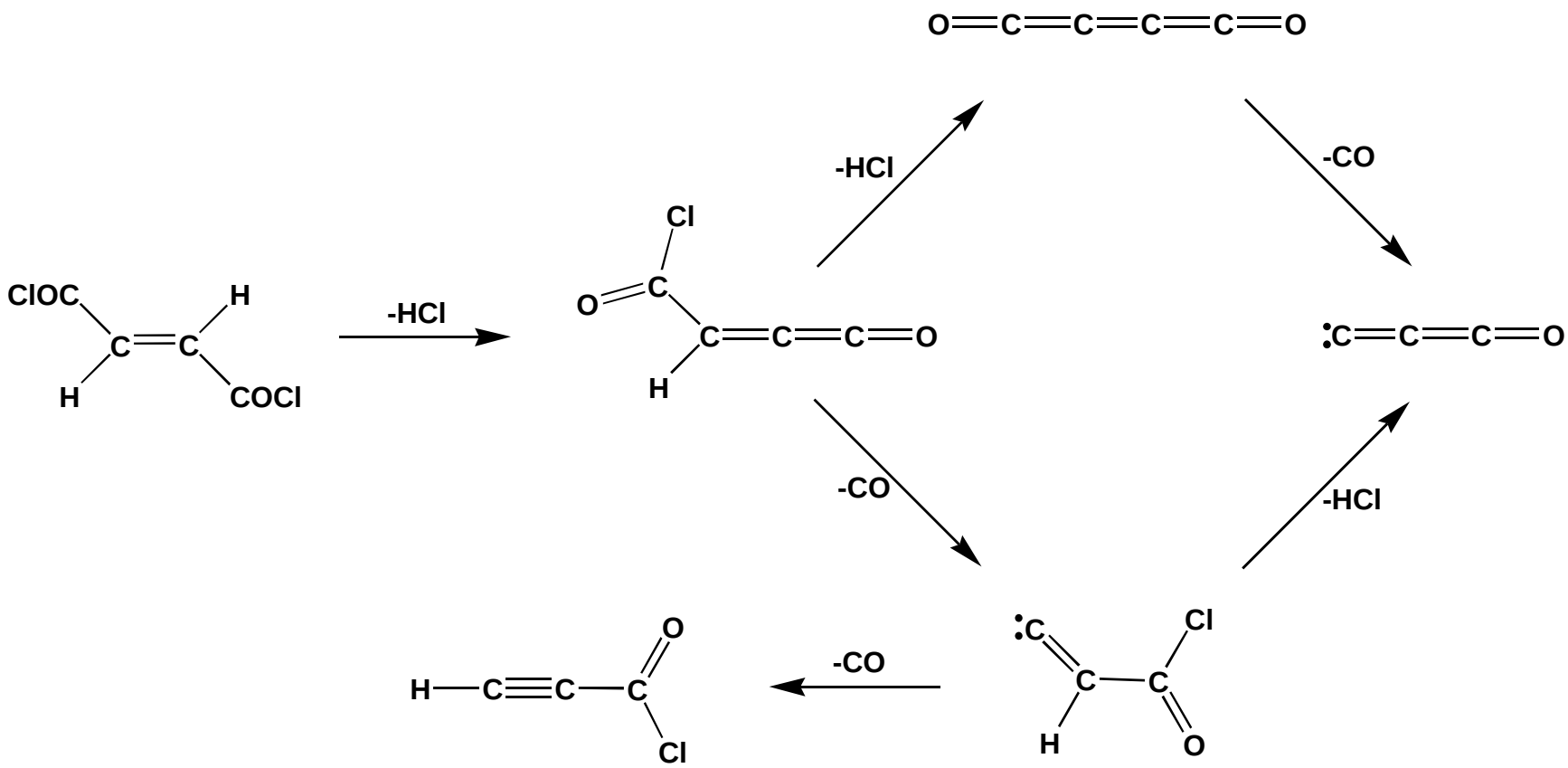

Figure 5.2 Reaction pathway for the production of C_3O from fumaroyl chloride pyrolysis as proposed by Brown and co-workers

5.3.1 Pyrolysis

In the present work, the most significant products observed following the pyrolysis of fumaroyl chloride were identified and characterised using FT-IR and GC-MS spectroscopy as HCl, CO, 2-propynoyl chloride and chloroacetylene. An increase in chloroacetylene at the expense of 2-propynoyl chloride at higher temperature is consistent with decarbonylation of the latter. The formation of *E*-3-chloro-2-propenoyl chloride (albeit in trace amount) is ascribed to the decarbonylation of starting material. The presence of a comparable quantity of the *Z* form can be rationalised in terms of *E*-*Z* isomerisation or decarbonylation of maleoyl chloride (the product derived from the isomerisation of starting material). Although the absence of maleoyl chloride (*Z*-2-butenedioyl dichloride) ostensibly precludes the latter, it is not inconceivable that the effective temperature of pyrolysis is such that decomposition of maleoyl chloride is initiated.

The low temperature post-pyrolysis FT-IR spectrum of fumaroyl chloride in both an Ar (dilution 2000 : 1) and SF_6 matrix (dilution 300 : 1) revealed a number of absorbance bands between 2300 and 2100 cm^{-1}. At 16 K, an intense band at 2128 cm^{-1} (2126 cm^{-1} in a SF_6 matrix) was observed that is ascribed to the acetylenic C≡C stretch of the stable pyrolysis product, 2-propynoyl chloride. A significant peak at 2137 cm^{-1} (2136 cm^{-1}) is assigned to uncomplexed CO. Weaker bands were observed at 2287, 2271, 2243 (a doublet centred at 2250 cm^{-1}) and 2109 cm^{-1} (2110 cm^{-1}), the peaks at 2287 and 2271 cm^{-1} evident only in experiments that utilised an Ar matrix (where initiation of reaction is heterogeneous). The absence of 1,2,3-butatriene-1,4-dione, the product effected from molecular dehydrochlorination of 4-oxo-2,3-butadienoyl chloride, is consistent with earlier studies [29, 30]. The dioxides of carbon possessing an even number of carbon atoms, of which 1,2,3-butatriene-1,4-dione is an example, are inherently unstable [2] and have often

eluded experimental identification [12]. On annealing an Ar matrix to 25 K, the absorbance band at 2287 cm^{-1} coalesced with the weaker band at 2271 cm^{-1}, affording a broad signal centred at 2277 cm^{-1}. The post-pyrolysis spectrum of SF_6 matrix trapped fumaroyl chloride at 16 K is illustrated in Figure 5.3.

The band at 2243 cm^{-1} (2246 and 2253 cm^{-1} in a SF_6 matrix) is ascribed to the transient species, tricarbon monoxide, and is in excellent agreement with the value reported by Brown and co-workers [30]. The peak at 2109 cm^{-1} is assigned to chloroacetylene; the low temperature spectrum of a pure sample (procured through the pyrolysis of *E*-1,2-dichloroethene) was spectroscopically identical with the band observed in the post-pyrolysis spectrum. A definitive assignment of the absorbance bands at 2287 and 2271 cm^{-1} is not possible in this investigation. It is likely that these peaks are attributable to the *syn* and *anti* conformers of 4-oxo-2,3-butadienoyl chloride, respectively. In the present work, the cumulenic stretch of the *syn* and *anti* conformers is calculated with scaling [31] at 2238 and 2237 cm^{-1}, respectively.

The formation of 4-oxo-2,3-butadienoyl chloride is ascribed to the molecular elimination of HCl from fumaroyl or maleoyl chloride. The absence of 4-oxo-2,3-butadienoyl chloride in a SF_6 matrix does not necessarily indicate that dehydrochlorination of starting material is heterogeneous in nature. The stable products derived from conventional pyrolysis (in an Ar matrix experiment) were comparable to those detected following IR LPHP, and can be accounted for only through a mechanism involving molecular dehydrochlorination of starting material. The absence of 4-oxo-2,3-butadienoyl chloride may be attributed to the difference in conditions, specifically pyrolysis temperature or duration.

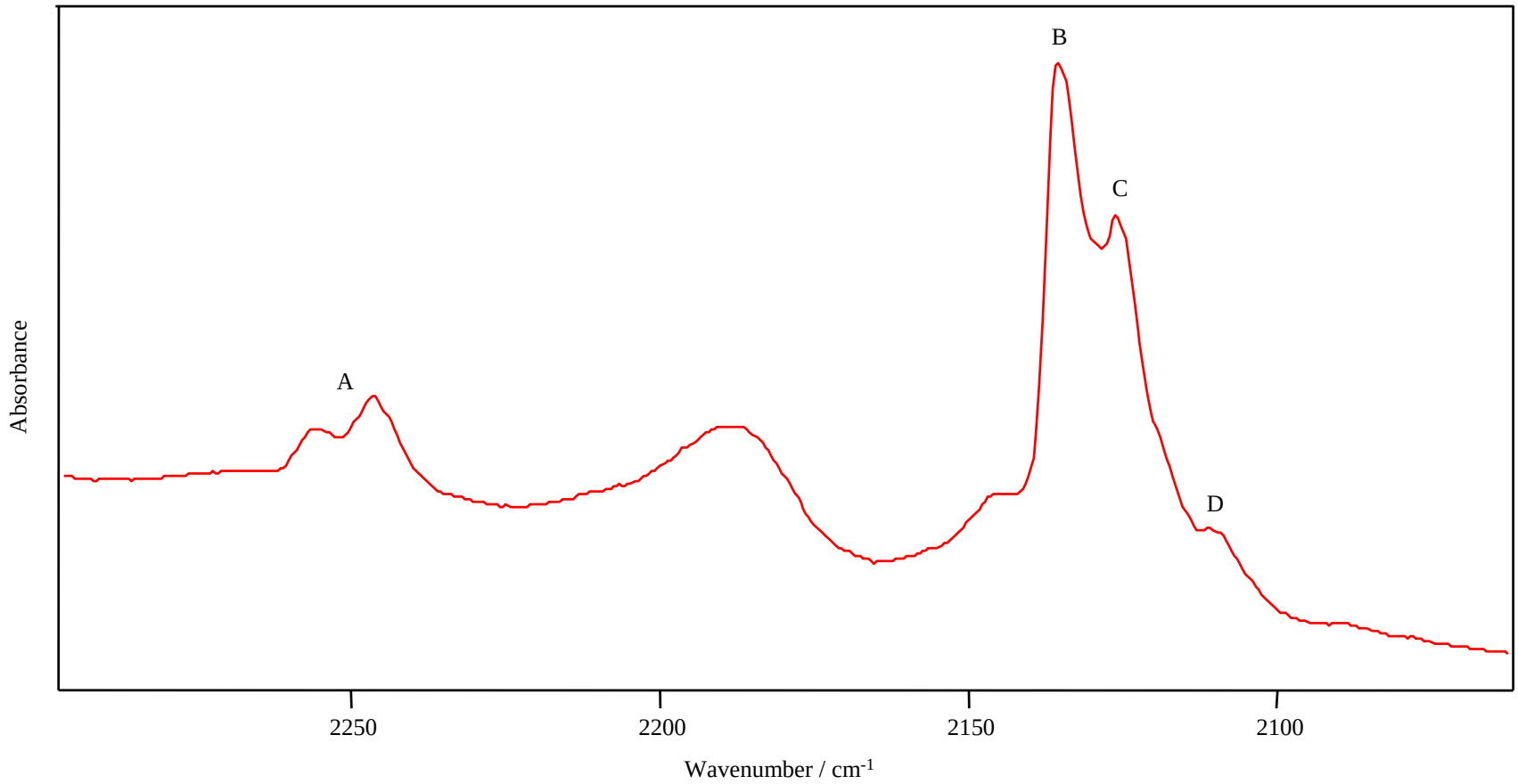

Figure 5.3 FT-IR spectrum of SF_6 matrix trapped (16 K) fumaroyl chloride after IR LPHP; A = C_3O; B =CO; C = 2-propynoyl chloride; D = chloroacetylene; unassigned peaks are attributable to SF_6

The predominant decomposition pathway of 4-oxo-2,3-butadienoyl chloride involves decarbonylation to yield 3-oxo-3-chloro-1-propenylidene. The subsequent rearrangement of this transient species (through insertion of the divalent carbon at the C_β–H bond) will yield 2-propynoyl chloride; the formation of 2-propynoyl chloride is also consistent with the molecular dehydrochlorination of *E* or *Z*-3-chloro-2-propenoyl chloride. The molecular elimination of HCl from 3-oxo-3-chloro-1-propenylidene is not a significant decomposition mechanism; the resultant species (tricarbon monoxide) was observed in only trace amount. A proposed scheme for the pyrolysis of fumaroyl chloride is illustrated in Figure 5.4.

5.3.2 Co-pyrolysis with $W(CO)_6$

In the present work, a sample of fumaroyl chloride and $W(CO)_6$ was exposed to low laser power; the most significant products were CO, benzene, acetyl chloride and acetylene, the latter observed in trace amount. The formation of acetylene is consistent with the selective abstraction of chlorine atoms, followed by successive homolytic loss of carbonyl groups from the resultant diradical. The generation of benzene (and the low yield of acetylene) is consistent with the trimerisation of acetylene, a process well known to be catalysed by transition metals [32-37].

The formation of acetyl chloride is consistent with the selective abstraction of a single chlorine atom to yield the 4-chloro-1,4-dioxo-2-butenyl radical; this rearranges to the 4-chloro-1,4-dioxo-3-buten-2-yl radical. The homolytic fragmentation of the C(2)–C(3) single bond (numbered from the chlorine-bearing carbon) with an accompanying hydrogen shift will effect formation of the chloroacetyl (1-oxo-2-chloroethyl) radical and

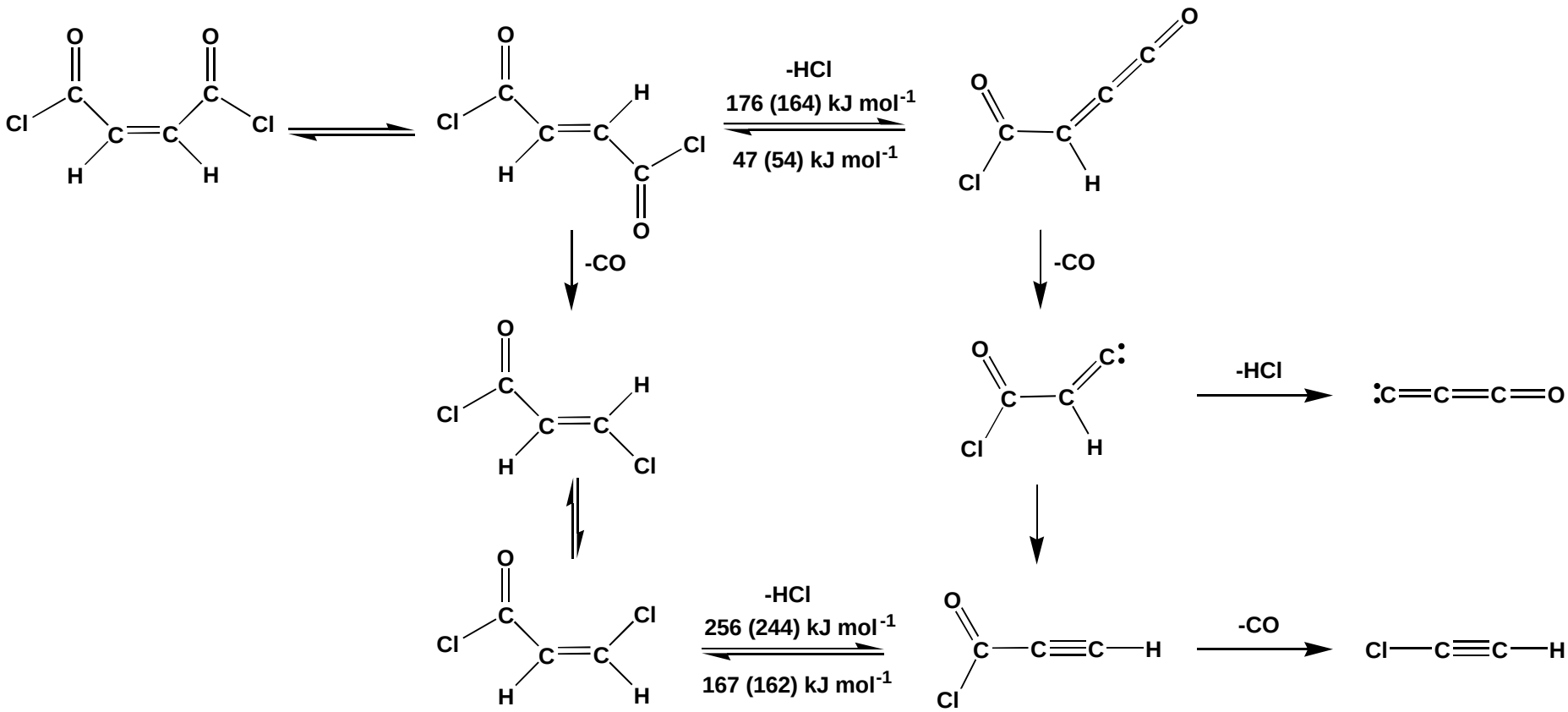

Figure 5.4 A proposed scheme for fumaroyl chloride IR LPHP with calculated activation energies for reversible dehydrochlorination; figures in parenthesis refer to maleoyl chloride, the *Z* isomer

oxoethenylidene; presumably, decarbonylation of the latter will yield elemental carbon. An alternative mechanism involving decarbonylation of 4-chloro-1,4-dioxo-3-buten-2-yl can not be discounted; a hydrogen shift in the resultant species with concomitant loss of carbon will also yield the chloroacetyl radical. The subsequent abstraction of atomic hydrogen by chloroacetyl will yield the observed acetyl chloride. A proposed scheme for fumaroyl chloride and $W(CO)_6$ pyrolysis is illustrated in Figure 5.5.

5.4 Succinyl Chloride

The decomposition of succinyl chloride (butanedioyl dichloride) has not been the subject of previous investigation. The reaction of sodium or potassium with succinyl chloride in dry xylene has been shown by Pearl and co-workers to yield succinic anhydride [38]. A mechanism was proposed in which K or Na effectively abstracts Cl from the acyl chloride.

5.4.1 Pyrolysis

In the present work, the products of succinyl chloride IR LPHP in the presence and absence of $W(CO)_6$ were characterised using FT-IR spectroscopy at both ambient and low (16 K) temperatures. The post-pyrolysis infrared spectra of succinyl chloride in the absence and presence of $W(CO)_6$ at ambient temperature is given in Figure 5.6. The products observed following the pyrolysis of succinyl chloride at low power were HCl, CO and acryloyl chloride; acetylene and chloroethene, the latter ascribed to decarbonylation of acryloyl chloride were detected at higher laser power.

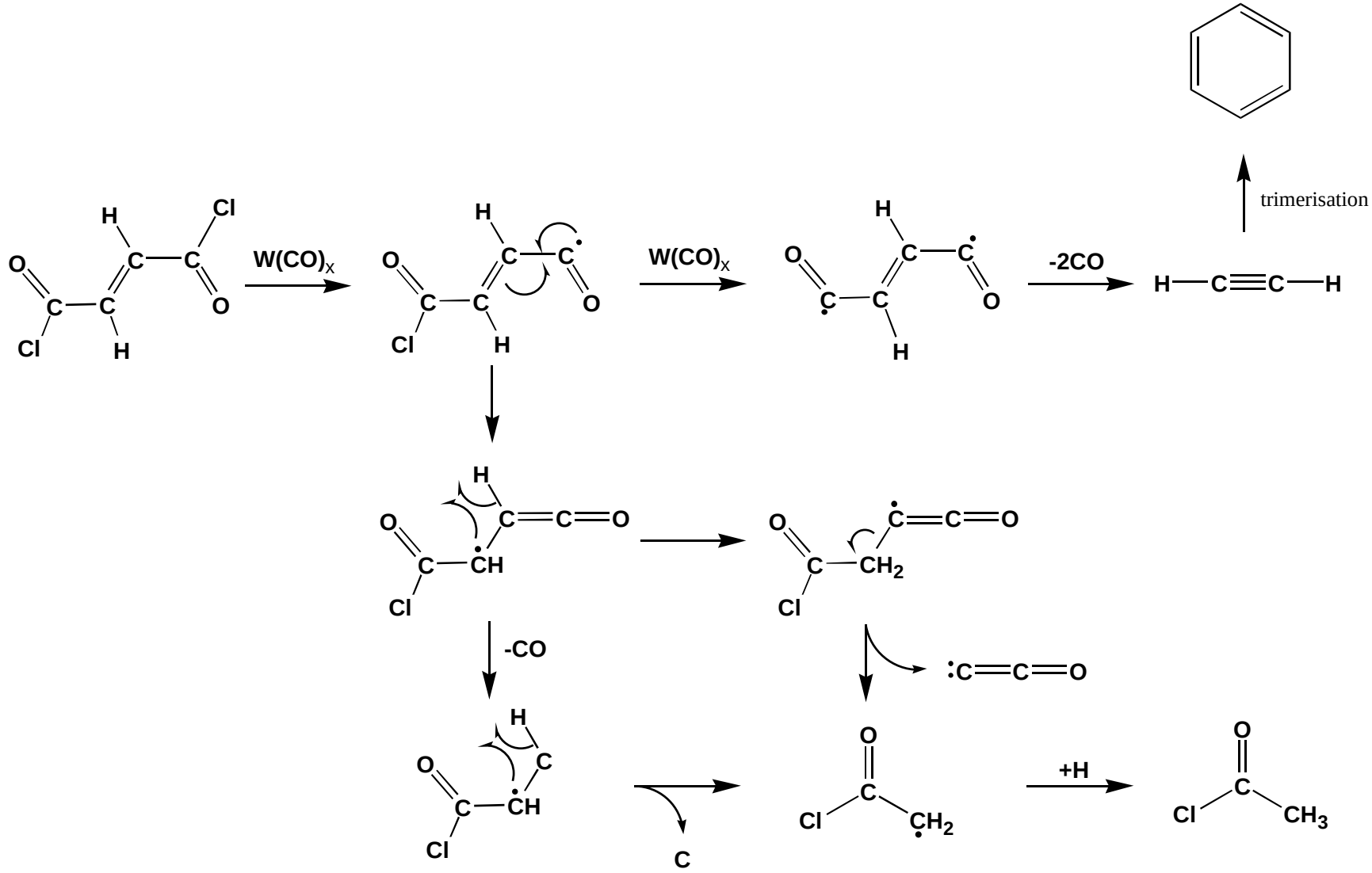

Figure 5.5 A proposed scheme for fumaroyl chloride and $W(CO)_6$ IR LPHP

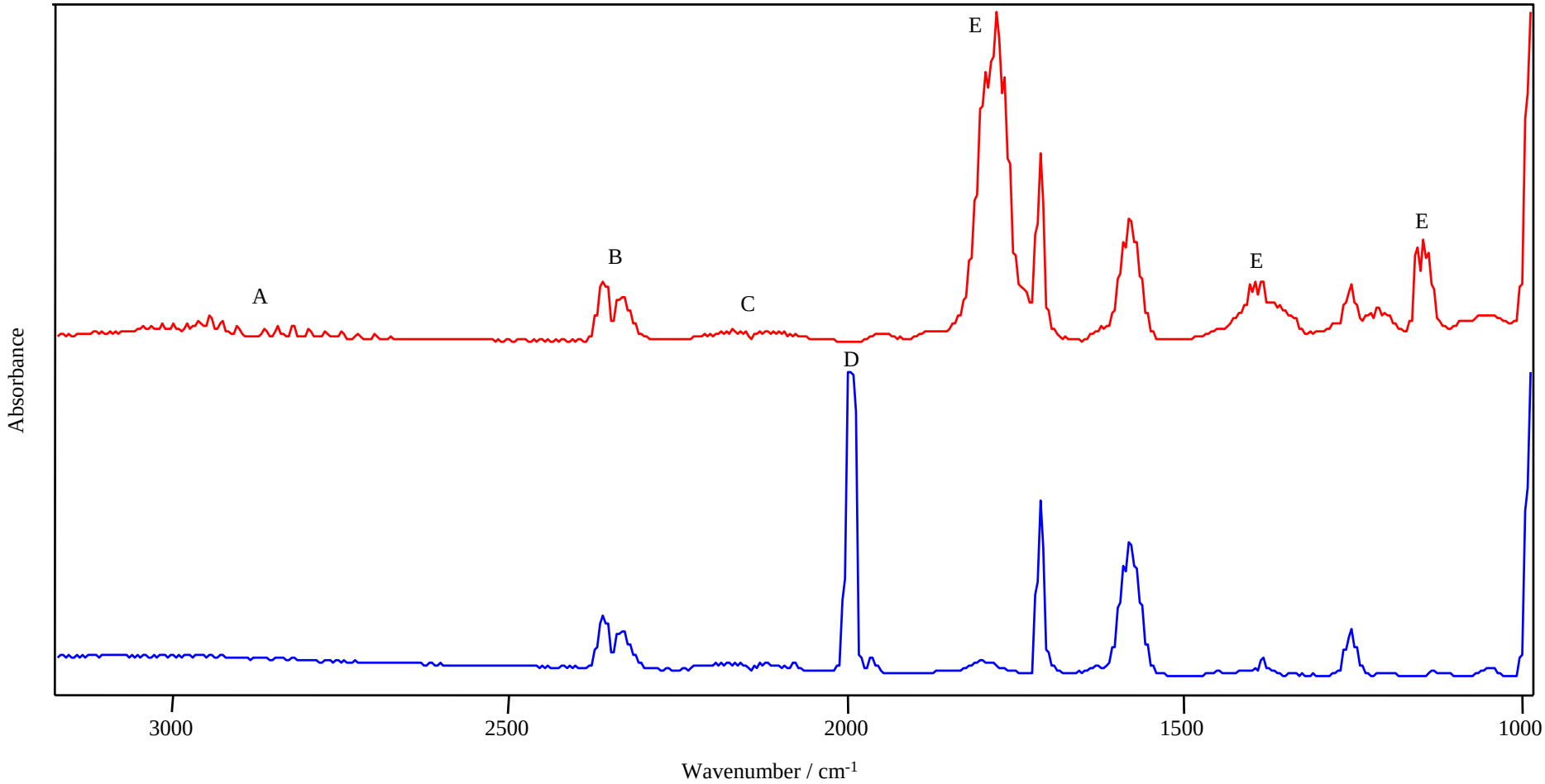

Figure 5.6 FT-IR spectra of the products of laser pyrolysis of succinyl chloride in the absence (—) and presence (—) of $W(CO)_6$; A = HCl; B = CO_2; C = CO; D = $W(CO)_6$; E = acryloyl chloride; unassigned peaks are attributable to SF_6; the CO_2 present is atmospheric in nature

The infrared spectra of Ar matrix trapped succinyl chloride (dilution 2000 : 1) following pyrolysis at 748 and 1023 K is illustrated in Figure 5.7. The post-pyrolysis (1023 K) spectrum revealed a series of absorbance bands between 2200 and 2100 cm^{-1} that was not unlike the post-pyrolysis spectra of 3-chloropropanoyl and acryloyl chloride. The most intense absorbance band, at 2122 cm^{-1}, was ascribed to the cumulenic stretch, ν_2, of methylene ketene (1,2-propadien-1-one), and is in agreement with the value (that was ascribed to the uncomplexed ketene) reported by Chapman and co-workers [39]. A number of weaker absorbance signals were also present at 2136, 2147, 2152 (shoulder) and 2169 cm^{-1}, the latter attributable to 3-chloro-1-propen-1-one. The formation of methylene ketene and 3-chloro-1-propene is consistent with the decomposition of acryloyl chloride (refer to section 4.5.1), which was observed in only trace amount under these conditions. The signal at 2147 cm^{-1} was comparable to that observed in the infrared spectrum of matrix trapped acryloyl and 3-chloropropanoyl chloride subsequent to pyrolysis at 1023 K, and has yet to be identified. The peak at 2136 cm^{-1} is ascribed to uncomplexed CO; the spectrum of an Ar matrix-isolated sample of pure CO was spectroscopically identical with the peak observed in the post-pyrolysis spectrum.

The infrared spectrum of Ar matrix trapped succinyl chloride (dilution 2000 : 1) following pyrolysis at 748 K was essentially devoid of the absorbance bands ascribed to methylene ketene and 3-chloro-1-propen-1-one; acryloyl chloride was observed at a significant level. In the region between 2200 and 2100 cm^{-1}, several peaks were observed at 2126, 2136, 2142, 2147 and 2152 cm^{-1}; the bands at 2147 and 2136 cm^{-1} were identical to those detected following the pyrolysis of succinyl chloride at 1023 K. In addition to these bands, there were two weak peaks at 1825 and 1875 cm^{-1} that may be ascribed to cyclopropenone; Breslow and Ryan observed cyclopropenone at 1835 and 1875 cm^{-1} [40]. A definitive

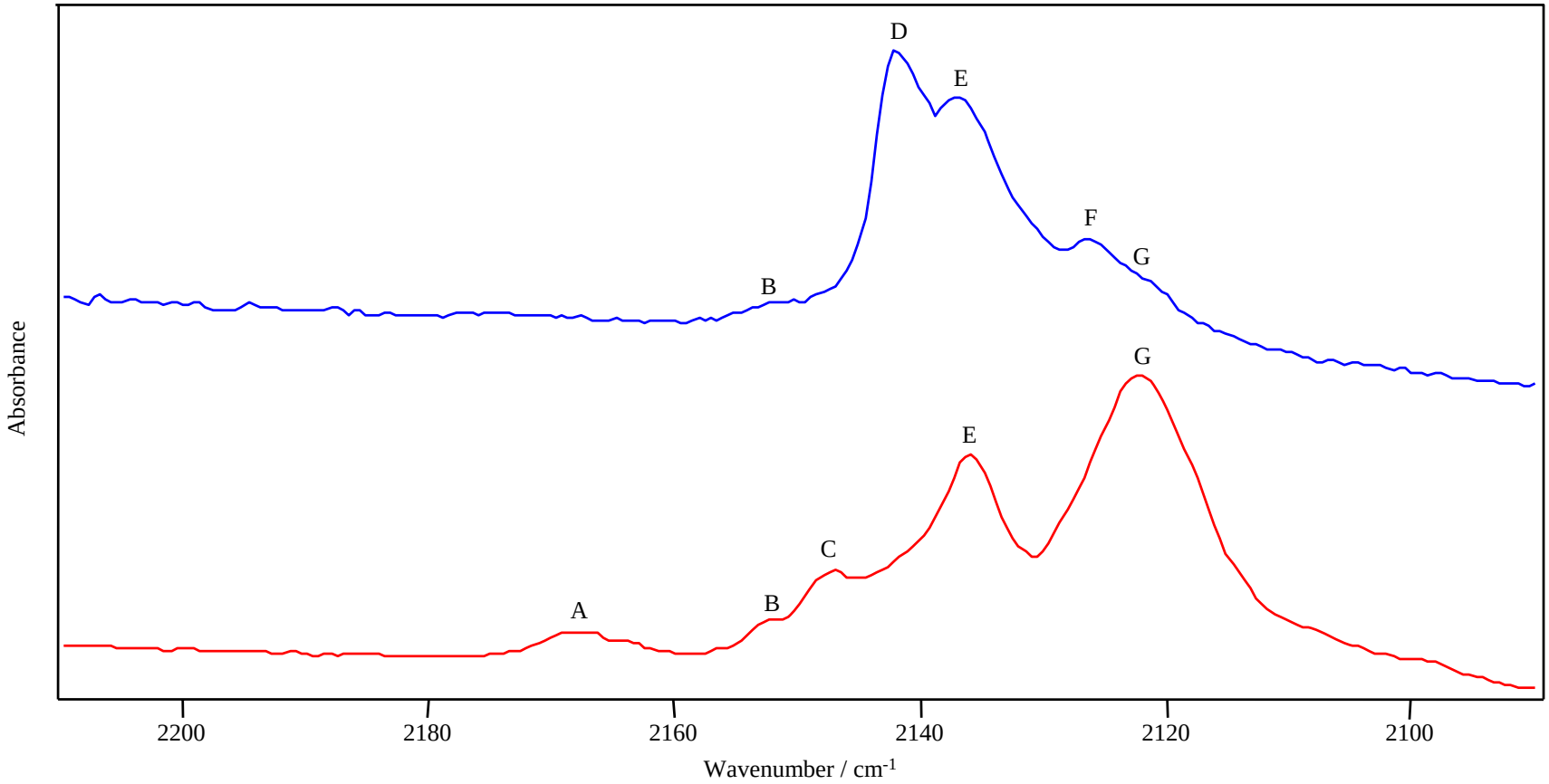

Figure 5.7 FT-IR spectra of Ar matrix trapped (16 K) succinyl chloride after pyrolysis at 748 (—) and 1023 K (—); A = 3-chloro-1-propen-1-one; B, C = unidentified; D = 4-oxo-3-butenoyl chloride; E = CO; F = 1,3-butadiene-1,4-dione; G = 1,2-propadien-1-one

assignment of the weak band at 2152 cm^{-1} was not possible in this study. The absorbance band at 2142 cm^{-1} is ascribed to 4-oxo-3-butenoyl chloride; in the present work, the cumulenic stretch, ν_2, of 4-oxo-3-butenoyl chloride was calculated with scaling [31] at 2152 cm^{-1}. The formation of this compound is consistent with the dehydrochlorination of starting material. There is no evidence to suggest that such a process is reversible; the absorbance bands ascribed to starting material did not increase at the expense of those assigned to HCl during the acquisition of a spectrum.

The band at 2126 cm^{-1} may be ascribed to 1,3-butadiene-1,4-dione; Maier and co-workers observed 1,3-butadiene-1,4-dione (procured through photolysis of the corresponding diazoketone) at 2125 cm^{-1} [41]. The formation of 1,3-butadiene-1,4-dione is consistent with the dehydrochlorination of 4-oxo-3-butenoyl chloride; conversely, the decarbonylation of 4-oxo-3-butenyl chloride will yield 3-chloro-3-oxo-propylidene, which can rapidly rearrange to acryloyl chloride. The predominant intramolecular reaction of an alkyl or dialkylcarbene is through insertion of the divalent carbon at the C_β–H or C_γ–H bond to yield the olefin or cyclopropane, respectively [25]. The absence of hydrogen at the γ-carbon of 3-chloro-3-oxo-propylidene precludes insertion at this position, resulting in the exclusive formation of acryloyl chloride through insertion at the C_β–H bond. It is evident that the predominant decomposition pathway of 4-oxo-3-butenoyl chloride involves decarbonylation; acryloyl chloride and (at higher laser power) its associated decomposition products were the most significant products (of a stable or transient nature) that were observed in this investigation.

The decarbonylation of 1,3-butadiene-1,4-dione will likely effect the formation of cyclopropenone. A theoretical study of the interconversion of 1,2-bisketenes (of which

1,3-butadiene-1,4-dione is an example), cyclopropenones and alkynes has been reported by Sung and co-workers [42]. The photolysis of Ar matrix isolated 1,3-butadiene-1,4-dione has been reported by Maier and co-workers [41]; cyclopropenone was observed in the post-photolysis spectrum at 1875 and 1848 cm^{-1}, and ascribed to decarbonylation of the bisketene. The formation of acetylene is consistent with subsequent decarbonylation of cyclopropenone; alternatively, the elimination of CO from 1,2-propadien-1-one will yield acetylene through rearrangement of the intermediate carbene. A proposed scheme for the pyrolysis of succinyl chloride is given in Figure 5.8.

5.4.2 Co-pyrolysis with $W(CO)_6$

The products derived from the pyrolysis of succinyl chloride in the presence of $W(CO)_6$ were identified as CO, propanoyl chloride, 2-chloro-1-propene, 2,2-dichloropropane, ethylene and propene. The formation of propanoyl chloride is consistent with the selective abstraction of atomic chlorine to yield the 4-chloro-1,4-dioxobutyl radical. The decarbonylation of this species will effect the formation of 3-chloro-3-oxopropyl, which can abstract atomic hydrogen to give the observed acyl chloride. The generation of ethylene (the most significant product detected in this investigation) is consistent with successive elimination of atomic chlorine and molecular CO from 3-chloro-3-oxopropyl.

It is apparent from experimental observation that the abstraction of atomic chlorine from starting material is not unique; peaks in the post-pyrolysis infrared spectrum that were ascribed to propanoyl chloride, 2,2-dichloropropane and 2-chloro-1-propene were found to decrease, albeit marginally, as the duration of pyrolysis was increased. The selective abstraction of atomic chlorine from propanoyl chloride will yield propanoyl, from which

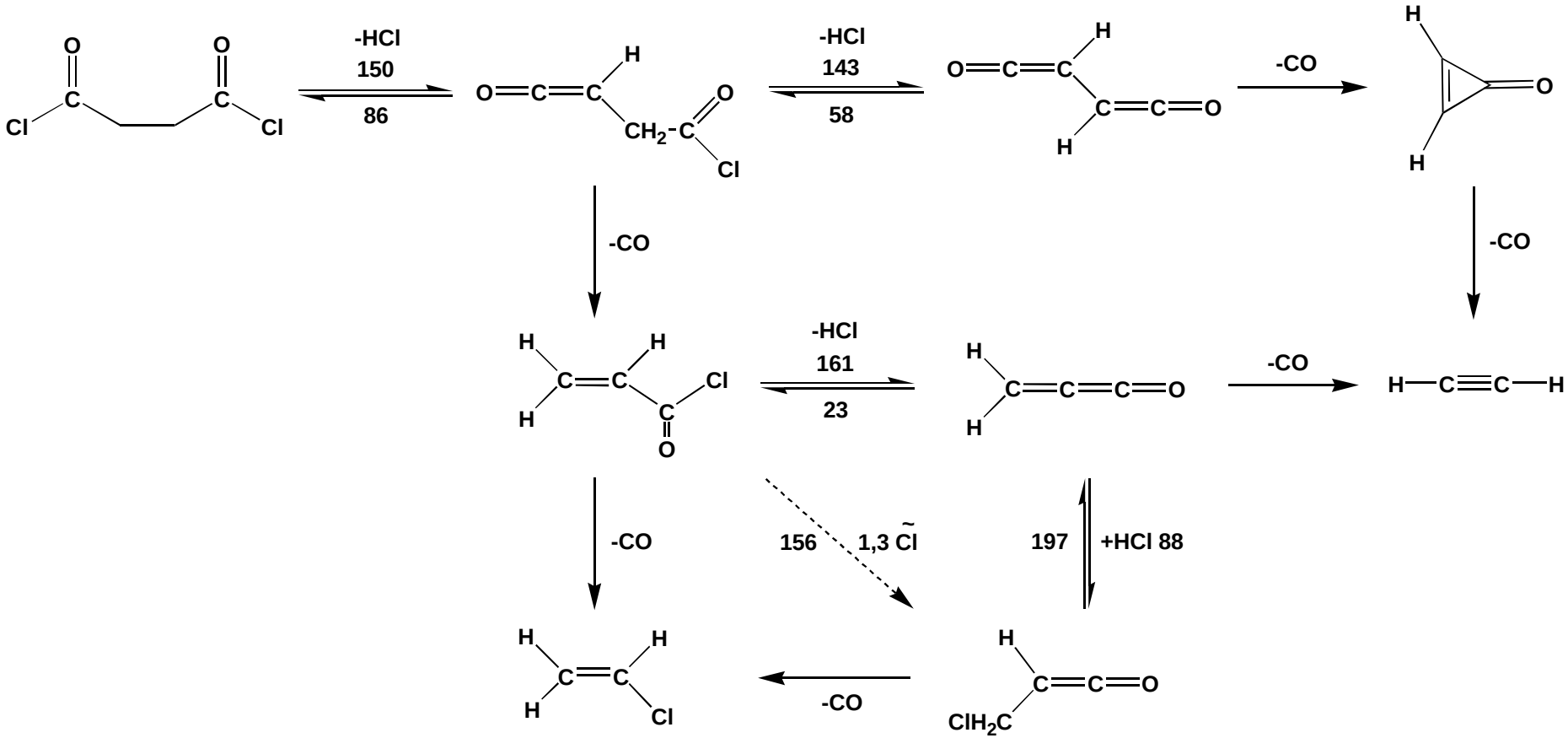

Figure 5.8 A proposed scheme for succinyl chloride IR LPHP; calculated activation energies for dehydrochlorination and 1,3-chlorine migration are in kJ mol^{-1}

the loss of CO will afford the ethyl radical; this can either undergo disproportionation, combination or decomposition (refer to section 4.3.2). The latter is known to proceed, primarily, through homolytic cleavage of the C_β–H bond to yield ethylene [43-49].

The abstraction of atomic chlorine from 2-chloro-1-propene and 2,2-dichloropropane will afford the 1-methylethenyl and 1-chloro-1-methylethyl radicals, respectively. It is conceivable that the latter expel atomic chlorine or hydrogen effecting the formation of propene (through rearrangement of the intermediate carbene) or 2-chloro-1-propene. The molecular elimination of HCl from 2,2-dichloropropane (which will effect the formation of 2-chloro-1-propene) can be discounted; the temperature at which a pure sample of 2,2-dichloropropane decomposed was significantly higher than that employed in this investigation. Moreover, HCl was detected in only trace amount following the pyrolysis of succinyl chloride in the presence of $W(CO)_6$.

The formation of propene is also consistent with abstraction of atomic hydrogen by 1-methylethenyl radicals. The addition of methylene to the double bond of ethylene with concomitant rearrangement of the resultant cyclopropane represents an additional pathway to propene. The formation of methylene may be ascribed to the decomposition of the 1-methylethenyl radical; cleavage of the C(1)–C(2) double bond (numbered from the radical centre) or, alternatively, the elimination of atomic hydrogen from methyl (afforded from scission of the single bond) will yield methylene.

The product ascribed to the combination of 1-methylethenyl (2,3-dimethyl-1,4-butadiene), which was detected in only trace amount following the pyrolysis of methacryloyl chloride in the presence of $W(CO)_6$ (refer section 4.7.2), was not observed in this investigation. It

was rationalised in section 4.7.2 that the inherent instability of 1-methylethenyl [50] would result in a low concentration of the radical; the absence of products consistent with the combination of 1-methylethenyl supports this proposition. The disproportionation of 1-methylethenyl will afford propene and allene or propyne; that the latter two products were not observed suggest that such a mechanism is not practicable.

The formation of 2,2-dichloropropane and 2-chloro-1-propene is consistent with a mechanism involving the selective abstraction of atomic oxygen from starting material. It is proposed that the driving force for reaction is formation of a tungsten-oxygen multiple bond, which has been estimated to be in excess of 577 kJ mol^{-1} [51]. While this is considerably less than the average dissociation energy of the C=O bond, which is equivalent to 743 kJ mol^{-1} [52], there are several cases where the bond dissociation energy is significantly lower. The dissociation energy of the C=O bond in acetone is of the order of 670 kJ mol^{-1} [53].

The transfer of oxygen to a tungsten compound has been promulgated by a number of workers; Brock and Mayer [54] reported the transfer of oxygen from phosphine oxide to a tungsten centre, a reaction they considered remarkable given the strength of the phosphorous-oxygen bond, which is approximately 540 kJ mol^{-1}. The oxidative addition of carbon-oxygen and carbon-nitrogen double bonds to $WCl_2(PMePh_2)_4$, in which the multiple bond is cleaved to form two divalent ligands, has been described by Bryan and Mayer [51]. The reaction of $WCl_2(PMePh_2)_4$ with a ketone or aldehyde was rapid and afforded the bis(η^2-ketone) or bis(η^2-aldehyde) complex, respectively. When the ketone was part of a five-membered ring, the complex was observed to rearrange with loss of ketone to give tungsten (VI) oxo-alkylidene products in high yield. The two-electron

oxidative addition of a heterocumulene was also reported; CO_2 was cleaved to form the oxo-carbonyl complex, $W(O)(CO)Cl_2L_2$. Bryan and Mayer considered these reactions extraordinary given the strength of the carbon-oxygen bonds being cleaved under very mild conditions.

In the present work, the pyrolysis of acetaldehyde and acetone (non-chlorinated species) was investigated in the presence of $W(CO)_6$ in an attempt to evaluate the practicability of oxygen abstraction. The most significant products derived from the pyrolysis of acetaldehyde or acetone with $W(CO)_6$ were consistent with the selective abstraction of atomic oxygen with rearrangement, or combination of the resultant carbene.

The selective abstraction of atomic oxygen from succinyl chloride will yield 1,4-dichloro-4-oxobutylidene; this can rearrange through intramolecular insertion at the C_δ–Cl bond to yield the activated cyclobutanone derivative, namely 2,2-dichlorocyclobutanone. The formation of four-, five- or six-membered rings by intramolecular insertion is quite exceptional [25]; however, it is conceivable that the predominant conformation of the intermediate carbene is such that insertion at the C_δ–Cl bond is favoured. The thermal decomposition of a simple cyclobutanone is reported to involve competition between α-cleavage with concomitant decarbonylation, and cycloreversion (2 + 2 cleavage) to the respective alkene and ketene [55]. The pyrolysis of cyclobutanone is initiated, almost exclusively, through cycloreversion to ethylene and ketene [56-58]; decarbonylation to cyclopropane (through a diradical intermediate) is a minor process.

It is proposed that the thermal decomposition of activated 2,2-dichlorocyclobutanone effect the exclusive formation of 2,2-dichlorocyclopropane through the elimination of molecular

CO. The fact that this compound was not detected in this study suggests that it may decompose under these conditions. The homolytic cleavage of the three-membered ring will afford a diradical intermediate (2,2-dichloro-1,3-propanediyl), which abstracts atomic hydrogen to form the 2,2-dichloropropyl radical; this either abstracts a further hydrogen atom to yield 2,2-dichloropropane, or loses atomic chlorine affording 2-chloro-1-propene. The formation of 2-chloro-1-propene is also consistent with the elimination of atomic chlorine from 2,2-dichloro-1,3-propanediyl to yield the 2-chloro-2-ethenyl radical; this can then abstract atomic hydrogen. A proposed pyrolysis scheme for succinyl chloride in the presence of $W(CO)_6$ is given in Figure 5.9.

5.5 Diglycoloyl Chloride

5.5.1 Pyrolysis

The decomposition of diglycoloyl chloride (2,2'-oxybisacetyl chloride) has not been the subject of previous investigation. In the present work, the stable products of diglycoloyl chloride IR LPHP were identified as HCl, CO, CO_2, chloromethane, chloroethene, acetyl chloride, chloroacetaldehyde, oxybischloromethane, ethylene, acetylene, methane and 1,2-dichloroethane, the latter observed in trace amount. A weak band was also detected in the post-pyrolysis gas chromatogram, which is ascribed to a mono-chlorinated species with a molecular weight equivalent to 106 g mol^{-1}.

The low temperature (16 K) post-pyrolysis FT-IR spectrum of diglycoloyl chloride in a SF_6 matrix (dilution 1000 : 1) revealed relatively few absorbance bands between 2200 and 2100 cm^{-1}. A peak at 2137 cm^{-1} is ascribed to uncomplexed CO; the spectrum of a SF_6

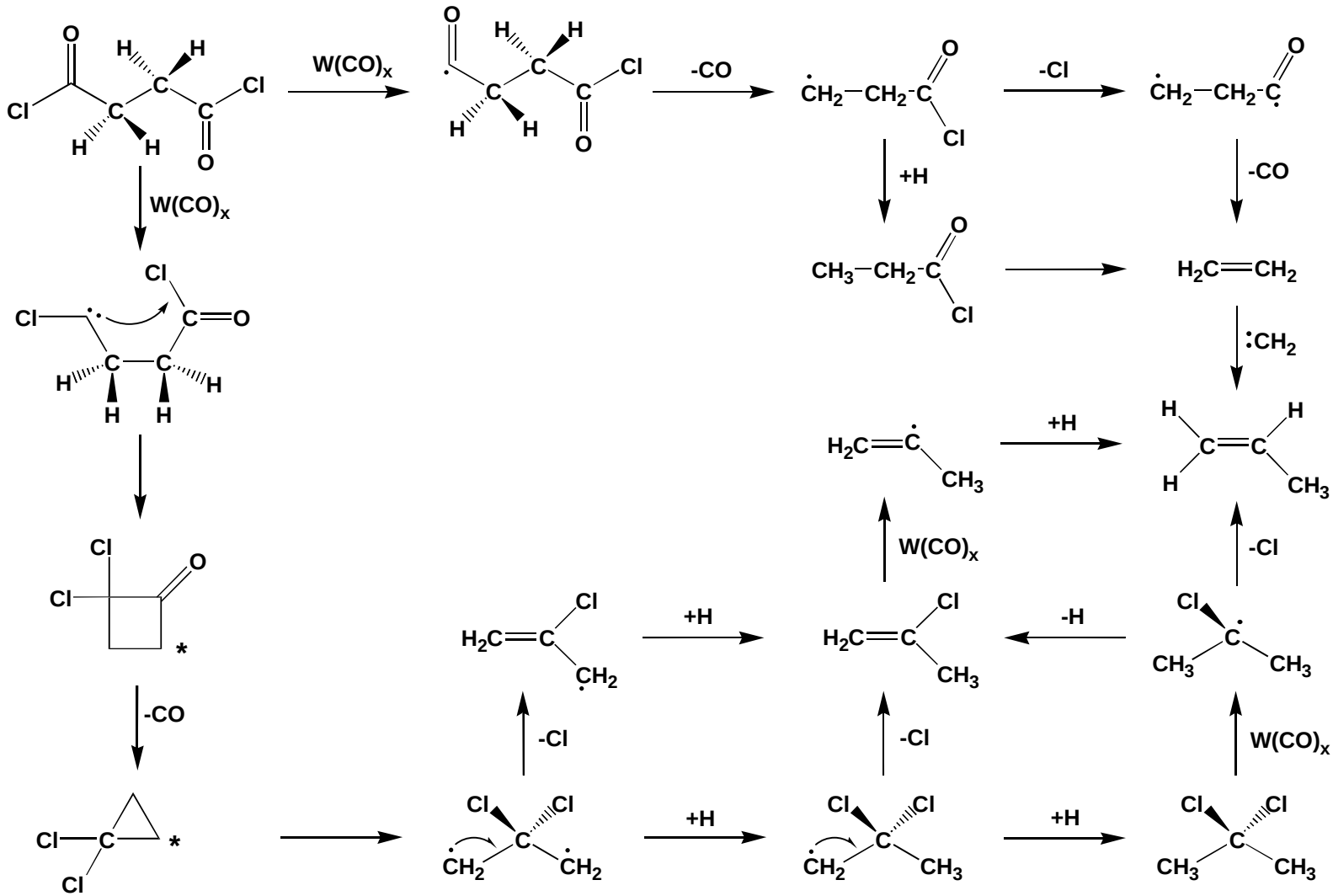

Figure 5.9 A proposed scheme for succinyl chloride and W $(CO)_6$ IR LPHP; activated species are labelled *****

matrix-isolated sample of pure CO was spectroscopically identical with the band observed in the post-pyrolysis spectrum. A band at 2144 cm^{-1}, which decreased in intensity in experiments that employed a restriction between the reaction cell and the cold stage (where the pyrolysate is collected), is ascribed to 2-(2-oxo-1-ethenyloxy)acetyl chloride. The formation of this species is consistent with molecular dehydrochlorination of diglycoloyl chloride. There was no evidence to suggest dehydrochlorination was reversible; the absorbance bands ascribed to starting material did not increase at the expense of HCl during the acquisition of a spectrum. In the present work, the cumulenic stretch, ν_2, of 2-(2-oxo-1-ethenyloxy)acetyl chloride was calculated with scaling [31] at 2162 cm^{-1}, which is in reasonable agreement with the frequency observed.

It is apparent from experiment that the decomposition of 2-(2-oxo-1-ethenyloxy)acetyl chloride involves exclusive elimination of molecular CO; there was no evidence to indicate formation of the dehydrochlorination product, namely 2,2'-oxybis-1-ethenone. It is conceivable that rearrangement of the resultant carbene take one of two forms: intramolecular insertion of the divalent carbon at the C_β–O bond to yield activated 3-oxo-propanoyl chloride, or intramolecular carbonyl addition of the divalent centre, which will generate vibrationally excited 2-chloro-1-ethenylformate. The intramolecular carbonyl addition of a diarylcarbene is reported to be the principal step in the photorearrangement of a quinoxaline-*N*-oxide to the corresponding isobenzofuran [59]. Insertion at a C–H bond, while expected to predominate [25], can be discounted; there was no hydrogen at the β position, and the product procured from insertion at the C_γ–H bond was not observed.

The presence of a weak band ascribed to a mono-chlorinated species with a molecular weight of 106 g mol^{-1} is consistent with the collisional deactivation of activated 2-chloro-

1-ethenylformate or 3-oxo-propanoyl chloride. The probability of collision is dependent on the total pressure; consequently, deactivating collisions are not significant in the present study where the total pressure was invariably low. The formation of acetyl chloride and chloroacetaldehyde is consistent with decarbonylation of activated 3-oxo-propanoyl chloride. The subsequent elimination of molecular CO from acetyl chloride or chloroacetaldehyde will yield chloromethane, a significant product at elevated temperature.

The decarboxylation of activated 2-chloro-1-ethenylformate with a concomitant hydrogen shift will afford chloroethene, the most significant product in this investigation. The formation of chloroethene is also consistent with the molecular dehydrochlorination of 1,2-dichloroethane. It is likely that the generation of acetylene involves the molecular elimination of HCl from chloroethene; certainly, the bands ascribed to acetylene became more intense, at the expense of those assigned to chloroethene, at higher temperature.

The formation of oxybischloromethane is consistent with the elimination of both carbonyl groups from diglycoloyl chloride. It is evident from the high yield of oxybischloromethane that this represents a significant decomposition route. The absence of chloromethoxyacetyl chloride (the product generated from the elimination of a single CO molecule) suggests that the elimination of a second CO molecule will rapidly follow that of the first under these conditions. It is conceivable that the elimination of molecular CO from the species effected through bis(dehydrochlorination) of oxybischloromethane will yield methylene; this either combines, or abstracts H to yield ethane and methane, respectively.

The homolytic fragmentation of the C–O bond in oxybischloromethane will yield the chloromethoxy and chloromethyl radicals; combination of the latter will afford the

observed 1,2-dichloroethane. Although the enthalpy of the C–O bond is considerably higher [52] than the calculated activation energies associated with molecular dehydrochlorination, it is likely that the reaction temperature is sufficient to initiate cleavage of the C–O bond. It is conceivable that the decomposition of the chloromethoxy radical involve molecular elimination of HCl with subsequent decarbonylation of the resultant species. A proposed scheme for the pyrolysis of diglycoloyl chloride is illustrated in Figure 5.10.

5.5.2 Co-pyrolysis with $W(CO)_6$

The most significant products observed following the pyrolysis of diglycoloyl chloride in the presence of $W(CO)_6$ at a slightly lower laser power were CO, chloromethoxyacetyl chloride, oxybischloromethane, chloromethoxymethane, acetone, propene, ethylene and methane. Decarbonylation of the species derived from the selective abstraction of atomic chlorine will yield the 2-chloro-2-oxoethoxymethyl radical. The decarbonylation of this compound will yield the chloromethoxymethyl radical, which can abstract atomic hydrogen to form the observed chloromethoxymethane. The formation of 2-chloro-2-oxoethoxymethyl and chloromethoxymethyl is also consistent with the abstraction of atomic chlorine from chloromethoxyacetyl chloride and oxybischloromethane, respectively.

The generation of chloromethoxyacetyl chloride and oxybischloromethane involves successive elimination of CO from starting material; the elimination of a single CO molecule will generate the observed chloromethoxyacetyl chloride, from which the loss of a second CO molecule will yield oxybischloromethane. These results reflect the

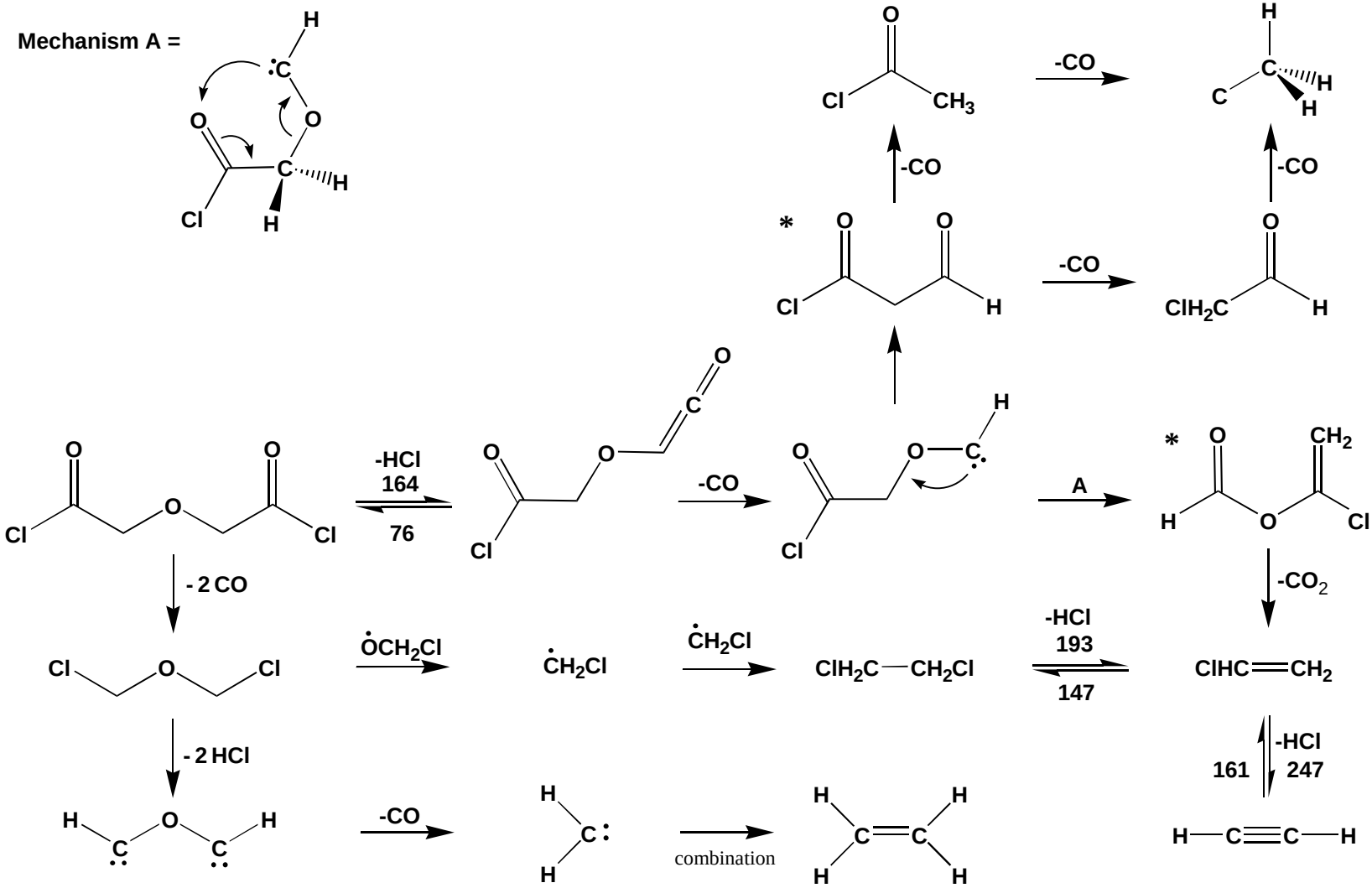

Figure 5.10 A proposed scheme for diglycoloyl chloride IR LPHP with calculated activation energies for dehydrochlorination in kJ mol^{-1}; activated species are labelled *****

comparatively mild conditions of pyrolysis in the presence of $W(CO)_6$; chloromethoxyacetyl chloride, which was not detected in the absence of $W(CO)_6$, is a significant product in this investigation.

The decomposition of the chloromethoxymethyl radical may involve homolytic cleavage of the C(1)–O single bond (numbered from the radical centre) to yield the chloromethoxy radical in addition to methylene. Tsang and Kiefer have investigated the unimolecular reactions of a number of polyatomic molecules [60]; the unimolecular rate expressions for the decomposition of larger radicals had activation energies between 120-160 kJ mol^{-1} and normal pre-exponential factors. It was proposed that these species were significantly less stable than the analogous alkanes and alkenes, and would rapidly generate highly reactive species such as methyl or atomic hydrogen. Combination of methylene will yield ethylene, while abstraction of hydrogen atoms by methylene will account for the observed methane. The formation of propene is consistent with the addition of methylene to the double bond of ethylene with rearrangement of the vibrationally excited cyclopropane intermediate.

The mechanism responsible for the formation of acetone is proposed to involve the selective abstraction of atomic oxygen from diglycoloyl chloride; the practicability of oxygen abstraction is evaluated in section 5.4.2. It is conceivable that rearrangement of the resultant species involve intramolecular insertion of the divalent carbon at the C_γ–O bond to yield a vibrationally excited epoxide derivative. Intramolecular insertion at a C_β–H or C_δ–H bond can be precluded, as the anticipated end products were not observed.

The decomposition of an epoxide, primarily, involves cleavage of a C–O bond to yield one of two diradical species [61]. The subsequent rearrangement of the diradical may take two

forms: migration of atomic hydrogen to oxygen will afford the unsaturated alcohol, while a hydrogen shift to carbon will effect the formation of the ketone or aldehyde. It is evident from experimental observation, specifically the exclusive formation of acetone, that rearrangement of the intermediate diradical involves homolysis of the C(4)–O bond (numbered from the carbonyl group) and is preceded or accompanied by the elimination of atomic chlorine and molecular CO. The resultant species may abstract hydrogen atoms to form the observed acetone. A proposed scheme for the pyrolysis of diglycoloyl chloride in the presence of $W(CO)_6$ is illustrated in Figure 5.11.

5.6 Conclusion

The results presented in this chapter confirm that $W(CO)_x$ species are effective and selective abstractors of atomic chlorine from the selected diacyl chlorides under comparatively mild conditions. Moreover, the investigation of the pyrolysis of succinyl and diglycoloyl chloride indicate that unsaturated $W(CO)_x$ species are also effective abstractors of atomic oxygen.

The decarbonylation of the species derived from the abstraction of a single chlorine atom will afford an intermediate species that can either abstract atomic hydrogen or lose a second chlorine atom. The subsequent decarbonylation of the species derived from the loss of a second chlorine atom will effect formation of a stable species, with the exception of methylene, which was generated from the pyrolysis of malonyl chloride. The aforementioned mechanism represents, in all but a single case, a significant decomposition pathway. The pyrolysis of diglycoloyl chloride did not involve the elimination of a second

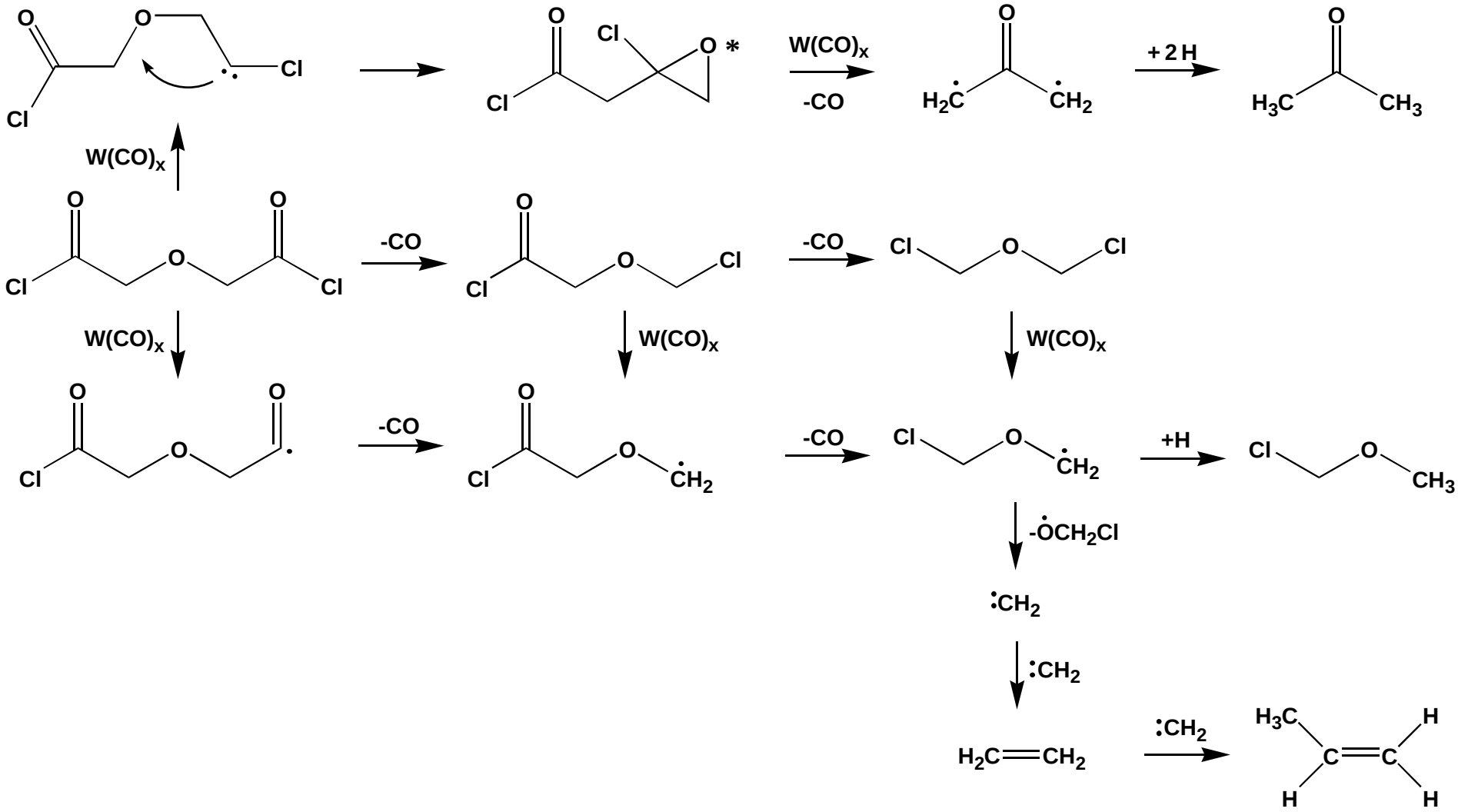

Figure 5.11 A proposed scheme for diglycoloyl chloride and W $(CO)_6$ IR LPHP; activated species are labelled *****

chlorine atom; presumably, fragmentation of the intermediate species (through homolysis of the C–O bond) was favoured.

The selective abstraction of atomic chlorine from starting material was not unique; in several cases a product could only be accounted for through a mechanism that involved Cl abstraction from a primary pyrolysis product. The decarbonylation of the diacyl chloride was not a predominant decomposition pathway; the product effected from the elimination of molecular CO was observed only following pyrolysis of diglycoloyl chloride in the presence of $W(CO)_6$.

The intramolecular insertion of the carbene afforded from the selective abstraction of a single oxygen atom was found to effect the formation of a cycloalkane derivative; insertion of the divalent carbon at the C_γ–O bond of the species derived from the pyrolysis of diglycoloyl chloride and $W(CO)_6$ yielded the corresponding epoxide. Intramolecular insertion at the C_δ–Cl bond of the carbene formed following pyrolysis of succinyl chloride in the presence of $W(CO)_6$ resulted in the formation of a cyclobutanone derivative.

The pyrolysis of the selected diacyl chlorides was initiated in the absence of $W(CO)_6$, primarily, through molecular elimination of HCl. The decomposition of the resultant ketene involved either homolytic loss of a carbonyl group to yield a carbene species, or molecular dehydrochlorination. The decarbonylation of the intermediate ketene predominated in all but a single case; chloroformyl ketene (which was procured through the pyrolysis of malonyl chloride) yielded carbon suboxide exclusively through molecular elimination of HCl. The decarbonylation of starting material was observed only following pyrolysis of fumaroyl or diglycoloyl chloride; reaction was limited, in the case of fumaroyl

chloride, to homolytic loss of a single carbonyl group, and was succeeded by molecular dehydrochlorination.

The predominant rearrangement of the carbene derived through successive dehydrochlorination and decarbonylation of starting material involved intramolecular insertion of the divalent carbon at the C_β–H bond or (where there was no C_β–H bond) the C_β–O bond; intramolecular carbonyl addition of the carbene was also practicable under these conditions. Decarbonylation of the product derived through rearrangement of the intermediate carbene is initiated at a higher laser power.

5.7 References

[1] G. R. Allen, N. D. Renner and D. K. Russell, *J. Chem. Soc., Chem. Commun.*, 1998, 703.

[2] T. T. Tidwell, *Ketenes,* John Wiley & Sons, New York, 1995 and references therein.

[3] *The Chemistry of Acyl Chlorides,* S. Patai, Ed., John Wiley & Sons, London, 1972.

[4] *The Chemistry of Ketenes, Allenes and Related Compounds,* S. Patai, Ed., John Wiley & Sons, New York, 1980.

[5] P. Zarras and O. Vogl, *Prog. Polym. Sci.*, 1991, **16**, 173.

[6] A. D. Allen, J. D. Colomvakos, I. Egle, R. Liu, J. Ma, R. M. Marra, M. A. McAllister and T. T. Tidwell, *Can. J. Chem.*, 1996, **74**, 457.

[7] A. D. Allen, R. Liu, J. Ma, M. A. McAllister, T. T. Tidwell and D. Zhao, *Pure Appl. Chem.*, 1995, **67**, 777.

[8] A. D. Allen, J. Ma, M. A. McAllister, T. T. Tidwell and D. Zhao, *Acc. Chem. Res.*, 1995, **28**, 265.

[9] N. Piétri, T. Chiavassa, A. Allouche, M. Rajzmann and J. Aycard, *J. Phys. Chem.*, 1996, **100**, 7034.

[10] N. Piétri, J. Aycard, A. Allouche, P. Verlaque and T. Chiavassa, *Spectrochim. Acta, Part A*, 1995, **51**, 1891.

[11] G. Maier, H. P. Reisenauer, H. Balli, W. Brandt and R. Janoschek, *Angew. Chem., Int. Ed. Engl.*, 1990, **29**, 905.

[12] D. Sülzle and H. Schwarz, *Angew. Chem., Int. Ed. Engl.*, 1990, **29**, 908.

[13] L. H. Reyerson, *Chem. Rev.*, 1930, **7**, 479.

[14] H. Ulrich, In *Cycloaddition Reactions of Heterocumulenes*, Academic Press, New York, 1967; pp. 110-121.

[15] T. Kappe and E. Ziegler, *Angew. Chem., Int. Ed. Engl.*, 1974, **13**, 491.

[16] T. Kappe, *Methoden der Organischen Chemie,* Theime Verlag, Stuttgart, 1993.

[17] L. Pandolfo, G. Facchin, R. Bertani, P. Ganis and G. Valle, *Angew. Chem., Int. Ed. Engl.*, 1994, **33**, 576.

[18] K. T. Potts, P. M. Murphy and W. R. Kuehnling, *J. Org. Chem.*, 1988, **53**, 2889.

[19] J. M. Oakes and G. B. Ellison, *Tetrahedron*, 1986, **42**, 6263.

[20] S. Polanc, M. C. Labille, Z. Janousek, R. Merenyi, M. Vermander, H. G. Viehe, B. Tinant, J. Piret-Meunier and J. P. Declercq, *New J. Chem.*, 1991, **15**, 79.

[21] W. T. Huntress, M. Allen and M. Delitsky, *Nature*, 1991, **352**, 316.

[22] G. Friedrichs and H. G. Wagner, *Z. Phys. Chem. (Munich)*, 1998, **203**, 1.

[23] Z. Cinar and Y. Inel, *Kim. Sanayi*, 1989, **31**, 49.

[24] Y. Osamura, K. Nishimoto, S. Yamabe and T. Minato, *Theor. Chim. Acta*, 1979, **52**, 257.

[25] W. Kirmse, *Carbene Chemistry,* Academic Press, New York, 1971.

[26] H. M. Frey, *Proc. Roy. Soc., Ser. A*, 1959, **250**, 409.

[27] H. M. Frey, *Proc. Roy. Soc., Ser. A*, 1959, **251**, 575.

[28] R. D. Brown, P. D. Godfrey, P. S. Elmes, M. Rodler and L. M. Tack, *J. Am. Chem. Soc*, 1985, **107**, 4112.

[29] D. McNaughton, D. McGilvery and F. Shanks, *J. Mol. Spec.*, 1991, **149**, 458.

[30] R. D. Brown, D. E. Pullin, E. H. N. Rice and M. Rodler, *J. Am. Chem. Soc.*, 1985, **107**, 7877.

[31] Calculated values are scaled by 2150.7 / 2349.1 (*i.e.* the observed signal for ketene in the gas phase / the calculated value for the cumulenic stretch of ketene).

[32] J. C. Bertolini, J. Massardiner and G. Dalmai-Imerdik, *J. Chem. Soc., Farad. Trans. I*, 1978, **74**, 1720.

[33] S. Lie, L. Wang, M. Xie, X. Guo and Y. Wu, *Catal. Lett.*, 1995, **30**, 135.

[34] P. M. Maitlis, *Pure Appl. Chem.*, 1973, **33**, 489.

[35] G. N. Schauzer and S. Eichlwer, *Chem. Ber.*, 1962, **95**, 550.

[36] F. Solymosi, A. Erdohelyi and A. Szoke, *Catal. Lett.*, 1995, **32**, 43.

[37] J. E. Germaine, *Catalytic Conversion of Hydrocarbons,* Academic Press, London, 1969.

[38] I. A. Pearl, T. W. Evans and W. M. Dehn, *J. Am. Chem. Soc.*, 1938, **60**, 2478.

[39] O. Chapman, M. Miller and S. Pitzenberger, *J. Am. Chem. Soc.*, 1987, **109**, 6867.

[40] R. Breslow and G. Ryan, *J. Am. Chem. Soc.*, 1967, **89**,

[41] G. Maier, H. P. Reisenauer and T. Sayrac, *Chem. Ber.*, 1982, **115**, 2192.

[42] K. Sung, D. Fang, D. Glenn and T. T. Tidwell, *J. Chem. Soc., Perkin Trans. II*, 1998, 2073.

[43] W. L. Hase, H. B. Schlegel, V. Balbyshev and M. Page, *J. Phys. Chem.*, 1996, **97**, 5354.

[44] L. F. Loucks and K. J. Laidler, *Can. J. Chem.*, 1967, **45**, 2795.

[45] M. C. Lin and M. H. Back, *Can. J. Chem.*, 1966, **44**, 2357.

[46] Y. Simon, J. F. Foucaut and G. Scacchi, *Can. J. Chem.*, 1988, **66**, 2142.

[47] A. B. Trenwith, *J. Chem. Soc., Faraday Trans. II*, 1986, **82**, 457.

[48] P. D. Pacey and J. H. Wimalasena, *J. Phys. Chem*, 1984, **88**, 5657.

[49] Y. Feng, J. T. Niiranen, Á. Bencsura, V. D. Knyazev, D. Gutman and W. Tsang, *J. Phys. Chem.*, 1993, **97**, 871.

[50] P. H. Scudder, *Electron Flow in Organic Chemistry,* John Wiley & Sons, New York, 1992.

[51] J. C. Bryan and J. M. Mayer, *J. Am. Chem. Soc.*, 1990, **112**, 2298.

[52] P. W. Atkins, *Physical Chemistry,* 4th Ed, Oxford University Press, Oxford, 1990.

[53] *CRC Handbook of Chemistry and Physics,* 60th Ed, R. C. Weast, Ed., CRC Press, Boca Raton, Fl., 1979.

[54] S. L. Brock and J. M. Mayer, *Inorg. Chem.*, 1991, **30**, 2138.

[55] R. F. C. Brown, *Pyrolytic Methods in Organic Chemistry,* Academic Press, New York, 1980.

[56] J. Metcalfe, H. A. J. Carless and E. K. C. Lee, *J. Am. Chem. Soc.*, 1972, **94**, 7235.

[57] A. T. Blades, *Can. J. Chem.*, 1969, **47**, 615.

[58] M. N. Das, F. Kern, T. D. Coyle and W. D. Walters, *J. Am. Chem. Soc.*, 1954, **76**, 6271.

[59] P. L. Kumler and O. Buchardt, *J. Am. Chem. Soc.*, 1968, **90**, 5640.

[60] W. Tsang and J. H. Kiefer, In *The Chemical Dynamics and Kinetics of Small Radicals,* K. Liu and A. Wagner, Eds., World Scientific, Singapore, 1995; pp. 58-119.

[61] R. J. Gritter, In *The Chemistry of the Ether Linkage,* S. Patai, Ed., Interscience, London, 1967; pp. 373-443.

Chapter Six

HALOGENATED THREE AND FOUR-MEMBERED RING COMPOUNDS

6.1 Introduction

The rearrangement of a cycloalkylmethyl radical to the corresponding alkyl radical has been the subject of intensive investigation, with a particular emphasis on the kinetics of reaction [1]. The rate constant for cleavage of the oxiranylmethyl to allyloxy radical has been estimated to be 10^{10} s^{-1} [2], approximately two orders of magnitude more rapid than the prototypical rearrangement of the cyclopropylmethyl to homoallyl radical [3]. In contrast, the cleavage of cyclobutylmethyl to 4-pentenyl radicals has a rate constant of $5 \cdot 10^{3}$ s^{-1} at 298 K [4]. A recent study by Crich and Mo concluded that 4-oxo-2-oxetanylmethyl radicals undergo facile ring opening with cleavage of the C(2)-O bond (numbered from the exocyclic carbon) to yield 1-oxo-3-butenyloxy radicals [1].

The principal intention of this study was to elucidate the reaction mechanisms of the aforementioned organic radical species by investigating the pyrolysis of the appropriate organohalide precursor in the presence of $W(CO)_6$. The IR LPHP of $W(CO)_6$ in the gas phase leads to unsaturated $W(CO)_x$ species; these prove to be very effective and selective abstractors of Cl atoms from a wide range of organic substrates, and offer a clean and low energy route into gas phase organic radical chemistry [5]. The chemistry of the resultant organic radical is dominated by the themes of combination, disproportionation, addition, abstraction, fragmentation and rearrangement; these have been described in section 1.1.3.

The decomposition of an organochlorine compound is initiated in the absence of $W(CO)_6$ by dehydrochlorination or C–Cl fission, the latter effecting formation of an organic radical. The molecular β-elimination of HCl from an organochlorine compound will afford the corresponding olefin through formation of an additional carbon-carbon bond; conversely,

in organochlorine compounds that do not possess a β-hydrogen, decomposition may proceed through molecular α-elimination of HCl yielding a carbene moiety [6, 7].

In this work, the gas phase thermal decomposition of a selection of cyclic organochlorine compounds, including cyclopropylmethyl chloride ((chloromethyl)cyclopropane), epichlorohydrin ((chloromethyl)oxirane), cyclobutylmethyl chloride (chloromethyl)-cyclobutane and 4-(bromomethyl)-2-oxetanone was initiated in the presence and absence of $W(CO)_6$ using IR LPHP. A combination of FT-IR, GC-MS and matrix isolation spectroscopy was employed to characterise reaction.

6.2 Cyclopropylmethyl Chloride

6.2.1 Pyrolysis

The decomposition of cyclopropylmethyl chloride ((chloromethyl)cyclopropane) has not been studied previously. In the present work, cyclopropylmethyl chloride was exposed to the output of a CW CO_2 laser in the absence and presence of $W(CO)_6$. The major product observed following pyrolysis of cyclopropylmethyl chloride in the absence of $W(CO)_6$ and at lower laser power (*i.e.* temperature) was 4-chloro-1-butene; 1-chloro-1-butene and, to a lesser extent, 3-chloro-2-methyl-1-propene were also detected. These results are consistent with isomerisation of starting material, the predominant pathway involving cleavage of the three-membered ring with a hydrogen shift, yielding 4-chloro-1-butene.

At higher temperature, isomerisation of starting material is accompanied by molecular elimination of HCl from 1-chloro-1-butene and 4-chloro-1-butene, yielding 1-butyne and

1,3-butadiene, respectively. There was no evidence to indicate dehydrochlorination of cyclopropylmethyl chloride; methylenecyclopropane, the expected product, was not detected in this investigation. It is possible, however, that at elevated temperature this species expeditiously decompose; certainly, rearrangement of methylenecyclopropane will afford 1,3-butadiene, which was observed at a significant level. The absence of C_β–H (relative to C–Cl) precludes β-elimination of HCl from 3-chloro-2-methyl-1-propene. It is likely that the major decomposition pathway of cyclopropylmethyl chloride involve β-elimination of HCl from the predominant C_4H_7Cl isomer, namely 4-chloro-1-butene.

The formation of ethylene and chloroethene, which were observed at significant levels, is consistent with heterolytic fragmentation of the C(2)–C(3) bond in 1-chloro-1-butene or 4-chloro-1-butene followed by a hydrogen shift. 1,2-butadiene was observed at a modest level in this investigation; this is consistent with rearrangement of 1-butyne. Indeed, at elevated temperature 1,2-butadiene was observed to increase at the expense of 1-butyne. A proposed pyrolysis scheme for cyclopropylmethyl chloride is illustrated in Figure 6.1.

6.2.2 Co-pyrolysis with $W(CO)_6$

The products derived from the pyrolysis of cyclopropylmethyl chloride in the presence of $W(CO)_6$ at low temperature were 4-chloro-1-butene, 1-chloro-1-butene, various C_4H_6, C_4H_8 and C_8H_{14} isomers, chloroethene, acetylene and benzene. The formation of 4-chloro-1-butene and 1-chloro-1-butene is consistent with isomerisation of starting material. 3-chloro-2-methyl-1-propene, which was observed in trace amount following pyrolysis of cyclopropylmethyl chloride alone, was not detected in this investigation. It is possible to rationalise isomerisation of cyclopropylmethyl chloride in the presence of $W(CO)_6$ (and,

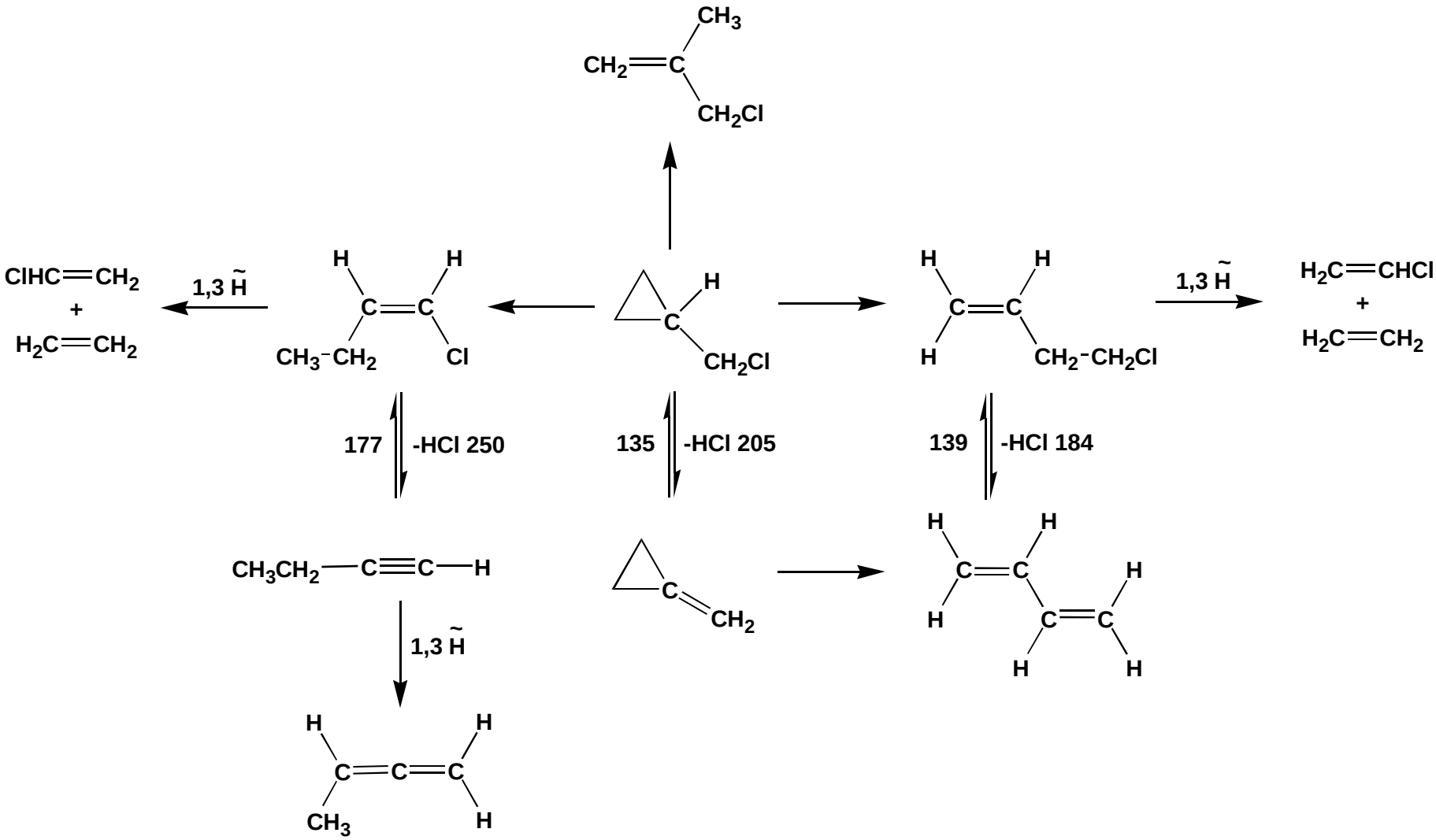

Figure 6.1 A proposed scheme for cyclopropylmethyl chloride IR LPHP; calculated activation energies for reversible dehydrochlorination are in kJ mol^{-1}

consequently, formation of 4-chloro-1-butene and 1-chloro-1-butene) in terms of pyrolysis temperature; the temperature required to initiate isomerisation of starting material in the absence of $W(CO)_6$ was approximately equivalent to that in the presence of $W(CO)_6$.

The formation of several C_4H_8, C_4H_6 and C_8H_{14} isomers is consistent with the selective abstraction of atomic chlorine from each of the C_4H_7Cl isomers to yield the corresponding C_4H_7 radical. These either combine, effecting formation of the various C_8H_{14} isomers, or undergo disproportionation to yield the corresponding C_4H_6 and C_4H_8 isomers. The absence of those products ascribed to combination or disproportionation of the cyclopropylmethyl radical suggests that radical rearrangement will precede self-reaction. The unimolecular conversion of cyclopropylmethyl to 3-butenyl is a fast radical rearrangement [3, 8-12] with activation energy of the order of 30 kJ mol^{-1} [10]. It is consequently not surprising that the products associated with cyclopropylmethyl combination and disproportionation were not detected in this study.

The selective abstraction of atomic chlorine from the C_4H_7Cl isomers, 1-chloro-1-butene and 4-chloro-1-butene, will afford 1-butenyl and 3-butenyl, respectively. The presence of several C_4H_6, C_4H_8 and C_8H_{14} isomers that are not ascribed to disproportionation or combination of the 1-butenyl or 3-butenyl radicals indicate rearrangement of either the self-reaction product or the radical prior to self-reaction. It is probable that rearrangement precedes self-reaction; the global minimum on the C_4H_7 potential energy surface comprises a resonance hybrid of the 2-butenyl and 1-methyl-2-propenyl radicals [13], while the analogous transition barriers have been calculated to be of the order of 125 kJ mol^{-1} [13]. Consequently, rearrangement to the resonance hybrid structure is thermodynamically and kinetically favoured. With reference to combination, this results in the formation of

2,6-octadiene, 3,4-dimethyl-1,5-hexadiene and 3-methyl-1,5-heptadiene (the latter derived from cross-combination) in addition to the species expected from the combination of 1-butenyl or 3-butenyl radicals.

The formation of chloroethene and ethylene, which were also detected at low temperature following pyrolysis in the absence of $W(CO)_6$, is consistent with heterolytic fragmentation of the C(2)–C(3) single bond in 1-chloro-1-butene or 4-chloro-1-butene followed by a hydrogen shift. The fact that ethylene was generated at a yield considerably higher than that expected suggests an additional formation mechanism. Moreover, the yield of chloroethene was lower than that anticipated. These results are consistent with the selective abstraction of Cl from chloroethene to yield the vinyl radical; this either combines to give 1,3-butadiene, which was also afforded from disproportionation of the C_4H_7 radical, or undergoes disproportionation to ethylene and acetylene.

The disproportionation to combination ratio of vinyl, which is reported to be of the order of 0.22 [14], predicts formation of 1,3-butadiene in preference to ethylene and acetylene, and indeed, this is observed. The production of benzene is ascribed to the trimerisation of acetylene, a process well known to be catalysed by transition metals [15-20], and will account for the low yield of acetylene observed. A proposed pyrolysis scheme for cyclopropylmethyl chloride in the presence of $W(CO)_6$ is illustrated in Figure 6.2.

6.3 Epichlorohydrin

The pyrolysis of epichlorohydrin ((chloromethyl)oxirane) in a single-pulse shock tube has been investigated by Gong and co-workers [21], with the conclusion that reaction proceeds

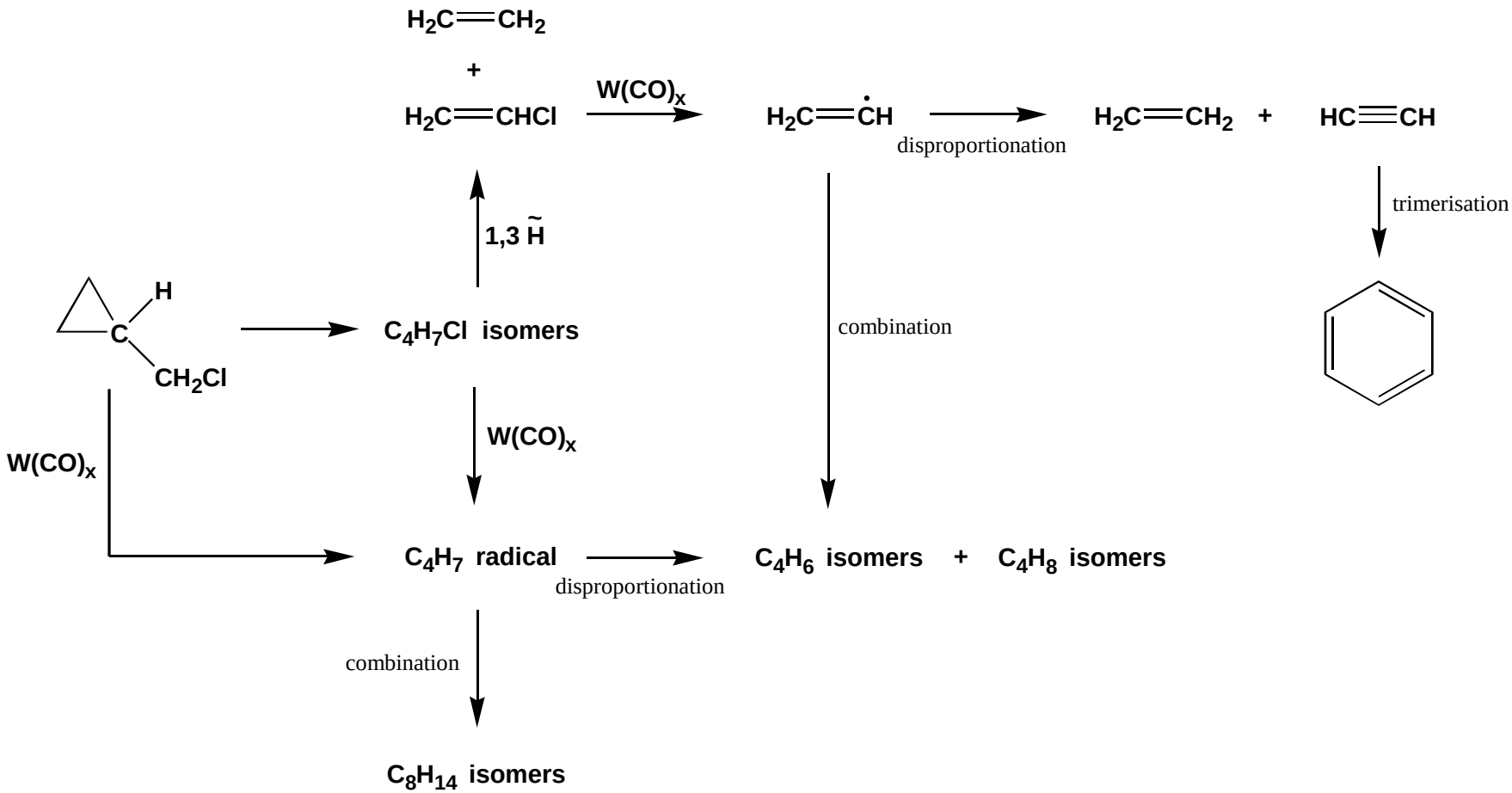

Figure 6.2 A proposed scheme for cyclopropylmethyl chloride and $W(CO)_6$ IR LPHP

through molecular elimination of HCl; the major products observed, in addition to HCl, were acetylene, ethylene, CO, acrolein (2-propenal) and formaldehyde.

6.3.1 Pyrolysis

In the present study, a sample of epichlorohydrin was exposed to the output of a CW CO_2 laser in the absence and presence of $W(CO)_6$. The pyrolysis of epichlorohydrin in the absence of $W(CO)_6$ at low temperature effected isomerisation of starting material, resulting in the formation of 3-chloropropanal through heterolytic fragmentation of the C(2)–O bond (numbered from the exocyclic group) with an accompanying hydrogen shift. The generation of 1-chloro-2-propanone (chloroacetone) at higher temperature is consistent with heterolytic cleavage of the C(3)–O bond with a concomitant hydrogen shift, and suggests that the C(3)–O bond is considerably stronger than the C(2)–O bond.

The isomerisation of starting material to 3-chloropropanal is accompanied by molecular elimination of HCl from the latter to yield acrolein. There was no evidence to indicate formation of methyleneoxirane, the product effected from the dehydrochlorination of epichlorohydrin. While this result ostensibly precludes such a mechanism, it is conceivable that the temperature required to initiate the elimination of HCl from epichlorohydrin is sufficient to decompose methyleneoxirane. The isomerisation or decarbonylation of methyleneoxirane will afford acrolein and ethylene, respectively, which were observed in this study. The formation of ethylene, which was detected in significant yield, is also consistent with the decarbonylation of acrolein. An alternative mechanism involving homolytic cleavage of the C(1)–C(2) bond in acrolein, followed by the abstraction of atomic hydrogen by the resultant species (vinyl) can be discounted. There was no evidence

to indicate combination of vinyl radical, which, given the reported disproportionation to combination ratio of 0.22 [14], should predominate.

The formation of acetaldehyde and chloromethane, which were detected at a significant level at elevated temperature, is consistent with homolytic fragmentation of the C(2)–C(3) bond in 3-chloropropanal. It is conceivable that the resulting species, which include the chloromethyl and acetyl radicals, abstract atomic hydrogen yielding, respectively, chloromethane and acetaldehyde. In a similar manner, homolytic fragmentation of the C(1)–C(2) bond will yield the formyl and 2-chloroethyl radicals. Presumably, the formyl radical affords CO through elimination of atomic hydrogen. The 2-chloroethyl radical can lose atomic hydrogen or chlorine to afford the observed chloroethene or ethylene, respectively. Theoretical calculations by Seetula [22] have shown that the predominant decomposition route for a β-chlorinated ethyl radical is through homolytic fragmentation of the weakest bond, namely C_β–Cl. A less significant mechanism involving the dissociation of the C_β–H bond is also practicable, given the relatively low enthalpy of that bond [23].

The absence of chloroethane and 1,4-dichlorobutane precludes disproportionation and combination of the 2-chloroethyl radical. This is consistent with the results presented in section 4.2.2 and 4.4.2, where the pyrolysis of $W(CO)_6$ with chloroacetyl and 3-chloropropanoyl chloride, respectively, was investigated. The presence of acetylene at higher temperature is consistent with the molecular dehydrochlorination of chloroethene, while the decarbonylation of acetaldehyde may account for the observed methane. A proposed pyrolysis scheme for epichlorohydrin is illustrated in Figure 6.3.

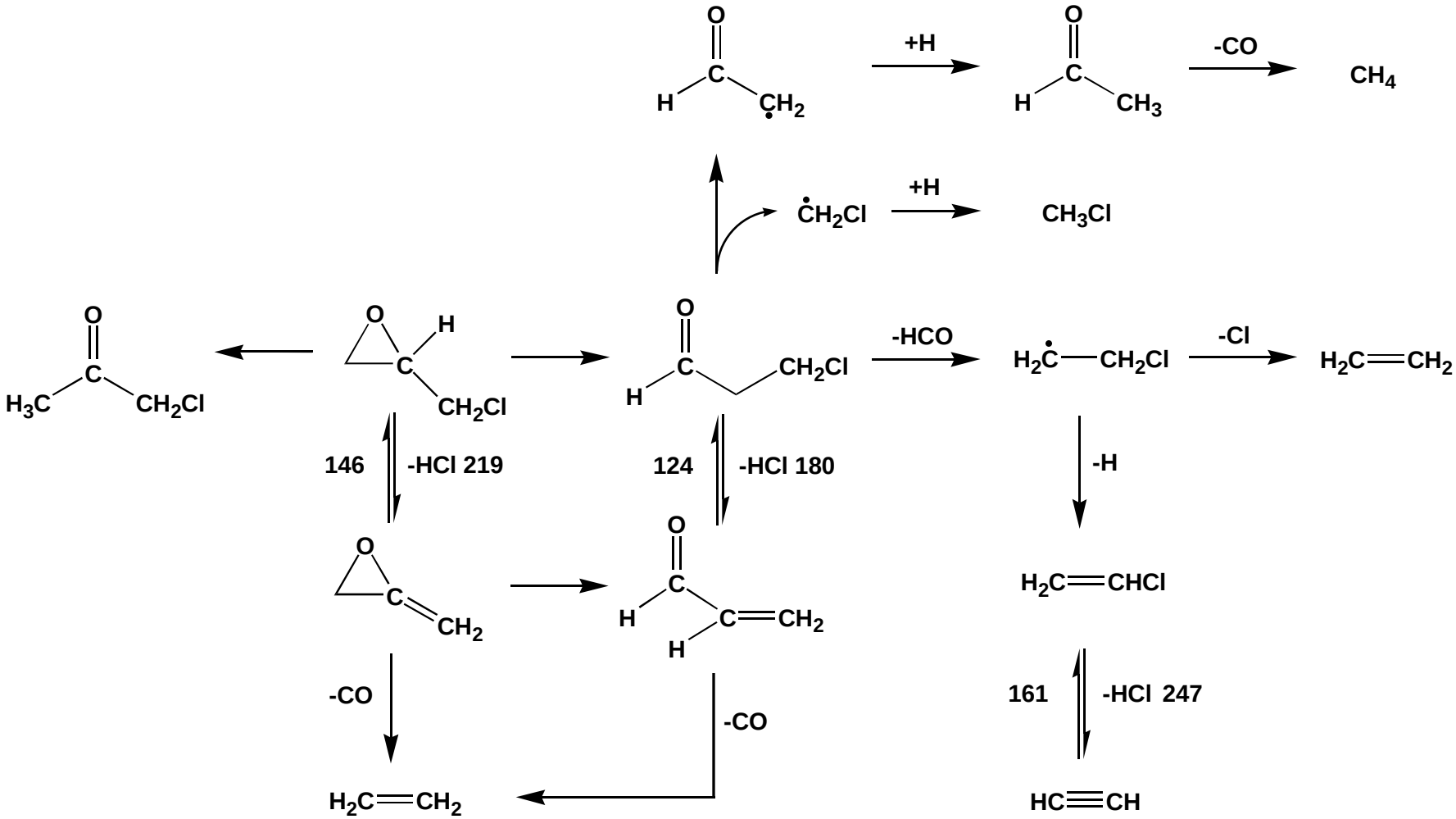

Figure 6.3 A proposed scheme for epichlorohydrin IR LPHP; calculated activation energies for reversible dehydrochlorination are in kJ mol^{-1}

6.3.2 Co-pyrolysis with $W(CO)_6$

The most significant products detected following IR LPHP of epichlorohydrin in the presence of $W(CO)_6$ at low power were 1,5-hexadiene, propene and 3-chloro-1-propene. Acrolein, ethylene and benzene, the latter increasing at the expense of 1,5-hexadiene as the duration of pyrolysis was extended, were observed in moderate yield. The generation of 3-chloro-1-propene is consistent with the selective abstraction of atomic oxygen from starting material, essentially the reverse reaction of alkene epoxidation [7]. The pyrolysis of succinyl and diglycoloyl chloride in the presence of $W(CO)_6$ (refer to sections 5.4.2 and 5.5.2, respectively) illustrated the practicability of oxygen abstraction by unsaturated $W(CO)_x$ species. Moreover, the pyrolysis of propylene oxide (the non-chlorinated analogue of epichlorohydrin) and $W(CO)_6$ yielded propene as the major product, presumably, through the selective abstraction of atomic oxygen.

The formation of 1,5-hexadiene and propene is consistent with the selective abstraction of atomic chlorine from 3-chloro-1-propene to yield the allyl (2-propenyl) radical. This either combines to yield 1,5-hexadiene, or abstracts atomic hydrogen to effect the formation of propene. The calculated Arrhenius parameters and rate constants for the abstraction of atomic hydrogen by allyl radicals from a number of hydrocarbons have been reported by Löser and co-workers [24]; calculated activation energies were in reasonable accord with experiment and did not exceed 100 kJ mol^{-1}. The absence of propane precludes disproportionation of the allyl radical, a result consistent with the reported disproportionation to combination ratio of 0.008 [25]. It is conceivable that the stoichiometric elimination of two hydrogen molecules from 1,5-hexadiene, with concomitant ring closure may yield benzene; certainly, generation of the latter was

accompanied by the decomposition of 1,5-hexadiene as the duration of pyrolysis was extended.

The generation of acrolein and ethylene is consistent with the selective abstraction of Cl from epichlorohydrin to yield the oxiranylmethyl radical. The elimination of H from the intermediate allyloxy radical formed through homolytic fragmentation of the C(2)–O bond (in oxiranylmethyl) will yield acrolein. The ring-opening rearrangement of a radical in which the unpaired electron is adjacent to an epoxide ring is known to proceed by homolytic cleavage of the C(2)–O bond unless scission of the C(2)–C(3) bond generates an allylic or benzylic radical [26]. The formation of ethylene is ascribed to decarbonylation of acrolein.

It is conceivable that the decomposition of the allyloxy radical also involve homolytic fragmentation of the C(3)–O bond, yielding the allyl radical. Tsang and Kiefer [27] have investigated the unimolecular reactions of large polyatomic molecules; the unimolecular rate expressions for the decomposition of larger radicals were found to have activation energies of the order of 120-160 kJ mol^{-1} and normal pre-exponential factors. It was concluded that such species are considerably less stable than the analogous alkanes and alkenes, and would rapidly generate highly reactive species such as methyl or atomic hydrogen.

It is evident from the distribution of products that the pyrolysis of epichlorohydrin in the presence of $W(CO)_6$ is initiated primarily through the selective abstraction of atomic oxygen as opposed to atomic chlorine. This is inconsistent with the relative strengths of the fragmenting C–O and C–Cl bonds, which are 743 and 348 kJ mol^{-1}, respectively [23]. It is

proposed that the driving force for reaction is formation of the W–O or W–Cl bond. The dissociation energy of the W–O multiple bond is estimated to be in excess of 577 kJ mol^{-1} [28], while the W–Cl diatomic bond energy (which is used to approximate the W–Cl bond strength) is 423 kJ mol^{-1} [29]. Consequently, formation of the W–O bond is favoured. A proposed pyrolysis scheme for epichlorohydrin in the presence of $W(CO)_6$ is illustrated in Figure 6.4.

6.4 Cyclobutylmethyl Chloride

6.4.1 Pyrolysis

The decomposition of cyclobutylmethyl chloride ((chloromethyl)cyclobutane) has not been previously investigated. In the present work, a sample of cyclobutylmethyl chloride alone was exposed to the output of a CW CO_2 laser to yield 3-chloro-1-propene, ethylene, allene and several C_5H_8 isomers, including methylenecyclobutane. There was some evidence to indicate isomerisation of starting material; a trace amount of each of the C_5H_9Cl isomers was detected. The formation of methylenecyclobutane, which was observed in significant yield, is ascribed to molecular dehydrochlorination of cyclobutylmethyl chloride.

The dissociation of cyclobutylmethyl chloride will yield 3-chloro-1-propene and ethylene through either a concerted or stepwise process. The thermal fission of a cyclobutane moiety by a concerted and allowed $\sigma^2s + \sigma^2a$ process is essentially the reverse of a $\pi^2s + \pi^2a$ cycloaddition of two alkenes [30], and will lead to retention of configuration in one alkene, and inversion in the other [6]. A stepwise process, in contrast, involves formation of a 1,4-diradical through homolytic cleavage of the C(2)–C(3) or C(2)–C(5)

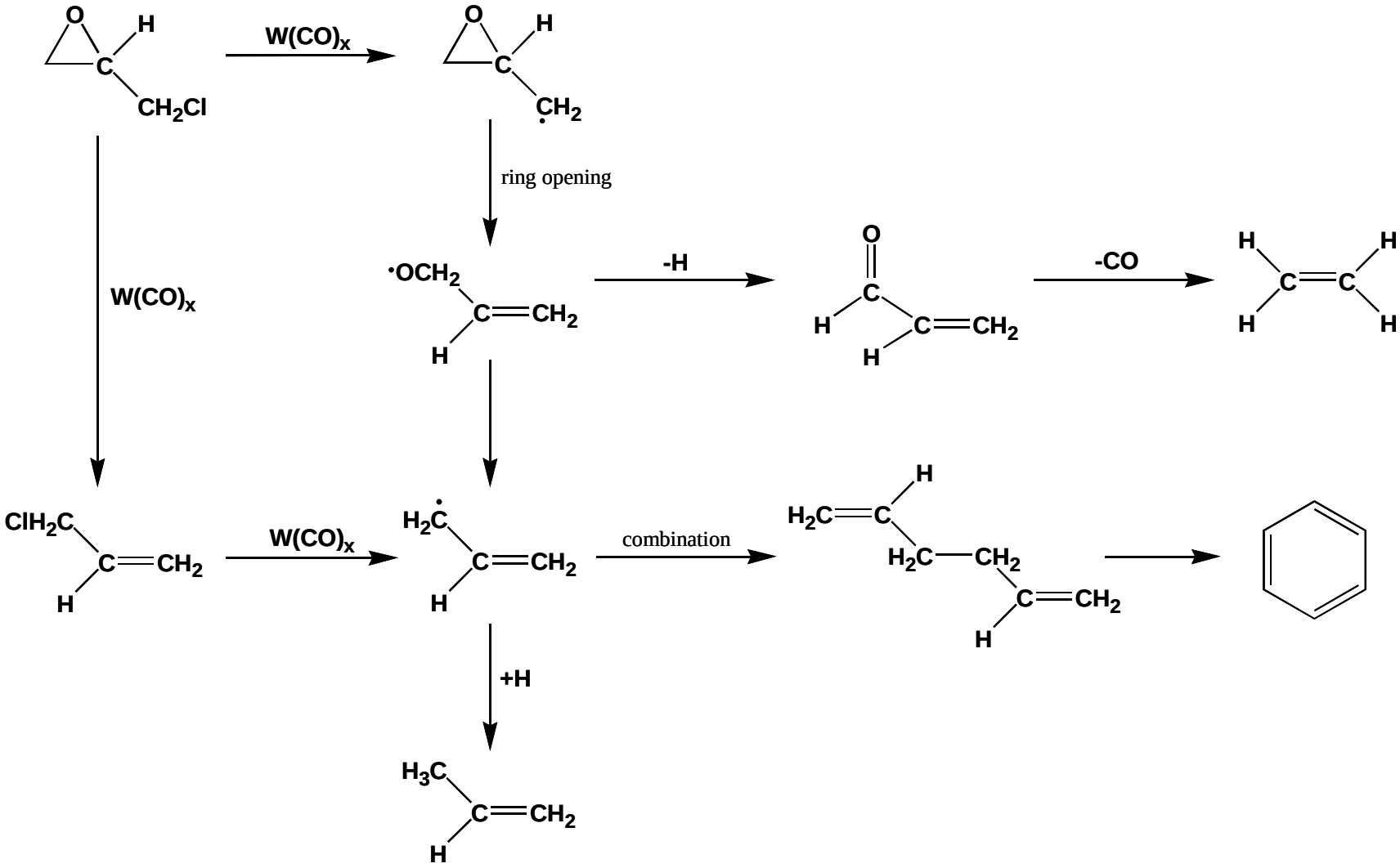

Figure 6.4 A proposed scheme for epichlorohydrin and $W(CO)_6$ IR LPHP

bond (numbered from the exocyclic carbon), followed by fragmentation of a second C–C bond. The variation in stereochemical outcome is dependent on the relative rates of radical fission of the first bond, rotations of the radical termini about the resultant single bonds, and fission of the second bond [6].

In an analogous manner, the dissociation of methylenecyclobutane will effect formation of allene and ethylene. The thermal dissociation of methylenecyclobutane has been investigated by Chesick [31], with the conclusion that reaction is non-concerted, as the activation energy of the concerted process is too high in such a small ring. Several other workers have reached a similar conclusion [32-34]. The formation of allene is also consistent with the molecular elimination of HCl from 3-chloro-1-propene; certainly, the yield of allene increased, at the expense of 3-chloro-1-propene, as the pyrolysis temperature was raised.

The presence of several C_5H_8 isomers, including cyclopentene and 1,4-pentadiene, in addition to methylenecyclobutane is consistent with isomerisation of the latter. The formation of cyclopentene indicates ring expansion, while the generation of 1,4-pentadiene presumably involves heterolytic fragmentation of the C(2)–C(5) bond, followed by a hydrogen shift. An alternative mechanism for formation of 1,4-pentadiene, involving molecular dehydrochlorination of 5-chloro-1-pentene (C_5H_9Cl isomer) can not be discounted. While only trace quantities of this isomer were detected, it is conceivable that the conditions of cyclobutylmethyl chloride pyrolysis are sufficient to decompose 5-chloro-1-pentene. A proposed pyrolysis scheme for cyclobutylmethyl chloride, without the mechanism responsible for the formation and depletion of each of the C_5H_9Cl isomers, which were formed in only trace amount, is illustrated in Figure 6.5.

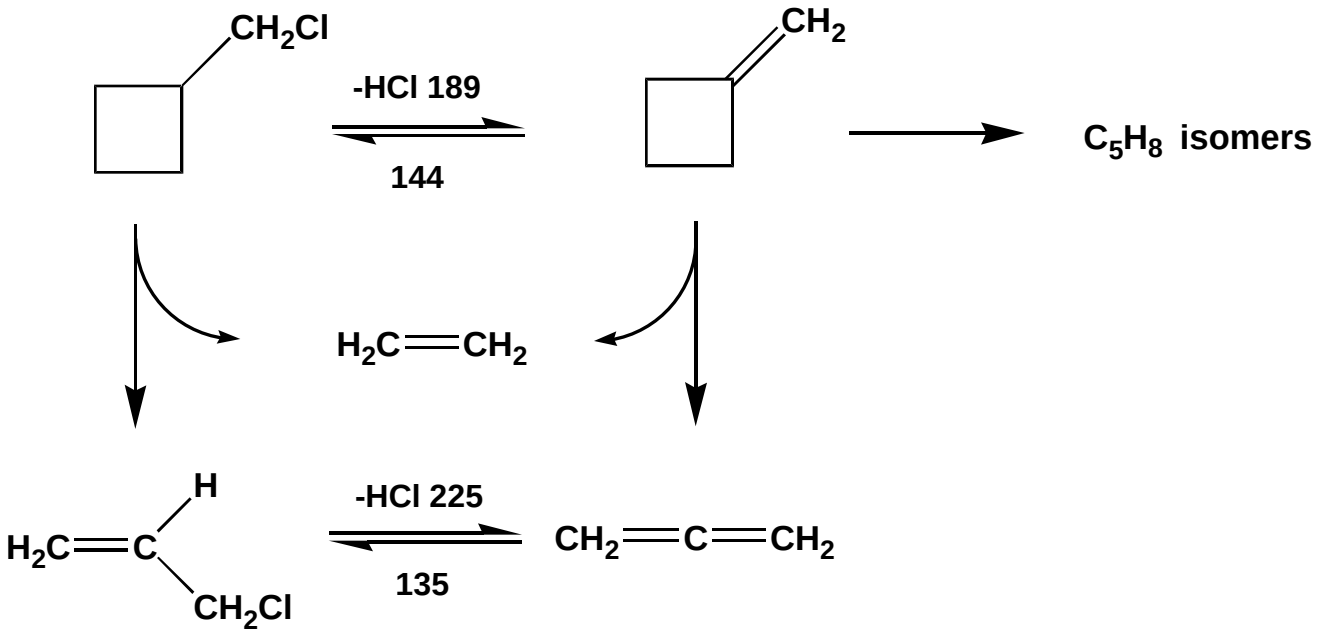

Figure 6.5 A proposed scheme for cyclobutylmethyl chloride IR LPHP with activation energies for dehydrochlorination in kJ mol^{-1}

6.4.2 Co-pyrolysis with $W(CO)_6$

The most significant product observed in the post-pyrolysis gas chromatogram of cyclobutylmethyl chloride and $W(CO)_6$, which is partially illustrated in Figure 6.6 with the post-pyrolysis gas chromatogram of cyclobutylmethyl chloride alone, was cyclopentene. This result is consistent with the selective abstraction of Cl to yield the cyclobutylmethyl radical; this rearranges though homolysis of the C(2)–C(3) or C(2)–C(5) bond to give the 4-pentenyl radical [4], which forms the thermodynamically more stable cyclopentyl radical through *endo*-mode cyclisation (intramolecular addition) [35]. The elimination of atomic hydrogen from cyclopentyl will yield cyclopentene.

The *endo*-mode cyclisation of 4-pentenyl is consistent with attack at the least substituted carbon atom, the preferred site of alkyl radical addition [36]. In contrast, intramolecular addition of a radical to an unsaturated group (most often a double bond) in the liquid phase is known to occur at the most substituted carbon [35], in many cases, yielding the less stable radical product. The cyclisation of 5-hexenyl proceeds in a highly selective manner affording the thermodynamically less stable cyclopentylmethyl radical through *exo*-mode intramolecular addition, and not the more stable cyclohexyl radical [37-39].

The formation of ethylene, propene and 1,5-hexadiene, which were detected at moderate levels, is consistent with dissociation of the 4-pentenyl radical; homolytic fragmentation of the C(2)–C(3) single bond (numbered from the radical centre) will afford the allyl radical and ethylene. The allyl radical will either combine, or abstract atomic hydrogen to form the observed propene. The disproportionation of allyl radical will effect the formation of propene and allene; that the latter is not observed suggests that such a mechanism is not

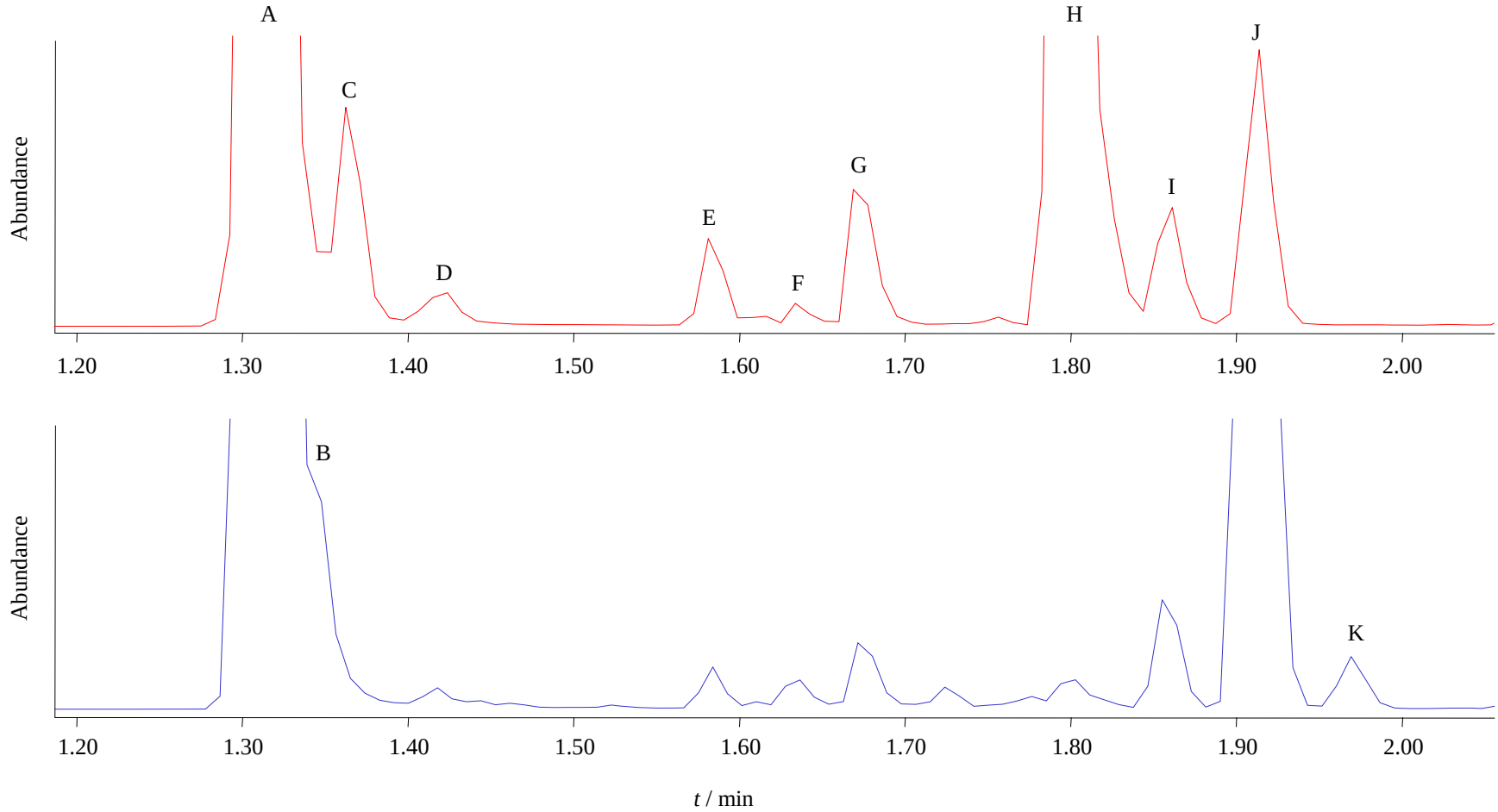

Figure 6.6 Partial gas chromatograph of the products of laser pyrolysis of cyclobutylmethyl chloride in the absence (—) and presence (—) of $W(CO)_6$; A = SF_6; B = propene; C = allene; D = unidentified; E = 1,4-pentadiene; F = acetone; G = ether; H = 3-chloro-1-propene; I = methylenecyclobutane; J = cyclopentene; K = cyclopentane; the small amount of ether and acetone evident in the upper and lower trace was present in the original sample

practicable. This is consistent with the reported disproportionation to combination ratio for the allyl radical of 0.008 [25].

The thermal decomposition of 4-pentenyl has been investigated at 1040 K < T < 1200 K by Tsang and Walker [40], with the conclusion that homolytic fragmentation of the C(2)–C(3) bond, while predominant, competes with *endo*-mode cyclisation. A similar result was reported from photolysis of the 4-pentenyl radical [41]. Tsang and Walker have derived an expression for the cyclisation (c) to dissociation (d) branching ratio:

$$\frac{k_c}{k_d} = (6.9 \pm 4) \cdot 10^{-3} \exp(2118 \pm 500/T)$$

The rate constant for cyclisation will exceed the dissociation rate constant at T < 430 ± 150 K. It is evident from the results of the present study that intramolecular cyclisation is the predominant decomposition mechanism, indicating an effective reaction temperature of less than 430 ± 150 K. It is important to note, however, that this value does not necessarily represent the temperature at the centre of the reaction cell (the hot zone); the 4-pentenyl radicals resulting from cyclobutylmethyl ring opening may migrate to a cooler region of the reaction cell prior to cyclisation or dissociation. The temperature evaluated from the pyrolysis study of *E*-1,2-dichloroethene in the presence of $W(CO)_6$ at a comparable laser power (refer to section 3.4) was considerably higher at 650 ± 150 K.

The formation of methylenecyclobutane and 1,4-pentadiene, which were observed at moderate levels, is consistent with the elimination of atomic hydrogen from the cyclobutylmethyl and 4-pentenyl radicals, respectively. The molecular dehydrochlorination of starting material can be discounted as an alternative pathway to methylenecyclobutane

since there was no evidence to indicate formation of HCl. The generation of 1,4-pentadiene may also involve the isomerisation of methylenecyclobutane though heterolytic fragmentation of the C(2)–C(3) or C(2)–C(5) bond, followed by a hydrogen shift. Cyclopentane was detected in moderate amount and is ascribed to abstraction of atomic hydrogen by the cyclopentyl radical. A proposed pyrolysis scheme for cyclobutylmethyl chloride in the presence of $W(CO)_6$ is given in Figure 6.7.

6.5 4-(Bromomethyl)-2-oxetanone

6.5.1 Pyrolysis

The pyrolysis of 4-(bromomethyl)-2-oxetanone has not been investigated previously. In the present work, a sample of 4-(bromomethyl)-2-oxetanone was exposed to the output of a CW CO_2 laser in the absence and presence of $W(CO)_6$. The most significant product observed following pyrolysis in the absence of $W(CO)_6$ and at lower laser power was 3-bromo-1-propene; this is consistent with the pericyclic decarboxylation of starting material. It is well known that simple β-lactones, of which 4-(bromomethyl)-2-oxetanone is an example, decompose readily to form CO_2 and an alkene at low temperature [6].

The generation of allene and HBr at higher temperature is consistent with molecular elimination of HBr from 3-bromo-1-propene. Conversely, the presence of propene and 1,5-hexadiene is consistent with elimination of Br to yield the allyl radical; this either combines, or abstracts atomic hydrogen to form the observed propene. Hettema and co-workers have illustrated the concurrent nature of decomposition of a brominated compound in the pyrolysis study of a series of halogenated acetic acids [42]. The pyrolysis

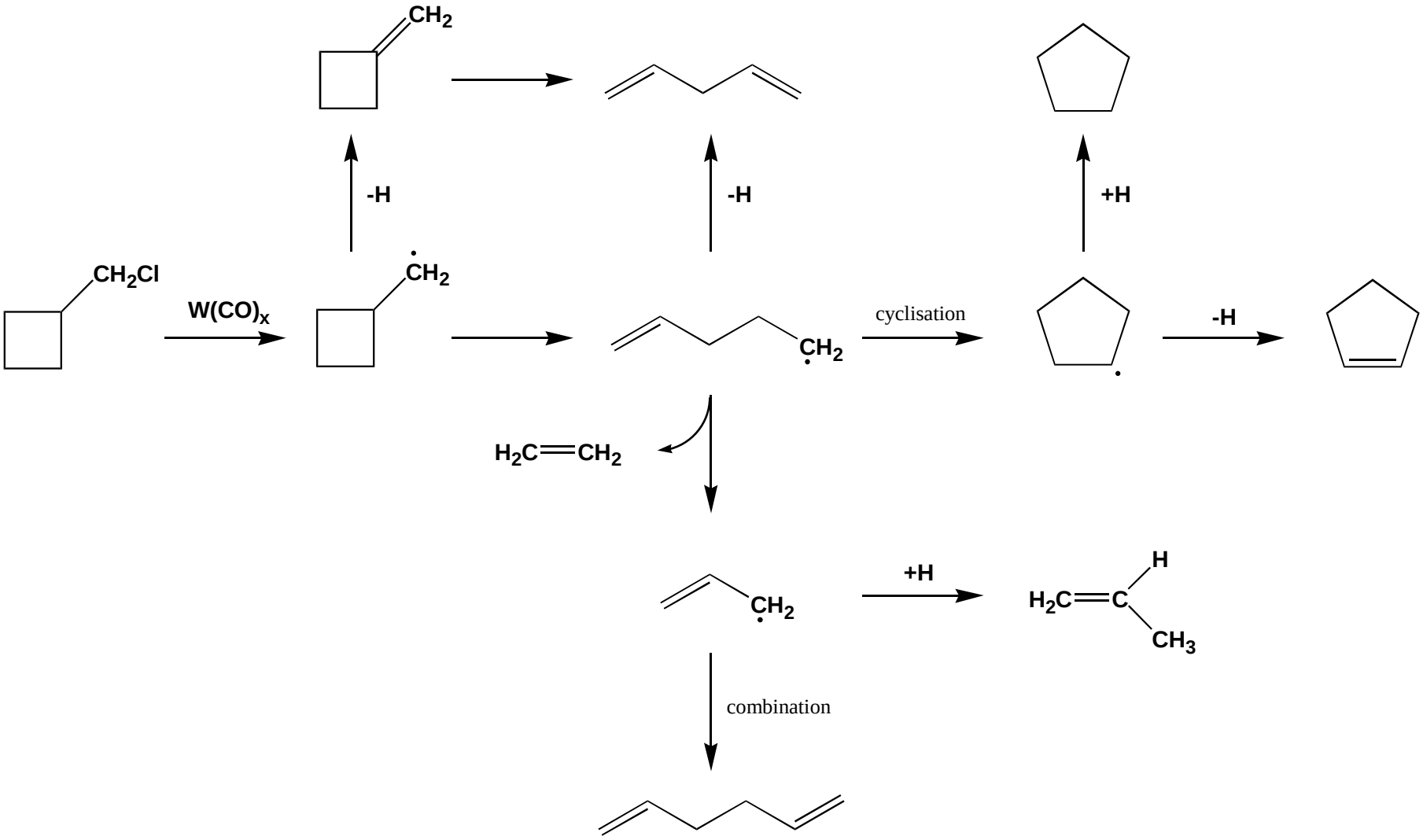

Figure 6.7 A proposed scheme for cyclobutylmethyl chloride and $W(CO)_6$ IR LPHP

of bromoacetic acid was found to proceed through two competing mechanisms: molecular elimination of HBr and C–Br homolysis.

It is conceivable that the stoichiometric elimination of two hydrogen molecules from 1,5-hexadiene with concomitant ring closure may yield the observed benzene; certainly, generation of the latter was accompanied by the decomposition of 1,5-hexadiene at higher temperature. A proposed scheme for pyrolysis of 4-(bromomethyl)-2-oxetanone is given in Figure 6.8.

6.5.2 Co-pyrolysis with $W(CO)_6$

On co-pyrolysis with $W(CO)_6$ at low laser power, the most significant products were propene, 1,5-hexadiene and acetone. The formation of propene and 1,5-hexadiene is consistent with the selective abstraction of Br to yield 4-oxo-2-oxetanylmethyl radicals; these undergo facile ring opening with cleavage of the C(2)–O bond (numbered from the exocyclic carbon) to give 1-oxo-3-butenyloxy radicals, which afford allyl following decarboxylation [1]. The allyl radical either combines, or abstracts atomic hydrogen to effect the formation of propene. It is evident from these results that the selective abstraction of atomic bromine by unsaturated $W(CO)_x$ species is a practicable mechanism; in fact, abstraction of Br is predicted to occur in preference to that of Cl, as the enthalpy of the C–Br bond is considerably less than that of the C–Cl bond [23].

The decomposition of substituted 4-oxo-2-oxetanylmethyl radicals was investigated by Crich and Mo [1], with the conclusion that the most likely mechanism (among those considered) involved homolytic cleavage of the C(2)–O bond (numbered from the radical

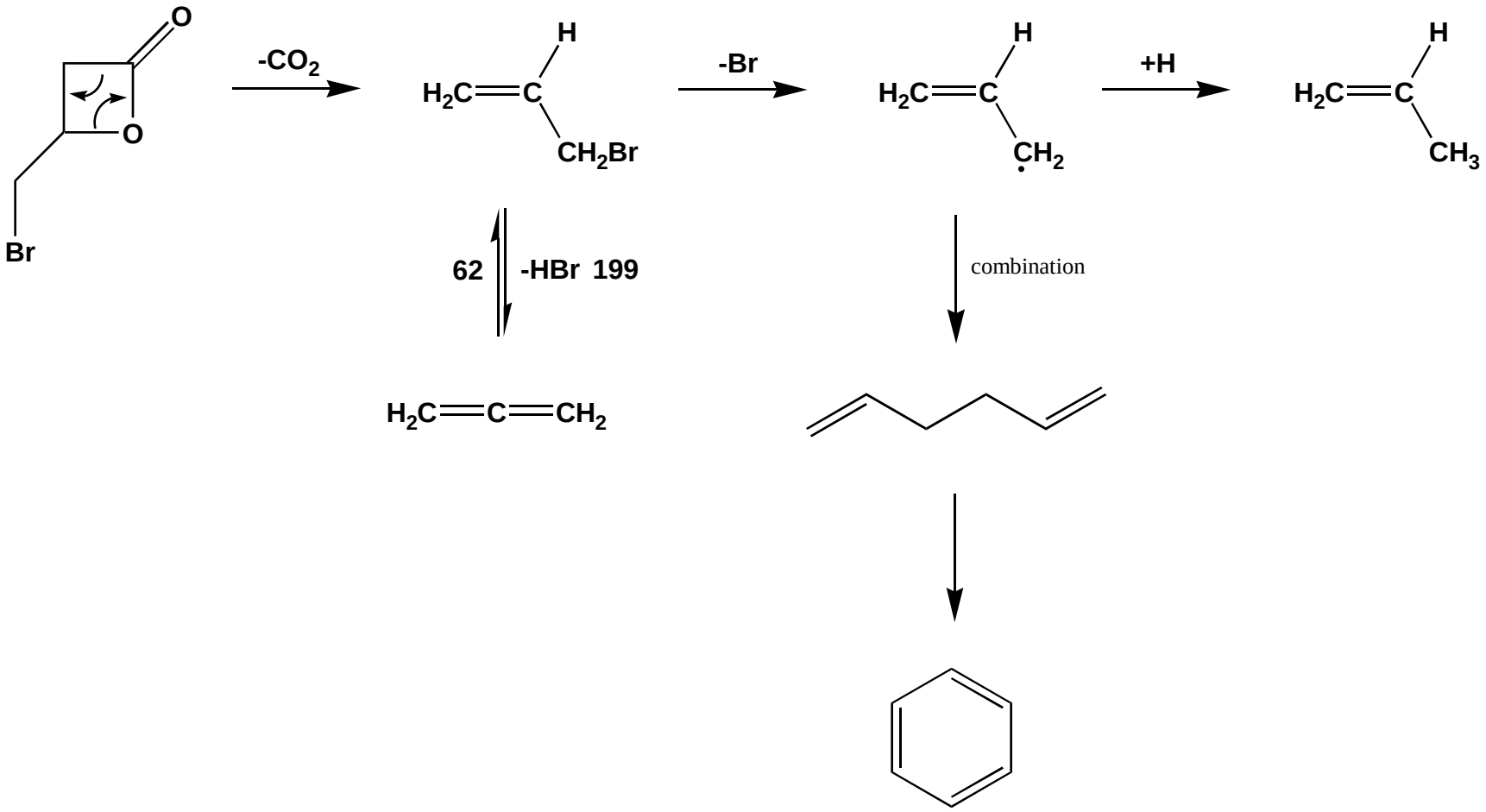

Figure 6.8 A proposed scheme for 4-(bromomethyl)-2-oxetanone IR LPHP

centre); interestingly, formation of the 3-oxobutanoyl radical through homolysis of the C(4)–O bond (with an accompanying hydrogen shift) was not considered. It is apparent from the present investigation that this mechanism can not be ignored; the formation of acetone is consistent with the decarbonylation of 3-oxobutanoyl to yield 2-oxopropyl radicals; these subsequently abstract atomic hydrogen to give the ketone.

The generation of 3-bromo-1-propene, albeit in trace amount, is consistent with the pericyclic decarboxylation of 4-(bromomethyl)-2-oxetanone. The thermal decomposition of 3-bromo-1-propene is limited to the selective abstraction of atomic bromine to yield the allyl radical; the absence of HBr and allene ostensibly preclude molecular dehydrobromination. This is consistent with the conditions employed; pyrolysis was initiated at a significantly lower temperature in the presence of $W(CO)_6$ than in the absence. It is conceivable that the formation of benzene, which was detected at a minor level, is ascribed to elimination of two hydrogen molecules from 1,5-hexadiene, with concomitant ring closure; certainly, decomposition of the latter was accompanied by formation of benzene as the duration of pyrolysis was extended. A proposed pyrolysis scheme for 4-(bromomethyl)-2-oxetanone with $W(CO)_6$ is illustrated in Figure 6.9.

6.6 Conclusion

The results presented in this chapter confirm that unsaturated $W(CO)_x$ species are effective and selective abstractors of Cl and O from a range of organochlorine compounds under comparatively mild conditions. Moreover, the investigation of the pyrolysis of 4-(bromomethyl)-2-oxetanone indicates that $W(CO)_x$ species are also effective and selective abstractors of atomic bromine. The selective abstraction of Cl or Br from starting

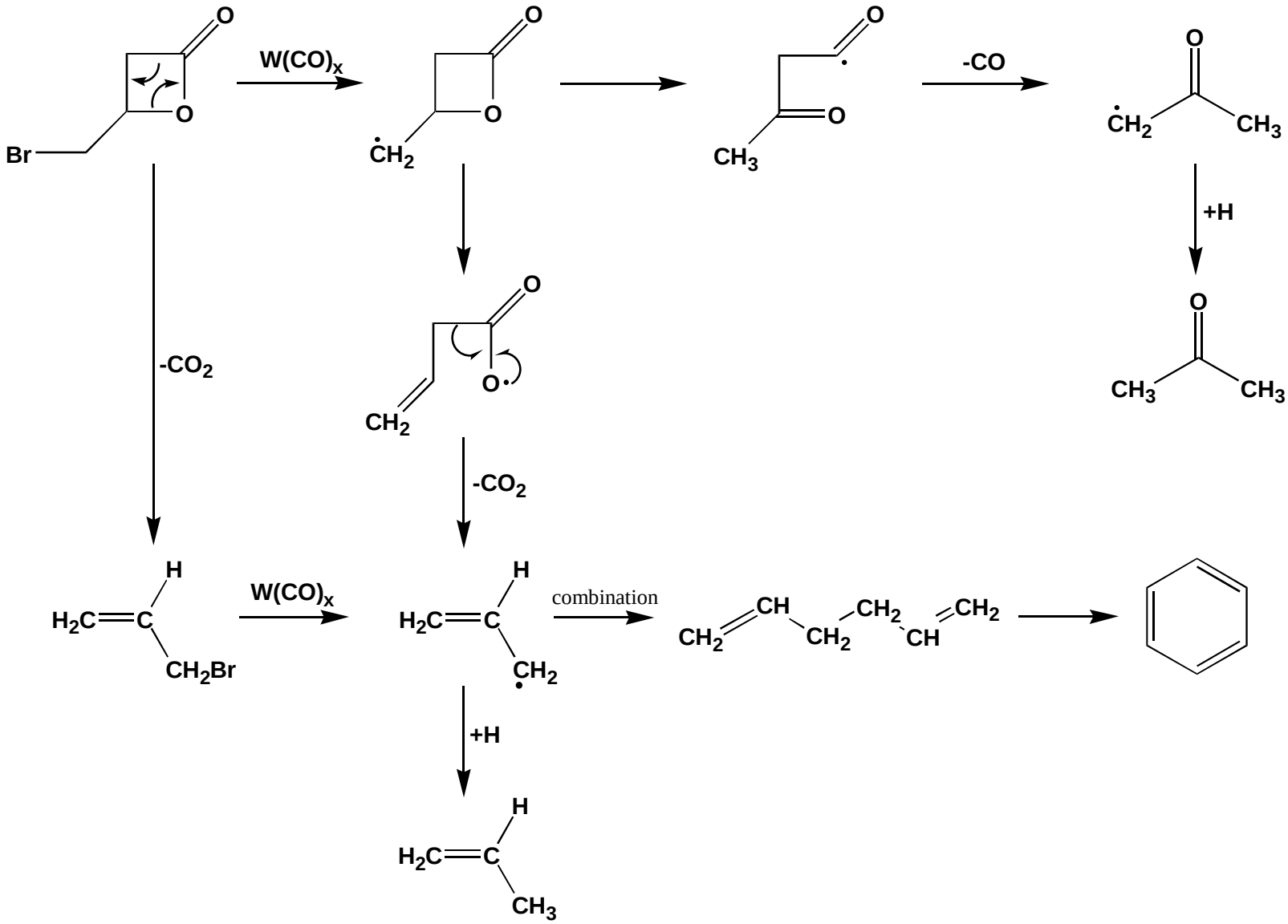

Figure 6.9 A proposed scheme for 4-(bromomethyl)-2-oxetanone and $W(CO)_6$ IR LPHP

material is succeeded by a ring-opening rearrangement involving homolysis of the C–C or (where available) C–O bond. The subsequent chemistry is dominated by the resulting organic radical moiety; observed end products are ascribed to combination and disproportionation (the two types of radical-radical reactions), intramolecular addition and fragmentation of the resultant species.

The combination or disproportionation of the species derived from the ring-opening rearrangement of the inaugural radical was a significant mechanism only following pyrolysis of cyclopropylmethyl chloride in the presence of $W(CO)_6$. In contrast, fragmentation was a predominant decomposition pathway, occurring in the pyrolysis of epichlorohydrin and 4-(bromomethyl)-2-oxetanone. Intramolecular addition was the predominant decomposition mechanism in the pyrolysis of cyclobutylmethyl chloride with $W(CO)_6$; presumably, the driving force for reaction was formation of the thermodynamically more stable cyclopentyl radical.

The selective abstraction of atomic oxygen was observed following the pyrolysis of epichlorohydrin in the presence of $W(CO)_6$ and effected formation of the corresponding alkene. The abstraction of atomic chlorine or bromine from starting material was not unique; in several cases a product could only be accounted for through a mechanism that involved Cl or Br abstraction from a primary pyrolysis product.

The pyrolysis of cyclopropylmethyl chloride and epichlorohydrin in the absence of $W(CO)_6$ and at lower temperature involved isomerisation of starting material through heterolytic cleavage of the three-membered ring; at higher temperature, this was accompanied by molecular dehydrochlorination. The dehydrochlorination of the product or

products effected from the isomerisation of starting material continued at higher temperature, and was accompanied by heterolytic or homolytic fragmentation. The pyrolysis of cyclobutylmethyl chloride and 4-(bromomethyl)-2-oxetanone involved dissociation (cycloreversion) of the four-membered ring through a concerted and allowed $\sigma^2s + \sigma^2a$ process; the cycloreversion of cyclobutylmethyl chloride was accompanied by the molecular elimination of HCl. The pyrolysis of the halogenated species derived from the cycloreversion of starting material initiated dehydrohalogenation; however, molecular elimination of HBr from 3-bromo-1-propene was found to compete with C–Br bond homolysis.

6.7 References

[1] D. Crich and X. Mo, *J. Am. Chem. Soc.*, 1998, **120**, 8298 and references therein.

[2] V. Krishnamurthy and V. H. Rawal, *J. Org. Chem.*, 1997, **62**, 1572.

[3] M. Newcombe and A. G. Glenn, *J. Am. Chem. Soc.*, 1989, **111**, 265.

[4] J. C. Walton, *J. Chem. Soc., Perkin Trans. II*, 1989, 173 and references therein.

[5] G. R. Allen, N. D. Renner and D. K. Russell, *J. Chem. Soc., Chem. Commun.*, 1998, 703.

[6] R. F. C. Brown, *Pyrolytic Methods in Organic Chemistry,* Academic Press, New York, 1980.

[7] J. McMurray, *Organic Chemistry,* 3rd Ed, Brookes/Cole Publishing Company, Pacific Grove, CA, 1992.

[8] A. Effio, D. Griller, K. U. Ingold, A. L. J. Beckwith and A. K. Serelis, *J. Am. Chem. Soc.*, 1980, **102**, 1734 and references therein.

[9] P. S. Engel, S. L. He, J. T. Banks, K. U. Ingold and J. Lusztyk, *J. Org. Chem.*, 1997, **62**, 1210.

[10] A. L. J. Beckwith and V. W. Bowry, *J. Am. Chem. Soc.*, 1994, **116**, 2710.

[11] V. W. Bowry, J. Lusztyk and K. U. Ingold, *J. Am. Chem. Soc.*, 1991, **113**, 5687.

[12] M. Newcombe, *Tetrahedron*, 1993, **49**, 1151.

[13] D. R. Kent, *J. Young Investigators*, 1999, **1**, www.jyi.org/articles/kent/kent.html.

[14] A. Fahr and A. H. Laufer, *J. Phys. Chem.*, 1990, **94**, 726.

[15] J. C. Bertolini, J. Massardiner and G. Dalmai-Imerdik, *J. Chem. Soc., Farad. Trans. I*, 1978, **74**, 1720.

[16] S. Lie, L. Wang, M. Xie, X. Guo and Y. Wu, *Catal. Lett.*, 1995, **30**, 135.

[17] P. M. Maitlis, *Pure Appl. Chem.*, 1973, **33**, 489.

[18] G. N. Schauzer and S. Eichlwer, *Chem. Ber.*, 1962, **95**, 550.

[19] F. Solymosi, A. Erdohelyi and A. Szoke, *Catal. Lett.*, 1995, **32**, 43.

[20] J. E. Germaine, *Catalytic Conversion of Hydrocarbons,* Academic Press, London, 1969.

[21] Y. Gong, H. Yang, Z. Qin and D. Han, *Beijing Daxue Xuebao, Ziran Kexueban*, 1991, **21**, 385.

[22] J. A. Seetula, *J. Chem. Soc., Faraday Trans.*, 1998, **94**, 1933.

[23] P. W. Atkins, *Physical Chemistry,* 4th Ed, Oxford University Press, Oxford, 1990.

[24] U. Löser, K. Scherzer and K. Weber, *Z. phys. Chemie, Liepzig*, 1989, **270**, 237.

[25] D. G. L. James and S. M. Kambanis, *Trans. Faraday Soc.*, 1969, **65**, 1350.

[26] D. J. Pasto, *J. Org. Chem.*, 1996, **61**, 252 and references therein.

[27] W. Tsang and J. H. Kiefer, In *The Chemical Dynamics and Kinetics of Small Radicals,* K. Liu and A. Wagner, Eds., World Scientific, Singapore, 1995; pp. 58-119.

[28] J. C. Bryan and J. M. Mayer, *J. Am. Chem. Soc.*, 1990, **112**, 2298.

[29] *CRC Handbook of Chemistry and Physics,* 60th Ed, R. C. Weast, Ed., CRC Press, Roca Baton, Fl., 1979.

[30] R. B. Woodward and R. Hoffmann, *The Conservation of Orbital Symmetry,* Academic Press, New York, 1970.

[31] J. P. Chesick, *J. Phys. Chem.*, 1961, **65**, 2170.

[32] W. J. Engelbrecht and M. J. De Vries, *J. S. Afr. Chem. Inst.*, 1970, **23**, 163.

[33] J. S. Chickos, *J. Org. Chem.*, 1979, **44**, 1515.

[34] R. L. Brandaur, B. Short and S. M. E. Kellner, *J. Phys. Chem.*, 1961, **65**, 2269.

[35] S. Dóbé and T. Bérces, In *Chemical Kinetics of Small Organic Radicals,* Z.B. Alfassi, Ed., CRC Press, Boca Raton, Fl., 1988; pp. 89-128.

[36] J. Fossey, D. Lefort and J. Sorba, *Free Radicals in Organic Chemistry,* John Wiley & Sons, Chichester, 1995.

[37] P. Schmid, D. Griller and K. U. Ingold, *Int. J. Chem. Kinet.*, 1979, **11**, 333.

[38] D. Lal, D. Griller, S. Husband and K. U. Ingold, *J. Am. Chem. Soc.*, 1974, **96**, 6355.

[39] D. J. Carlson and K. U. Ingold, *J. Am. Chem. Soc.*, 1968, **90**, 7047.

[40] W. Tsang and J. A. Walker, *J. Phys. Chem.*, 1992, **96**, 8378.

[41] K. W. Watkins and D. K. Olsen, *J. Phys. Chem.*, 1972, **76**, 1089.

[42] H. Hettema, N. R. Hore, N. D. Renner and D. K. Russell, *Aust. J. Chem.*, 1997, **50**, 363.

Chapter Seven

CONCLUSIONS AND FUTURE WORK

The pyrolysis of a number of halogenated compounds in the absence and presence of $W(CO)_6$ has been investigated using infrared laser powered homogeneous pyrolysis (IR LPHP). The chemistry of these compounds in the absence of $W(CO)_6$ was dominated by the themes of dehydrohalogenation (where available) and C–X bond homolysis (where X = halogen). It is anticipated that the results pertaining to the decomposition of several selected halogenated species in the absence of $W(CO)_6$ may contribute to the existing literature.

The molecular elimination of HCl from the acyl and diacyl chlorides (with the exception of methacryloyl chloride) effected the formation of a transient ketene species. These were detected using a combination of matrix isolation and tuneable diode laser (TDL) spectroscopy; IR LPHP-TDLS may be utilised in future work to further characterise these ketene species. The subsequent decarbonylation of the ketene predominated in all but a single case, yielding the analogous carbene; chloroformyl ketene (which was procured through the pyrolysis of malonyl chloride) afforded carbon suboxide exclusively through molecular dehydrochlorination.

The rearrangement of the resultant carbene involved intramolecular insertion of the divalent carbon at the C_β–H bond or (where there was no C_β–H bond) the C_β–O bond; intramolecular carbonyl addition was also a practicable mechanism. The predominant reaction of a carbene possessing a single carbon atom involved combination or abstraction.

The results pertaining to pyrolysis of the selected halogenated compounds in the presence of $W(CO)_6$ confirm that unsaturated $W(CO)_x$ species are effective and selective abstractors of Cl and Br atoms under comparatively mild conditions. The chemistry of the resulting

organic radical moiety is dependent on the precursor. Decarbonylation of the species derived from the selective abstraction of atomic chlorine from the acyl chlorides resulted in an organic radical species that dominated the subsequent chemistry. The observed end products were ascribed to combination, disproportionation, abstraction and fragmentation of this organic radical species.

The decarbonylation of the species derived from the abstraction of a single chlorine atom from the diacyl chlorides yielded an intermediate species that could either abstract atomic hydrogen or lose a second chlorine atom. The subsequent decarbonylation of the species derived from the loss of a second chlorine atom effected formation of a stable species, with the exception of methylene that was generated from the pyrolysis of malonyl chloride.

The selective abstraction of atomic chlorine or atomic bromine from the exocyclic carbon of a three or four-membered ring was succeeded by a ring-opening rearrangement involving homolysis of the C–C or (where available) C–O bond. The subsequent chemistry was dominated by the resulting organic radical moiety; observed end products were ascribed to combination, disproportionation, intramolecular addition and fragmentation of this species.

The results presented in this thesis also indicate that unsaturated $W(CO)_x$ species are effective abstractors of atomic oxygen from a range of halogenated compounds under comparatively mild conditions. The selective abstraction of atomic oxygen was observed following the pyrolysis of epichlorohydrin in the presence of $W(CO)_6$ and effected the formation of the corresponding alkene. The intramolecular insertion of the carbene derived

from the abstraction of a single oxygen atom from succinyl or diglycoloyl chloride led to a cycloalkane derivative that rapidly decomposed.

The pyrolysis of a halogenated or oxygenated compound in the presence of unsaturated $W(CO)_x$ species provides a clean and low-energy route into gas phase organic radical and carbene chemistry. A number of radical and carbene reactions have been illustrated in the present study by investigating the pyrolysis of an appropriate organohalide precursor in the presence of $W(CO)_6$. There is, however, scope for further work; an investigation into the pyrolysis mechanisms of compounds containing other heteroatoms (*e.g.* group 15 or other group 16 elements) with $W(CO)_6$ would be advantageous. The pyrolysis mechanisms of any number of organic species possessing a heteroatom with $W(CO)_6$ is also possible using this novel technique.